LINOLEIC ACID-DERIVED OXYLIPIDS MODIFY MAMMARY ENDOTHELIAL BARRIER INTEGRITY DURING INFLAMMATION

By

Valerie Eubanks Ryman

A DISSERTATION

Submitted to
Michigan State University
in partial fulfillment of the requirements
for the degree of

Comparative Medicine and Integrative Biology - Doctor of Philosophy

2016

ABSTRACT

LINOLEIC ACID-DERIVED OXYLIPIDS MODIFY MAMMARY ENDOTHELIAL BARRIER INTEGRITY DURING INFLAMMATION

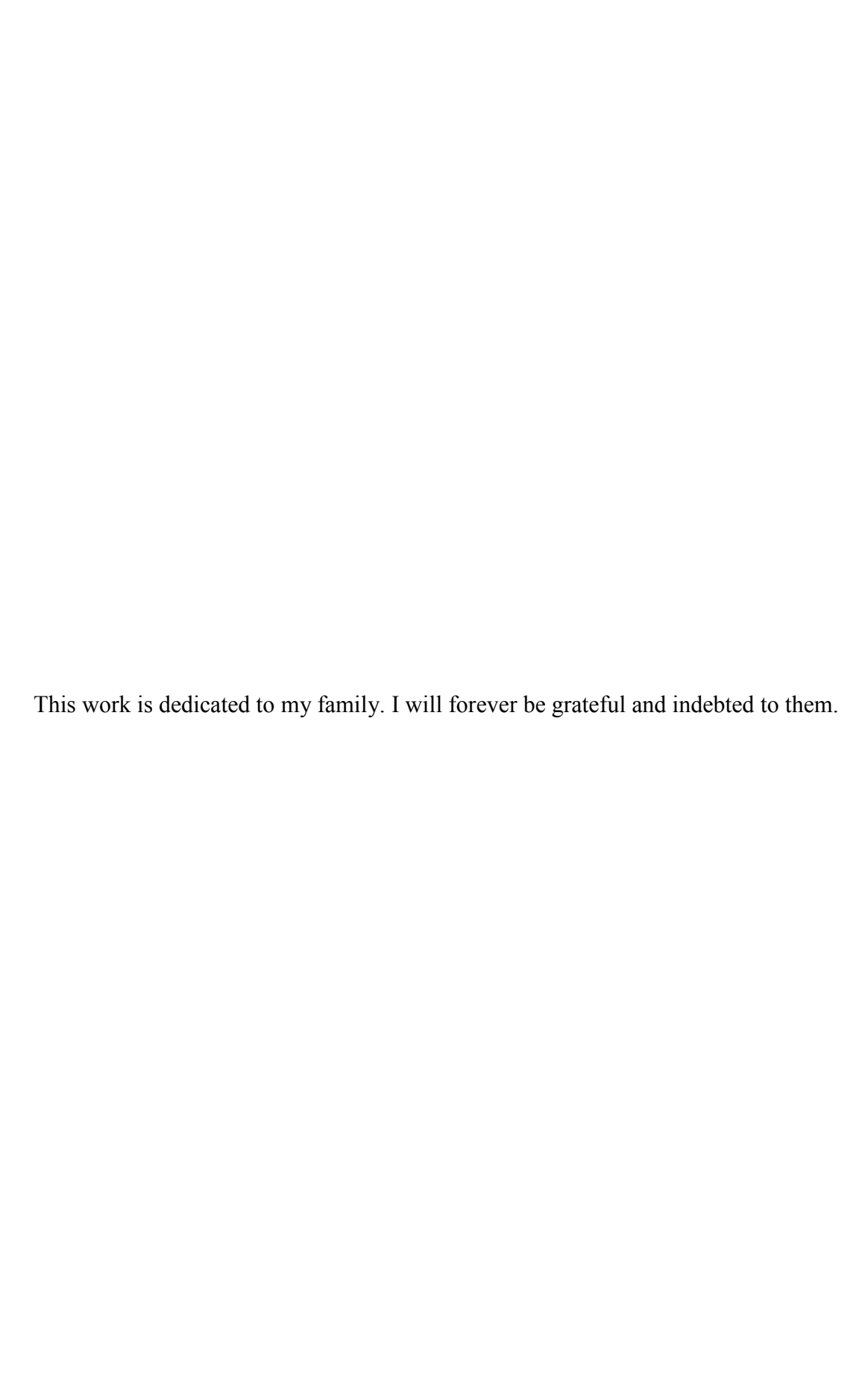
By

Valerie Eubanks Ryman

Bovine Streptococcus uberis mastitis results in severe damage of mammary tissue due to uncontrolled inflammation. Endothelial dysfunction is implicated in the development of uncontrolled inflammation. Oxylipids are potent lipid mediators that orchestrate pathogeninduced inflammatory responses and an abundance or imbalance of some oxylipids may contribute to pathogenesis of disease. Oxylipids are derived from polyunsaturated fatty acids (PUFA) in the cell membranes, and the enzymatic oxygenation products of linoleic acid (LA) were previously shown to modulate endothelial cell responses. Thus, the hypothesis for chapter 2 was that LA metabolites, 9- and 13-hydroxyoctadecadienoic acid (HODE), are increased during S. uberis mastitis and contribute to an inflammatory phenotype in endothelial cells. The LAderived oxylipids were predominant and 9- and 13-HODE were significantly increased in S. uberis-infected mammary tissue. The initial oxygenation product of LA induced a proinflammatory phenotype in bovine mammary endothelial cells (BMEC), but 13-HODE did not change BMEC phenotype. Previous research demonstrated that 13-HPODE induced apoptosis in endothelial cells, which may disrupt the continuous, single-cell layer necessary for mediating a successful, self-limiting inflammatory response to S. uberis. However, the relative contribution of specific LA-oxygenation products to endothelial integrity was unknown. The hypothesis for chapter 3 was that S. uberis-induced LA-derived 15-LOX-1 oxygenation products impair mammary endothelial barrier integrity by apoptosis. Findings demonstrated that the BMEC may not be a primary source of 13-HODE in response to S. uberis. Bovine monocytes were evaluated

as a potential source of synthesized 13-HODE in response to S. uberis exposure. Subsequent results suggested that exposure of cultured BMEC monolayers to 13-HPODE, but not 13-HODE, reduced endothelial barrier integrity and apoptosis and necrosis may contribute, in part, to impairment. Based on previous literature, the proposed mechanism for 13-HPODE induced apoptosis was lipid peroxidation and co-exposure with an antioxidant in the current study prevented the adverse effects of 13-HPODE. Given the potential importance of LA-derived oxylipids during S. uberis mastitis, the final objective was to change the PUFA substrate in an effort to modify predominant oxylipid pools. Other than LA, other PUFA substrates include arachidonic acid (ArA), eicosapentaenoic acid (EPA), and docosahexaenoic acid (DHA). Linoleic acid may be used for *de novo* synthesis of ArA and α -linolenic acid (ALA) may be used for de novo EPA and DHA synthesis. The hypothesis for chapter 4 was that supplementation of PUFA would change bovine leukocyte FA content and respective oxylipid profiles from ex vivo microbial-challenged leukocytes. Results demonstrated an ability to modify the ALA content of leukocytes following ALA supplementation but not EPA and DHA content, suggesting that dosing and timing of ALA supplementation may be important for increasing EPA and DHA. Supplementing ALA changed S. uberis-induced oxylipids derived from LA and ArA. Even though LA supplementation did not modify leukocyte PUFA content, S. uberis-induced LA and ArA-derived oxylipids were significantly decreased. Future investigations are required to determine how supplemental PUFA, without changing content, could mediate oxylipid biosynthesis. Furthermore, the ability of changing ALA content to modify ArA and LA oxylipids, but no change in ArA or LA content, is an important finding and supports the idea that the abundance of increase may not be as important as the ratio of PUFA.

Copyright by VALERIE EUBANKS RYMAN 2016



ACKNOWLEDGEMENTS

I would like to acknowledge the many people and organizations that contributed to my professional development as a research scientist and to the development of all of the work within this document. Dr. Lorraine Sordillo served as my major advisor and kindly provided extensive time, thoughtful guidance, and endless support. My committee members, Drs. Julia Busik, Jane Maddox, and James Wagner, proved to be invaluable resources in learning to critically evaluate my research. Continuous funding was instrumental in completing my degree and was from an endowment from the Matilda R. Wilson Fund (Detroit, MI), the Agriculture and Food Research Initiative Competitive Grants Program of the USDA National Institute for Food and Agriculture (2011-67015-30179 and 2015-67011-23012), the Rackham Research Endowment, and Michigan State University AgBioResearch. Technical assistance from countless Meadow Brook Immunobiology lab members contributed to successful completion of this work. Last, but not least, I acknowledge my family and friends for their love, support, and patience.

TABLE OF CONTENTS

LIST OF TABLES	X
LIST OF FIGURES	xii
CHAPTER 1	1
ROLE OF ENDOTHELIAL CELLS IN BOVINE MAMMARY GLAND HEALTH AND	1
DISEASE	1
Abstract	
Introduction	
Endothelial cells contribute to the specialized structure of the mammary gland	
Mammary gland growth and development	
Onset of milk synthesis and secretion	
Mammary gland involution.	
Endothelial cells prevent mastitis by orchestrating inflammation	
Endothelial cells modulate changes in vascular tone and blood flow during	
inflammation	11
Vascular permeability is altered during inflammation	
Leukocyte movement increases across the mammary endothelium during	10
inflammation	17
Resolution of inflammation is necessary to prevent vascular and mammary tissue	
damage	21
Endothelial dysfunction as an underlying cause for immunopathology	
Oxidative stress negatively affects antioxidant pathways and oxylipid	c
biosynthesis	26
Oxidative stress contributes to decreased nitric oxide	
Prolonged or excessive inflammation induces apoptosis of endothelial cells	
Conclusions	
Acknowledgements	
Acknowledgements	50
CHAPTER 2	31
QUANTIFICATION OF BOVINE OXYLIPIDS DURING INTRAMAMMARY	
STREPTOCOCCUS UBERIS INFECTION	31
Abstract	32
Introduction	33
Materials and Methods	36
Chemicals and reagents	36
Streptococcus uberis 0140J challenge for quantification of oxylipids in mammary	
tissue	36
Streptococcus uberis UT888 challenge for quantification of oxylipids in milk	
samples	
Extraction and LC/mass spectrometry (LC/MS) quantification of oxylipids	39

13-HODE and 13-HPODE stimulation of bovine mammary endothelial cells (BMEC) for
COX-2 mRNA expression	
Preparation of 13-HPODE	42
Statistical analysis	43
Results	
Clinical signs of intramammary infection following S. uberis challenge	44
Mammary tissue oxylipid profiles in <i>S. uberis</i> -infected mammary tissue	
Milk oxylipid profiles in S. uberis-challenged dairy cows	
Response of BMEC following 13-HODE and 13-HPODE exposure	
Discussion	
Conclusion	54
Acknowledgements	54
CIVA PEED A	
CHAPTER 3	55
APOPTOSIS OF ENDOTHELIAL CELLS BY 13-HPODE CONTRIBUTES TO	
IMPAIRMENT OF ENDOTHELIAL BARRIER INTEGRITY	
Abstract	
Introduction	
Reagents	
Preparation of <i>Streptococcus uberis</i> for <i>in vitro</i> challenge	
Isolation and culture of primary bovine manimary endomenar cens (BMEC)	
Primary BMEC and monocyte mRNA quantification	
Extraction and quantification of oxylipids	
Preparation of 13-HPODE	
Electric Cell-Substrate Impedance Sensing assay: Endothelial barrier integrity	
Measurement of apoptosis and necrosis	
Statistical analysis	
Results	
S. uberis exposure induced inflammatory marker expression, but not oxylipid	00
biosynthetic enzyme expression, in BMEC	66
BMEC 13-HODE and 13-oxoODE biosynthesis was not changed following <i>S. uberis</i>	
exposure	
S. uberis exposure induced expression of inflammatory markers, including oxylipid	
biosynthetic enzyme expression, in bovine monocytes	66
13-HODE, but not 13-oxoODE, biosynthesis by bovine monocytes was upregulated	
following heat-killed <i>S. uberis</i> exposure	67
Mammary endothelial barrier integrity is decreased during 13-HPODE treatment	
Apoptosis and necrosis of BMEC was increased by 13-HPODE treatment	
N-acetylcysteine ameliorates 13-HPODE-induced apoptosis and necrosis of BMEC.	
N-acetylcysteine rescues 13-HPODE-induced impairment of endothelial integrity	
Discussion	
Conclusions	73
Acknowledgements	73

SUPPLEMENTATION OF LINOLEIC ACID (C18:2N-6) OR A-LINOLENIC ACID (C18:3N-3) CHANGES OXYLIPID BIOSYNTHESIS FOLLOWING EX VIVO MICROBIAL EXPOSURE
EXPOSURE
EXPOSURE
Introduction
Materials and Methods
Chemicals and reagents
Chemicals and reagents
Microbial agonist ex vivo challenge of blood leukocytes from non supplemented and supplemented animals
Microbial agonist ex vivo challenge of blood leukocytes from non supplemented and supplemented animals
supplemented animals 81 Whole blood processing for quantification of FA and oxylipids 82 Solid phase extraction of FA and oxylipids in WBC and cultured plasma 83 LC-MS quantification of FA 84 LC-MS/MS quantification of oxylipids 85 Statistical analysis 85 Results 86 White blood cell FA concentrations following supplementation of LA and ALA 86 FA following microbial challenge without PUFA supplementation 86 Microbial challenge-induced FA and oxylipid changes following LA and ALA supplementation 87 Discussion 88 Conclusions 95 Acknowledgements 95 CHAPTER 5 97 SUMMARY AND CONCLUSIONS 97 Chapter 2 99
Solid phase extraction of FA and oxylipids in WBC and cultured plasma LC-MS quantification of FA LC-MS/MS quantification of oxylipids Statistical analysis Results Results White blood cell FA concentrations following supplementation of LA and ALA FA following microbial challenge without PUFA supplementation Microbial challenge-induced FA and oxylipid changes following LA and ALA supplementation S7 Discussion R8 Conclusions S95 Acknowledgements S95 CHAPTER 5 S97 SUMMARY AND CONCLUSIONS S97 Chapter 2 S99
Solid phase extraction of FA and oxylipids in WBC and cultured plasma LC-MS quantification of FA LC-MS/MS quantification of oxylipids Statistical analysis Results Results White blood cell FA concentrations following supplementation of LA and ALA FA following microbial challenge without PUFA supplementation Microbial challenge-induced FA and oxylipid changes following LA and ALA supplementation S7 Discussion R8 Conclusions S95 Acknowledgements S95 CHAPTER 5 S97 SUMMARY AND CONCLUSIONS S97 Chapter 2 S99
LC-MS quantification of FA 84 LC-MS/MS quantification of oxylipids 85 Statistical analysis 85 Results 86 White blood cell FA concentrations following supplementation of LA and ALA 86 FA following microbial challenge without PUFA supplementation 86 Microbial challenge-induced FA and oxylipid changes following LA and ALA supplementation 87 Discussion 88 Conclusions 95 Acknowledgements 95 CHAPTER 5 97 SUMMARY AND CONCLUSIONS 97 Chapter 2 99
Statistical analysis
Statistical analysis
White blood cell FA concentrations following supplementation of LA and ALA 86 FA following microbial challenge without PUFA supplementation 86 Microbial challenge-induced FA and oxylipid changes following LA and ALA supplementation 87 Discussion 88 Conclusions 95 Acknowledgements 95 CHAPTER 5 97 SUMMARY AND CONCLUSIONS 97 Chapter 2 99
FA following microbial challenge without PUFA supplementation 86 Microbial challenge-induced FA and oxylipid changes following LA and ALA supplementation 87 Discussion 88 Conclusions 95 Acknowledgements 95 CHAPTER 5 97 SUMMARY AND CONCLUSIONS 97 Chapter 2 99
FA following microbial challenge without PUFA supplementation 86 Microbial challenge-induced FA and oxylipid changes following LA and ALA supplementation 87 Discussion 88 Conclusions 95 Acknowledgements 95 CHAPTER 5 97 SUMMARY AND CONCLUSIONS 97 Chapter 2 99
Microbial challenge-induced FA and oxylipid changes following LA and ALA supplementation
supplementation 87 Discussion 88 Conclusions 95 Acknowledgements 95 CHAPTER 5 97 SUMMARY AND CONCLUSIONS 97 Chapter 2 99
Discussion 88 Conclusions 95 Acknowledgements 95 CHAPTER 5 97 SUMMARY AND CONCLUSIONS 97 Chapter 2 99
Acknowledgements
CHAPTER 5
SUMMARY AND CONCLUSIONS 97 Chapter 2 99
SUMMARY AND CONCLUSIONS 97 Chapter 2 99
Chapter 299
•
Chapter 2
Chapter 3
Chapter 4104
APPENDICES
Appendix A. Authorization to publish Chapter 1 in dissertation
Appendix B. Authorization to publish Chapter 2 in dissertation
Appendix C. Tables
Appendix D. Figures
Appendix E. Preparation of 13-HPODE
Appendix F. Electric Cell-Substrate Impedance Sensing Experimental Protocol160
REFERENCES

LIST OF TABLES

Table 1. Summary of inflammatory mediator production during bovine mastitis
Table 2. Bovine primers for qRT-PCR
Table 3. Oxylipid concentrations in mammary tissue obtained from uninfected cows and cows challenged with <i>S. uberis</i> (pg/ng of tissue). ¹
Table 4. Oxylipid concentrations in milk from cows that did not establish <i>S. uberis</i> mastitis after intramammary challenge (pg/μL of milk)
Table 5. Oxylipid concentrations in milk from cows that established <i>S. uberis</i> mastitis after intramammary challenge (pg/μL of milk)
Table 6. Fatty acid composition of linoleic acid (LA) and α-Linolenic acid (ALA) infusions117
Table 7. Ingredient and nutrient composition of the treatment diet ¹
Table 8. Concentration (mM) of plasma FA following <i>ex vivo</i> microbial exposure ¹ 119
Table 9. Concentration (μM) of significantly changed plasma oxylipids following <i>ex vivo</i> microbial exposure ^{1,2}
Table 10. Changes in plasma FA from PUFA-supplemented cows following <i>ex vivo S. uberis</i> challenge
Table 11. Changes in plasma oxylipids from PUFA-supplemented cows following <i>ex vivo S. uberis</i> challenge ¹
Table 12. Changes in plasma FA from PUFA-supplemented cows following <i>ex vivo</i> LPS challenge
Table 13. Changes in plasma oxylipids from PUFA-supplemented cows following <i>ex vivo</i> LPS challenge ¹
Table 14. Concentration (μM) of plasma oxylipids not significantly changed following <i>ex vivo</i> microbial exposure ^{1,2}
Table 15. Changes in plasma oxylipids from PUFA-supplemented cows following <i>ex vivo S. uberis</i> challenge ¹

Table 16.	Changes in plasma of	xylipids from	PUFA-supplemented	cows following	ex vivo LPS
challenge	l			-	129

LIST OF FIGURES

Figure 1A. During homeostasis, endothelial cells maintain adequate vascular tone, permeability, and leukocyte migration. B. At the onset of infection-induced inflammation, endothelial cells acquire new properties to facilitate clearance of the bacteria. Activated endothelial cell expression adhesion molecules and produce increased concentrations of reactive oxygen species, vasoactive lipid mediators, and cytokines. Increased vasodilation and chemokines elicit neutrophils to adhere to and cross the endothelium. Some endothelial cells may exhibit morphological changes during inflammation, those of which are eliminated during the resolution and wound healing phase of inflammation. C. An unregulated immune response results in prolonged activation of endothelial cells and accumulation of activated neutrophils at the endothelial surface causing irreversible cell damage. Oxidative stress as a result of accumulated ROS, free radicals, and lipid hydroperoxides further contributes to cellular damage and apoptosis of endothelial cells.
Figure 2. Means of oxylipid concentrations in tissue from uninfected cows (n=3) are displayed in open bars and means of oxylipid concentrations in tissue from <i>S. uberis</i> -infected cows (n=5) are displayed in closed bars. The concentration of tissue 6-keto-PGF _{1α} , PGE ₂ , PGF _{2α} , and 5-oxoETE (A) was significantly greater in <i>S. uberis</i> -infected mammary tissue. Similarly, the concentration of 9-HODE and 13-HODE (B), and the 9-HODE:9-oxoODE ratio (C) was significantly greater in <i>S. uberis</i> -infected mammary tissue. Values are means \pm SEM expressed in pg of oxylipid per mg of tissue or as a ratio of oxylipids. *Significance declared at $P \le 0.05$
Figure 3. Means of relative mRNA expression in tissue from uninfected cows (n=3) are displayed in open bars and means of relative mRNA expression in tissue from <i>S. uberis</i> -infected cows (n=5) are displayed in closed bars. Pro-inflammatory marker (A) and oxylipid biosynthetic enzyme (B) mRNA expression of tissue from uninfected (n=3) and <i>S. uberis</i> (014J)-infected cows (n=5). The mRNA expression is expressed as $2^{-\Delta\Delta Ct} \pm SE$. Significance declared for differences in ΔCt at $P \le 0.05$.
Figure 4. Means of oxylipid concentrations in milk from cows that failed to establish <i>S. uberis</i> mastitis (n=3) are displayed in open bars and means of oxylipid concentrations in milk from cows that established <i>S. uberis</i> mastitis (n=5) are in closed bars. Increased HODE was significant 7 d post-challenge in cows that established a <i>S. uberis</i> intramammary infection (A). In contrast, the milk 13-HODE:13-oxoODE ratio (B) and the milk 13-HODE:9-HODE ratio (C) was greater on the d of challenge and 3 d post-challenge in milk from cows that did not establish <i>S. uberis</i> mastitis compared to milk from cows that established mastitis. Values are means \pm SEM expressed in pg of oxylipid per μ L of milk or as a ratio of oxylipids. *Significance declared at <i>P</i>

Figure 5. Means of oxylipid concentrations in milk from cows that failed to establish *S. uberis* mastitis (n=3) are displayed in open bars and means of oxylipid concentrations in milk from cows that established *S. uberis* mastitis (n=3) are in closed bars. The concentration of milk 6-keto-PGF_{1 α} (A) and 11-HETE (B) was different on the d of challenge between dairy cows that

did not establish S. uberis mastitis compared to cows that established mastiti	s. Values	are means
± SEM expressed in pg of oxylipid per μL of milk. *Significance declared at	$t P \le 0.05$	513 <i>6</i>

Figure 6. A) The mRNA expression of pro-inflammatory COX-2 was not different after 4 h 13-HODE exposure. (10 and 50 μ M n=7 and 100 μ M n=4). B) The mRNA expression of pro-inflammatory COX-2 was significantly greater after 4 h exposure to 30 μ M 13-HPODE (n=5). The positive control was LPS and was significantly greater during both experiments (A, B). The mRNA expression is expressed as $2^{-\Delta\Delta Ct} \pm SE$. Significance declared for differences in ΔCt at $P \le 0.05$.

Figure 9. Mean changes in mRNA expression of bovine monocyte oxylipid biosynthetic enzymes (A, B), a marker of monocyte activation (C) and inflammatory cytokines (D, E). Media controls are displayed as open bars. Positive control is 4 hr LPS and displayed in closed bars. Light grey bars represent *S. uberis* supernatant exposure for 4 hr and 36 hr. Dark grey bars represent heat-killed *S. uberis* exposure for 4 hr and 36 hr. The mRNA expression is expressed as $2^{-\Delta\Delta Ct} \pm SE$. Asterisks (*) denote differences between media control and positive control (LPS) as tested by Student's t-tests. Letters that differ between control time points, 4 hr and 36 hr separately, denote significant differences between control and among treatments as measured by an ordinary one-way ANOVA with Tukey's post hoc correction. For example, 4 hr exposure to heat-killed *S. uberis* upregulated COX-2 mRNA expression compared to control but 4 hr exposure to *S. uberis* supernatant did not (Figure 3A). Additionally, COX-2 mRNA expression after *S. uberis* supernatant exposure (Figure 3A). A similar relationship can be described for 36 hr exposure of bovine monocytes to heat-killed and *S. uberis* supernatant. Significance declared for all tests using ΔCt at $P \le 0.05$ (n=4 for 15-LOX-1, IL-6, and IL-10; n=3 for COX-2 and iNOS)................141

Figure 10. Oxylipid biosynthesis following 4 hr LPS (black bars) or *S. uberis* exposure. Media controls are displayed as open bars. Light grey bars represent *S. uberis* supernatant exposure for 4 hr and 36 hr. Dark grey bars represent heat-killed *S. uberis* exposure for 4 hr and 36 hr. Oxylipid biosynthesis is expressed as ng of oxylipid/mL of media. Oxylipid biosynthesis is expressed as ng of oxylipid/mL of media. Asterisks (*) denote differences between media control and positive control (LPS) as tested by Student's t-tests. Letters that differ between control time

points, 4 hr and 36 hr separately, denote significant differences between control and among treatments as measured by an ordinary one-way ANOVA with Tukey's post hoc correction. For example, 4 hr exposure to <i>S. uberis</i> supernatant or heat-killed <i>S. uberis</i> did not modify 13-HODE biosynthesis, whereas 36 hr exposure to heat-killed <i>S. uberis</i> did increase 13-HODE biosynthesis. No letters are displayed in Figure 4B as no differences were detected in any time points. Significance for differences declared at $P \le 0.05$ (n=4).
Figure 11. Mean normalized resistance across time during media control ($\stackrel{\bullet}{\bullet}$) and 150 μM 13-
HPODE (•) is displayed in Figure 5A. Mean normalized resistance for 100 μM 13-HODE (
) exposure up to 6 hr is displayed in Figure 5B. Mean normalized resistance across time
during media control ($\stackrel{\bullet}{\bullet}$) and 25 ng/mL LPS ($\stackrel{\bullet}{\bullet}$) is displayed in Figure 5C. Resistance for each group is normalized to prior to treatment addition. Significance declared for differences between media control and 13-HPODE at specific time points by Mann-Whitney tests ($P \le 0.05$).
Figure 12. YOPRO®-1 and propidium iodide staining displayed as fold change over media control after 6 hr (Figure 6A & B) and 24 hr (Figure 6C & D) 13-HPODE exposure. Media controls are displayed in open bars and 13-HPODE treatments are in light grey bars. Positive control (1 hr 2mM H_2O_2 exposure) YOPRO®-1 and propidium iodide staining is displayed in Figure 6A & B and are the black bars. Different letters demonstrate a significant difference among media control and 13-HPODE treatments determined by one-way ANOVA with Tukey's post hoc correction. An asterisk (*) represents a significant difference between medial control and H_2O_2 as determined by Student's t-tests. Significance declared at $P \le 0.05$
Figure 13. Mean change in caspase $3/7$ activity displayed as fold change over media control (open bar) after 6 hr 13-HPODE (light grey bars) or 1 mM H_2O_2 exposure for 6 hr (black bar, positive control). Different letters demonstrate a significant difference among media control and 13-HPODE treatments determined by one-way ANOVA with Tukey's post hoc correction. An asterisk (*) represents a significant difference between medial control and H_2O_2 as determined by Student's t-tests. Significance declared at $P \le 0.05$
Figure 14. YOPRO-1 and propidium iodide staining displayed as fold change over media control (open bar) after 6 hr 150 μ M 13-HPODE (light grey bars) or 6 hr co-exposure with 150 μ M 13-HPODE or N-acetylcysteine (NAC, light grey bars). Different letters demonstrate a significant difference among media control and treatments as determined by a one-way ANOVA with Tukey's post hoc correction. Significance declared at $P \le 0.05$
Figure 15. Mean normalized resistance across time during media control (→), 150 μM 13-
HPODE ($\ \ \ \ \ \ \ \ \ \ \ \ \ \ \ \ \ \ $

Figure 16. Mean amount (ng) of PUFA and SFA normalized to DNA (ng) following supplementation of the ethanol carrier (CON), LA at 45 g/d, and ALA at 45 g/d. Figures 1A-E depicts quantified PUFA (LA, ALA, ArA, EPA, and DHA). Figures 1F-G depicts quantified SFA (palmitic acid, oleic acid, and stearic acid). Letters in Figure 1B represent significant differences across treatments groups as determined by a non-parametric one-way ANOVA with Dunn's correction ($P \le 0.05$).
Figure 17. Normalized average sum of n-6 FA, n-6 FA, ratio of n-6/n-3, and ratio of LA/ALA following supplementation of the ethanol carrier (CON), LA at 45 g/d, and ALA at 45 g/d. Figure 2A represents the normalized sum of n-6 PUFA (LA and ArA). Figure 2B represents the normalized sum of n-3 PUFA (ALA, EPA, and DHA). Figure 2C represents the ratio of total n-6 to n-3 (n-6/n-3). Figure 2D represents the ratio of LA to ALA (LA/ALA). Letters in Figure 2C & D represent significant differences across treatments groups as determined by an non-parametric one-way ANOVA with Dunn's correction ($P \le 0.05$). 1 CON vs. ALA, $P = 0.0895$
Figure 18. Summary of proposed mechanisms for 13-HPODE-induced apoptosis. (1) 13-hydroperxyoctadecadienoic acid (13-HPODE) may promote lipid peroxidation of endothelial membranes and contribute to increased lipid peroxyl radicals capable of propagating lipid peroxidation in the mitochondrial membrane. An inability to reduce pro-oxidant contributes to sustained increase in the permeability of the mitochondrial membrane and likely results in activation of intrinsic pathway of apoptosis. (2) 4-hydroxynonenal (4-HNE) may be formed as an end product of lipid peroxidation or from 13-HPODE cleaved from the membrane. Increased 4-HNE may activate cytoplasmic p53, which can promote transcription and translation of proteins that promote apoptosis. Conversely, 4-HNE is diffusible and can interact with the Fas death ligand to contribute to activate of the extrinsic apoptosis pathway through either caspase 8
activation or apoptosis signal-regulating kinase 1 (ASK-1).

CHAPTER 1 ROLE OF ENDOTHELIAL CELLS IN BOVINE MAMMARY GLAND HEALTH AND DISEASE

Valerie E. Ryman¹, Nanda Packiriswamy¹, and Lorraine M. Sordillo^{1*}

¹ College of Veterinary Medicine, Michigan State University, East Lansing, MI 48824, USA

*Corresponding author

Dr. Lorraine M. Sordillo,
Department of Large Animal Clinical Sciences
College of Veterinary Medicine
Michigan State University
sordillo@msu.edu
Tel: (517) 432-8821

Fax: (517) 432-8822

Published in Anim Health Res Rev, 2015, 16(2), 135-49. Copyright form located in appendix.

Abstract

The bovine mammary gland is a dynamic and complex organ composed of various cell types that work together for the purpose of milk synthesis and secretion. A layer of endothelial cells establishes the blood-milk barrier, which exists to facilitate the exchange of solutes and macromolecules necessary for optimal milk production. During bacterial challenge, however, endothelial cells divert some of their lactation function to protect the underlying tissue from damage by initiating inflammation. At the onset of inflammation, endothelial cells tightly regulate the movement of plasma components and leukocytes into affected tissue. Unfortunately, endothelial dysfunction as a result of exacerbated or sustained inflammation can negatively affect both barrier integrity and the health of surrounding extravascular tissue. The objective of this review is to highlight the role of endothelial cells in supporting milk production and regulating optimal inflammatory responses. The consequences of endothelial dysfunction and sustained inflammation on milk synthesis and secretion are discussed. Given the important role of endothelial cells in orchestrating the inflammatory response, a better understanding of endothelial function during mastitis may support development of targeted therapies to protect bovine mammary tissue and mammary endothelium.

Keywords: Endothelial cells, inflammation, mammary gland, mastitis

Introduction

The mammary gland is a specialized organ in female mammals that evolved for the purpose of milk synthesis and secretion to feed offspring. Due to advancements in genetic selection, however, the lactating dairy cow produces milk volumes that far exceed the neonate's nutritional requirement. As an example, the bovine neonate consumes approximately 25 pounds of milk at 30 days of age if allowed *ad libitum* consumption, whereas the average commercial dairy cow produces on average 4 times more milk (Jasper and Weary, 2002). In addition to the remarkable milk volume synthesized by the mammary gland, milk is also rich in nutrients including protein, carbohydrates, fats, minerals, and vitamins (Haug et al., 2007). The ability of the mammary gland to synthesize and secrete milk requires a structure that is as unique as its function. In particular, the vascular endothelium is fundamental for the mammary gland to grow and develop and to initiate and sustain milk production. A thin, single layer of mammary capillary endothelial cells forms a semipermeable barrier that facilitates the exchange of serum components to provide oxygen, remove carbon dioxide, and transfer solutes and macromolecules for cellular energy and metabolism (Andres and Djonov, 2010, Prosser et al., 1996). Endothelial cells also support the robust synthesis and secretion of milk by facilitating a high rate of transfer of blood-derived components including amino acids and glucose that are necessary for milk production (Mattmiller et al., 2011, Aleman et al., 2009). To maintain adequate delivery of milk components and substrates, endothelial cells directly orchestrate vascular tone, blood fluidity, and vascular permeability to support both the vasculature and underlying milk-producing tissue (Prosser et al., 1996).

In addition to supporting lactation physiology, the endothelium also plays a direct role in orchestrating host defense to infectious bacterial pathogens. The mammary gland is exposed to outside environment through the teat canal. If bacteria are able to penetrate the teat end barrier, then the efficiency of mammary gland inflammatory responses will determine if mastitis manifests. Vascular endothelial cells play a central role in the facilitating movement of soluble and cellular host defense mechanisms into mammary tissues during the initial stages of bacterial invasion. An efficient inflammatory response will recognize and eliminate invading bacteria promptly without causing any discernable changes to mammary tissues (Aitken et al., 2011a). When the initial inflammatory response fails to prevent the establishment of bacterial infection, however, clinical and/or chronic mastitis will cause impaired milk yield and quality. Indeed, mastitis costs the United States dairy industry an estimated 2 billion dollars a year due to reduced milk production, discarded milk following antibiotic treatment, veterinary costs, and replacement animal costs (National Mastitis Council, 2004). Inadequate inflammatory responses can be attributed to deficiencies in normal endothelial cell functions. Endothelial dysfunction is characterized as facilitating the unregulated accumulation of leukocytes at the site of infection, enhanced leakage of plasma proteins into mammary tissues, and disruption in blood flow that contributes to mammary tissue damage and loss of function (Knepler et al., 2001, Scalia and Lefer, 1998, Cassuto et al., 2014). Thus, optimal endothelial cell functions are needed to tightly regulate inflammatory responses and prevent immunopathology during bacterial invasion.

Because endothelial cells play a central role in mammary gland health, knowledge of the delineating factors between a successful self-limiting inflammatory response and immunopathology is critical. The review will cover three major topics that discuss how and why:

1) endothelial cells are necessary for the growth and development of the unique mammary gland,
2) endothelial cells modify their phenotype to orchestrate the initiation and resolution of
inflammation, and 3) endothelial dysfunction contributes to immunopathology and subsequent
tissue damage. A better understanding of the biological mechanisms regulating endothelial cell
function is essential for optimizing mammary gland health and increasing the efficiency of milk
production in dairy cattle.

Endothelial cells contribute to the specialized structure of the mammary gland Mammary gland growth and development

Mammogenesis, the first stage of mammary gland development, culminates in the formation of a complex epithelial and endothelial network. Previous studies show that a disruption in the normal progression of murine mammogenesis hinders the ability of the mammary gland to adequately secrete milk (Rossiter et al., 2007). Mammogenesis begins during embryogenesis and continues following the birth of the succeeding neonate, at which time it overlaps with the onset of lactation. Studies on mammogenesis were conducted in rat and mice, and from those studies the development of the bovine mammary endothelium can be inferred (Abdul Awal et al., 1996, Matsumoto et al., 1992, Rossiter et al., 2007, Yasugi et al., 1989). The mammary endothelium is composed of a thin layer of simple squamous endothelial cells, and along with myoepithelial cells and connective tissue, forms a complex vascular network known as the mammary vasculature. A unique feature of the mammary gland vasculature is the basket-like capillary beds surrounding bronchi-like alveoli clusters as demonstrated in murine models (Yasugi et al., 1989). Capillary beds surrounding alveoli maximize the surface area for exchange of oxygen and nutrients. To further facilitate exchange, but also maintain a selective barrier, the endothelial

surface is largely continuous with some minor areas of fenestration. A continuous endothelium is an uninterrupted layer of cells that restricts the free movement of large solutes and proteins, but allows for exchange of water and other very small molecules (Michel and Curry, 1999, Clough, 1991, Levick and Smaje, 1987). Fenestrations are small pores in endothelial cells that permit passage of small molecules and proteins. Development of the murine and human mammary endothelium establishes a semipermeable barrier that is primarily continuous with some areas of fenestration, which suggests the bovine mammary gland maintains a similar structure (Matsumoto et al., 1992, Stirling and Chandler, 1976). To further facilitate nutrient transfer for optimal mammary growth, mammogenesis is characterized by an increase in cell number and surface area to provide a maximal interface for nutrient transfer and milk secretion. In murine models, the increase in surface area of the luminal endothelium occurs early in pregnancy by the formation of microvilli and marginal folds on individual endothelial cells (Matsumoto et al., 1992). Evidence of increased endothelial surface area by the formation of microvilli and marginal folds, minor areas of fenestrations, and basket-like capillary beds surrounding alveoli suggest that optimal mammary function is unequivocally dependent on mammary structure.

Onset of milk synthesis and secretion

Lactogenesis is the acquisition of functional properties enabling the mammary gland to synthesize and secrete large volumes of milk. While much of the research regarding lactogenesis focuses on the differentiation of epithelial cells, endothelial cells also experience structural and functional changes in an effort to support initial and sustained milk production. For example, the number of mitochondria increases in rat mammary endothelial cells, conceivably for the increased energy required for maintaining blood flow, vascular tone, and regulating transport of

components needed for milk synthesis (Abdul Awal et al., 1996). Pinocytotic vesicles also increase in rat endothelial cells to support efficient transportation of plasma solutes and molecules, such as glucose (Abdul Awal et al., 1996). Recent research demonstrates that several glucose transporter molecules (GLUT) are expressed in the bovine mammary gland including GLUT1, GLUT3, GLUT4, GLUT5, GLUT8, and GLUT12, named according to their order of discovery. In the bovine mammary gland, the mRNA expression of GLUT1, GLUT8, and GLUT12 increased substantially from late in gestation to early lactation (Zhao and Keating, 2007). Similarly, the mRNA and protein expression of glucose GLUT1 was significantly increased in mammary tissue from early lactation cows compared to non-lactating cows (Komatsu et al., 2005). Mammary tissue from early-lactation dairy cows exhibited increased GLUT1, which was localized to endothelial cells and epithelial cells, compared to 15 days prior to the onset of lactation (Mattmiller et al., 2011). Though the mechanisms that stimulate increased expression of GLUT1 during late pregnancy and early lactation are unclear, previous research demonstrates that hypoxia in the mammary gland elicits a hypoxia inducible factor-α dependent mechanism that results in GLUT1 upregulation (Shao et al., 2014). In contrast, the regulation of GLUT4 expression is not clear. Some research suggests GLUT4 increases during late lactation in bovine mammary tissue, whereas others suggest that GLUT4 is not expressed in mammary tissue (Komatsu et al., 2005, Mattmiller et al., 2011). However, the expression of glucose transporters, GLUT1 and GLUT4, by primary bovine mammary endothelial cell (BMEC) was confirmed in an *in vitro* study (Mattmiller et al., 2011). Since glucose transport is a rate-limiting step in optimal lactation, more investigation into the role of GLUT in mammary endothelial is necessary. Nonetheless, the localization of glucose transporters to the endothelium and increased mRNA expression in BMEC from lactating cows suggests endothelial cells play an active role in metabolism and nutrient transfer during lactation.

In conjunction with increased transport molecules, murine models demonstrated increased capillary permeability during early lactation, which would support enhanced transfer of fluids and molecules for milk synthesis (Matsumoto et al., 1994). To further support nutrient transfer, capillaries with thinner walls were in closer contact with the alveoli during late pregnancy and early lactation compared to late lactation (Matsumoto et al., 1992). Perhaps most telling about the importance of the mammary vasculature in rats is that the development of the vasculature, measured as number of capillaries per individual lobular ductule, surpassed alveolar lobular ductule development during lactation (Ramirez et al., 2012). Though additional research is still required in dairy cattle, research in other species support the notion that changes in both structure and optimal function of the bovine vasculature during lactogenesis directly affect the ability of epithelial cells to synthesize milk components.

Mammary gland involution

To support maximal milk production in the next lactation, a period of involution is needed for regeneration of bovine mammary tissues (Holst et al., 1987). Dairy cows milked continuously until calving produced approximately 75% less milk compared to the twin given a 60-day non-milking period prior to calving (Swanson, 1965). Involution across species involves a regression in lobulo-alveoli complexity, decreased cell number, and a loss of milk-synthesizing function (Djonov et al., 2001, Holst et al., 1987, Tatarczuch et al., 1997, Walker et al., 1989). Involution in murine, goat, and dairy cow mammary glands suggests epithelial cells experience apoptosis at

a very high rate following cessation of milking (Wilde et al., 1997). However, other bovine studies demonstrate very little epithelial cell loss during involution even though alveolar lumen area decreases (Holst et al., 1987). Nonetheless, previous research in lactating goats suggests that induction of epithelial cell apoptosis may be initiated by accumulation of milk in the mammary gland (Quarrie et al., 1994). Whether regression of the bovine vasculature occurs during involution is not clear, although changes in the endothelium during murine and sheep involution may be used to infer changes in the bovine. In the involuting mouse mammary gland, capillary density decreases to a density similar to early pregnancy (Pepper et al., 2000). Studies in sheep suggest that a decrease in mammary capillary density may be a result of endothelial apoptosis. During involution of the ovine mammary gland, apoptosis of endothelial cells was observed in addition to the presence of apoptotic bodies found within the cytoplasm of healthy endothelial cells (Tatarczuch et al., 1997). Interestingly, murine models of involution featured endothelial cell apoptosis that was preceded by epithelial cell apoptosis (Djonov et al., 2001). The timing of endothelial cell apoptosis relative to epithelial apoptosis suggests the endothelial cells may be adapting to or dying from an altered microenvironment. However, the major temporal differences between epithelial and endothelial regression during sheep and rat mammary gland involution was not demonstrated, thus more research is required to understand these processes (Tatarczuch et al., 1997, Walker et al., 1989). Degradation of the proteins in the basement membrane also occurs during involution and matrix metalloproteinases (MMP) are largely responsible for this event. Data demonstrate that MMP1 and MMP14 are increased in epithelial cells during late involution, whereas MMP-2 was only localized to mammary endothelial cells and only during involution (Rabot et al., 2007). In a human umbilical vein endothelial cell (HUVEC) model, withdrawal of growth factor to induce apoptosis resulted in increased MMP-2

expression in apoptotic endothelial cells (Levkau et al., 2002). Activation of MMP-2 in HUVEC enables association of MMP-2 with receptors for fibronectin and vitronectin, both glycoproteins responsible for the formation of the extracellular matrix and cell adhesion, suggesting apoptosis of endothelial cells during mammary gland involution may be integrin-mediated (Levkau et al., 2002). Apoptosis may not be solely responsible for decreased vascular networks in the murine mammary gland where capillary regression was noted in the absence of apoptotic endothelial cells (Djonov et al., 2001). The conflicting research in rodent models and the limited amount of research in involuting bovine mammary glands suggests that more research is needed to better understand the role of endothelial cells in the remodeling process.

Endothelial cells prevent mastitis by orchestrating inflammation

The inflammatory response is a complex, tightly regulated series of events to protect the normal milk-synthesizing function of the bovine mammary gland from mastitis-causing organisms.

Endothelial cells regulate a wide variety of homeostatic mechanisms including maintenance of proper vascular tone, regulation of vascular permeability, modulation of blood fluidity, and regulation of immune responses for protection of the mammary gland during pathogen exposure (Aitken et al., 2011a, Prosser et al., 1996). Exposure of microbes and microbial components initially triggers a response from epithelial cells and resident macrophages to produce and release a variety of inflammatory mediators including cytokines and oxylipids (Table 1). The inflammatory mediators initially recruit phagocytic immune cells and robustly activate endothelial cells. Human and murine models indicate vasodilation of capillaries and increased vascular permeability are necessary for the influx of neutrophils to contain pathogens and limit extravascular tissue damage (van Nieuw Amerongen and van Hinsbergh, 2002, Bazzoni and

Dejana, 2004). Endothelial cells also promote active resolution of inflammation to protect the integrity of the vasculature and interstitial tissue (Kadl and Leitinger, 2005). During mastitis, however, the inflammatory response can either be inefficient, excessive, or prolonged resulting in severe tissue and vascular damage. Thus, it is necessary to differentiate between a normal inflammatory response (self-limiting) and immunopathology (mastitis). The following sections will discuss the change in endothelial cell phenotype needed to orchestrate an efficient inflammatory response.

Endothelial cells modulate changes in vascular tone and blood flow during inflammation A change in blood flow and vascular tone, characterized by the degree of constriction relative to dilation, is among the initial responses of the vasculature during pathogen exposure (Kobayashi et al., 2013, Lacasse et al., 1996, Prosser et al., 1996). Myoepithelial cells and endothelial cells work synergistically to either constrict or relax in response to signals primarily produced by endothelial cells (Prosser et al., 1996). Endothelial cells produce a variety of vasoactive mediators, such as nitric oxide (NO), prostacyclin (PGI₂), endothelin-1, and histamine, that function in an autocrine, juxtacrine, and paracrine manner to regulate myoepithelial contraction or relaxation. The most well studied endothelial-derived regulators of vascular tone during homeostasis are NO and PGI₂ in lactating goats, though less is known in the bovine (Nishida et al., 1992, Lacasse et al., 1996, Nielsen et al., 1995). At the onset of inflammation, eNOS is activated as a result of increased intracellular calcium. Activation of eNOS metabolizes arginine to citrulline and NO. Subsequently, NO activates guanylyl cyclase to produce cGMP, which inhibits calcium influx into the endothelial cell allowing relaxation of the actin cytoskeleton (Busse and Mulsch, 1990). In lactating goats, infusion of the mammary external pudendal artery with an eNOS inhibitor significantly reduces mammary blood flow (Lacasse et al., 1996). Mice deficient in eNOS fail to exhibit an early change in the vasculature and the later phase is markedly reduced, suggesting without eNOS activation the inflammatory response cannot be efficiently mounted or proceed normally (Bucci et al., 2005).

Similar to eNOS activation and NO biosynthesis, constitutive cyclooxygenase-1 (COX-1) is activated by an increase in intracellular calcium to facilitate the synthesis of PGI₂, an oxylipid. An oxylipid is an oxidized fatty acid and may be synthesized enzymatically or nonenzymatically from many different fatty acids, such as arachidonic acid and linoleic acid. Increased calcium also activates cytosolic phospholipase A₂, which cleaves fatty acids from membrane phosphatidylcholine to generate a free fatty acid and lysophosphatidylcholine moiety (Lombardo et al., 1986). During early inflammation, COX-1 oxidizes arachidonic acid to prostaglandin G₂ (PGG₂), which is quickly reduced to PGH₂ by intrinsic peroxidase activity of COX-1 (Fitzpatrick and Soberman, 2001). Next, PGH₂ is converted to PGI₂ by PGI₂ synthase. Activation of the PGI₂ receptor, a G-protein coupled receptor (GPCR), causes an increase in adenylyl cyclase-dependent cAMP and subsequent vasodilation as a result of protein kinase A activation (Murata et al., 1997). Furthermore, sustained PGI₂ is dependent on COX-2 and also is activated by increased calcium, but its optimal expression and activity requires transcript and translation induced by pro-inflammatory mediators. Increased expression of COX-2 would aide in sustaining vasodilation during the progression of inflammation. In lactating goats, infusion of the external pudendal artery with PGI₂ increased blood flow in the mammary gland, whereas infusion with a PGI₂ synthase inhibitor significantly decreased mammary blood flow suggesting the endothelium is sensitive to changes in NO and can alter mammary blood flow (Lacasse et al., 1996, Nielsen et al., 1995). A change in mammary blood flow following PGI₂ and NO exposure suggests that the vasculature in the bovine mammary gland is sensitive to potent vasodilatory mediators. By modulating vascular tone, endothelial cells strive to provide an optimal endothelial surface to facilitate rolling, attachment, and migration of leukocytes to control infection and inflammation.

Though vasodilation is critical to the progression of an appropriate immune response, vasoconstriction during the very early stages of infection and inflammation is protective in the event of mechanical injury and bleeding. Because vasoconstriction limits blood flow, and therefore may compromise the health of the mammary tissue, the release of vasoconstrictors is short-lived and balanced by the sustained release of vasodilators (Prosser et al., 1996). Two vasoconstrictors that are rapidly synthesized at the onset of inflammation are platelet-activating factor (PAF) and thromboxane A₂ (TXA₂). Lysophosphatidylcholine, a lipid moiety generated following the cleavage of arachidonic acid from phosphatidylcholine, acts as a precursor for the production of PAF (Lombardo et al., 1986). Early production of PAF in BMEC and bovine aortic endothelial cells (BAEC) was confirmed following LPS exposure (Corl et al., 2008, Corl et al., 2010). In murine pulmonary artery endothelial cells, PAF also induced increased production of NO suggesting the presence of a negative feedback loop to prevent sustained vasoconstriction (Predescu et al., 2013). Another well-known vasoconstrictor produced during inflammation is TXA₂, an unstable oxylipid that is degraded to TXB₂. The biosynthesis of TXA₂ is similar to PGI₂ except that thromboxane synthase converts PGH₂ to TXA₂. Interestingly, BAEC stimulated with a TXA₂ mimetic induced the synthesis of the PGI₂, further supporting a negative feedback loop established by the production of vasoconstrictors (Clesham et al., 1992). In fact, the balance

of TXA₂ and PGI₂ may be more important than absolute concentrations in modulating vascular tone. The production of vasoconstrictors, which also contributes to vasodilator release, suggests that modulation of vascular tone during the initial inflammatory response is tightly regulated to prevent unnecessary damage to blood vessels and interstitial tissue.

In conjunction with changes in vascular tone, reduced blood fluidity also is required during the inflammatory response. During early inflammation, endothelial cells initiate and propagate coagulation by increasing procoagulant properties and decreasing anticoagulants. In BAEC and HUVEC models, thrombus formation is initiated by up regulation of tissue factor expression in response to bacterial toxins and cytokines (Crossman et al., 1990, Nawroth and Stern, 1986, Fei et al., 1993). The coagulation cascade, initiated by the binding of tissue factor to factor VIIa, acts on factor X to form Factor Xa, which in turn complexes with prothrombin, Factor Va, and calcium to produce thrombin (Rao and Rapaport, 1987, Nawroth and Stern, 1986). Thrombin then converts fibringen to fibrin resulting in the formation of a fibrin clot, thus slowing blood flow at the site of coagulation. Much of the research on the modulation of coagulation in bovine endothelial cells is focused on the effect of cytokines. In BAEC, tumor necrosis factor- α (TNF- α) exposure decreases the expression of thrombomodulin, a major regulatory mechanism of coagulation that prevents the formation of thrombin by generating active protein C (Nawroth and Stern, 1986). Further supporting the effect of pro-inflammatory cytokines on BAEC, TNF-α dose-dependently decreased activated protein C, an antioxidant serine protease that inactivates Factor Va and VIIIa (Conway and Rosenberg, 1988). Antithrombin, another anticoagulant factor, binds to heparin-like glycosaminoglycans on the endothelial luminal surface to prevent serine protease activity (Olson et al., 2010). However, research suggests pro-inflammatory cytokines,

reduce the expression of heparin sulfate, the major target for antithrombin, by about 50% in porcine aortic endothelial cells (Kobayashi et al., 1990). Furthermore, thrombin increased cytokine-induced leukocyte migration across a HUVEC monolayer and in an *in vivo* rabbit dermal inflammation model, supporting the idea that the coagulation cascade is critical for inflammation (Drake et al., 1992). The purpose of coagulation is to reduce blood fluidity to prevent the systemic spread of bacteria and toxins, as well as, enhance leukocyte contact with the endothelial cells to facilitate leukocyte migration.

Vascular permeability is altered during inflammation

Endothelial cells mediate the type and quantity of solutes and leukocytes that move back and forth between tissue and blood using selective cellular junctions (Bazzoni and Dejana, 2004). Perturbation of the endothelium alters endothelial junctions and permeability leading to leakage of plasma proteins and leukocytes. Several endothelial junction proteins can control vascular permeability by regulating cell to cell contact and thus forming a highly selective barrier (Blum et al., 1997, Jiang et al., 1998). The series of events modulating bovine mammary vascular permeability during inflammation is unknown, but previous studies suggest inflammatory mediators and toxins produced during a normal inflammatory response directly alter endothelial junctions (Bannerman et al., 1998, Zhang et al., 2013). Studies using HUVEC models demonstrate that endothelial tight junctions are loosened by GPCR activation in response to various extracellular mediators, including fatty acids and cytokines (Blum et al., 1997, Jiang et al., 1998, Michel and Curry, 1999, Goeckeler and Wysolmerski, 1995). Tight junctions are composed of transmembrane proteins (e.g., claudins and occludins) and cytosolic proteins (zona occludins), which bridge to cytoskeleton actin filaments. Similarly, in a HUVEC model of

inflammation LPS decreased endothelial tight junction proteins concomitant with increased monolayer permeability (Zhang et al., 2013). Claudin-5 (a tight junction protein) deficient mice exhibited a leaky blood-brain barrier with larger molecules able to move across this extremely restrictive barrier (Nitta et al., 2003). Unrestricted movement of macromolecules may contribute to destruction of extravascular tissue and allow systemic infection. Tight junctions are not the only cell connections altered during inflammation. Exposure of bovine pulmonary artery endothelial cells to LPS destabilized endothelial adherens junctions by cleaving β -catenin, thereby disrupting the anchor to the cell cytoskeleton (Bannerman et al., 1998). Additionally, blocking VE-cadherin binding in HUVEC increased permeability to solutes and leukocytes suggesting any modulation in endothelial junction expression may severely alter the course of inflammation (Hordijk et al., 1999). Thus, without proper organization and function of tight junctions and adherens junctions in the mammary endothelium, exchange of solutes and cells is dysregulated and may contribute to tissue damage due to accumulation of plasma components. However, some rearrangement or modulation of endothelial junctions must occur to facilitate effective clearance of mastitis-causing pathogens by phagocytic immune cells.

In dairy cows, most research on barrier permeability is focused on epithelial cells without considering the important contributions of endothelial cells. Early studies suggested that an increase in sodium and chloride in milk from cows with mastitis was indicative of epithelial barrier disruption (Linzell and Peaker, 1972). However, researchers also appreciated the presence of serum albumin in milk as indicative of increased permeability at the blood-milk barrier (Kobayashi et al., 2013). Endothelial cells and associated endothelial junctions directly contribute to changes in milk components, such as albumin. Albumin is one of the most

important proteins that regulate oncotic pressure and disruption of oncotic pressure typically causes edema in interstitial tissue (Rippe et al., 1979). Additionally, albumin can bind many different molecules and act as a chaperone across the endothelium (Spector, 1975). Thus, increased albumin in secretory products, i.e., milk, would indicate radical changes at the endothelium. A similar occurrence is demonstrated during early involution, when albumin concentration in milk increases (Breau and Oliver, 1985, Poutrel et al., 1983). The increase in serum albumin may be related to a minimal increase in vascular permeability to support passive immunoglobulin transfer during early involution. In contrast, the increased concentration of serum albumin in early involution may simply be an artifact of decreased milk production with no appreciable change yet in plasma protein transfer (Poutrel et al., 1983). Understanding how the endothelium regulates vascular permeability is necessary for discovering new and innovative therapies to prevent systemic infection, as well as add insight to the complex changes that occur during mammary regression.

Leukocyte movement increases across the mammary endothelium during inflammation

The movement of leukocytes into the infected tissue is critical to prevent the progression of mastitis. Leukocytes present in the blood stream are not innately adhesive, but do interact with the endothelium. Under basal conditions neutrophils roll along the vascular barrier and communicate through random and reversible interactions with neutrophil surface selectins. Neutrophil leukocyte-selectin (neutrophil associated; L-selectin) association with the murine endothelium allows contact, but not tethering, capture, or firm adhesion (Ley et al., 1995, Kaplanski et al., 1993). The purpose of neutrophil rolling is to survey the vasculature for cytokines, oxylipids, or reactive oxygen species (ROS) signaling microbial infection (Ley et al.,

1995). The production of ROS is increased during early inflammation due to increased adenosine triphosphate (ATP) production through the electron transport chain and as a result of respiratory burst by phagocytic cells (Aon et al., 2012, Parnham et al., 1987). At the initiation of inflammation, activation of GPCRs induces the release of pre-synthesized platelet-selectin (Pselectin) from specialized endothelial organelles called Weibel-Palade bodies as demonstrated in HUVEC (McEver et al., 1989). Binding of P-selectin to leukocyte-associated P-selectin glycoprotein ligand-1 forms a tight, but reversible, attachment between endothelial cells and leukocytes. In BMEC, the mRNA expression of P-selectin is increased following exposure to TNF-α and in P-selectin deficient mice, rolling of neutrophils on the endothelial surface and neutrophil migration are reduced, illustrating the vital role of initial P-selectin binding in leukocyte migration (Mayadas et al., 1993, Aitken et al., 2011b). Capture, but not firm adhesion, of neutrophils is complete with endothelial-selectin (E-selectin), but its transcription and expression requires gene transcription and translation. In both BMEC and HUVEC, increased temporal synthesis and expression of P-selectin and E-selectin is the result of various inflammatory mediators, including cytokines and ROS (Scholz et al., 1996, Maddox et al., 1999, Aitken et al., 2011b). Stimulation of BMEC with TNF-α induced an increase in E-selectin expression at 3 hours and 6 hours, whereas P-selectin expression was only significantly increased at 3 hours (Maddox et al., 1999). The time-dependent expression of adhesion molecules involved in tethering and capture during inflammation further supports the temporal, cooperative effort between P- and E-selectin that must exist in the bovine mammary gland. The contribution of endothelial cells to tethering and capture of neutrophils during inflammation is unequivocal and necessary for an appropriate, timely response.

Firm adhesion follows capture of leukocytes and is necessary for diapedesis of leukocytes into the inflamed tissue. Firm adhesion is achieved by neutrophil ligand binding to intercellular adhesion molecule-1 (ICAM-1), ICAM-2, and vascular cell adhesion molecule-1 (VCAM-1) (Sans et al., 1999). Macrophage-1 antigen binds to endothelial ICAM-1, whereas lymphocyte function associated antigen-1 preferentially binds ICAM-2. *In vivo* data during bovine mammary gland inflammation is limited regarding firm adhesion, but murine and human studies provide information about endothelial cells in orchestrating leukocyte adhesion and migration (Hafezi-Moghadam et al., 2007, Sans et al., 1999). Very late antigen-4 (VLA-4) is the ligand for VCAM-1, and when VLA-4 is blocked on rat leukocytes, adhesion to the endothelium is significantly reduced (Hafezi-Moghadam et al., 2007). In a rat model of colitis, blockade of ICAM-1 slightly reduced leukocyte adhesion, but blockade of VCAM-1 prevented all adhesion of leukocytes to colonic venules suggesting VCAM-1 may be the predominant molecule in firm adhesion (Sans et al., 1999). In bovine in vitro models, several studies demonstrated the ability to increase the expression of ICAM-1 and VCAM-1 following exposure to TNF-α and PAF (Sordillo et al., 2005, Corl et al., 2008). Additionally, a mixture of saturated and unsaturated fatty acids increased the expression of ICAM-1 in BAEC (Contreras et al., 2012a, Contreras et al., 2012b, Aitken et al., 2011b). In contrast, omega-3 fatty acids reduced ICAM-1 and VCAM-1 expression in cytokine-stimulated human endothelial cells (De Caterina et al., 1994). Furthermore, arachidonic acid-derived 15-hydroperoxyeicosatetraenoic acid (15-HPETE) and linoleic acidderived 13-hydroperoxyoctadecadienoic acid, both produced early in the inflammatory response, induced an increase in BAEC and HUVEC ICAM-1 expression at low doses (Sordillo et al., 2008, Friedrichs et al., 1999). Rapid biosynthesis of oxylipids supports robust and acute expression of endothelial adhesion molecules to expedite neutrophil migration into the infected

tissue. The sensitivity of the endothelium to fatty acids and oxylipids is important because it suggests that the inflammatory response may be modulated with only small changes in autocrine, juxtacrine, and paracrine mediators.

Though research focusing on the process of leukocyte migration is limited, there is no doubt that endothelial-leukocyte cooperation is necessary to successfully bring neutrophils to the site of infection. Platelet-endothelial cell adhesion molecule-1 (PECAM-1) is thought to be the primary molecule that mediates migration of leukocytes between across the endothelium through the formation of homodimers between endothelial cells and neutrophils (Schenkel et al., 2002). Though there was no change in BMEC PECAM-1 mRNA expression following TNF- α exposure, previous human studies showed that blocking neutrophil PECAM-1 or HUVEC prevents transmigration, suggesting without PECAM-1 binding an efficient inflammatory response would not occur (Muller et al., 1993, Aitken et al., 2011b). Moreover, expression of PECAM-1 was upregulated in an *in vivo* murine model following exposure to cytokines, such as IL-1β and TNF-α, (Thompson et al., 2001). Additionally, PECAM-1 receptors may rearrange and move to junctional complexes to support leukocyte migration. For example, TNF-α and IFNγ induced PECAM-1 redistribution on the HUVEC (Romer et al., 1995). Expression of PECAM-1 during bovine mammary inflammation is not well characterized and requires further exploration. However, based on other human and murine inflammatory models, it is appreciated that an optimal inflammatory response requires a coordinated effort between endothelial cells and surrounding cell types to facilitate neutrophil migration to the site of inflammation.

Resolution of inflammation is necessary to prevent vascular and mammary tissue damage

The process of active resolution is not completely understood, but current research suggests that there is a switch from a pro-inflammatory to an anti-inflammatory/pro-resolving cellular phenotype (Serhan et al., 2008a). A proper inflammatory response is self-limiting with the final phase being resolution. The sequence of events that lead to resolution of inflammation and tissue repair is not well defined due to the involvement of many different cells and pathways. Thus, the topics and order of discussion for the following endothelial mechanisms is based on their hierarchal importance in reducing leukocyte migration and promoting tissue repair.

Endothelial cells are sensitive to ROS and free radicals, collectively called pro-oxidants, and during inflammation there is increased pro-oxidant production surrounding and within endothelial cells (Zweier et al., 1994). Intracellular pro-oxidants are derived from the mitochondrial electron transport chain during ATP production and extracellular pro-oxidants are predominantly derived from nicotinamide adenine dinucleotide phosphate (NADPH) oxidase activity during phagocytic respiratory burst (Aon et al., 2012, Karlsson et al., 1995). The continued presence of pro-oxidants can contribute to the development of oxidative stress. Oxidative stress is an imbalance of antioxidant mechanisms and pro-oxidant molecules resulting in damage to cellular lipids, proteins, and DNA (Sordillo et al., 2009). To mediate resolution, antioxidants must be produced to counteract the damaging effects of pro-oxidants. The most well-studied enzymatic antioxidant defenses include glutathione peroxidase (GPx), superoxide dismutase (SOD), and thioredoxin reductase (TrxR) (Aon et al., 2012, Bowler et al., 2004). Superoxide dismutase either adds or removes an electron from O2⁻ to form O2 or H2O2, which will be catalyzed to oxidized glutathione and H2O by GPx (Bowler et al., 2004). The *in vivo*

action of TrxR, GPx, and SOD is unknown during self-limiting bovine mammary gland inflammation, but *in vitro* models in bovine, murine, and human endothelial cells provide an opportunity to discuss how the lack of antioxidants defenses promotes inflammation. The overexpression of GPx-1 protected BAEC-derived NO production in an endothelial injury model (Weiss et al., 2001). Conversely, deficiency of GPx-1 during TNF-α stimulation in human microvascular endothelial cells exacerbated the expression of VCAM-1 and ICAM-1 and subsequently enhanced ROS production (Lubos et al., 2011). Mice deficient in extracellular endothelial-derived SOD demonstrated significantly exaggerated lung inflammation characterized by robust and sustained pro-inflammatory cytokine production (Bowler et al., 2004). Importantly, neutrophil infiltration was persistent in SOD knockout mice, which was consistent with sustained endothelial adhesion molecule expression, suggesting clearance of pro-oxidants by endothelial cells is critical for decreased leukocyte migration and resolution of inflammation (Bowler et al., 2004).

While GPx and SOD directly reduce ROS and free oxygen radicals, TrxR reduces oxidized thioredoxin so that it may reduce other pro-oxidants (Trigona et al., 2006). Following low dose H₂O₂ exposure in HUVEC, thioredoxin mRNA and protein expression was significantly increased indicating its role in antioxidant defense (Haendeler et al., 2004). Interestingly, TrxR can also reduce GPx in human plasma after pro-oxidant quenching suggesting redundancy in antioxidant defense system (Bjornstedt et al., 1994). However, it is unknown whether this occurs in the bovine mammary gland or in the mammary endothelial cells. Overall these studies suggest that for a self-limiting inflammatory response to occur, adequate antioxidants and antioxidant enzymes must be available to counteract increased pro-oxidants during inflammation.

Another new and burgeoning area of research that involves active resolution of inflammation is the production of anti-inflammatory and pro-resolving lipid mediators. The major classes of antiinflammatory and pro-resolving oxylipids include resolvins (RV), protectins (PD), and lipoxins (LX), which are synthesized from fatty acids. The RV are synthesized from eicosapentaenoic acid (EPA) and docosahexaenoic acid (DHA) and PD are derived from DHA. Resolvins derived from EPA are enzymatically formed by the sequential oxidation of cytochrome P450 and 5-LOX, whereas DHA-derived RV (RvD) are generally derived by the sequential oxidation 15-LOX and 5-LOX, similar to AA-derived LX. On the other hand, PD is formed by 15-LOX oxidation and subsequent hydrolysis. There is not a great deal of *in vivo* bovine research available for review in this new area, however, research in in vitro bovine models demonstrate the anti-inflammatory effects of increased EPA and DHA on cellular phenotype and subsequent oxylipid production. For example, in BAEC increased omega-3 fatty acid content (DHA and EPA) reduced pro-inflammatory cytokine expression, adhesion molecule expression, ROS production, and pro-inflammatory oxylipid production (Contreras et al., 2012a). Also, the production of DHA-derived oxylipids including RvD and PD, and AA-derived LXA4 was increased in BAEC exposed to increased omega-3 fatty acids (Contreras et al., 2012a). In a HUVEC model of inflammation, RvD₁ prevented the reorganization of tight junction proteins and abrogated any changes in vascular permeability induced by LPS (Zhang et al., 2013). Similar to RV function, PD also has the ability to promote endothelial barrier function. In human microvascular endothelial cells, PD1 effectively prevented the LTB4-induced migration of neutrophils (Serhan et al., 2006). In addition, PD1 administration also was able to abrogate the inflammatory response after induction of murine peritonitis (Serhan et al., 2006). Thus, research

suggests that administration of omega-3 derived oxylipids may be beneficial in preventing immunopathogenesis, however the complexity of oxylipid biosynthesis necessitates further research in human and veterinary species.

Oxylipids derived from omega-6 fatty acids may also play a very important role in protecting the endothelial barrier. Arachidonic acid-derived LX are primarily synthesized with the cooperative effort of both 5-LOX and 15-LOX (Serhan et al., 2008b). Lipoxins inhibit chemotaxis and migration of neutrophils, reduce ROS production, and prevent activation of nuclear factor-κB (NF-κB) (Serhan et al., 2008a). In the context of endothelial barrier integrity, LXA4 prevents LPS- or PAF-induced increased vascular permeability suggesting LXA4 acts as an anti-inflammatory protector of the endothelium (Ereso et al., 2009). In addition, LXA4 induces IL-10 production in a HUVEC model while concomitantly inhibiting production of pro-inflammatory cytokines and vascular adhesion molecules (Baker et al., 2009). Consequently, active resolution is dependent on the contribution of potent anti-inflammatory oxylipids and given their ability to modulate many aspects of inflammation warrants continued research in human and veterinary species.

As oxylipids may directly modulate cytokine production to promote resolution, other negative feedback loops and checkpoints also exist to prevent sustained inflammation. Cytokine expression, as a result of NF-κB signaling, is a major pro-inflammatory pathway activated following the detection of bacterial pathogens (Nadjar et al., 2005). Thus, it makes sense that NF-κB signaling should be tightly regulated to prevent sustained activation. One such checkpoint is inhibition of NF-κB signaling pathway by inhibitor of κB (IκB). The inhibitor IκBα prevents

NF-κB binding, and thus prevents activation of pro-inflammatory gene expression. Though IκBα is degraded at the onset of inflammation, sustained activation of NF-kB initiates the expression of IκB, which acts as a negative feedback loop (de Martin et al., 1993). Additionally, IκBα may directly decrease the expression of IL-1, IL-6, IL-8, and VCAM in porcine aortic endothelial cells (Wrighton et al., 1996). Aside from pro-inflammatory cytokines, endothelial cells also produce anti-inflammatory cytokines including IL-10, IL-1 receptor agonist (IL-1ra), and transforming growth factor- β (TGF- β), which decrease the expression of pro-inflammatory cytokines and also promote tissue repair (Cromack et al., 1993). In HUVEC, exposure to TGF-β decreased both baseline E-selectin and TNF-α-stimulated E-selectin mRNA and protein expression by more than 50% (Gamble et al., 1993). Though the mechanism by which tissue repair is initiated remains unclear, TGF-β contributes substantially through activation of angiogenesis and induction of matrix component synthesis (Ferrari et al., 2009, Ignotz and Massague, 1986). Decreased expression of pro-inflammatory cytokines, in conjunction with increased anti-inflammatory cytokines and growth factors, is necessary for controlling chronic inflammatory and immunopathology.

Endothelial dysfunction as an underlying cause for immunopathology

Bovine mastitis results when there is not a self-limiting inflammatory response and may be a result of endothelial cell dysfunction. Endothelial dysfunction can contribute to an aberrant inflammatory response as a result of breakdown of tight junction proteins, loss of barrier integrity, increased attachment of leukocytes and platelets, and in the most severe cases, leading to sepsis and tissue hypoperfusion (Levi et al., 1997, Winn and Harlan, 2005, van Nieuw Amerongen and van Hinsbergh, 2002). Based on previous *in vitro* BMEC and BAEC studies, as

well as research in other species and disease models as a reference, it is possible to speculate how endothelial cell dysfunction can contribute to immunopathology during mastitis (Figure 1). The following sections discuss the impact of sustained inflammation and accumulation of prooxidants on endothelial function and survival.

Oxidative stress negatively affects antioxidant pathways and oxylipid biosynthesis

Oxidative stress contributes to immunopathology by modulating endothelial function. During inflammation, endothelial metabolism is increased to support a variety of mechanisms, including increased adhesion molecule expression, cytokine expression, and antioxidant pathways (Kadl and Leitinger, 2005). Functional roles of antioxidant systems may be decreased due to quenching by existing ROS and free radicals, down regulation of transcriptional expression, and inactivation of antioxidant enzymes (Blum and Fridovich, 1985). In BAEC, reduced TrxR activity during oxidative stress resulted in decreased heme oxygenase-1 (HO-1), an enzyme that catalyzes the degradation of ROS-inducing free heme (Trigona et al., 2006, Fortes et al., 2012). Decreased HO-1 would exacerbate oxidative stress and potentially result in endothelial cell death. In fact, pro-apoptotic markers were increased during oxidative stress in BAEC, a finding that was correlated to decreased HO-1 and TrxR (Trigona et al., 2006). *In vitro* BMEC models shed further light on how oxidative stress affects cellular function eventually leading to endothelial dysfunction. Endothelial cells (BMEC and BAEC) increased production of TXB₂ and PAF, and decreased production of PGI₂ during oxidative stress potentially compromising maintenance of vascular tone (Cao et al., 2000, Weaver et al., 2001). Additionally, changes in endothelial cell metabolism during oxidative stress resulted in the accumulation of bioactive oxylipids, such as 15-HPETE (Weaver et al., 2001). Arachidonic acid-derived 15-HPETE is a

lipid hydroperoxide derived by 15-LOX oxidation and can have similar effects on endothelial cell health as ROS. Such changes in oxylipid biosynthesis during oxidative stress can cause apoptosis of bovine endothelial cells, which may lead to disruption of the endothelial barrier (Sordillo et al., 2005). Our understanding of these mechanisms during bovine mastitis is less clear; however, *in vitro* reports support the contention that oxidative stress can compromise endothelial integrity.

Oxidative stress contributes to decreased nitric oxide

In human diseases, endothelial dysfunction is classically characterized as the reduced availability of NO resulting in altered vascular tone and blood flow. The availability of NO ensures that the mammary vasculature remains relaxed, as opposed to being in a state of vasoconstriction (Ohashi et al., 1998). Chemical inhibition of eNOS in HUVEC induces intracellular oxidative stress contributing to increased adhesion of neutrophils (Niu et al., 1994). During a dysfunctional inflammatory response, NO levels may be reduced dramatically as a result of several different mechanisms. First, reduced NO may be a function of eNOS uncoupling. Uncoupling of eNOS occurs when available O₂ is oxidized to form superoxides preventing its combination with Larginine to generate NO (Vasquez-Vivar et al., 1998). In addition to reduced NO synthesis, superoxide, generated during oxidative stress, is toxic to endothelial cells and other cells if not reduced by superoxide dismutase. Aside from superoxide production by eNOS uncoupling, activated neutrophils arrested at the endothelial barrier produce superoxide and other ROS/free radicals by the action of NADPH oxidase (Aon et al., 2012, Karlsson et al., 1995). The excess ROS further uncouples eNOS by oxidizing BH4, a cofactor for eNOS activity (Xia et al., 1998). Though eNOS activation or uncoupling during bovine mastitis is unknown, accumulation of

neutrophils at the endothelial interface was demonstrated during *Streptococcus uberis* mastitis along with destruction of the surrounding tissue (Thomas et al., 1994). Levels of NO also may be reduced by ROS consumption. Accumulation of activated neutrophils would allow for increased ROS production, such as superoxide, at the endothelial surface, which would be able to act on NO directly rather than affecting eNOS activity. Peroxynitrite, formed by the reaction of NO and superoxide, induced barrier dysfunction, endothelial protein oxidation, and cytoskeleton rearrangement in porcine pulmonary artery endothelial cells (Knepler et al., 2001). Thus, reduced NO through eNOS uncoupling or quenching by oxygen radicals prevents endothelial cells from maintaining proper vascular tone and perpetuates a dysfunctional endothelial phenotype.

Prolonged or excessive inflammation induces apoptosis of endothelial cells

The end result of persistent endothelial dysfunction is apoptosis, which may be activated through both intrinsic and extrinsic pathways. Apoptosis of endothelial cells would compromise the mammary endothelium thereby disrupting the semi-permeable endothelial barrier. The extrinsic pathway is initiated through receptor activation by death ligands, including TNF-α and LPS. Exposure of BMEC to TNF-α induced a pro-apoptotic response suggesting cytokines meant to activate endothelial cells to facilitate pathogen clearance may also damage the gatekeeper cells at the blood-milk barrier (Aitken et al., 2011b). Furthermore, apoptosis was documented during oxidative stress in a BAEC model supporting the intrinsic pathway of apoptosis (Sordillo et al., 2005, Trigona et al., 2006). The intrinsic pathway is activated by cellular DNA damage and/or accumulation of intracellular ROS, which causes mitochondrial damage triggering apoptosis. During bovine mastitis, ROS and free radicals accumulate at the endothelial barrier due to the activated nature of endothelial cells and activated neutrophils that are migrating or immobilized

at the barrier (Thomas et al., 1994). Previous HUVEC models demonstrate oxygen radicals activate protein kinase D and ASK-1/JNK activation, which activates the JNK/p38 MAPK apoptosis pathway (Zhang et al., 2005). Additionally, a HUVEC model demonstrated that apoptotic endothelial cells possess procoagulant and prothrombotic properties including increased platelet adhesion and decreased thrombomodulin, heparin sulfate, and tissue factor pathway inhibitor (Bombeli et al., 1997, 1999). Furthermore, caspase cleavage during apoptosis directly disrupts adherens junctions, allowing the transfer of plasma proteins and fluid in bovine pulmonary artery endothelial cells (Bannerman et al., 1998). During bovine mastitis, it seems likely that an inability to rectify the inflammatory response may be due to damaged and apoptotic endothelial cells. Unfortunately, it is unclear when the inflammatory response can be targeted to prevent destruction of the bovine mammary vascular endothelium and represents a substantial gap in our current knowledge.

Conclusions

Endothelial cells are no longer viewed as static barriers at the interface between blood and tissue. Endothelial cells regulate transfer of solutes and macromolecules, leukocyte migration, vascular tone, and blood flow during homeostasis and inflammation. The ability of a thin layer of endothelial cells to serve such a prominent role is directly related to their proximity to the circulation and to the underlying interstitial tissue. Specifically, capillaries encircling milk-producing alveoli in the bovine mammary gland offer increased surface area for the principle functions of lactation and immune surveillance. However, research is still limited outlining the role of endothelial cell in initiation and resolution of mammary inflammation. Through modulation of vascular tone and blood fluidity, vascular permeability, and endothelial

adhesiveness, the endothelium enables the progression of a self-limiting inflammatory response to support clearance of the pathogen and protect the milk-producing tissue. However, mediators that are important for progression of mastitis and clearance of pathogens may also be responsible for damage to alveoli in the mammary gland. In particular, oxidative stress is especially detrimental to endothelial function and survival. Thus, understanding how endothelial activation becomes endothelial dysfunction represents a point of potential therapeutic intervention, e.g, preventing or ameliorating oxidative stress. Future studies should focus on the mechanisms that initiate the switch from activation to resolution. Such research would be important to modify exacerbated and sustained inflammatory responses that contribute to inflammatory-based diseases such as boyine mastitis.

Acknowledgements

This work is supported by the National Institute of Food and Agriculture, U.S. Department of Agriculture, under Agreement No. 2015-67011-23012 and Agreement No. 2011-67015-30179.

CHAPTER 2 QUANTIFICATION OF BOVINE OXYLIPIDS DURING INTRAMAMMARY STREPTOCOCCUS UBERIS INFECTION

V.E. Ryman¹, G.M. Pighetti², J.D. Lippolis³, J.C. Gandy¹, C.M. Applegate¹, and L.M. Sordillo¹*

College of Veterinary Medicine, Michigan State University, East Lansing, MI 48824, USA
 Department of Animal Science, University of Tennessee, Knoxville, TN 37996, USA
 Periparturient Diseases of Cattle Research Unit, National Animal Disease Center, USDA-Agricultural Research Service, Ames, IA 50010, USA

*Corresponding author

Dr. Lorraine M. Sordillo,
Department of Large Animal Clinical Sciences
College of Veterinary Medicine
Michigan State University
sordillo@msu.edu
Tel: (517) 432-8821

Fax: (517) 432-8822

Published in Prostaglandins Other Lipid Mediat, 2015, 121(Part B), 207-17. Copyright form located in appendix.

Abstract

Streptococcus uberis mastitis results in severe mammary tissue damage in dairy cows due to uncontrolled inflammation. Oxylipids are potent lipid mediators that orchestrate pathogen-induced inflammatory responses, however, changes in oxylipid biosynthesis during S. uberis mastitis are unknown. Thus, the current objective was to determine how oxylipid concentrations change in milk and mammary tissues during different stages of S. uberis mastitis. Increased arachidonic acid and linoleic acid-derived oxylipids were significantly increased in S. uberis-infected bovine mammary tissue. Linoleic acid metabolites, hydroxyoctadecadienoic acid (HODE) and oxooctadecadienoic acid, predominated in tissue and milk. Furthermore, in vitro exposure of bovine mammary endothelial cells to 13-hydroperoxyoctadecadienoic acid, upstream metabolite of HODE, significantly increased cyclooxygenase-2 expression, but 13-HODE exposure had no effect. The findings in the current study indicate lipidomic profiling may explain some of the dynamics of inflammation during bacterial challenge, however continued research is necessary to determine sample compartments which best reflect disease pathogenesis.

Keywords: Oxylipids; inflammation; mastitis; eicosanoid; cyclooxygenase; lipoxygenase

Introduction

Mastitis, an inflammation of the mammary gland, negatively impacts the U.S. dairy industry by reducing milk yield and quality (Aitken et al., 2011). Whereas many pathogens cause bovine mastitis, Streptococcus uberis is a major pathogen of concern as it results in severe tissue damage and significant milk production losses related to an ineffective inflammatory response (Pedersen et al., 2003). Mastitis causes by S. uberis infections present as acute or subclinical, which may persist as chronic infections with associated inflammation (Phuektes et al., 2001). The major cause of S. uberis-induced pathology is the sustained migration of leukocytes into the secretory tissue resulting in irreversible damage. Histopathological data from S. uberis-infected mammary tissue indicate that colonization of S. uberis can survive aggressive neutrophil infiltration into mammary tissues and cause the development of chronic disease (Hill et al., 1994; Burvenich et al., 2004). The underlying mechanisms regulating the initiation and resolution of mammary gland inflammatory responses to S. uberis are unclear. Previous research in bovine mastitis suggests that the composition of oxylipid profiles within affected tissues may regulate the severity and duration of the localized inflammatory response. For example, the milk lipoxin A₄ (LXA₄) to leukotriene B₄ (LTB₄) ratio was lower in cows suffering from chronic mastitis compared to healthy cows (Boutet et al., 2003). Similarly, the concentration of arachidonic acid (AA)-derived oxylipids, such as prostaglandins and thromboxane, significantly increased during clinical mastitis (Giri et al., 1984; Atroshi et al., 1987). As such, the ability of the host to respond quickly and eliminate mastitis-causing pathogens may be directly influenced by the production of pro- and anti-inflammatory oxylipids (Atroshi et al., 1990; Boutet et al., 2003; Aitken et al., 2011a). Though previous research has quantified a limited number of oxylipids during clinical mastitis, it is now recognized that the lipidome is extensive and complex. Advancing the current

understanding of the bovine lipidome can be used to develop novel, targeted therapies to control tissue damage related to an unregulated inflammatory response, such as mastitis.

Predominant fatty acid substrates used for oxylipid biosynthesis in both humans and dairy cows are polyunsaturated fatty acids (PUFA), including AA and linoleic acid (LA) (Ramsden et al., 2012; Raphael et al., 2014). Fatty acid substrates are cleaved from the phospholipid membrane by phospholipase A₂, and may undergo non-enzymatic and enzymatic oxidation. Non-enzymatic pathways are primarily mediated by reactive oxygen species (ROS) and free radicals formed as end products of the electron transport chain and as byproducts of phagocyte-associated nicotinamide adenine dinucleotide phosphate (NADPH) oxidase (Morrow et al., 1990). In general, non-enzymatic oxidation of lipids occurs by a hydroxyl radical attack of hydrogen and subsequent O₂ interaction to form a lipid peroxyl radical, which can damage cell membranes and propagate lipid peroxidation (Micciche et al., 2005; Sordillo et al., 2005). Enzymatic pathways that predominantly catalyze oxylipid biosynthesis are cyclooxygenase (COX), lipoxygenase (LOX), and cytochrome (CYP). The COX and LOX enzymes oxidize PUFA by removing a hydrogen, allowing 2 O₂ to interact forming a lipid hydroperoxide (Hamberg and Samuelsson, 1967). Intrinsic peroxidase activity of COX enzymes reduces AA-derived PGG₂ to the hydroxyl, PGH₂ and subsequent enzymatic metabolism yields several different prostaglandins and thromboxanes (Hamberg and Samuelsson, 1967). Linoleic acid-derived hydroperoxides are reduced to hydroxyl oxylipids by antioxidant mechanisms, such as glutathione peroxidases or non-enzymatic quenching (Noguchi et al., 2002; Trigona et al., 2006; Suardiaz et al., 2013). Hydroxyl oxylipids can then be enzymatically dehydrogenated to ketones (Bergholte et al., 1987; Altmann et al., 2007). Oxidation of AA by LOX also synthesizes leukotrienes and lipoxins,

which require the coordination of multiple enzymes, i.e., LXA₄ biosynthesis requires 15-LOX, 5-LOX, and epoxide hydrolases (Serhan et al., 2008a). Lastly, CYP catalyzes a NADPH-dependent monooxygenation of AA and subsequent metabolism to form several oxylipids including 12-HETE, epoxyeicosatrienoic acids, and dihydroxyeicosatrienoic acids.

Given the breadth of oxylipid species and limited research in bovine models, it is difficult to pinpoint predominant pathways during bovine disease. Inflammatory-based disease models in humans suggest that oxylipid therapy may be used to control unregulated inflammation in veterinary species as well (Buckley et al., 2014). Determining how a targeted bovine lipidome changes during disease may be used to assess disease progression and severity. Previous research supports the predominance of LA as a substrate for oxidation, suggesting an abundance of LAderived oxylipids during health and disease (Ramsden et al., 2012; Raphael et al., 2014). The initial product of LA oxidation is hydroperoxyoctadecadienoic acid (HPODE) and the sequential metabolism of HPODE to hydroxyoctadecadienoic acid (HODE) to oxooctadecadienoic acid (oxoODE) synthesizes oxylipids that may have very different inflammatory functions. For example, 13-HPODE is associated with increased adhesion molecules and apoptosis, whereas 13-oxoODE is a potent ligand for an anti-inflammatory nuclear receptor (Altmann et al., 2007). Additionally, different isoforms of LA-derived metabolites are synthesized depending on the mode of oxidation. Oxidation of LA by 15-LOX-1 primarily yields 13-HPODE, whereas 9-HPODE is primarily produced during non-enzymatic oxidation (Oliw et al., 1996). However, HPODE is rapidly reduced to stable HODE, and thus, are measured during disease. For example, 9-HODE and 13-HODE are predominant in plasma from healthy individuals and may be increased during oxidative stress and inflammatory-based diseases, such as atherosclerosis

(Quehenberger et al., 2010; Ramsden et al., 2012). The purpose of this study was to document oxylipid changes in the milk and mammary tissue of dairy cows during different stages of *S. uberis* mastitis. The hypothesis was that LA metabolites, 9- and 13-HODE, are increased during *S. uberis* mastitis and contribute to an inflammatory phenotype in endothelial cells.

Materials and Methods

Chemicals and Reagents

HPLC-grade acetonitrile, HPLC-grade methanol, formic acid, sodium selenite, insulin, heparin, transferrin, ethylenediaminetetraacetic acid (EDTA), triphenylphosphine (TPP) were purchased from Sigma-Aldrich (St. Louis, MO). Diethyl ether and butylated hydroxy toluene (BHT) were purchased from ACROS Organics (Fair Lawn, NJ). Antibiotic/antimycotic and all bovine Taqman® primers were purchased from Thermo Fisher Scientific (Waltham, MA). Deuterated and nondeuterated standards were purchased from Cayman Chemical (Ann Arbor, MI). Indomethacin was from Cayman Chemical (Ann Arbor, MI). Magnesium sulfate was purchased from Avantor Performance Materials, Inc. (Central Valley, PA) and sodium borate from Fisher Science Education (Nazareth, PA). Fetal bovine serum was purchased from Hyclone Laboratories, Inc. (Logan, Utah).

Streptococcus uberis 0140J challenge for quantification of oxylipids in mammary tissue

The National Animal Disease Center animal care and use committee approved all animal-related procedures used in this study (Protocol ARS-2620). Five healthy, mid-lactation Holstein dairy cows were infused with an average of approximately 600 CFU of *S. uberis*, strain 0140J into 1 mammary gland. The dose of *S. uberis* was based on previous preliminary experiment with this

strain, which gave a reproducible infection rate of >95%. The mammary gland was cleaned with water to remove all debris and then dried thoroughly. The cow was milked and then the teat end was disinfected with a 70% ethanol solution and allowed to dry. Using a sterile teat cannula, bacteria were infused into one mammary gland. After infusion, the teat end was held closed and the bacterial inoculum was massaged upward into the main cistern. The mammary gland was further massaged to ensure distribution of the inoculation. All teats were then dipped in a standard iodine-based teat dip. Challenged cows were monitored symptoms of clinical disease including increased rectal temperature, increased somatic cell count in milk, and abnormalities in mammary gland and milk appearance. Mammary gland abnormalities included pain, swelling, heat, redness, or hardening of the mammary gland and milk abnormalities included a watery consistency, flakes, clots, or pus. At the onset of clinical symptoms, cows were euthanized and parenchymal mammary tissue was excised and either placed in a sterile vial alone (oxylipid quantification) or in RNAlater (mrNA quantification) and snap frozen in liquid nitrogen (Qiagen, Venlo, Limburg). Samples were stored at -80°C (oxylipid quantification) or -20°C until processing. Adhesion molecule, proinflammatory cytokine, and oxylipid biosynthetic enzyme mRNA expression was quantified by qRT-PCR using the RNeasy Mini Kit (Qiagen, Venlo, Limburg) following the manufacturer's protocol. Samples were run in triplicate with ribosomal protein S9 (RPS9) as the endogenous control. Gene expression was calculated using the Δ Ct method for statistical analysis and also using the $2^{-\Delta\Delta Ct}$ method for graphical purposes (Mattmiller et al., 2014). All bovine primers are displayed in Table 2.

Streptococcus uberis UT888 challenge for quantification of oxylipids in milk samples

The University of Tennessee-Knoxville Animal Care and Use Committee preapproved all animal use and care (Protocol 1982-0111). The challenge strain of S. uberis (UT888) was originally isolated from a clinical case of mastitis and has since been used in other S. uberis challenge trials (Rambeaud et al., 2003). A frozen stock of S. uberis UT888 was thawed and grown in Todd Hewitt Broth at 37°C until turbid. The culture was serially diluted in phosphate buffered saline (PBS) to 2,000 CFU/mL. Prior challenge studies, both preliminary and published, demonstrated that the challenge dose had an infection rate of 75-80% (Rambeaud et al., 2003). Approximately 1 week prior to calving, mammary secretion samples were aseptically collected to screen for the presence of bacteria in the mammary gland. Immediately following the morning milking on the day of challenge, 8 healthy Holstein dairy cows were infused with 5 mL of the dilute S. uberis inoculum. Briefly, the mammary gland was cleaned to remove debris and then the cow was milked. The teat end was then disinfected with a 70% ethanol solution and allowed to dry, after which, bacteria were infused into one mammary gland using a sterile cannula. The teat end was held closed and massaged upward into the main cistern and mammary gland. Teats were dipped in a standard iodine-based teat dip. All cows were challenged within 3 d of calving. Similar to details discussed in section 2.2, challenged cows were monitored for signs of clinical disease including increased rectal temperature, increased somatic cell count, abnormalities in the milk and mammary gland. Following intramammary challenge, post-plating revealed that dairy cows received an average dose of approximately 2,100 CFU/mL. Rectal temperatures were recorded prior to challenge (day 0) and 12 h later followed by every 24 h through 7 d post-challenge. Milk samples were aseptically collected on day 0 (prior to challenge) and every 12 h after intramammary challenge through 3.5 d and again on 7 d post-challenge. Milk samples were

collected for bacterial CFU counts, somatic cell count (SCC), and oxylipid quantification.

Samples collected for oxylipid quantification were snap frozen in liquid nitrogen and stored at -80°C until processing. Milk bacterial CFU counts were determined by growth on blood agar plates and were evaluated using established guidelines (NMC, 1999). Milk SCC were determined by the Tennessee Dairy Herd Information Association laboratory (Knoxville, TN).

Extraction and LC/mass spectrometry (LC/MS) quantification of oxylipids

Mammary tissue ranging in weight from 56.8 mg to 150.8 mg was pulverized by a Sartorius-Mikro Dismembrator S (Sartorius Stedium Biotech, Aubagne, France) at 1,800 rpm for 2 min and suspended in HPLC-grade water:MeOH (3:2 v/v) to allow a mixture of 60% MeOH for protein precipitation. Antioxidant reducing agent at 4 μL/mL and a mixture of internal standards containing 0.01% formic acid was added. Antioxidant and reducing agent was prepared with 50% MeOH, 25% EtOH, and 25% HPLC-grade water containing 0.54 mM EDTA 0.9 mM BHT, 3.2 mM TPP, and 5.6 mM indomethacin. The internal standards mixture contained the following deuterated oxylipids (0.1 ng/μl, 10 ng total): LTB_{4-d4}, TxB_{2-d4}, PGF_{2α-d4}, PGE_{2-d4}, PGD_{2-d4}, 13(S)-HODE_{-d4}, 6-keto PGF_{1α-d4}, 9(S)-HODE_{-d4}, 12(S)-HETE_{-d8}, 15(S)-HETE_{-d8}. Tissue suspensions were sonicated at 4°C for 1 min and stored at -20°C for 48 h. Samples were then centrifuged at 4000 x g for 30 min at 4°C and supernatant transferred to a tube with 39 mL of HPLC water and 39 μL formic acid to increased MeOH to 5% in preparation for solid phase extraction.

An aliquot of 300 μ L of milk was mixed with 2.7 mL of 6% trifluoroacetic acid using a vortex, and centrifuged at 14,000 x g for 10 min at 4°C to precipitate casein. Next, casein-precipitated supernatant was added to 5 mL -20°C methanol, antioxidant/reducing agent at 4 μ L/mL

containing 0.01% formic acid, and 200 μ L of an internal standard mixture. Antioxidant/reducing agent and internal standards were similar for mammary tissue and milk samples. Milk samples were vortexed and stored at -20°C over night then centrifuged at 4,700 x g for 20 min at 4°C.

Tissue and milk oxylipids were isolated from the sample supernatant by solid phase extraction using Waters Oasis HLB 12cc Polymeric Reversed Phase 500 mg extraction cartridges (Waters, Milford, MA). Cartridges were preconditioned with 6 mL MeOH, followed by 6 mL HPLCgrade water. Samples were loaded onto preconditioned columns followed by washing with 6 mL 40% MeOH. Columns were then dried under full vacuum at room temperature for 4 min and oxylipids were eluted in 6 mL methanol:acetonitrile (50:50 v/v). Flow rate for solid phase extraction was maintained at 1 drip/sec. Extract was dried at room temperature in Savant SpeedVac (Thermo Electron Corp., West Palm Beach, FL) and resuspended in 200 µl acetonitrile:water:formic acid (37:63:0.02 v/v/v) for analysis. Lastly, resuspended residues were centrifuged at 14,000 x g for 30 min at 4°C to remove any residual debris and an aliquot of 125 μL was transferred to a HPLC vial. Oxylipids were analyzed using 2 distinct liquid chromatography-mass spectrometry (LC/MS) methods based on techniques previously described (Contreras et al., 2012b). Briefly, both methods used reverse-phase LC on a Waters Acquity UPLC BEH C18 1.7 μM column (2.1 x 100 mm). The flow rate was 0.6 mL/min at 35°C. The quadropole MS was in electrospray negative ionization mode and voltage was -3 kV with the turbo ion spray source temperature at 450°C. The isocratic mobile phase for method 1 was acetonitrile:water:formic acid (45:55:0.01 v/v/v) and analysis time was 15 min. Method 2 had an isocratic mobile phase consisting of acetonitrile:MeOH:water:formic acid (47.4:15.8:26.8:0.01 v/v/v/v) and analysis time of 10 min. A total of 26 oxylipids were quantified by matching mass-1

and retention time with corresponding deuterated internal standard abundance and calibrated to a linear 5-point standard curve (R²>0.99). Oxylipids quantified by Waters Empower Z software (Waters, Milford, MA) for tissue and milk samples were as follows: 8-iso PGF₂₀, PGE₂, PGD₂, PGF_{2α}, 6-ketoPGF_{1α}, TXB₂, LTB₄, LTD₄, LXA₄, 5-HETE, 5-oxoETE, 8-HETE, 11-HETE, 12-HETE, 12-oxoETE, 15-HETE, 15-oxoETE, 20-HETE, 7(S)-Maresin-1, Protectin D1, Resolvin D1, and Resolvin D2. Oxylipid concentrations in tissue were normalized per mg of tissue processed and milk oxylipids were normalized per µL of milk processed. The limit of detection was determined by spiking samples with known standard concentrations of each oxylipid and found to be 0.01 ng/µL, the lowest point of each standard curve. Additionally, the following ratios were calculated: 5-HETE:5-oxoETE, 12-HETE:12-oxoETE, 15-HETE:15-oxoETE, 9-HODE:9-oxoODE, 13-HODE:13-oxoODE, and 13-HODE:9-HODE. Ratios were calculated to determine the change, if any, in degree of metabolism or enzymatic versus non-enzymatic oxidation (Raphael et al., 2014). Pro- and anti-inflammatory oxylipids quantified were chosen based on previous research in bovine inflammation models (Anderson et al., 1986; Atroshi et al., 1987; Contreras et al., 2012a; Contreras et al., 2012b; Raphael et al., 2014).

13-HODE and 13-HPODE stimulation of bovine mammary endothelial cells (BMEC) for COX-2 mRNA expression

The BMEC were isolated from the supra-mammary artery of healthy dairy cows based on limited dilution cloning techniques described previously (Aherne et al., 1995). The 13-HPODE was prepared using the procedure outlined in section 2.4.1. The 13-HODE was purchased from Cayman Chemicals (, Ann, Arbor, MI). The BMEC were exposed to several doses of 13-HPODE or 13-HODE in the current study based on previous reports (Setty et al., 1987; Friedrichs et al.,

1999; Trigona et al., 2006). For 13-HODE and 13-HPODE exposure, BMEC were used from passage 8 through passage 10 in F12K medium containing 10% fetal bovine serum (FBS), 100U/mL antibiotic/antimycotic solution, 20 mM HEPES buffer, 10 μg/l insulin, 100 μg/ml heparin, 5 µg/ml transferrin and 10 ng/ml sodium selenite. Prior to 13-HODE or 13-HPODE stimulation, BMEC were seeded on 100 mm culture dishes at 2 x 10⁶ cells/mL and in 96-well dishes at 1 x 10⁴ cells/mL for cell viability. Approximately 12 h later, 10% FBS F12K media was replaced with 5% FBS F12K media with all other ingredients remaining the same. After 4 h of media replacement, BMEC were stimulated with 13-HODE for 1, 2, 4, and 8 h or 13-HPODE for 2 and 4 h. The 13-HODE doses tested were 1, 10, 50, and 100 µM. The 13-HPODE doses tested were 2, 10, and 30 µM. Lipopolysaccharide (LPS, Sigma-Aldrich, St. Louis, MO) at 25 ng/μL for 2 h was used as a positive control. Cell viability was measured using the CellTiter-Glo® luminescent cell viability assay (Promega, Madison, WI) according to manufacturer's protocol and previous research (Contreras et al., 2012a). Total RNA was isolated using the RNeasy Mini Kit (Qiagen, Venlo, Limburg) following the manufacturer's protocol. Samples were run in triplicate and RPS9, TATA-box binding protein (TBP), and phosphoglycerate kinase 1 (PGK1) were endogenous controls. Gene expression was calculated using the Δ Ct method for statistical analysis and also using the $2^{-\Delta\Delta Ct}$ method for graphical purposes (Mattmiller et al., 2014). All bovine primers used in the current study are displayed in Table 1.

Preparation of 13-HPODE. The 13-HPODE was prepared according to previous research with some modifications on a Shimadzu LC-photo diode array detector system (Kyoto, Japan) (Funk et al., 1976). Briefly, 50 mg of LA (Sigma-Aldrich, St. Louis, MO) was stirred with 300,000 U of soybean lipoxidase type V (Sigma-Aldrich, St. Louis, MO) in 30 mL 0.15M

(pH 9) sodium borate buffer for 1 h on ice. The reaction was guenched to pH 3 with 1N HCl and 60 mL HPLC diethyl ether was added. The extracts were washed with 30 mL water and dried over magnesium sulfate to remove water. Extracts were resuspended in 2 mL of mobile phase solution which consisted of HPLC-grade hexane:isopropanol (96.1:3.9 v/v) The extracts were injected in 200 µL aliquots onto a 250 x 4.6 mm Luna column (Phenomenex, Torrence, CA) at room temperature and the prepared 13-HPODE fraction was collected based on pre-injected 13-HPODE standard (Cayman Chemical, Ann Arbor, MI). The method used an isocratic mobile phase with a flow rate was 6 mL/min and a retention time of approximately 4 min for 13-HPODE at 234 nM. A linear 13HPODE (Cayman Chemical, Ann Arbor, MI) standard curve (0.096 μM-60 μM) was generated using a 150 x 4.6 Silica normal phase column (Phenomenex, Torrence, CA). The isocratic mobile phase was the same as for preparation of 13-HPODE and the flow rate was 1 mL/min. The prepared 13-HPODE fraction injected in a 20 µL aliquot and was quantified based on its peak area compared to the standard curve at approximately 4 min. At the time of experiment, solvent was dried and 13-HPODE was resuspended in serum-free F12k media for cell application.

Statistical analysis

Statistical analyses to determine temporal changes in milk SCC, rectal temperature, milk bacterial CFU, and milk production were performed for each experimental group using the MIXED procedure of SAS (SAS Inst Inc., Cary, NC) with time as a repeated measure and cow as a random effect. Least square mean differences were adjusted by the Tukey-Kramer method. Significant ANOVA results were further analyzed by the Student's t-test at specific time points. Statistical analyses to determine differences in tissue oxylipids between uninfected and *S. uberis*-

infected mammary tissue was performed using unpaired Student's t-tests. To determine if there were any temporal differences in milk oxylipid profiles across time in *S. uberis*-infected cows, oxylipid concentrations were tested using the MIXED procedure of SAS (SAS Inst Inc., Cary, NC) with time as repeated measure and cow as a random effect. Least square mean differences were adjusted by the Tukey-Kramer method. Significant ANOVA results were further analyzed by the Student's t-test at specific time points. To compare milk oxylipid concentrations from cows that failed to establish a *S. uberis* infection versus cows did establish an intramammary infection unpaired Student's t-tests were performed for each time point (d 0, d 3, and d 7). The mRNA expression data from mammary tissue was analyzed by Student's t-tests using the Δ Ct to determine differences between uninfected control tissue and *S. uberis*-infected mammary tissue. The mRNA expression data from BMEC exposed to 13-HODE and 13-HPODE was analyzed by ANOVA (SAS Inst Inc., Cary, NC) using the Δ Ct to determine differences between doses and time points. Least square mean differences were adjusted by the Tukey-Kramer method. Significance was declared at $P \le 0.05$ for all tests.

Results

Clinical signs of intramammary infection following S. uberis challenge

S. uberis-infected cows challenged in both models demonstrated clinical symptoms, including appearance of abnormalities in the mammary gland and milk, approximately 3.5 d following intramammary challenge. Though milk somatic cell count and milk *S. uberis* CFU numerically increased following *S. uberis* challenge in all infected cows, there was not a significant change. However, peak rectal temperature was significantly increased to 40.6±0.3271°C and 40.7±0.5320°C in early-lactation and mid-lactation dairy cows, respectively, infected with *S*.

uberis compared to d 0. Milk yield did not significantly change following challenge in cows challenged with *S. uberis* relative to d 0 (prior to challenge). Uninfected cows did not display clinical symptoms during the challenge periods.

Mammary tissue oxylipid profiles in S. uberis-infected mammary tissue

All 26 oxylipids measured were detected in tissue samples taken from dairy cows challenged with *S. uberis* 0140J (Table 3 and Figure 2A,B). The biosynthesis of PGE₂, PGF_{2 α}, 6-keto-PGF_{1 α}, 5-oxoETE, 9-HODE, and 13-HODE was greater in *S. uberis*-infected tissue compared to uninfected tissue (Figure 2A and B). Similarly, the 9-HODE:9-oxoODE ratio was higher in *S. uberis*-infected tissue samples in comparison to uninfected tissue (Figure 2C).

A significant increase in the mRNA expression of pro-inflammatory cytokines (IL-6 and IL-1β) and adhesion molecules ICAM-1, VCAM-1, and E-selectin was observed in *S. uberis*-infected tissue (Figure 3A). Similarly, there was a significant increase in COX-2 mRNA expression in *S. uberis*-infected mammary tissue (Figure 3B). The mRNA expression of other oxylipid biosynthetic enzymes (15-LOX-1, 5-LOX, and COX-1) did not significantly change following *S. uberis* challenge.

Milk oxylipid profiles in S. uberis-challenged dairy cows

In total, 23 out of 26 measured oxylipids were detected in milk samples (Table 4 and 5) with lipoxin A₄, 7(*S*)-Maersin-1, and 12-oxoETE not detected in milk samples. Unexpectedly, no significant temporal changes in oxylipid biosynthesis were observed following the establishment of *S. uberis* mastitis (n=5) in the current study. Because there was a subset of cows that did not

establish an infection after *S. uberis* intramammary challenge (n=3) in the current study, oxylipid biosynthesis was compared on d 0, 3 d post-challenge, and 7 d post-challenge between cows that established infection and those that did not following challenge. The biosynthesis of HODE (9-and 13-HODE collectively) was significantly increased 7 d post-challenge in cows that established *S. uberis* mastitis following challenge compared to cows that did not establish a *S. uberis* intramammary infection (Figure 4A). In contrast, the 13-HODE:13-oxoODE ratio and 13-HODE:9-HODE ratio was significantly increased on the d of challenge and also 3 d post-challenge in cows that did not establish an intramammary infection (Figure 4B and C). The concentration of 6-keto PGF_{1 α} was greater prior to challenge (d 0) in milk from cows that failed to establish a S. uberis infection compared to those that did (Figure 5A), whereas 11-HETE was greater prior to challenge (d 0) in milk from cows that established an intramammary infection compared to those that did not (Figure 5B).

Response of BMEC following 13-HODE and 13-HPODE exposure

After 8 h of exposure to 13-HODE, BMEC viability decreased by 5%, 3%, and 13% during 10, 50, and 100 μ M exposure, respectively. However, there was not a significant change in the mRNA expression of COX-2 at any dose (1, 10, 50, or 100 μ M) or time point (1, 2, 4, or 8h) (Figure 6A). The results were consistent with the additional doses and time points. The mRNA response following 2h LPS exposure (positive control) was significantly increased. After 4 h of exposure to 13-HPODE, there was a significant decline in viability by 13, 16, and 21% for 2, 10, and 30 μ M, respectively. There was a significant increase in COX-2 mRNA expression after 4 h exposure to 30 μ M 13-HPODE (Figure 6B). There was a similar increase in COX-2 mRNA

expression following 2 h exposure to LPS (positive control). There was no significant difference at 2 h for any dose and 2 and 10 μ M for 4 h.

Discussion

The current study provides a unique perspective on how oxylipid profiles change at the onset of clinical mastitis in tissue and the temporal expression of oxylipids in milk. In the present study, *S. uberis*-challenged cows displayed clinical symptoms of disease, which was consistent with mRNA expression of several pro-inflammatory markers. Thus, it was expected to find significant changes in oxylipid biosynthesis following *S. uberis* intramammary challenge. Indeed, oxylipids derived from different fatty acid substrates (AA and LA) and oxidation pathways (enzymatic and non-enzymatic) were detected and significantly increased. A change in oxylipids from various PUFA sources illustrates the complexity of oxylipid biosynthesis in this targeted LC/MS array consisting of 26 oxylipids. It is fathomable that an expanded lipidome may demonstrate additional substrates and pathways sensitive to bacterial challenge in the bovine mammary gland.

The findings in the current study are consistent with data from murine infection models suggesting a robust and rapid increase in oxylipid biosynthesis during the initial stages of the inflammatory response coincides with onset of clinical disease (Blaho et al., 2009; Balvers et al., 2012; Tam et al., 2013). Of those oxylipids measured at the onset of clinical symptoms, similarities between the profiles in the current study and previous murine bacterial challenge models, such as PGE₂ and 5-oxoETE, suggest the involvement of similar biosynthetic pathways during initial inflammatory responses (Blaho et al., 2009; Balvers et al., 2012). However, a murine endotoxin challenge model highlighted the differences in oxylipid profiles depending on

the sample type, i.e. various tissues and plasma (Balvers et al., 2012). Comparably, in the present study there were no temporal changes in oxylipid biosynthesis in milk during S. uberis mastitis, which is in contrast to tissue oxylipid profiles from S. uberis-infected cows. One explanation for the difference in tissue and milk oxylipid profiles is the potential source of the lipid mediators. Mammary tissue samples are composed primarily of epithelial cells, leukocytes, endothelial cells, few myoepithelial cells, and lipid-rich membranes fragments from damaged cells. Thus, intracellular oxylipids from various cell types, intracellular oxylipids transported extracellularly by fatty acid binding proteins, and oxylipids esterified to membrane fragments are quantifiable in mammary tissue (Dickinson Zimmer et al., 2004). In contrast, milk oxylipid profiles would represent a smaller, more specific selection of oxylipids in the mammary gland, i.e., oxylipids synthesized intracellularly then transported into the alveolar lumen by fatty acid binding proteins and oxylipids esterified to fragments of membranes. Additionally, some oxylipids may be formed while the fatty acid substrate is still esterified to the lipid membrane or formed in the cytosol and reincorporated into the lipid membrane (Kozak et al., 2002; Morgan et al., 2009). For example, murine peritoneal macrophages synthesize phospholipid-esterified 12-HETE following in vitro calcium ionophore stimulation and in lung inflammation in an in vivo murine model (Morgan et al., 2009). Additionally, previous research demonstrates the ability for some cell types, such as porcine coronary endothelial cells, to incorporate 20-HETE into the phospholipid membrane (Kaduce et al., 2004). Thus, esterified oxylipids would not be transported into the ductal lumen of alveoli and, as such, not detected in milk. Further mastitis studies quantifying oxylipid profiles would benefit from obtaining several different sample types during disease to understand how local mammary inflammation may change oxylipids in plasma, urine, milk, and mammary tissue. Identifying the appropriate samples indicative of disease pathology is important for identifying lipid biomarkers of disease and any potential therapies that may arise as a result of lipidomic profiling.

In addition to differences in sample type, the method of oxylipid quantification and experimental design in this study compared to earlier trials also warrants discussion. In the current study, there were no changes in the temporal expression of oxylipids in milk; however, past mastitis studies demonstrated robust increases in several AA-derived oxylipids including prostaglandins, lipoxin, leukotriene, and thromboxane (Giri et al., 1984; Anderson et al., 1986; Atroshi et al., 1987; Atroshi et al., 1990). However, previous studies utilized antibody-based radioimmunoassays and enzyme-linked immunosorbent assays to quantify oxylipids (Maskrey and O'Donnell, 2008). Antibodies may cross-react among oxylipids due to subtle structural differences among oxidized lipids, which could result in overestimation of oxylipid concentrations (Il'yasova et al., 2004). Thus, it is not surprising that results in the current study did not support previous reports. Furthermore, earlier mastitis trials quantified oxylipids during naturally occurring mastitis or gram-negative pathogen-induced mastitis, which does not allow for initial bacterial counts or assessment of oxylipid profiles during the progression of infection (Giri et al., 1984; Zia et al., 1987; Atroshi et al., 1990). Because oxylipids are both rapidly produced and rapidly metabolized into different metabolites, a challenge model that can control dose and time of challenge offers a clearer picture of oxylipid dynamics during disease

While advancements in our understanding of the field of oxylipid biosynthesis are evident, the contribution that different bacterial strain may have on oxylipid profiles during disease is unclear. In the current study, a different encapsulated *S. uberis* strain was utilized in each model;

however, the onset of clinical disease and associated symptoms in infected cows were similar. Murine viral infection and sepsis models demonstrate dissimilar oxylipid profiles following challenge with strains having low pathogenicity versus high pathogenicity, but there are currently no studies that explore if different bacterial strains induce distinct oxylipid biosynthesis yet similar clinical outcomes (Chiang et al., 2012; Tam et al., 2013). While the two strains of *S. uberis* in the present study caused similar clinical symptoms at about 3.5 d, knowing distinct profiles induced by various bacterial strains would be important for tailoring dietary and pharmacologic treatment according to predominant mastitis-causing strains in dairy herds.

Regardless of differences in oxylipid profiles from milk and tissue, the predominance of LAderived metabolites (HODE and oxoODE) was consistent between models in all control and challenged cows. The predominance of HODE and oxoODE was not surprising given the LArich diet that dairy cows and humans consume (Ramsden et al., 2012; Raphael et al., 2014). With respect to significant changes in *S. uberis*-infected mammary tissue, increase in total 9- and 13-HODE also may be a reflection of increased HPODE that is rapidly reduced to the hydroxyl form related to its instability (Sandstrom et al., 1995; Friedrichs et al., 1999; Aitken et al., 2011a). Exposure to HPODE, especially 13-HPODE, induced apoptosis in T cells and endothelial cells suggesting 13-HPODE is particularly detrimental to cell survival and tissue health (Sandstrom et al., 1995; Tampo et al., 2003). Linoleic acid-derived HODE isomers, 9- and 13-, can further be metabolized by NAD+ dehydrogenation to 9- and 13-oxoODE resulting in potent anti-inflammatory oxylipids (Bull et al., 1996; Nagy et al., 1998). In epithelial cells and macrophages, the oxoODEs robustly activate PPARγ, which contributes to limiting pro-inflammatory responses by reducing the expression of pro-inflammatory cytokines (Nagy et al., 1998; Altmann

et al., 2007). Thus, the increased 9-HODE:9-oxoODE ratio in infected tissues following *S. uberis* 0140J challenge reflects an accumulation of unstable HPODE and stable HODE, as well as reduced metabolism to anti-inflammatory oxoODE. Previous studies suggest that prolonged availability of HPODE and HODE, and less oxoODE, may result in an inability to control inflammation (Vangaveti et al., 2010). As such, the extent of LA metabolism may influence the inflammatory response by impacting vascular barrier integrity and function. In the bovine mammary gland, an inability to resolve inflammation may lead to death of endothelial cells and would allow increased exchange of plasma components contributing to edema and mammary tissue damage (Ereso et al., 2009).

Though there is some evidence to suggest that LA-derived oxylipids modify vascular function, it is unknown how they contribute to mastitis pathogenesis and affect vascular phenotype. To address the direct impact of the most prevalent oxylipid identified from the present *in vivo* data on vascular phenotype, primary BMEC were exposed to 13-HPODE and 13-HODE, following which COX-2 mRNA expression was quantified. Expression of COX-2 is highly inducible in response to extracellular and internal pro-inflammatory stimuli, such as NF- κB activation, hypoxia, and ROS (Schmidt et al., 1995; Schmedtje et al., 1997; Meade et al., 1999). There was a significant increase in COX-2 mRNA expression following 4 h exposure to 30 μM 13-HPODE, whereas there were no significant changes in COX-2 mRNA expression following 13-HODE exposure. The significant increase in COX-2 mRNA expression following 4 h exposure to 30 μM 13-HPODE, suggests 13-HPODE acts as a pro-inflammatory oxylipid in inducing COX-2 expression compared to the reduced 13-HODE. Similarly, previous studies in human colorectal cells showed that LA hydroperoxides, which includes 9- and 13-HPODE, significantly increase

COX-2 mRNA (Jurek et al., 2005). In contrast, Friedrichs et al. (Friedrichs et al., 1999) demonstrated a more robust response in human umbilical vein endothelial cell adhesion molecule expression following 13-HODE exposure in contrast to 13-HPODE exposure, however the timing and dose of 13-HPODE was higher (50 μM) than the current study (30 μM). A higher dose was not used in the current study because cell viability was compromised during longer periods of exposure. Further studies are needed to determine the extent of 13-HPODE and 13-HODE effects on BMEC, however *in vitro* data suggest a future question to be addressed is whether an accumulation of HPODE results in more severe disease pathology, whereas rapid reduction to HODE protects tissue from damage. Furthermore, the ability of 13-oxoODE to ameliorate inflammation needs to be explored since there seems to be reduced metabolism during *S. uberis* mastitis. Identifying and targeting specific downstream enzymatic pathways (e.g., dehydrogenation to divert metabolism to oxoODE) could alter the balance of oxylipids, which may prove to be more efficacious than current approaches targeting major upstream enzymatic pathways, such as NSAID therapy.

Differences in the ratio of pro-inflammatory to anti-inflammatory LA-derived oxylipids suggest the balance of oxylipids may be important in identifying cows at risk for disease or even modulating inflammation to mediate disease progression. In the present study, retrospective assessment of milk oxylipids from cows that were challenged and developed S. uberis mastitis could be compared to cows challenged but did not develop a S. uberis mammary infection to understand if profiles potentially contributed to disease resistance or disease progression. Indeed, the differences in the 13-HODE:9-HODE ratio, 6-ketoPGF_{1 α}, and 11-HETE prior to challenge and shortly after challenge in dairy cows that established mastitis versus those that did not

suggest that specific oxylipid profiles or instrumental factors in the microenvironment, might influence the inflammatory response after bacterial challenge. In the case of an increased 13-HODE: 9-HODE ratio, oxidation of LA by 15-LOX-1 primarily yields 13-HPODE, whereas 9-HPODE is generally formed by non-enzymatic oxidation (Vangaveti et al., 2010). Increased abundance of 13-HODE compared to 9-HODE suggests greater 15-LOX-1 activity or enhanced antioxidant defenses thus reducing non-enzymatic oxylipid biosynthesis (Friedrichs et al., 1999; Vangaveti et al., 2010). Previous transcriptomic data from S. uberis-infected (wild-type strain 233) mammary tissue revealed enhanced antioxidant defenses after challenge against damaging oxygen and nitrogen radicals; however, these data do not explain the differences prior to challenge in the current study (Swanson et al., 2009). Although conjecture, an increased 13-HODE:9-HODE ratio, in advance of an inflammatory challenge, may be advantageous in limiting an overwhelming immune response that controls the infection and also protects the surrounding tissue. Tam et al. (2013) reported a significant increase in the 13-HODE:9-HODE ratio during the resolution phase in a murine model of influenza infection, whereas the opposite was true during the clinical phase, suggesting an increased 13-HODE:9-HODE ratio is reflective of a healthier microenvironment. Increased antioxidant defenses in advance of bacterial challenge also may be supported by lower 11-HETE biosynthesis as 11-HETE is generated by ROS and free radical-mediated non-enzymatic oxidation of AA. However, a bioactive role of 11-HETE at the onset of inflammation remains to be determined. Perhaps, oxylipid profiles prior to challenge indicate the effectiveness of other systems, such as antioxidant enzymes and redox pathways, rather than acting as bioactive molecules.

Conclusion

The profiling of oxylipids in veterinary medicine can be an effective way of assessing the dynamics of the inflammatory response to microbial challenges. However, the current study demonstrated differential oxylipid profiles during different stages of *S. uberis* mastitis and in different sample compartments, milk versus tissue. The current findings suggest that the choice of biological sample type may be important in understanding how oxidized lipids change in response to pathogen challenge. Furthermore, current technology using LC tandem electrospray ionization triple quadrupole MS is capable of quantifying close to 160 oxylipids in one sample, (Wang et al., 2014). Expanding the profile of oxylipids measured may enable identification of other key biosynthetic pathways, such as the CYP oxidation pathway, that may either optimize or impair mammary gland inflammatory responses (Mavangira et al., 2015). Though the current study identified differences in the effect of LA-derived oxylipids on endothelial function, future studies need to be done to determine if altering oxylipid profiles can in fact protect against the development of mastitis or protect the mammary gland from severe damage.

Acknowledgements

The authors acknowledge the resources and staff of the Michigan State University Research Technology Support Facility Mass Spectrometry Core, especially Drs. Dan Jones and Scott Smith. This work was funded, in part, through grants (2011-67015-30179 and 2015-67011-23012) from the Agriculture and Food Research Initiative Competitive Grants Programs of the USDA National Institute for Food and Agriculture and by an endowment from the Matilda R. Wilson Fund (Detroit, MI).

CHAPTER 3 APOPTOSIS OF ENDOTHELIAL CELLS BY 13-HPODE CONTRIBUTES TO IMPAIRMENT OF ENDOTHELIAL BARRIER INTEGRITY

Valerie E. Ryman¹, Nanda Packiriswamy¹, and Lorraine M. Sordillo^{1*}

¹ College of Veterinary Medicine, Michigan State University, East Lansing, MI 48824, USA

*Corresponding author

Dr. Lorraine M. Sordillo,
Department of Large Animal Clinical Sciences
College of Veterinary Medicine
Michigan State University
sordillo@msu.edu
Tel: (517) 432-8821

Fax: (517) 432-8822

Abstract

Inflammation is an essential host response during bacterial infections such as bovine mastitis. Endothelial cells are critical for an appropriate inflammatory response and loss of vascular barrier integrity is implicated in the pathogenesis of *Streptococcus uberis*-induced mastitis. Previous studies suggested that accumulation of 15-lipoxygenase-1 (15-LOX-1) oxygenation products of linoleic acid (LA) may contribute to vascular dysfunction. The initial 15-LOX-1 LA product, 13-hydroperoxyoctadecadienoic acid (HPODE), can induce endothelial death and the reduced metabolite, 13-hydroxyoctadecadienoic acid (HODE), can be abundantly produced during vascular activation. The relative contribution of specific LA-derived metabolites on impairment of mammary endothelial integrity is unknown. Our hypothesis was that S. uberisinduced LA-derived 15-LOX-1 oxygenation products impair mammary endothelial barrier integrity by apoptosis. Exposure of bovine mammary endothelial cells (BMEC) to S. uberis did not increase 15-LOX-1 LA metabolism. However, S. uberis challenge of bovine monocytes demonstrated monocytes may be a significant source of 13-HODE. Exposure of BMEC to 13-HPODE, but not 13-HODE, significantly reduced endothelial barrier integrity and increased apoptosis. Changing oxidant status by co-exposure to an antioxidant during 13-HPODE treatment prevented adverse effects of 13-HPODE, including amelioration of apoptosis. A better understanding of how the oxidant status of the vascular microenvironment impacts endothelial barrier properties could lead to more efficacious treatments for S. uberis mastitis.

Keywords: 13-hydroperoxyocatadecadienoic acid, endothelial cells, barrier integrity, apoptosis

Introduction

Inflammation contributes to a variety of human and veterinary diseases, including mastitis. Bovine mastitis caused by *Streptococcus uberis* results in severe damage to milk-producing tissues as a result of an uncontrolled inflammatory response. Previous clinical and histopathological data suggested disruption of the endothelial barrier contributed to disease pathology. For example, *S. uberis* intramammary challenge studies reported a loss in the blood-milk barrier as indicated by a sustained increase of plasma proteins in milk (Bannerman et al., 2004a). Similarly, histopathological analysis demonstrated that neutrophils accumulated in mammary tissue up to several days after *S. uberis* intramammary challenge indicating an inability of the endothelium to limit leukocyte influx across the blood-milk barrier (Thomas et al., 1994, de Greeff et al., 2013). Subcutaneous edema after intramammary *S. uberis* challenge also indicated an inability to preserve a selectively permeable vascular barrier (Pedersen et al., 2003). The mechanisms that may cause endothelial dysfunction during *S. uberis* mastitis are undefined, but some fatty acid-derived oxylipids were implicated in contributing to development of dysfunctional endothelial responses (Sordillo et al., 2005, Szklenar et al., 2013).

Oxylipids are synthesized from esterified PUFA that are cleaved from the phospholipid membrane by cytosolic phospholipase A₂. Cleaved PUFA are often oxidized through several different enzymatic pathways including 15-lipoxygenase (15-LOX) (Morrow et al., 1990, Buczynski et al., 2009). Initial enzymatic oxygenation products can be further enzymatically metabolized by a variety of down stream enzymes including hydrolases and dehydrogenases (Schmelzer et al., 2005, Altmann et al., 2007). Additionally, initial oxygenation products during oxylipid biosynthesis may be reduced depending on the redox status of the cellular environment.

For example, enzymatic oxidation of linoleic acid (LA) by 15-LOX-1 predominately yields 13-hydroperoxyoctadecadienoic acid (13-HPODE) and can be reduced to 13-hydroxyoctadecadienoic acid (13-HODE) by antioxidants/reducing agents, such as the glutathione (Kuhn et al., 2015). Dehydrogenation of 13-HODE to an anti-inflammatory 13-oxooctadecadienoic acid (13-oxoODE) can occur by the action of NADPH-dependent fatty acid dehydrogenases (Altmann et al., 2007). Since LA oxidation and metabolism is a sequential process, 13-HPODE biosynthesis is required for the subsequent generation of 13-HODE and 13-oxoODE. Current literature supports an important role for some LA-derived 15-LOX-1 oxylipids in a normal inflammatory response (Henricks et al., 1991, Friedrichs et al., 1999, Dwarakanath et al., 2004). However, previous data also suggested 13-HPODE biosynthesis induced death of various cell types and was associated with severe inflammatory-based diseases (Haimovitz-Friedman et al., 1997, Hasdai et al., 1999).

A recent study proposed that LA-derived oxylipids may be responsible for contributing to *S. uberis* pathogenesis (Ryman et al., 2015). Authors specifically highlighted the potential contribution of the 15-LOX-1 oxidation pathway to disruption of the endothelial barrier (Ryman et al., 2015). Various studies showed that 13-HODE induced vascular activation and could play a role in regulating endothelial barrier integrity during inflammation (Buchanan et al., 1985, Szklenar et al., 2013). The initial 15-LOX-1 LA oxygenation product, 13-HPODE, was implicated in contributing to apoptosis of endothelial cells, which could be a key event contributing to endothelial dysfunction (Tampo et al., 2003, Dhanasekaran et al., 2004, Dhanasekaran et al., 2005). However, the capacity of specific LA oxygenation products to compromise the mammary endothelial barrier during *S. uberis* mastitis is unknown. Thus, the

hypothesis for the current study was that *S. uberis*-induced LA-derived 15-LOX-1 oxygenation products impair mammary endothelial barrier integrity by apoptosis.

Materials and Methods

Reagents

High performance liquid chromatography (HPLC)-grade acetonitrile, HPLC-grade methanol, formic acid, sodium selenite, insulin, heparin, transferrin, ethylenediaminetetraacetic acid (EDTA), triphenylphosphine (TPP), sodium selenite, soybean lipoxidase type V, and linoleic acid were purchased from Sigma—Aldrich (St. Louis, MO). Diethyl ether and butylated hydroxy toluene (BHT) were purchased from ACROS Organics (Fair Lawn, NJ). YOPRO®-1 and propidium iodide stains were from Thermo Fisher Scientific (Waltham, MA).

Antibiotics/antimycotics, trypsin-EDTA, glutamine, and bovine collagen were from Life Technologies (Carlsbad, CA). All bovine Taqman® primers were purchased from Applied Biosystems (Foster City, CA). Deuterated oxylipid standards, nondeuterated oxylipid standards, and indomethacin were purchased from Cayman Chemical (Ann Arbor, MI). Magnesium sulfate was purchased from Avantor Performance Materials, Inc. (Central Valley, PA) and sodium borate from Fisher Science Education (Nazareth, PA). Fetal bovine serum was purchased from Hyclone Laboratories, Inc. (Logan, Utah). The HEPES buffer, HAM's F-12k, and RPMI 1640 was from Corning Inc. (Corning, NY).

Preparation of Streptococcus uberis for in vitro challenge

Streptococcus uberis was streaked on a blood agar plate to enable collection of 3 pure colony forming units (CFU). The 3 CFU were added to 100 mL RPMI 1640 medium containing 5%

fetal bovine serum (FBS), 300 mg/mL L-glutamine, and 0.1 μ M sodium selenite. The suspension was shaken at 37°C for 13 hr to exponential growth phase. For BMEC challenge experiments, the bacterial suspension was centrifuged at 11,000 x g for 30 min at 4°C. After centrifuging, the supernatant was filtered through a filter with a pore size of 0.22 μ M. For monocyte challenge experiments, filtered supernatant was utilized as described and also bacterial suspension was heat-killed in a 65°C water bath for 45 min.

Isolation and culture of primary bovine mammary endothelial cells (BMEC)

Mammary endothelial cells were collected from the supra-mammary artery of healthy Holstein dairy cows based on techniques described previously (Aherne et al., 1995). The BMEC were purified by limited cloning techniques and then cultured in Ham's F-12K medium containing 10% FBS, 20 mM HEPES, antibiotics and antimycotics (100 U/mL consisting of penicillin, streptomycin, and amphotericin B), heparin (100 μ g/mL), insulin (10 μ g/mL), transferrin (5 μ g/mL), and sodium selenite (10 η g/mL). Cells were revived from liquid nitrogen at pass 4 and used up to passage 10. For experiments involving exposure to *S. uberis*, cells were seeded the day before at 2.5 × 10⁶ cells/100 mm cell culture dish. The *S. uberis* supernatant was diluted 1:3 for challenge and BMEC were incubated for 4 hr and 36 hr at 37°C. Lipopolysaccharide (LPS) at 25 η g/mL was added for 4 hr as a positive control.

Isolation and culture of primary bovine monocytes

Peripheral blood mononuclear cells (PBMC) were collected from healthy Holstein dairy cows by methods previously described (Contreras et al., 2010). Primary monocytes were isolated from PBMC by the plate adherence method in RPMI 1640 medium containing 5% fetal bovine serum

(FBS), 300 mg/mL L-glutamine, antibiotics and antimycotics (100 U/mL consisting of penicillin, streptomycin, and amphotericin B), and 0.1 μM sodium selenite (O'Boyle et al., 2012). The PBMC and monocytes were collected and prepared fresh for each replicate. For *S. uberis* challenge of monocytes, PBMC were seeded the day of at 8 × 10⁷ cells/100 mm cell culture dish with approximately 10% cell adherence after 3 hr and 3 subsequent washes. After the washes, either *S. uberis* supernatant or heat-killed *S. uberis* was added for 4 hr and 36 hr. The multiplicity of infection for heat-killed *S. uberis* challenge was an average of 54:1. The *S. uberis* supernatant was diluted 1:3 for challenge. Monocytes were incubated for 4 hr and 36 hr at 37°C. Lipopolysaccharide at 25 ng/mL was added for 4 hr as a positive control.

Primary BMEC and monocyte mRNA quantification

Total mRNA was isolated with the RNeasy Mini Kit (Qiagen, Venlo, Limburg) following the manufacturer's instructions. Samples were run in triplicate with β-actin, TATA-box binding protein (TBP), and phosphoglycerate kinase 1 (PGK1) as endogenous controls. Target genes to assess BMEC inflammatory phenotype were cyclooxygenase-2 (COX-2), 15-LOX-1, vascular cell adhesion molecule-1, intercellular adhesion molecule-1, and intereukin-8 (IL-8). Thermal cycling conditions for BMEC were as follows: 95 °C for 20 s; stage 2, 95 °C for 3 s; stage 3, 60 °C for 30 s; with 40 replications through stages 2 and 3. Primary monocyte cDNA required amplification and was amplified using TaqMan PreAmp Kit (Applied Biosystems Inc.). Target genes to assess monocyte inflammatory phenotype were COX-2, 15-LOX-1, inducible nitric oxide synthase (iNOS), IL-10, and IL-6. Thermal cycling conditions for monocytes were as follows: stage 1: 50°C for 2 min, stage 2: 95°C for 10 min, stage 3: 95°C for 15 s, and stage 4: 60°C for 1 min, with 40 replicates of stages 3 and 4. Gene expression was calculated using the

 Δ Ct method for statistical analysis and also using the $2^{-\Delta\Delta$ Ct} method for graphical purposes (Aitken et al., 2011b, Raphael et al., 2014).

Extraction and quantification of oxylipids

Oxylipids were extracted from the supernatant after S. uberis challenge in monocytes and BMEC based on techniques previously described (Mattmiller et al., 2014). Briefly, supernatant was collected and an antioxidant reducing agent at 4 µL/mL and a mixture of internal standards containing 0.01% formic acid was added. Antioxidant and reducing agent was prepared with 50% MeOH, 25% EtOH, and 25% HPLC-grade water containing 0.54 mM EDTA 0.9 mM BHT, 3.2 mM TPP, and 5.6 mM indomethacin. The internal standards mixture contained the following deuterated oxylipids (0.1 ng/µL, 10 ng total): LTB_{4-d4}, TxB_{2-d4}, PGF_{2a-d4}, PGE_{2-d4}, PGD_{2-d4}, 13(S)- $HODE_{-d4}$, 6-keto $PGF_{1\alpha-d4}$, 9(S)- $HODE_{-d4}$, 12(S)- $HETE_{-d8}$, 15(S)- $HETE_{-d8}$. The solution was brought up to 60% (v/v) methanol to facilitate protein precipitation. Samples were centrifuged at 4000 x g for 30 min at 4 °C. Supernatant was aspirated and diluted to 5% (v/v) methanol and kept cold prior to extraction through column cartridges Prior to passing samples, the Phenomenex Strata-X 33u Polymeric Reverse-Phase Columns (500 mg/12 ml, Phenomenex, Torrance, CA) were conditioned with 6 ml methanol then 6 ml water. After conditioning, samples were run through the column and then washed with 40% methanol. The column was dried completely and then oxylipids were eluted from the columns in methanol/acetonitrile (50:50; v/v). Samples were dried in a Sevant SVD121P SpeedVac (Thermo Scientific, Waltham, MA), resuspended in acetonitrile/water/formic acid (37:63:0.02; v/v/v) and centrifuged at 14,000 x g for 30 min. Supernatant was aspirated and transferred to chromatography vials prior to liquid

chromatography-mass spectrometry (LC-MS) quantification. Oxylipids were quantified according to previously described methods (Ryman et al., 2015).

Preparation of 13-HPODE

The 13-HPODE was prepared according to previous reports with modifications on a Shimadzu LC-photo diode array detector system (Kyoto, Japan) (Funk et al., 1976). Briefly, 30 mL 0.15 M (pH 9) sodium borate buffer was mixed with 50 mg of LA and 300,000 U of soybean lipoxidase type V. The suspension was stirred for 1 h on ice. The oxidation reaction was stopped by lowering the pH to 3 with 1N HCl. Immediately, 60 mL HPLC diethyl ether was added and extracts were washed with 30 mL water. After separation and dispensing of water, the extracts were dried over magnesium sulfate to remove remaining water. Extracts were resuspended in 2 mL of HPLC-grade hexane:isopropanol (96.1:3.9 v/v) and injected in 200 μL aliquots onto a 250 × 4.6 mm Luna column (Phenomenex, Torrence, CA) at room temperature. The prepared 13-HPODE fraction was collected based on pre-injected 13-HPODE standard. The method used an isocratic mobile phase (hexane:isopropanol, 96.1:3.9 v/v) with a flow rate was 6 mL/min. A linear 13-HPODE standard curve (0.48–300 μM) was generated on a reverse-phase LC on a Waters Acquity UPLC BEH C18 1.7 μM column (2.1 × 100 mm). The flow rate was 0.6 mL/min at 35 °C and the quadropole MS was in electrospray negative ionization mode. The voltage was −3 kV with the turbo ion spray source temperature at 450 °C. The mobile phase was acetonitrile:MeOH:water:formic acid (47.4:15.8:26.8:0.01 v/v/v/v) and had an analysis time of 10 min. The concentration of 13-HPODE in the synthesized and collected fraction was quantified by Waters Empower Z software (Waters, Milford, MA) according to the 5-point standard curve.

Electric Cell-Substrate Impedance Sensing assay: Endothelial barrier integrity

For assessment of endothelial barrier integrity, BMEC were plated on bovine collagen-coated wells with gold electrodes and grown to confluence. Electric currents passing through the monolayer were continuously measured by the Electric Cell-Substrate Impedance Sensing system (ECIS, Applied Biophysics, Inc., Troy, NY). Approximately 4-6 hr prior to treatment addition, media was changed to 0% FBS Ham's F12k media containing 20 m*M* HEPES, antibiotics and antimycotics (100 U/mL consisting of penicillin, streptomycin, and amphotericin B), heparin (100 μg/mL), insulin (10 μg/mL), transferrin (5 μg/mL), and sodium selenite (10 ng/mL). Resistance across the monolayer was monitored up to 24 hr after treatment addition. Resistance was normalized to the time point immediately prior to treatment addition.

Measurement of apoptosis and necrosis

Apoptosis and necrosis was measured using by co-staining with YOPRO®-1 and propidium iodide from a commercial kit (Thermo Fisher Scientific, Waltham, MA). Briefly, BMEC were seeded in 100 mm cell culture dishes overnight. The media was then changed to 0% FBS media containing 20 mM HEPES, antibiotics and antimycotics (100 U/mL consisting of penicillin, streptomycin, and amphotericin B), heparin (100 μg/mL), insulin (10 μg/mL), transferrin (5 μg/mL), and sodium selenite (10 ng/mL) for approximately 4 hr. Treatments were added for 6 hr and 24 hr depending on experiment. Fluorescence was determined by flow cytometry according to manufacturer's protocols. Amount of apoptosis or necrosis was expressed as fold change over media control. Apoptosis was also measured by the Apo-ONE® Homogeneous Caspase-3/7 kit (Promega, Madison, WI) according to manufacturer's protocols at 6 hr post-treatment. Amount of apoptosis or necrosis was expressed as fold change over media control.

Statistical analysis

Differences in BMEC mRNA expression of select oxylipid biosynthetic enzymes, select adhesion molecules, and a chemotactic cytokine between respective time point controls and treatments (LPS and S. uberis supernatant) were determined by Student's t-tests. Differences in oxylipid biosynthesis for BMEC between control and treatments at each time point were tested in the same manner. Similarly, differences in bovine monocyte mRNA expression of select oxylipid biosynthetic enzymes, a marker of monocyte activation, and inflammatory cytokines between respective time point controls and LPS treatments were determined by Student's t-tests. Differences between control, S. uberis supernatant, and heat-killed S. uberis among time points was determined by ordinary one-way ANOVA with Tukey's post hoc correction. Differences in oxylipid biosynthesis for bovine monocytes exposed to S. uberis supernatant and heat-killed S. uberis were tested in the same manner. To determine differences at specific points in normalized resistance for all barrier integrity experiments between control and 13-HPODE, 13-HODE, or LPS treatments, Mann-Whitney tests were performed. Fold change in apoptosis and necrosis (flow cytometry and caspase 3/7 activity) over control were determined by ordinary one-way ANOVA with Tukey's post hoc correction. Effect of several doses of N-acetylcysteine coexposure with 13-HPODE was also tested by ordinary one-way ANOVA with Tukey's post hoc correction.

Results

S. uberis exposure induced inflammatory marker expression, but not oxylipid biosynthetic enzyme expression, in BMEC

Oxylipid biosynthetic enzyme mRNA expression (COX-2 and 15-LOX-1) was not significantly increased after 4 hr or 36 hr exposure to *S. uberis* supernatant (Figure 7A & B). In contrast, the mRNA expression of ICAM-1 and IL-8 was significantly increased after 4 hr exposure to *S. uberis* supernatant and VCAM-1 mRNA expression was significantly increased after 36 hr exposure (Figure 7C, D, & E). Exposure to LPS (positive control) demonstrated a significant increase in all genes tested after 4 hr (Figure 7).

Exposure to *S. uberis* did not induce any significant changes in 13-HODE and 13-oxoODE biosynthesis after 4 and 36 hr (Figure 8A & B). Increased 13-oxoODE, but 13-HODE, was significant after 4 hr LPS exposure (Figure 8B).

S. uberis exposure induced expression of inflammatory markers, including oxylipid biosynthetic enzyme expression, in bovine monocytes

The mRNA expression of COX-2 was significantly upregulated by the following treatments and time points: 4 hr *S. uberis* supernatant, 4 hr heat-killed *S. uberis*, and 36 hr heat-killed *S. uberis* (Figure 9A). The mRNA expression of 15-LOX-1 was significantly upregulated the following treatments and time points: 4 hr *S. uberis* supernatant and 36 hr heat-killed *S. uberis* (Figure 9B). The mRNA expression of iNOS was significantly upregulated after 4 hr and 36 hr exposure to both *S. uberis* supernatant and heat-killed *S. uberis* (Figure 9C). The mRNA expression of IL-6

was significantly upregulated by the following treatments and time points: 4 hr *S. uberis* supernatant and 36 hr heat-killed *S. uberis* (Figure 9D). The mRNA expression of IL-10 was significantly upregulated after 4 hr exposure to heat-killed *S. uberis* (Figure 9E). Exposure to LPS demonstrated a significant increase in all genes tested after 4 hr (Figure 9).

13-HODE, but not 13-oxoODE, biosynthesis by bovine monocytes was upregulated following heat-killed S. uberis exposure

Increased 13-HODE, but not 13-oxoODE was significant after 36 hr heat-killed *S. uberis* exposure (Figure 10A). Exposure to *S. uberis* supernatant for 4 and 36 hr failed to induce significant changes in 13-HODE and 13-oxoODE biosynthesis (Figure 10A & B). Similarly, bovine monocytes to LPS for 4 hr did not induce significant changes in 13-HODE and 13-oxoODE biosynthesis. (Figure 10A & B).

Mammary endothelial barrier integrity is decreased during 13-HPODE treatment

Cultured endothelial barrier integrity was significantly decreased by 150 μ M 13-HPODE from 2 hr post-exposure until 12 hr post-exposure compared to media control at the respective time points (Figure 11A). A 6 hr time point and 24 hr time point was used for subsequent determination of apoptosis and necrosis following 13-HPODE treatment. Barrier integrity was unchanged during exposure to 100 μ M 13-HODE (Figure 11B). Treatment of endothelial monolayers with 25 ng/mL LPS was the positive control for all ECIS experiments. Treatment with LPS consistently reduced barrier integrity within 2 hr post-treatment application (Figure 11C).

Apoptosis and necrosis of BMEC was increased by 13-HPODE treatment

Exposure of BMEC to 150 μM 13-HPODE for 6 hr significantly increased YOPRO®-1 staining over control indicating an increase in early apoptosis, whereas 0.5 μM and 30 μM 13-HPODE did not (Figure 12A). Similarly, exposure of BMEC to 150 μM 13-HPODE for 6 hr significantly increased propidium iodide staining over control indicating an increase in late apoptosis/primary necrosis, but 0.5 μM and 30 μM 13-HPODE did not (Figure 12B). There were no significant differences in apoptosis or necrosis after 24 hr 13-HPODE exposure (Figure 12C & D). Exposure to 2 mM H₂O₂ for 1 hr (positive control) demonstrated a significant increase YOPRO®-1 and propidium iodide staining (Figure 12A & B). Exposure of BMEC to 150 μM 13-HPODE for 6 hr significantly increased caspase 3/7 activity but 0.5 μM and 30 μM did not (Figure 13). Exposure to 1 mM H₂O₂ for 6 hr (positive control) demonstrated a significant increase in caspase 3/7 activity (Figure 13).

N-acetylcysteine ameliorates 13-HPODE-induced apoptosis and necrosis of BMEC

Co-exposure of BMEC to 150 μM 13-HPODE and 3 doses of N-acetylcysteine (0.1 mM, 1 mM, and 10 mM) prevented 13-HPODE-induced early apoptosis as demonstrated by decreased YOPRO®-1 staining over control (Figure 14A). Co-exposure of BMEC to 150 μM 13-HPODE and 2 doses of N-acetylcysteine (1 mM, and 10 mM) prevented 13-HPODE-induced late apoptosis/early necrosis as demonstrated by decreased propidium iodide staining over control (Figure 14B).

N-acetylcysteine rescues 13-HPODE-induced impairment of endothelial integrity

Co-exposure of BMEC monolayer to 150 μ M 13-HPODE and 1 mM N-acetylcysteine prevented a significant decrease in endothelial barrier integrity compared to exposure of 150 μ M 13-HPODE alone (Figure 15).

Discussion

Endothelial cells play an active role in inflammation in response to recognition of bacteria and bacterial products. One way in which activated endothelial cells may mediate the inflammatory response is through the enzymatic production of oxylipids (Weaver et al., 2001, Sordillo et al., 2005, Contreras et al., 2012b). Consistent with increased adhesion molecule expression in S. uberis-infected mammary tissue, our data demonstrated increased ICAM-1 and VCAM-1 expression in BMEC following exposure to S. uberis supernatant (Ryman et al., 2015). In contrast, expression of COX-2 and 15-LOX-1 mRNA in BMEC was not significantly changed by S. uberis exposure (Ryman et al., 2015). Previous murine studies suggested that COX-2 expression was dependent on recognition of pathogen associated molecular patterns by host pathogen receptors, such as toll like receptors (TLR) (Fukata et al., 2006). In the case of S. *uberis*, a recent study demonstrated an inability of heat-killed and live S. *uberis* to induce TLR-2 signaling in mammary epithelial cells (Gunther et al., 2016). Though our study did not evaluate TLR activity, failure to activate the BMEC TLR-2 pathway could result in a failure to induce significant expression of oxylipid biosynthetic enzymes, especially 15-LOX-1. Consistent with a failure to induce 15-LOX-1 mRNA expression, BMEC did not significantly increase 15-LOX-1 LA-derived oxygenation products. Additionally, the oxylipid profiles induced by BMEC during S. uberis exposure did not mimic previously described S. uberis-infected mammary tissue

profiles (Ryman et al., 2015). Most importantly, biosynthesis of 13-HODE by BMEC was not increased by *S. uberis* supernatant exposure suggesting that BMEC may not be an important source of 15-LOX-1 LA-derived oxygenation products in response to *S. uberis* supernatant.

Demonstrating that endothelial cells may not be an important source of 13-HODE during S. uberis exposure required evaluation of other potential oxylipid sources during an inflammatory response. In murine studies, the macrophages demonstrated the highest expression of 12/15-LOX and represented a significant source of 15-LOX-derived oxylipids (Huo et al., 2004, Mattmiller et al., 2014). Resident macrophages also are instrumental in alerting the surrounding mammary cells that a perceived insult is present (Aitken et al., 2011a). Therefore, we developed a primary bovine monocyte S. uberis-challenge model and showed that heat-killed S. uberis increased 15-LOX-1 expression and 13-HODE biosynthesis. Current findings were in contrast to *in vivo S*. uberis intramammary challenge, which did not demonstrate a significant increase in 15-LOX-1 mRNA expression in S. uberis-infected mammary tissue (Ryman et al., 2015). Collection of S. uberis-infected tissue may have occurred after peak 15-LOX-1 expression, especially because increased 13-HODE biosynthesis in S. uberis-infected mammary tissue supported increased 15-LOX-1 activity (Ryman et al., 2015). Additionally, the relative contribution of macrophages expression 15-LOX-1 compared to mammary epithelial cells and infiltrating neutrophils in infected tissue was not known (Thomas et al., 1994). Heat-killed S. uberis, but not S. uberis supernatant, exposure of bovine monocytes induced a significant increase in 13-HODE biosynthesis and may suggest optimal monocyte 15-LOX-1 activation requires recognition of bacteria by host pathogen recognition receptors, such as TLR-2 (Gunther et al., 2016). Nonetheless, our data suggested that bovine monocytes represented a more important source of

13-HODE, and potentially 13-HPODE, than mammary endothelial cells during *S. uberis* exposure. Investigating BMEC oxylipid biosynthesis in response to *S. uberis*-induced monocytederived oxylipid profiles could be beneficial for further understanding *S. uberis* pathogenesis. Additionally, future studies may evaluate the relative contributions of 13-HODE during *S. uberis* exposure by other mammary cells, including mammary epithelial cells and infiltrating neutrophils.

Our results demonstrated the capability of 13-HPODE, but not 13-HODE, to modify endothelial monolayer integrity. No other study evaluated the effect of 13-HODE on endothelial barriers, but a previous study demonstrated that arachidonic acid-derived hydroxyls were capable of reducing bovine microvascular retinal endothelial barrier integrity (Othman et al., 2013). The difference between the effects of arachidonic acid-derived hydroxyls and 13-HODE on barrier integrity could be due to endothelial cell origin as BMEC were from the macrovasculature whereas retinal endothelial cells were from the microvasculature (Kelly et al., 1998). In contrast to 13-HODE, we showed 13-HPODE reduced mammary endothelial barrier, but the reduction was not sustained throughout the duration of the treatment period suggesting an ability of the endothelial cells to overcome the adverse affects of 13-HPODE. During an inflammatory response to bacterial infection, however, there may be repeated exposure to newly synthesized 13-HPODE, which may not allow the endothelial barrier to recover. Though we anticipated 13-HPODE would decrease barrier integrity, confirmation of 13-HODE being unable to modify barrier integrity in our model was essential. Reduction of 13-HPODE generates 13-HODE and thus treatment with 13-HPODE would most likely contribute to increased exposure to 13-HODE as well. Other studies have showed differential effects of 13-HPODE and 13-HODE on endothelial

activation, but the present study was the first to demonstrate different effects on endothelial monolayer integrity (Friedrichs et al., 1999). In support of compromised barrier integrity, additional functional studies would be useful to evaluate how 13-HPODE may contribute to enhanced vascular permeability to macromolecules or uncontrolled leukocyte transmigration.

Apoptosis and necrosis of endothelial cells disrupts the continuous, single-cell layer necessary for orchestrating an effective and self-limiting inflammatory response. The current study demonstrated induction of apoptosis and necrosis of BMEC in conjunction with decreased barrier integrity. Our findings were consistent with previous work that demonstrated 13-HPODEinduced apoptosis in bovine aortic endothelial cells (Tampo et al., 2003, Dhanasekaran et al., 2004, Dhanasekaran et al., 2005). Though not evaluated in the current study, previous data suggested that 13-HPODE induced mitochondrial dysfunction resulting in the activation of the intrinsic pathway for apoptosis (Dhanasekaran et al., 2004, Dhanasekaran et al., 2005). For example, exposure of bovine aortic endothelial cells to 13-HPODE increased the activity of intrinsic pathway caspases 3 and 9, and was associated with a loss in mitochondrial function (Dhanasekaran et al., 2005). The primary proposed mechanism by which 13-HPODE induces apoptosis is by lipid peroxidation of cell membranes (Catala, 2009). Phospholipids in cell membranes contain an abundance of esterified PUFA and are extremely susceptible to lipid hydroperoxide attack. Propagation of lipid peroxidation occurs by decomposition of lipid hydroperoxides by transition metals to generate lipid alkoxyls (LO•), and lipid peroxyl radicals (LOO•) (Buettner, 1993). The lipid peroxyl radicals can act as pro-oxidants and attack membrane-esterified PUFA to generate additional LO•, LOO•, and LOOH, such as 13-HPODE. Peroxidation of lipid membranes initiated by extracellular 13-HPODE may contribute to an

irreversible increase in mitochondrial permeability and permanent loss of function (Vercesi et al., 1997). Thus preventing accumulation of lipid peroxides and other pro-oxidants may be protective or beneficial in limiting the effects of 13-HPODE (Hill-Kapturczak et al., 2003). Overall, the data from the current study demonstrated that shifting oxidant status in the endothelial microenvironment during 13-HPODE treatment by promoting reduction of pro-oxidants with an antioxidant may limit initiation and propagation of lipid peroxidation, thus preventing apoptosis and impaired barrier integrity.

Conclusions

The tightly regulated, self-limiting inflammatory response is dependent on optimal endothelial function and maintenance of the endothelial barrier. Some oxylipids may reduce the ability of endothelial cells to orchestrate an optimal inflammatory response. Thus, our study defined a potential source and role for 15-LOX-1 LA metabolites. Our data showed that bovine monocytes, but not BMEC, may be an important source of 15-LOX-1 oxygenation products of LA during *S. uberis* exposure. Furthermore, exposure of BMEC to 13-HPODE, but not 13-HODE, contributed to impaired mammary endothelial barrier integrity and apoptosis of BMEC. We also showed that oxidant status during 13-HPODE treatment may contribute to cell death and barrier integrity. Elucidating the mechanisms by which oxidant status mediates vascular function may be critical to developing targeted therapies for bovine mastitis.

Acknowledgements

The authors acknowledge the technical assistance Jeff Gandy and Jennifer Devries. This work was funded, in part, through grants (2011-67015-30179 and 2015-67011-23012) from the

Agriculture and Food Research Initiative Competitive Grants Programs of the USDA National Institute for Food and Agriculture and by an endowment from the Matilda R. Wilson Fund (Detroit, MI).

CHAPTER 4 SUPPLEMENTATION OF LINOLEIC ACID (C18:2N-6) OR A-LINOLENIC ACID (C18:3N-3) CHANGES OXYLIPID BIOSYNTHESIS FOLLOWING *EX VIVO*MICROBIAL EXPOSURE

Valerie E. Ryman¹, Nanda Packiriswamy¹, Bo Norby¹, Sarah M. Schmidt², Adam L. Lock², and Lorraine M. Sordillo^{1*}

¹ College of Veterinary Medicine, Michigan State University, East Lansing, MI 48824, USA
² Department of Animal Science, Michigan State University, East Lansing, MI 48824, USA

*Corresponding author

Dr. Lorraine M. Sordillo,
Department of Large Animal Clinical Sciences
College of Veterinary Medicine
Michigan State University
sordillo@msu.edu
Tel: (517) 432-8821

Fax: (517) 432-8822

Abstract

Oxylipids are derived from polyunsaturated fatty acids (PUFA) in cellular membranes and the relative abundance or balance of oxylipids may contribute to disease pathogenesis. Previous studies documented unique oxylipid profiles from cows with either coliform or *Streptococcus* uberis mastitis, suggesting that lipid mediator biosynthesis may be dependent on type of microbial agonist. However, changing the essential fatty acid (FA) content of leukocytes also may be critical to the relative expression of oxylipid profiles and the outcome of bacterial infection. There is no information in dairy cows describing how changing cellular PUFA content will modify oxylipids in the context of a microbial challenge. Therefore, the hypothesis was that supplementation of essential FA would change bovine leukocyte PUFA content and the expression of leukocyte-derived oxylipids following ex vivo microbial-challenge. To address the hypothesis, blood samples were collected from 6 cows before and after PUFA supplementation with linoleic acid (LA) and α -linolenic acid (ALA) and fatty acid content of leukocytes was quantified. Oxylipid biosynthesis was assessed after culture with *Streptococcus uberis* or lipopolysaccharide and was compared to oxylipid profiles of unstimulated leukocytes. Supplementation of ALA significantly increased ALA content of leukocytes, whereas supplementing LA had no effect. Though LA supplementation did not change leukocyte content, it did reduce S. uberis-induced arachidonic acid- and LA-derived oxylipids compared to S. uberis exposure without supplementation. Notably, ALA supplementation increased lipopolysaccharide-induced anti-inflammatory oxylipids from arachidonic acid and LA. Future investigations are needed to understand how activation of the leukocyte and availability of membrane PUFA interact to contribute to differential oxylipid biosynthesis.

Key words: oxylipid, polyunsaturated fatty acid, Streptococcus uberis, lipopolysaccharide

Introduction

The outcome of bovine mastitis may be dependent, in part, on potent lipid mediators derived from polyunsaturated fatty acids PUFA. Specifically, the oxygenation of PUFA following cleavage from the phospholipid membrane generates a profile of pro- and anti-inflammatory oxylipids. The profile of pro- and anti-inflammatory oxylipids may depend on the specific causative pathogen and its capability to induce different immune recognition and signaling pathways (Bannerman et al., 2004a; Mavangira et al., 2015; Ryman et al., 2015). For example, a diverse oxylipid profile was robustly upregulated in milk during severe Gram-negative coliform mastitis, whereas oxylipid profiles were not changed in milk during clinical Gram-positive Streptococcus uberis mastitis (Mavangira et al., 2015; Ryman et al., 2015). Coliform mastitis is characterized by an acute, robust inflammatory response with clinical symptoms appearing in as little as 8 h after challenge (Bannerman et al., 2004b; Moyes et al., 2014). In contrast, the uncontrolled inflammatory response to S. uberis does not result in clinical symptoms until several days after infection and may develop into a chronic inflammatory disease (Pedersen et al., 2003; Thomas et al., 1994). Thus, understanding oxylipid biosynthesis in the context of different microbial challenges may be critical for developing optimal nutritional and pharmacological strategies to manage disease prevalence and severity.

Several PUFA, including linoleic acid (LA, C18:2n-6), arachidonic acid (ArA, C20:4n-6), eicosapentaenoic acid (EPA, C20:5n-3), and docosahexaenoic acid (DHA, C22:6n-3), are the predominant substrates for oxylipid biosynthesis. The PUFA are esterified to the phospholipid membrane and are released by the action of calcium-dependent cytosolic phospholipase A₂ (Buczynski et al., 2009). An increase in intracellular calcium is induced by a variety of agonists

but a major stimulus is the recognition of bacterial pathogen-associated molecular patterns (PAMP) by host pathogen recognition receptors (PRR) (Chiang et al., 2012). Enzymatic and non-enzymatic pathways oxidize cleaved PUFA to create a complex network of oxylipids (Buczynski et al., 2009). Enzymatic oxidation pathways include the cyclooxygenase (COX), lipoxygenase (LOX), and cytochrome P450 (CYP) pathways. Non-enzymatic oxidation is mediated by reactive oxygen species and free radicals. Initial peroxidation products, such as prostaglandin (PG) G₂ and hydroperoxyoctadecadienoic acid, are immediately reduced to stable analogues, such as hydroxyoctadecadienoic acids (HODE), and hydroxyeicosatetraenoic acids (HETE) (Serhan and Petasis, 2011; Smith et al., 2011; Sordillo et al., 2005). Reduced oxylipids, such as hydroxyls and epoxides, also may serve as substrates for metabolism to dehydrogenase and hydrolase products, such as oxoeicosatetraenoic acids (oxoETE) and dihydroxyeicosapentaenoic acid (DiHETE) (Ramsden et al., 2012). The regulatory effects of oxylipids on inflammation may depend on method of oxidation and the degree of metabolism. For example, 5-LOX-derived 5-oxoETE induced neutrophil degranulation and leukocyte chemotaxis in various models (Hosoi et al., 2005; O'Flaherty et al., 1994). In contrast, 15-LOXderived lipoxin A₄ (LXA₄) prevented disruption of the rat small bowel mesenteric endothelial barrier during LPS challenge (Ereso et al., 2009). Interestingly, the precursor to LXA₄, 15hydroperoxyeicosatetraenoic acid, induced apoptosis of bovine aortic endothelial cells in an oxidative stress model (Sordillo et al., 2005).

In addition to the method of oxidation and degree of metabolism, one of the major factors that can alter oxylipid profiles is the availability of PUFA substrate. Linoleic acid and α -linolenic acid (ALA, C18:3n-3) are essential fatty acids (FA) that must be provided in the diet because de

novo synthesis requires desaturase enzymes that are absent in mammals (Nakamura and Nara, 2003). Dietary LA contributes to LA content in phospholipid membranes but also can be used for de novo ArA synthesis. Similarly, ALA can be used for EPA and DHA de novo synthesis. The de novo synthesis of ArA, EPA, and DHA requires a series of desaturation, elongation, and potentially β-oxidation events (Marcel et al., 1968; Sinclair et al., 2002). In monogastrics, feeding essential fatty acids (LA and ALA) or other PUFA derived from essential fats (ArA, EPA, and DHA) changed the FA profile of plasma and various tissues (Ramsden et al., 2012). Similarly, previous research showed that abundance and type of PUFA contained within the phospholipid membrane can be altered by the diet and influence the outcome or status of disease (Calder, 2008; Min et al., 2014; Raphael and Sordillo, 2013). For example, supplementation of obese pregnant women with 1200 mg EPA and 800 mg DHA resulted in decreased systemic markers of inflammation (Haghiac et al., 2015). One of the ways in which supplementation of PUFA is thought to mediate disease severity is through the biosynthesis of oxylipids. Supplementation of humans with 1008 mg EPA and 672 mg DHA contributed to greater EPAderived oxylipids, but not DHA-derived oxylipids (Schuchardt et al., 2014). Conversely, reducing nutritional LA in humans resulted in decreased abundance of plasma LA-derived oxylipids (Ramsden et al., 2012). In dairy cows, nutritional supplementation of PUFA is more challenging because isomerization and biohydrogenation of dietary PUFA by rumen microbes contributes to saturated FA biosynthesis from PUFA (Glasser et al., 2008; Jenkins et al., 2008). Recent studies utilized abomasal supplementation of PUFA to modify milk fat, but PUFA content of cells and tissues was not investigated, so it is unclear if abomasal supplementation changes cellular PUFA content as well as if there is any effect on oxylipids during inflammation. Thus, the hypothesis for the current study was that supplementation of PUFA would change

bovine leukocyte FA content and respective oxylipid profiles from *ex vivo* microbial-challenged leukocytes.

Materials and Methods

Chemicals and reagents

Liquid chromatography/mass spectrometry (LC-MS) grade acetonitrile, LC-MS methanol, formic acid, ethylenediaminetetraacetic acid (EDTA), and triphenylphosphine (TPP) were purchased from Sigma-Aldrich (St. Louis, MO. USA). Standards, deuterated and non-deuterated, and indomethacin were purchased from Cayman Chemical (Ann Arbor, MI, USA). Butylated hydroxy toluene (BHT) was purchased from ACROS (New Jersey, USA).

Supplementation of FA by abomasal infusion

All experimental procedures were approved by the Institutional Animal Care and Use Committee at Michigan State University. Six ruminally-fistulated multiparous mid-lactation Holstein cows (91.7 ± 8.36 days in milk) from the Michigan State University Dairy Field Laboratory (East Lansing, MI) were blocked by milk yield and randomly assigned to a treatment sequence in a replicated 3x3 Latin square design experiment with a 7-d preliminary period and three 7-d treatment periods separated by a 7-d washout periods (Lock et al., 2007). Prior to the first treatment period, all cows were fitted with an abomasal infusion line. All lines were flushed daily with water and ethanol during the treatment periods to ensure proper delivery of the FA infusion treatments into the abomasum. Treatments consisted of an ethanol carrier infusion (CON), LA infusion, and ALA infusion. The LA infusion blend was comprised of 82% safflower oil, 17% high omega flax oil, and 1% palm oil. The ALA infusion blend was comprised of 93%

high omega flax oil, 6% palm oil, and 2% safflower oil. Fat blends were dissolved in ethanol prior to infusion and administered at a dose of approximately 62 g/d with LA or ALA comprising approximately 40 g/d (Table 6). Daily infusions were divided and administered at 6-h intervals throughout each 7-d treatment period. The infusions were administered at 0500, 1100, 1700, and 2300 h. Blood was collected in 4 mM EDTA anticoagulant prior to each treatment period and after 7-d infusion period. Blood samples were transported back to the laboratory on ice for immediate collection to quantify FA in white blood cells (WBC) or for *ex vivo* challenge with microbial agonists. *Ex vivo* challenge with microbial agonists is described in the next section.

Cows were housed individually in tie stalls throughout the experiment. Access to feed was blocked from 0800 to 1000 h daily to allow for collection of orts and distribution of feed. Feed intake was measured daily and cows were fed at 115% of expected dry matter intake at 1000 h each day. Water was available *ad libitum* at all times. Stalls were bedded with sawdust and cleaned twice daily. The cows were milked twice daily at 0330 and 1630 h. The composition of the diet was a standard total mixed ration with mineral and vitamin supplementation (Table 7). The dry matter content of the forages was determined twice weekly and the diets were adjusted as needed.

Microbial agonist ex vivo challenge of blood leukocytes from non supplemented and supplemented animals

Heat killed *S. uberis* was prepared by first collection 3 pure *S. uberis* colony forming units (CFU) from a blood agar plate. The 3 CFU were added to 100 mL RPMI 1640 medium (Cellgro, Manassas, VA) containing 5% fetal bovine serum, 300 mg/mL L-glutamine, and 0.1 μM

selenium. The bacterial suspension was shaken at 37°C for 13 hr to exponential growth phase. After that time, the suspension was heat-killed in a 65°C water bath for 45 min. Suspensions were aliquoted at 10° CFU *S. uberis*/mL and frozen at -20°C until use. Ultrapure LPS (Invivogen, San Diego, CA) was purchased at a stock of 5 mg/mL and kept at -20°C until use. Blood samples from cows abomasally infused with ethanol carrier, LA, or ALA were aliquoted into pre-labeled 50 mL tubes and either 10⁷ CFU *S. uberis*/mL or 1 μg/mL LPS were added. Samples were gently rotated for mixing then incubated in a 37°C water bath for 4 h.

Whole blood processing for quantification of FA and oxylipids

Whole blood collected from animals in the 3 treatment groups (CON, LA, and ALA), but not cultured with microbial agonists, was collected and immediately spun at 4,816 x g for 20 min to enable separation of buffy coat. The buffy coat fraction was collected and deposited into a separate 50 mL tube. Ammonium-Chloride-Potassium lysing buffer (20 mL) was added and incubated for 4 min at room temperature to remove contaminating erythrocytes. To neutralize excess lysis buffer, 20 mL of PBS was added after incubation. The samples were spun at 4,816 x g for 5 min and the supernatant containing lysed erythrocyte fractions was discarded. The pellet was resuspended in 20 mL of PBS and washed twice. Lastly, the supernatant was discarded and the WBC pellet was stored at -80°C until further analysis. Whole blood collected from animals in the 3 treatment groups (CON, LA, and ALA) then cultured with microbial agonists (LPS and heat-killed *S. uberis*) for 4 h was centrifuged at 4,816 x g for 20 min at room temperature. A 2 mL aliquot of plasma then was collected and immediately flash frozen in liquid nitrogen until solid phase extraction.

Solid phase extraction of FA and oxylipids in WBC and cultured plasma

The WBC pellets were thawed on ice and resuspended in 600 µL of PBS. A 40 µL aliquot was collected for quantification of total DNA in each sample to normalize FA levels (Mattmiller et al., 2014; Silva et al., 2013). Total DNA was quantified using Broad Range Quant-iT DNA Assay kit (Life Technologies) according to manufacturer's instructions. Samples were sonicated after addition of 15 μL of internal standards and 4 μL of antioxidant reducing agent. The antioxidant reducing agent mixture was 0.9 mM of BHT, 0.54 mM EDTA, 3.2 mM TPP, and 5.6 mM indomethacin in 50% methanol, 25% ethanol, and 25% water. Samples were immediately frozen in liquid nitrogen and stored at -80°C. The internal standard mixture contained 0.25 µM 5(S)-HETE d_8 , 0.25 μ M 15(S)-HETE d_8 , 0.5 μ M 8(9)-epoxyeicosatrienoic acid (EET) d_{11} , 0.5 μ M PGE2 d_9 , 0.25 μ M 8,9- dihydroxyeicosatrienoic acid (DHET) d_{11} , 50 μ M AA d_8 , 2 μ M 2arachidonoyl glycerol d_8 and 0.2 μ M arachidonoyl ethanolamide d_8 . A volume of 900 μ L methanol was added to each sample. To release FA from cell membranes, samples were hydrolyzed with 3 mM potassium hydroxide and incubated at 45°C for 45 min. Samples were cooled, acidified to a pH < 3 using hydrochloric acid, and centrifuged at 4,816 x g for 45 min at 4°C. Supernatants were collected for solid phase extraction. For 4 h cultured plasma samples, all plasma aliquots were thawed on ice. A volume of 4 μL antioxidant reducing agent, 15 μL internal standards, and 2 µL formic acid was added. A volume of 5 mL methanol was added and the sample was vigorously vortexed for 2 min. Samples were incubated for 15 min at room temperature and then centrifuged at 14,000 x g for 10 min at 4°C. The supernatant was aspirated and added to 95 mL high performance liquid chromatography (HPLC) grade water and 95 µL formic acid. Solid phase extraction was conducted with Oasis HLB 12cc (500mg) LP Extraction Columns (Waters, Medford, Mass. USA) pre-conditioned with 6 mL of methanol followed by 6

mL of HPLC water. Sample extracts were loaded onto the columns and then washed with 6 mL of 20% methanol. Columns were dried under full vacuum for 4 min and extracts were eluted with 6 mL of methanol:acetonitrile 50:50 (V:V). Solvents were removed under vacuum using a Savant SpeedVac. Oxylipid extracts were reconstituted in 150 μ L of methanol:water (2:1) and centrifuged at 14,000 x g for 15 min at 4°C. The supernatant was transferred to a chromatography vial, topped with argon, and stored at -20°C until analysis.

LC-MS quantification of FA

The FA were quantified based on previously described techniques (Ryman et al., 2015). Briefly, reverse-phase LC on a Waters Acquity ultra performance LC BEH C18 1.7 μM column (2.1 x 100 mm) was used at a flow rate of 0.6 mL/min at 35°C. The quadropole MS was in electrospray negative ionization mode and voltage was -3 kV with the turbo ion spray source temperature at 450°C. The isocratic mobile phase for method 1 was acetonitrile:water:formic acid (45:55:0.01 v/v/v) and 15 min analysis time. Method 2 had an isocratic mobile phase consisting of acetonitrile:methanol:water:formic acid (47.4:15.8:26.8:0.01 v/v/v/v) and 10 min analysis time. A total of 5 PUFA, 2 SFA, and 1 MUFA were quantified by matching mass-1 and retention time with corresponding deuterated internal standard abundance and calibrated to a linear 5-point standard curve (R²>0.99). Fatty acids quantified by Waters Empower Z software (Waters, Milford, MA) for cultured plasma samples and hydrolyzed cell pellets were as follows: LA, ALA, ArA, EPA, DHA, palmitic acid, oleic acid, and stearic acid. The limit of detection was established as the lowest point of each standard curve.

LC-MS/MS quantification of oxylipids

Oxylipids were quantified based on techniques previously described (Mavangira et al., 2015). Briefly, a Waters Acquity UPLC coupled to a Waters Xevo TQ-S triple quadrupole mass spectrometer (Waters, Milford, MA) was employed. Mobile phase A was HPLC water with 0.1% formic acid, and mobile phase B was acetonitrile. Flow rate across the C18 HPLC column was 0.3 mL/min. Linear gradient steps were programmed in the following manner (A/B ratio): time 0 – 0.5 min (99/1), to (60/40) at 2.0 min; to (20/80) at 8.0 min; to (1/99) at 9.0 min; 0.5 min; held at (1/99) until min 13.0; then return to (99/1) at 13.01 min, and held at this condition until 15.0 min. Oxylipids were detected using electrospray ionization in negative-ion mode. Cone voltages and collision voltages were optimized using Waters QuanOptimize software (Mavangira et al., 2015).

Statistical analysis

Differences in FA and oxylipid concentrations due to *S. uberis* or LPS stimulation compared to unstimulated samples without PUFA supplementation (CON group) were determined by Student's t-tests. Determination of differences across treatments (CON, LA, and ALA) in WBC FA content was made by non-parametric one-way ANOVA with Dunn's correction. Differences in plasma FA and plasma oxylipid profiles among treatments following ex vivo microbial agonist exposure (CON, LA, and ALA) were tested as a three-treatments three periods cross-over analysis with random affect of cow nested within sequence by a PROC MIXED model. Tukey's correction was applied for multiple tests. Significance was set at $P \le 0.05$ for all tests.

Results

White blood cell FA concentrations following supplementation of LA and ALA

There was no change in LA content of WBC following LA supplementation (Figure 16A). Similarly, supplementing LA did not affect other PUFA (ALA, ArA, EPA, and DHA), saturated fatty acid (SFA) (palmitic acid and stearic acid), or monounsaturated fatty acid (MUFA) (oleic acid) (Figure 16B-H). In contrast, ALA content of WBC increased ($P \le 0.05$) following ALA supplementation (Figure 16B). Additionally, the ratio of LA/ALA after ALA supplementation decreased ($P \le 0.05$) relative to the non-supplemented group (CON) and LA supplemented groups (Figure 17D). There were no differences in other FA following ALA supplementation (Figure 16A, C-H). Similarly, there was no change in the sum of n-6 PUFA (Figure 2A), sum of n-3 PUFA (Figure 17B), or the ratio of n-6/n-3 following PUFA supplementation (Figure 17C).

FA following microbial challenge without PUFA supplementation

Whole blood exposed to heat-killed *S. uberis* for 4 h resulted in numerical decreases in all plasma PUFA, but only plasma ArA was significantly decreased ($P \le 0.05$) (Table 8). In contrast, whole blood exposed to LPS for 4 h did not reveal any differences in plasma FA (Table 8). Heat-killed *S. uberis* exposure of whole blood induced an increase ($P \le 0.05$) in LA-derived, ArA-derived, and EPA-derived oxylipids from the LOX and CYP oxidation pathways (Table 9). Heat-killed *S. uberis* increased biosynthesis of 13-oxooctadecadienoic acid (oxoODE), 15-oxoETE, 12-HETE, 14,15-DiHETE, and 17,18-DiHETE ($P \le 0.05$) (Table 9). Oxylipids not significantly changed in response to *S. uberis* are displayed in Table 14.

All oxylipids changed by LPS exposure ($P \le 0.05$) were derived from ArA and represented all 3 enzymatic pathways: COX, LOX, and CYP (Table 9). Lipopolysaccharide challenge increased 12- hydroxyheptadecatrienoic acid ($P \le 0.05$), but decreased 5,6-LXA₄ and 11,12- epoxyeicosatrienoic acid ($P \le 0.05$). The ratio of 11,12-EET/11,12-DHET was also decreased ($P \le 0.05$) suggesting a greater abundance of the downstream DHET compared to EET during LPS exposure relative to unstimulated plasma oxylipid profiles from bovine leukocytes. However, since the ratio of 11,12-EET/11,12-DHET is below 1, there is an abundance of DHET regardless of inflammatory challenge. Oxylipids not significantly changed in response to LPS are displayed in Table 14.

Microbial challenge-induced FA and oxylipid changes following LA and ALA supplementation

Linoleic acid supplementation increased ($P \le 0.05$) S. uberis-induced plasma ArA (Table 10) and changed the S. uberis-induced biosynthesis of 4 oxylipids ($P \le 0.05$): 12,13-epoxyoctadecadienoic acid (EpOME), 9-oxooctadecadienoic acid (oxoODE), 15-oxoETE, and 9-HETE (Table 11) compared to the non-supplemented group (CON). The S. uberis-induced biosynthesis of 12,13-EpOME, 9-oxoODE, and 15-oxoETE was decreased by LA supplementation relative to non-supplemented (CON) S. uberis exposure. Conversely, ALA supplementation increased ($P \le 0.05$) S. uberis-induced 9-HETE biosynthesis relative to non-supplemented (CON). The S. uberis-induced biosynthesis of ArA-derived CYP metabolite, 20-HETE, decreased ($P \le 0.05$) following ALA supplementation relative to LA supplementation, though there was no difference relative to non-supplemented (CON). A decrease ($P \le 0.05$) in S. uberis-induced plasma 12,13-EpOME also was demonstrated from ALA-supplemented cows

relative to non-supplemented (CON). *S. uberis*-induced oxylipids that were not significantly changed by treatments are in Table 15.

Supplementation of LA did not change LPS-induced plasma FA relative to non-supplemented (CON) (Table 12). There was an increase ($P \le 0.05$) in LPS-induced ArA following ALA supplementation relative to LA supplementation, though there were no differences relative to non-supplemented (CON). Supplementation of LA did not change LPS-induced plasma oxylipids. In contrast, LPS-induced 9-oxoODE, 13-oxoODE, and 5,6 LXA4 were all increased ($P \le 0.05$) due to ALA supplementation (Table 13). The LPS-induced plasma 9-oxoODE biosynthesis from ALA-supplemented cows was also significantly greater than LPS-induced plasma 9-oxoODE in cultured plasma from LA-supplemented cows. LPS-induced oxylipids that were not significantly changed by treatments are in Table 16.

Discussion

The availability or relative abundance of cellular PUFA content contributes to distinct oxylipid profiles during homeostasis and disease. Indeed, altering PUFA content in host cells is being pursued as a strategy to modify oxylipid biosynthesis in hopes of mitigating inflammation and reducing disease severity (Duda et al., 2009; Min et al., 2014; Raphael and Sordillo, 2013). Supplementation of ALA significantly increased ALA content of WBC in the present trial. However, supplementation of ALA did not result in increased EPA and DHA content of WBC, perhaps as a consequence of insufficient dose or not enough time with supplementation. A recent review concluded, based on a summary of ALA-supplementation trials, up to 40 g/d (a high dose for humans) and as many as 42 wk was required to consistently modify EPA content, with little

to no appreciable change in DHA content (Brenna et al., 2009). Additionally, elongase and desaturase enzyme activities were not evaluated in the study but may affect ALA conversion because the same elongase and desaturase enzymes may metabolize both LA and ALA (Guillou et al., 2010). Thus, the abundance of LA in the diet and in the leukocyte may outcompete ALA for elongation and desaturation. While our data does not fully support this claim because there was no change in LA or ArA content following ALA supplementation, we also did not measure all intermediary PUFA that have the ability to compete for elongases and desaturases (Patterson et al., 2012). Previous research also suggested there is no discrimination between incorporation of n-6 or n-3 PUFA and that the availability of PUFA in the phospholipid membrane is reflective of dietary intake (Dougherty et al., 1987; Lands et al., 1982). Though the potential for a maximal level of PUFA incorporation has yet to be thoroughly considered, an *in vitro* epithelial cell line study demonstrated that 50% of maximal incorporation of ALA was achieved by 10-20 µg/mL, whereas 50% of maximal incorporation of LA was at only 5-10 μg/mL (Bryan et al., 2001). Furthermore, previous research also indicated a potential negative effect of excess PUFA on the ability to incorporate PUFA by acyltransferases. In humans pre-fed a high LA diet prior to receiving LA or ALA, acyltransferase activity appeared reduced compared to humans pre-fed a high SFA diet (Emken et al., 1994). Authors hypothesized that the high LA in the prefed diet might decrease acyltransferase mRNA synthesis, support increase transport to the mitochondria for β -oxidation, or divert excess PUFA to adipose tissue for storage. Although conjecture, current and previous data suggest supplementation of PUFA already in abundance may prohibit further incorporation or changes in WBC PUFA content.

A complex network of oxylipids is synthesized in response to a variety of stimuli, including bacteria and bacterial-derived agonists. Previous studies supported the differential biosynthesis of oxylipids to Gram-negative and Gram-positive agonists, perhaps as a result of PAMP recognition during bovine mastitis (Mayangira et al., 2015; Ryman et al., 2015; Tam, 2013). Thus, it was not surprising that ex vivo exposure to LPS and S. uberis resulted in different oxylipid profiles because LPS mediates the inflammatory response through toll like receptor (TLR)-4, whereas the response to S. uberis is generally considered to be TLR-2 dependent (Bannerman et al., 2004a). The most striking difference in oxylipid profiles within the current study was that LPS contributed to a reduction in oxylipids with anti-inflammatory properties, whereas the inverse was true for S. uberis. Exposure to LPS in the current study reduced anti-inflammatory LXA₄ and 11,12-EET biosynthesis, which previous studies demonstrated could prevent endothelial barrier disruption and reduce pro-inflammatory cytokine expression (Ereso et al., 2009; Schmelzer et al., 2005). In contrast, S. uberis exposure induced biosynthesis of oxylipids that are ligands for activation of a nuclear receptor called peroxisome proliferator-activated receptor-y (PPAR-y) that can inhibit pro-inflammatory nuclear factor-κB (NF-κB) signaling (Shiraki et al., 2005; Snyder et al., 2015; Zhao et al., 2004). The significance of these changes in the context of mastitis was not elucidated in the current study, but highlighted a need to understand if different PRR signaling pathways directly mediates oxylipid biosynthesis in a similar way as the innate immune response (Strandberg et al., 2005).

The inflammatory response to LPS during coliform mastitis contributes to the production of lipid mediators from many different cell types. Thus, it was not surprising that there were fewer changes in oxylipids induced by *ex vivo* LPS exposure of leukocytes compared to milk and

plasma profiles during coliform mastitis (Mavangira et al., 2015). The contribution of replicating E. coli bacteria, sustained exposure to endotoxin secretion, and the participation of a variety of cells and tissues probably led to a more diverse oxylipid profile. Furthermore, the ex vivo model could not capture the contribution of adipose tissue lipolysis, which may be important as it is proposed to be the primary source of nonesterified FA during endotoxin-mediated inflammation (Moyes et al., 2014; Zu et al., 2009). This limitation may be supported by the absence of any changes in nonesterified LA in the current study compared to almost a 3-fold increase measured in milk and plasma during bovine coliform mastitis (Mayangira et al., 2015). Though there were limitations with the current model, ex vivo exposure of WBC may be critical in understanding the specific contributions to oxylipid biosynthesis of blood leukocytes during LPS exposure. In fact, some similarities in oxylipid biosynthesis were detected between ex vivo and in vivo studies. Decreased anti-inflammatory 5,6-LXA₄ and 11,12-EET in the current study was consistent with plasma oxylipids during coliform mastitis, but inverse to the change in milk oxylipids (Mayangira et al., 2015). Authors hypothesized that the inverse relationship between milk and plasma oxylipids may be the result, in part, of a breakdown in the blood-milk barrier. Our findings may suggest there also was a decrease in the oxylipid production from blood cells contributing to reduced plasma expression during coliform mastitis.

Oxylipids profiles induced by *S. uberis* in the current study also were in contrast to previous work. For example, intramammary *S. uberis* challenge did not induce changes in milk oxylipids whereas the current study demonstrated increases in ArA-, LA-, and EPA-derived oxylipids (Ryman et al., 2015). The lack of changes in milk oxylipids following intramammary *S. uberis* challenge compared to current findings may be attributed, in part, to the difference in oxylipid

profile size and dilution of oxylipids in milk. For example, the current study included a much wider oxylipid profile, especially including more CYP- and EPA-derived oxylipids than the previous work (Ryman et al., 2015). A wider profile in the current study is the reason we were able to report increased 14,15-DiHETE and 17,18-DiHETE, though their functions in the inflammatory response are unknown. Similarly, 12-HETE was not previously quantified in milk or tissue from S. uberis challenge, but the inflammatory properties are contradictory depending on the model and warrant further investigation (Bolick et al., 2005; Kronke et al., 2009). While 13-oxoODE and 15-oxoETE, both ligands for PPAR-γ, were quantified in milk and tissue from S. uberis challenge animals similar to the current study, only ex vivo exposure of leukocytes to S. *uberis* resulted in increased biosynthesis. The inconsistency of 13-oxoODE and 15-oxoETE biosynthesis between the current study and intramammary S. uberis challenge may be a function of different stages of inflammation, in the case of S. uberis tissue, and dilution of oxylipids in milk limiting the detection of appreciable changes. A final important finding was that, in general, significantly changed S. uberis-induced oxylipids (oxoODEs, oxoETEs, and DiHETEs) represented a greater degree of metabolism from their precursors. It is unknown how S. uberis recognition may influence the activity of downstream enzymatic metabolism in leukocytes, but may be important when developing pharmacologic intervention strategies during mastitis.

Aside from the potential effect of pathogen recognition pathways, oxylipid profiles heavily depend on availability of cellular PUFA content. In the current study, the goal of LA supplementation was to modify cellular PUFA content and also alter microbial agonist-induced oxylipid profiles. However, we showed in the present study that LA supplementation did not modify PUFA content, but could have affected other levels of oxylipid biosynthesis regulation,

including oxidation pathway and degree of metabolism, during microbial exposure (Mavangira et al., 2015; Ramsden et al., 2012). Our data supports a potential effect of LA supplementation on oxidation pathway during *S. uberis* exposure because oxylipids that changed represented different enzymatic (12,13-EpOME from CYP and 15-oxoETE from 15-LOX-1) and nonenzymatic oxidation pathways (9-oxoODE). However, the effect of LA supplementation on degree of metabolism was not conclusive as there were no changes in the ratios of upstream hydroxyls (e.g., HETE) to downstream ketones (e.g., oxoETE) following *S. uberis* exposure. The reason for a decrease in these specific oxylipids is unclear, but previous data demonstrated an inhibitory effect of PUFA on some CYP isoforms and the ability of 15-LOX-1 to undergo suicide inactivation due to its own metabolites (Wiesner et al., 2003; Yao et al., 2006).

Additional studies are required to understand how supplemental PUFA, without a change in cellular PUFA content, may negatively affect enzymatic FA oxidation pathways, especially in the context of microbial challenge.

Feeding whole linseed as a source of ALA rather than fish oil supplementation is a more common approach to increase n-3 fats in milk because milk composition is negatively affected (Petit et al., 2002). Thus, it is important to understand if ALA supplementation is beneficial in promoting anti-inflammatory and pro-resolving oxylipid biosynthesis during microbial exposure. Our results suggested that supplementing ALA at the current dose and duration is not sufficient to alter oxylipids from EPA- and DHA, which was consistent with an inability to alter EPA and DHA content. In fact, supplementation with ALA suggested increased lipid peroxidation because *S. uberis*-induced non-enzymatically-derived 9-HETE relative to no PUFA supplementation. Increased ALA content in leukocytes, with no appreciable decreases in other PUFA, would

increase the availability of PUFA for lipid peroxidation (Guido et al., 1993). Lipid peroxidation is implicated in dysfunctional inflammatory responses and inflammatory-based diseases (Catala, 2009). However, other markers of lipid peroxidation like the ArA-derived isoprostanes were not increased with ALA supplementation, thus it cannot be concluded that the synthesis of 9-HETE was reflective of a detrimental event. In contrast to 9-HETE during S. uberis exposure, ALAsupplementation contributed to greater LPS-induced biosynthesis of anti-inflammatory oxylipids, 9-oxoODE, 13-oxoODE, and 5,6-LXA₄. Biosynthesis of LXA₄ is instrumental in decreasing leukocyte recruitment and migration, as well as promoting resolution of inflammation (Serhan, 1994). Similarly, 9- and 13-oxoODE are ligands for anti-inflammatory PPAR-γ (Itoh et al., 2008; Nagy et al., 1998). Adding exogenous 9-oxoODE to a macrophage model of oxidative stress deficient in 9-oxoODE decreased TNF-α release (Mattmiller et al., 2014). Perhaps decreasing the ratio of LA/ALA in leukocytes, as our study showed after ALA supplementation, contributed to the presentation of a more anti-inflammatory profile regardless of the oxylipid substrate (Poulsen et al., 2008). Our study strongly illustrated the need to evaluate a diverse array of oxylipids following manipulation of PUFA content or PUFA supplementation. Evaluation of PUFA supplementation, both n-6 and n-3, through the careful analysis of a more diverse oxylipid profile may be critical to identifying specific and novel methods of controlling disease severity and duration. Additionally, given the use of linseed for ALA rather than fish oil for EPA and DHA in dairy cattle, future studies are needed to determine whether it is possible to sufficiently increase EPA- and DHA-derived oxylipids with ALA supplementation. Perhaps increased EPAand DHA-derived oxylipids are not required if increasing the abundance of anti-inflammatory n-6 derived oxylipids, such as lipoxins and oxoODEs, can be consistently achieved.

Conclusions

Oxylipid biosynthesis during microbial exposure is dependent on several factors, including type of agonist and PUFA availability. Supplementation of ALA increased ALA content of WBC and decreased the ratio of LA/ALA, but no change in EPA and DHA content suggested that dose or duration of ALA supplementation may be important for enhanced EPA and DHA content. Consistent with no change in EPA and DHA content after ALA supplementation, microbialinduced EPA- and DHA-derived oxylipids were not increased after ALA supplementation. However, LPS-induced anti-inflammatory oxylipids from n-6 FA were increased following ALA supplementation. Perhaps the ratio of LA/ALA content is equally, if not more, important in mediating oxylipid biosynthesis during microbial challenge than absolute abundance. Furthermore, data indicated that LA supplementation could affect S. uberis-induced oxylipid biosynthesis without changing PUFA content in bovine leukocytes suggesting that supplemental PUFA can affect other levels of oxylipid biosynthesis, like method of oxidation or degree of oxylipid metabolism. Though oxylipid profiles are inherently dependent on phospholipid PUFA content, the interaction with pathogen recognition pathways could contribute to modification of other regulatory levels of oxylipid biosynthesis, such as method of oxidation. The data presented in this manuscript are essential to enhancing our understanding of PUFA and oxylipid biosynthesis during different microbial exposures in the dairy cow.

Acknowledgements

This work funded from the Matilda R. Wilson Fund (Detroit, MI), the Agriculture and Food Research Initiative Competitive Grants Program of the USDA National Institute for Food and Agriculture (2011-67015-30179 and 2015-67011-23012), Rackham Research Endowment, and

Michigan State University AgBioResearch. Technical assistance provided by Jeff Gandy and Courtney Preseault was instrumental in the completion of these experiments.

CHAPTER 5 SUMMARY AND CONCLUSIONS

The broad goal of this dissertation was to determine the contribution of linoleic acid oxygenation products on endothelial integrity and viability during inflammation. Inflammation is necessary to quickly and sufficiently resolve bacterial infections. Previous data in our lab and others suggested that an imbalance in fatty acid oxygenation products, called oxylipids, could contribute to dysfunctional inflammatory responses during mastitis. Oxylipids are synthesized from lipid membrane-derived polyunsaturated fatty acids (PUFA) by enzymatic and nonenzymatic pathways. Endothelial cells robustly produce and respond to oxylipids, which can modulate inflammatory responses. However, during Streptococcus uberis mastitis endothelial dysfunction is implicated as a potential cause for uncontrolled inflammation. Since linoleic acid (LA) is the most predominant PUFA in dairy cows and LA oxygenation products were previously shown to influence vascular activation and viability, this dissertation focused on the potential contribution of LA-derived oxylipids to mediate endothelial dysfunction during S. uberis mastitis. Chapter 2 demonstrated that the LA hydroxyl metabolite, 13hydroxyoctadecdienoic acid (13-HODE), was increased following intramammary S. uberis challenge. In chapter 2 and other studies, 13-HODE and the initial oxygenation product of LA metabolism, 13-hydroperoxyoctadecadeinoic acid (13-HPODE), were demonstrated to activate, and in some cases, kill endothelial cells. The contribution of the specific LA metabolites to compromise endothelial barrier integrity was not known. Thus, chapter 3 sought to define a role for 13-HODE and 13-HPODE in compromised barrier integrity. We showed that 13-HPODE, but not 13-HODE reduced endothelial barrier integrity. Apoptosis and necrosis were implicated in contributing to the adverse effects of 13-HPODE. Finally, chapter 4 defined the ability to change the PUFA content of leukocytes and subsequently modify the oxylipid profiles during microbial challenge. Understanding the limitations of changing microbe-induced oxylipid

profiles may be essential to develop strategies to modify fatty acid metabolism in the oxylipid network and potentially alter the inflammatory phenotype.

Chapter 2

Oxylipid profile induced during S. uberis mastitis was unknown prior to completion of objective 1. Thus, chapter 2 aimed to define changes in a carefully selected oxylipid profile during different stages of S. uberis mastitis. The most interesting finding in the first study was the predominance of LA-derived oxylipids, HODE and 13-oxooctadecadeinoic acid (13-oxoODE), regardless of infection status. Greater quantities of LA-derived oxylipids were not necessarily surprising given that dairy cows receive a diet high in LA and previous work demonstrated a predominance of 9 and 13-HODE in plasma from periparturient dairy cows (Raphael et al., 2014). This was the first study, however, to show increased 9- and 13-HODE in S. uberisinfected mammary tissue relative to uninfected tissue. In contrast, 9- and 13-HODE were not increased in milk from S. uberis challenged animals, possibly from oxylipid retention within the mammary tissues due to oxygenation of esterified PUFA or re-esterification of products after synthesis (Kozak et al., 2002, Morgan et al., 2009). These findings also highlighted the difference in microbial agonists in inducing oxylipid biosynthesis because a previous study found increased 9- and 13-HODE in milk from cows with severe bovine coliform mastitis (Mavangira et al., 2015). The difference in HODE biosynthesis between coliform mastitis and S. *uberis* mastitis could be related to pathogen signaling pathways and subsequent magnitude of response.

In particular, the findings in chapter 2 indicated the potential importance of the 15-LOX-1 derived linoleic acid oxygenation products. The initial oxygenation product is capable of killing cells in various models, but especially endothelial cells (Tampo et al., 2003, Dhanasekaran et al., 2004, Dhanasekaran et al., 2005). Several previous reports indicated that 13-HODE was capable of inducing vascular activation, cytokine production, and even oxylipid biosynthesis (Setty et al., 1987, Friedrichs et al., 1999, Szklenar et al., 2013). Thus, the final piece of this chapter demonstrated that bovine mammary endothelial cells (BMEC) were capable of differentially responding to 13-HPODE versus 13-HODE by assessing the mRNA expression of the inducible oxylipid biosynthetic cyclooxygenase-2 enzyme. Our data showed that 13-HPODE at 30 μM significantly increased cyclooxygenase-2 mRNA expression, whereas 13-HODE did not induce any change. The importance of 13-HPODE and its ability to compromise the inflammatory response, especially by inducing death of endothelial cells, was illustrated in previous studies and provided the framework and rationale for *in vitro* investigation in chapter 3.

Lastly, the final point reflects on differences in oxylipid profiles from chapter 2 compared to the findings in chapter 4 following ex vivo challenge with *S. uberis*. The assessed oxylipid profile compromised a snapshot of the total lipidome, but was carefully selected based on criteria to include variety of oxylipids (Wang et al., 2014). Thus, inclusion factors included published evidence of pro- and anti-inflammatory functions, expression within tissue of interest, diversity of PUFA substrates, diversity of oxidation pathways, and representative of varying degrees of metabolism. A limitation in the second chapter of this dissertation is that the oxylipid profile did not include a larger selection of oxylipids from the CYP and non-enzymatic oxidation pathways, as well as an abundance of EPA- and DHA-derived oxylipids. However, this limitation is

retrospective because at the time experiments from chapter 2 were conducted, the importance and functions of oxylipids included in our later array were less well defined than our chosen profile. Additionally, technical advancements in lipidomics allowed for an expanded, yet still focused, oxylipid profile in chapter 4.

Chapter 3

The first task in chapter 3 was to develop an endothelial cell S. uberis challenge model to investigate the potential relative contribution of BMEC to 13-HODE biosynthesis. The BMEC responded to S. uberis exposure with increased adhesion molecules and IL-8 mRNA expression, but failed to induced COX-2 and 15-LOX-1 mRNA. Expression of COX-2 is considered highly inducible in all cell types by various agonists, however, there is some evidence to support that COX-2 expression may be dependent on pathogen recognition pathways during bacterial infection (Fukata et al., 2006). In in vitro human and murine macrophage models, activation of TLR-7 was responsible, in part, for activation of DHA oxidation and metabolism pathways (Koltsida et al., 2013). Perhaps optimal activation of oxylipid biosynthetic enzymes in BMEC requires activation of a pathogen recognition pathway, though the specific pathway to implicate is not clear. Nonetheless, BMEC did not produce 13-HODE in response to S. uberis supernatant. Similarly, previous studies demonstrated that bovine aortic endothelial cells were capable of synthesizing 13-HODE, however there was not a significant increase during LPS exposure (Contreras et al., 2012a, Contreras et al., 2012b). It appeared that BMEC may not represent a predominant source of 13-HODE in response to S. uberis alone though we cannot rule out the possibility that BMEC could produce 13-HODE in response to other inflammatory mediators, including oxylipids.

Because endothelial cells did not represent a significant source of 13-HODE in our current model other potential sources were considered. The tissue macrophage is the predominant leukocyte in the healthy mammary gland and is capable of contributing a variety of inflammatory mediators, including oxylipids, to the inflammatory milieu. In mice, a 15-LOX-1 equivalent is expressed in the highest amounts in macrophages (Huo et al., 2004). It is unknown if the same is true in the bovine species, but a previous study was able to detect 15-LOX-1 mRNA in peripheral blood mononuclear cells (Raphael et al., 2014). Though correlations could not be established between 15-LOX-1 mRNA and HODE biosynthesis, the protein abundance and activity of 15-LOX-1 was not quantified and may be different than mRNA expression. Given the importance of macrophages and the potential activity of 15-LOX-1, developing a primary bovine monocyte *S. uberis* challenge model was the next logical step and demonstrating increased 13-HODE biosynthesis by monocytes would recapitulate, to a degree, the *in vivo* findings from *S. uberis*-infected mammary tissue.

We were able to demonstrate a significant increase in 13-HODE biosynthesis in conjunction with increased 15-LOX-1 mRNA expression following exposure of bovine monocytes to heat-killed *S. uberis*. Interestingly, *S. uberis* supernatant did not induce 13-HODE biosynthesis and only minimally induced 15-LOX-1 mRNA expression at 4 hr, which may support the claim made previously that optimal biosynthesis of LA oxygenation products requires activation of pathogen recognition pathways (Fukata et al., 2006). Though demonstrating increased 13-HODE by bovine monocytes suggested that they represent a potential significant source of 15-LOX-1 oxidized products from LA, it does not negate the contribution of other cells to the oxylipid pool

in *S. uberis*-infected mammary tissue. Mammary epithelial cells would be one of the first cell types to recognize and respond to *S. uberis*, aside from leukocytes in the milk, and previous work demonstrated the ability of human airway and bovine mammary epithelial cells to synthesize oxylipids in response to various non-microbial agonists (Erlemann et al., 2007, Piotrowska-Tomala et al., 2012). Given the interaction of many different cell types within the mammary gland, defining *S. uberis*-induced oxylipid profiles in a dual cell monocyte/endothelial cell or epithelial cell/endothelial cell model may be a critical next step.

The second part of chapter 3 was to determine if 13-HODE or 13-HPODE decreased endothelial barrier integrity and if apoptosis may contribute to this phenotype. Findings demonstrated that 13-HPODE, but not 13-HODE, decreased barrier integrity. Subsequently, data showed that induction of apoptosis and necrosis may contribute to decreased barrier integrity. The ability to prevent apoptosis, necrosis, and impaired barrier integrity by co-exposure to an antioxidant provided support for the potential involvement of lipid peroxidation in mediating the detrimental effects of 13-HPODE (Catala, 2009). Reduction of the pro-oxidant load by antioxidants may limit pro-oxidant attack of lipid membranes thus enabling endothelial cells to overcome adverse outcomes induced by 13-HPODE. In chapter 3, a proposed result of lipid peroxidation is mitochondrial dysfunction induced by the irreversible enhancement of mitochondrial membrane permeability (Vercesi et al., 1997). Activation of the intrinsic apoptotic pathway may also be mediated by the end product of lipid peroxidation, 4-hydroxynonenal (4-HNE), of which 13-HPODE is a primary precursor. The mechanisms of its action are incompletely understood but several reports provided evidence for the ability of 4-HNE to activate cytoplasmic p53, thus promoting transcription and translation of pro-apoptotic proteins (Chaudhary et al., 2010,

Abarikwu et al., 2012). Additionally, 4-HNE may also activate the extrinsic pathway of apoptosis but it can diffuse out of the cell and interact with the Fas death ligand (Chaudhary et al., 2010, Dalleau et al., 2013). Thus, future investigations are warranted to determine the pathways by which 13-HPODE mediates apoptosis as it most likely contributes to multiple events.

Chapter 4

Since our findings in the chapters 2 and 3 demonstrated the potential importance of oxylipids profiles during microbial exposure, identifying an ability to modify profiles may be instrumental in altering the course of a disease. Several strategies are currently employed to modify oxylipid profiles and include nutritional modulation of dietary PUFA, pharmacologic inhibition of major oxidation pathways, and recently, pharmacologic inhibition of some downstream oxylipid metabolic pathways. Whereas pharmacologic intervention can be used to limit clinical symptoms or prevent severe disease, nutritional modulation with supplementation of dietary PUFA can be preemptive by contributing to the formation of oxylipids with pro- and anti-inflammatory properties. Thus, the goal of chapter 4 was to modify microbial-induced oxylipid biosynthesis through the manipulation of leukocyte PUFA content by PUFA supplementation.

There were three major findings in chapter 4. First, we demonstrated that the pathogens that are known to activate different recognition signaling pathways, such as toll like receptors, in host cells contributed to different oxylipid profiles (Aitken et al., 2011, Gunther et al., 2016). *Ex vivo* exposure of leukocytes to Gram-positive *S. uberis* induced the biosynthesis of several oxylipids with anti-inflammatory properties, where LPS exposure reduced the biosynthesis of some anti-

inflammatory oxylipids. Our findings for each microbial agonist was compared to previous *in vivo* work and both similarities and differences were found. Milk and plasma from cows with coliform mastitis demonstrated a more diverse profile compared to *ex vivo* LPS exposure which would be expected given the contribution of a wide variety of tissues and complex milieu of inflammatory mediators (Mavangira et al., 2015). Specifically, reduced biosynthesis of 5,6-LXA and 11,12-EET after *ex vivo* LPS exposure was consistent with plasma oxylipids in cows with coliform mastitis, suggesting that a reduction in some oxylipids in the blood during coliform mastitis may be the result of decreased biosynthesis by blood leukocytes. Of course, the impact of blood-milk barrier disruption on plasma oxylipid profiles should not be negated. Previous *in vivo* findings may be a reflection of both barrier disruption and decreased oxylipid biosynthesis from leukocytes (Ereso et al., 2009, Kobayashi et al., 2013).

No similarities in oxylipid profiles were detected between *ex vivo S. uberis* exposure of blood leukocytes and milk or mammary tissue from *S. uberis*-challenged cows (Ryman et al., 2015). We were unable to draw any comparisons with the DiHETEs because they were not included in the *in vivo* profile panel, but others hypothesize that DiHETEs may not have any relevant biological activity and are only an indication that the anti-inflammatory precursor was biosynthesized(Zhao et al., 2004, Ryman et al., 2015). Similarly, 12-HETE was not included our *in vivo* profile, but the likelihood of detection is unclear. Origin of 12-HETE is generally considered platelet-derived, though there is some evidence a bovine leukocyte-type 12-LOX exists (Wong et al., 2001, Porro et al., 2014). Lastly, 13-oxoODE and 15-oxoETE were measured in the current *ex vivo* model and were increased, whereas the previous *in vivo S. uberis* challenge study found no significant change (Ryman et al., 2015). A marginal change in milk

oxylipids could be a result of fluid dilution or oxylipids were retained within mammary tissues by esterification to phospholipids (Morgan et al., 2009). Though we measured oxylipids in *S. uberis* mammary tissue, samples were not hydrolyzed and thus would not capture the expression of potentially retained oxylipids. The inconsistency with *S. uberis*-infected mammary tissue may be a result of different stages of lactation at collection, as tissue was obtained 3 days post-challenge compared to a 4 hr exposure period in the *ex vivo* model (Ryman et al., 2015). Though additional studies are needed to understand how prominent a role oxylipid biosynthesis by blood leukocytes plays in *S. uberis* mastitis, our findings indicate that different pathogens are capable of inducing different oxylipid profiles.

The second major finding was that even though LA supplementation did not alter leukocyte PUFA content, oxylipid biosynthesis was significantly altered. Supplementation with LA decreased LA- and ArA-derived oxylipids from the CYP and LOX pathways. Since PUFA substrate in leukocytes did not change and may not have contributed to a change in lipid mediator biosynthesis, differential oxylipid profiles may be due to modification of oxidation pathways or an effect of the degree of metabolism of oxygenation products. Previous work demonstrated the ability of LA to inhibit some CYP isoforms (Yao et al., 2006). Similarly, suicide inactivation of 15-LOX-1 by its own metabolites can contribute to decreased biosynthetic activity (Wiesner et al., 2003). Indeed, our *ex vivo* model demonstrated increased 15-oxoETE, the ketone derivative of 15-LOX-1 ArA metabolism, before LA supplementation and then was decreased after LA supplementation. The functional properties of the oxylipids significantly decreased by LA supplementation (12,13-EpOME, 9-oxoODE, and 15-oxoETE) were collectively shown by others to have anti-inflammatory or protective functions during disease

(Zhao et al., 2004, Shiraki et al., 2005). Our findings may further support the idea that excessive intake of LA may promote an imbalance of pro- and anti-inflammatory oxylipids (Patterson et al., 2012).

The third major finding was that ALA supplementation increased ALA content of leukocytes and changed microbial agonist-induced oxylipid biosynthesis, but did not specifically change EPAand DHA-derived oxylipids. The present study was the first to investigate the effect of ALA supplementation on cellular PUFA content in bovine cells. Fish oil negatively affects milk composition and for this reason linseed is instead supplemented as a source of ALA to increase beneficial n-3 content in milk (Petit et al., 2002). However, our findings suggest that supplementation of ALA may not necessarily be positive in all respects, though we did not evaluate the effect of supplementation on the inflammatory phenotype. An increase in S. uberisinduced 9-HETE after ALA supplementation indicated that non-enzymatic lipid peroxidation had occurred (Guido et al., 1993). In contrast to the potential detrimental effect of lipid peroxidation by ALA supplementation, LPS-induced biosynthesis of ArA-derived and LA-derived oxylipids with anti-inflammatory functions were increased relative to non-supplemented. It is possible that by reducing the ratio of LA/ALA in leukocytes, the biosynthesis of anti-inflammatory oxylipids over pro-inflammatory oxylipids was fostered, though the mechanism is unclear (Patterson et al., 2012). Thus, our data showed that it was not necessary to decrease n-6 PUFA content, or increase EPA and DHA content, to modify oxylipid profiles. Perhaps intermediary PUFA and oxygenation productions that we did not measure contributed to differential oxylipid biosynthesis (Levin et al., 2002). Our data suggested that perhaps supplementation with ALA, instead of EPA and DHA, in dairy cows may still promote biosynthesis of anti-inflammatory

oxylipids derived from n-6 fatty acids. However, additional studies are needed to determine if any functional differences in the immune response are evident with increased cellular ALA content and increased anti-inflammatory oxylipids from n-6 PUFA.

APPENDICES

Appendix A. Authorization to publish Chapter 1 in dissertation

CAMBRIDGE UNIVERSITY PRESS LICENSE TERMS AND CONDITIONS

May 19, 2016

This Agreement between Valerie Ryman ("You") and Cambridge University Press ("Cambridge University Press") consists of your license details and the terms and conditions provided by Cambridge University Press and Copyright Clearance Center.

3847161037297 License Number Apr 13, 2016 License date

Licensed Content Publisher Cambridge University Press Licensed Content Animal Health Research Reviews

Publication

Licensed Content Title Role of endothelial cells in bovine mammary gland health and

Licensed Content Author Valerie E. Ryman, Nandakumar Packiriswamy and Lorraine M.

Sordillo

Licensed Content Date Aug 25, 2015

Licensed Content Volume

Number

16

Licensed Content Issue 02

Number

135

Start page End page 149

Type of Use Dissertation/Thesis

Requestor type Author Portion Full article

Author of this Cambridge Yes University Press article

Author / editor of the new Yes

Order reference number None Territory for reuse World

Title of your thesis /

dissertation

Oxidized linoleic acid oxylipids modify mammary barrier

integrity during inflammation

Expected completion date Jun 2016 Estimated size(pages)

Requestor Location Valerie Ryman

9134 E. Coleman Rd.

HASLETT, MI 48840 **United States** Attn: Valerie Ryman

Billing Type Invoice

Billing Address Valerie Ryman

9134 E. Coleman Rd.

HASLETT, MI 48840 **United States** Attn: Valerie Ryman

Total 0.00 USD

Terms and Conditions

Appendix B. Authorization to publish Chapter 2 in dissertation

ELSEVIER LICENSE TERMS AND CONDITIONS

May 19, 2016

This is a License Agreement between Valerie Ryman ("You") and Elsevier ("Elsevier") provided by Copyright Clearance Center ("CCC"). The license consists of your order details, the terms and conditions provided by Elsevier, and the payment terms and conditions.

All payments must be made in full to CCC. For payment instructions, please see information listed at the bottom of this form.

Supplier Elsevier Limited

The Boulevard, Langford Lane Kidlington, Oxford, OX5 1GB, UK

Registered Company

Number

1982084

Customer name Valerie Ryman Customer address 9134 E. Coleman Rd. HASLETT, MI 48840

License number 3847090595095 License date Apr 13, 2016 Licensed content publisher Elsevier

Licensed content

publication

Prostaglandins and Other Lipid Mediators

Licensed content title Quantification of bovine oxylipids during intramammary

Streptococcus uberis infection

V.E. Ryman, G.M. Pighetti, J.D. Lippolis, J.C. Gandy, C.M. Licensed content author

Applegate, L.M. Sordillo

Licensed content date

September 2015 121

Licensed content volume number

Licensed content issue number

Number of pages 11 Start Page 207 **End Page**

Type of Use reuse in a thesis/dissertation

Portion full article

both print and electronic Format

Are you the author of this Yes

Elsevier article?

Will you be translating?

Title of your

Oxidized linoleic acid oxylipids modify mammary barrier

thesis/dissertation integrity during inflammation

Expected completion date Jun 2016 Estimated size (number of 150

pages)

Elsevier VAT number GB 494 6272 12 Permissions price 0.00 USD

VAT/Local Sales Tax 0.00 USD / 0.00 GBP

0.00 USD

Terms and Conditions

Appendix C. Tables

Table 1. Summary of inflammatory mediator production during bovine mastitis

Models	Selected findings	References
Experimental in	ntramammary challenge	
LPS	\uparrow mammary tissue TNF α , COX-2, LF, LZ, and iNOS mRNA	(Schmitz et al., 2004)
LPS	\spadesuit plasma PGE ₂ , 15-keto-PGF _{2α} , LTB ₄ , and LTC ₄ and milk TXB ₂	(Piotrowska-Tomala et al., 2012, Anderson et al., 1986)
E. coli	Severity correlated with \uparrow plasma TNF- α and milk PGE ₂	(Pezeshki et al., 2011)
E. coli	↑ milk IL-1, IL-6, IL-8, complement fragment C5a, and TNFα	(Shuster et al., 1997)
E. coli	\uparrow milk IL-1β, IL-12, IFN-γ, IL-8, IL-10, and TNFα	(Bannerman et al., 2004b)
K. pneumoniae	\uparrow plasma PGF _{2α} and milk histamine, 5-HT, TxB ₂ , PGE ₂ , and PGF _{2α}	(Zia et al., 1987)
S. marcescens	\uparrow milk IL-1β, IL-8, IL-10, IL-12, IFN-γ, TNF-α, and C5a	(Bannerman et al., 2004a)
S. aureus	ightharpoonup milk IL-1β, IL-12, IFN-γ, IL-10	(Bannerman et al., 2004b)
S. uberis	\uparrow milk IL-1β, IL-8, IL-10, IL-12, IFN-γ, TNF-α, and C5a	(Bannerman et al., 2004a, Rambeaud et al., 2003)
Natural infection	on	
Mixed bacteria	\uparrow milk PGF _{2α} , PGE ₂ , and TXB ₂ , LXA ₄ , and LTB ₄ in milk	(Boutet et al., 2003, Atroshi et al., 1987)
E. coli	↑ milk 6-keto PGF _{1α} , PGE ₂ , HODE, 5-HETE, 15-HETE and plasma 6-keto PGF _{1α} , PGE ₂ , and RvD ₂	(Mavangira et al., 2015)
E. coli or	↑ plasma coagulation parameters including ATT,	(Ismail and
S. aureus	and PT time	Dickinson, 2010)
S. aureus	↑ mammary tissue TGF-β protein expression	(Andreotti et al., 2014)

^{↑=}Increased, LF=Lactoferrin, LZ=lysozyme, LPS=Lipopolysaccharide, IL=Interleukin, TNF-α=Tumor necrosis factor-α, COX-2=Cyclooxygenase-2, iNOS=Inducible nitric oxide synthase, PG=Prostaglandin, LT=Leukotriene, TX=Thromboxane, IFN-γ=Interferon-γ, 5-HT=Serotonin, HODE=Hydroxyoctadecadienoic acid, HETE=Hydroxyeicosatetraenoic acid, RvD=Resolvin, ATT=Activated partial thromboplastin time, PT=Prothrombin time, TGF=Transforming growth factor-β

Table 2. Bovine primers for qRT-PCR.

Gene ^a	Reference sequence	TaqMan® assay ID ^b
RPS9	NM_001101152.2	Bt03272016_m1
PGK1	NM_001034299.1	Bt03225857_m1
ACTB	NM_173979.3	Bt03279174_g1
ICAM-1	NM_174348.2	Bt03213911_m1
VCAM-1	NM_174484.1	Bt03279189_m1
E-selectin	NM_17418.2	Bt03213082_m1
IL-6	NM_173923.2	Bt03211905_m1
IL-8	NM_173925.2	Bt03211906_m1
IL-1β	NM_174093.1	Bt03212741_m1
15-LOX-1	NM_174501.2	Bt03214775_m1
15-LOX-2	NM_001205703.1	Bt04284773_m1
5-LOX	NM_001192792.1	Bt04297609_m1
COX-1	NM_001105323.1	Bt03817775_m1
COX-2	NM_174445.2	Bt03214492_m1

^a RPS9=ribosomal protein S9; PGK1=phosphoglycerate kinase; ACTB=β-actin; ICAM-1=intercellular adhesion molecule-1; VCAM-1=vascular adhesion molecule-1; 15-LOX-1=15lipoxygenase-1; 15-LOX-2=15-lipoxygenase-2; 5-LOX=5-lipoxygenase; COX-1=cyclooxygenase-1; COX-2=cyclooxygenase-2. b Life Technologies, Carlsbad, CA.

Table 3. Oxylipid concentrations in mammary tissue obtained from uninfected cows and cows

challenged with S. uberis (pg/ng of tissue)¹

Oxylipid ²		ted (n=3)	Infected (n=5)		
Oxylipid	Mean	SEM	Mean	SEM	
8-iso PGF _{2α}	0.19	0.19	1.61	0.80	
TXB2	0.00	0.00	0.27	0.24	
PGD_2	0.16	0.16	0.00	0.00	
LXA_4	0.99	0.53	2.26	0.16	
$\mathrm{LTB_4}$	0.69	0.35	1.59	0.81	
LTD_4	105.67	56.10	57.21	26.54	
RvD_1	0.13	0.04	0.20	0.07	
RvD_2	0.05	0.02	0.14	0.09	
PD_1	6.37	2.80	18.18	6.78	
7(<i>S</i>)-Maresin 1	0.28	0.16	0.32	0.28	
5-HETE	0.35	0.25	0.39	0.10	
8-НЕТЕ	2.40	1.38	6.72	4.34	
11-HETE	0.48	0.41	0.19	0.08	
12-HETE	0.24	0.14	0.35	0.09	
12-oxoETE	0.34	0.15	1.21	0.90	
15-HETE	0.65	0.41	0.81	0.29	
15-oxoETE	0.74	0.30	0.73	0.20	
20-HETE	0.16	0.07	0.51	0.25	
9-oxoODE	5.49	3.09	12.70	5.01	
13-oxoODE	2.74	1.10	8.83	5.51	
5-HETE:5-oxoETE	1.11	0.60	0.49	0.07	
12-HETE:12-oxoETE	0.78	0.31	2.29	1.24	
15-HETE:15-oxoETE	0.74	0.34	1.27	0.44	
13-HODE:13-oxoODE	0.38	0.04	5.90	3.78	
13-HODE:9-HODE	0.43	0.09	0.48	0.11	

¹ Table displays oxylipids that were not different between *S. uberis*-infected mammary tissue and control tissue.

² PG = prostaglandin; TX = thromboxane; LT = leukotriene; RvD = resolvin D; PD = protectin; HETE = hydroxyeicosatetraenoic acid; HODE = hydroxyoctadecadienoic acid; oxoODE = oxooctadecadienoic acid.

Table 4. Oxylipid concentrations in milk from cows that did not establish *S. uberis* mastitis after

intramammary challenge (pg/µL of milk)

Oxylipid ¹ –	$\frac{c \left(pg \right) \mu E \sigma^2}{0^2}$		3	3		7	
	Mean	SEM	Mean	SEM	Mean	SEM	
8-iso PGF _{2α}	0.00	0.00	0.07	0.07	0.07	0.07	
PGE,	0.44	0.44	0.07	0.07	0.30	0.20	
PGF_{2lpha}^{2}	0.59	0.20	0.52	0.27	0.44	0.13	
TXB_2	1.78	1.22	1.63	1.21	0.52	0.41	
PGD_2	1.63	1.19	0.30	0.07	0.22	0.22	
LTB_4	0.15	0.15	0.19	0.10	0.00	0.00	
LTD_4	24.53	24.53	31.59	24.75	30.44	27.85	
RvD_1	0.22	0.13	0.00	0.00	0.00	0.00	
RvD_2	0.30	0.20	0.07	0.07	0.00	0.00	
PD_1	3.43	1.06	5.13	0.77	6.55	1.07	
5-HETE	0.00	0.00	0.12	0.07	0.00	0.00	
5-oxoETE	4.98	2.57	0.17	0.03	0.66	0.29	
8-HETE	0.00	0.00	0.25	0.13	0.47	0.11	
12-HETE	18.40	9.54	0.12	0.07	0.11	0.11	
15-HETE	0.13	0.13	3.92	1.94	0.71	0.24	
15-oxoETE	20.46	10.70	0.17	0.03	0.26	0.07	
20- HETE	0.00	0.00	0.20	0.02	0.77	0.40	
13-HODE	1.92	0.47	1.34	0.06	2.13	0.50	
13-oxoODE	2.83	1.01	2.05	1.31	3.64	0.79	
9-HODE	1.64	0.72	1.85	0.75	3.31	0.49	
9-oxoODE	6.83	1.27	7.71	4.76	22.27	3.31	
9-HODE:9-oxoODE	0.22	0.06	0.31	0.06	0.15	0.03	
5-HETE:5-oxoETE	6.83	1.27	7.71	4.76	22.27	3.31	
15-HETE:15-oxoETE	0.22	0.06	0.31	0.06	0.15	0.03	

¹ PG = prostaglandin; TX = thromboxane; LT = leukotriene; RvD = resolvin D; PD = protectin; HETE = hydroxyeicosatetraenoic acid; oxoETE = oxoeicosatetraenoic acid; HODE = hydroxyoctadecadienoic acid; oxoODE = oxooctadecadienoic acid.

 $^{^{2}}$ 0 = prior to intramammary infusion on d of challenge, 3 = 3 d post-challenge, 7 = 7 d post-challenge, n=3 for all time points.

Table 5. Oxylipid concentrations in milk from cows that established *S. uberis* mastitis after

intramammary challenge (pg/μL of milk)

	0 1101) ²	3	3		7	
Oxylipid ¹	Mean	SEM	Mean	SEM	Mean	SEM	
8-iso PGF _{2α}	0.04	0.04	0.09	0.09	0.18	0.08	
PGE_2	0.22	0.10	0.30	0.18	0.22	0.10	
$PGF_{2\alpha}$	0.42	0.13	0.40	0.18	0.46	0.15	
TXB_2	0.44	0.34	1.24	0.87	0.36	0.15	
PGD_2	0.22	0. 12	0.40	0.19	0.36	0.23	
LTB_4	0.24	0.24	0.16	0.12	0.24	0.15	
LTD_4	17.38	6.36	123.29	95.72	414.53	317.41	
RvD_1	0.10	0.06	0.40	0.18	0.24	0.15	
RvD_2	0.22	0.07	0.27	0.13	0.18	0.08	
PD_{1}	14.67	5.48	53.11	33.24	90.00	55.27	
5-HETE	0.80	0.69	0.98	0.40	0.98	0.56	
5-oxoETE	0.40	0.22	0.93	0.42	2.76	2.20	
8-HETE	0.31	0.21	0.49	0.25	0.98	0.60	
12-HETE	0.31	0.19	0.44	0.20	1.33	0.84	
15-HETE	0.71	0.45	0.84	0.28	0.98	0.30	
15-oxoETE	1.24	0.45	2.31	1.54	2.22	1.67	
20-HETE	2.09	1.65	1.20	0.50	8.20	5.54	
13-HODE	4.93	2.58	3.02	0.90	5.69	2.01	
13-oxoODE	91.47	62.51	33.42	13.39	45.33	19.05	
9-HODE	8.31	3.64	9.82	3.45	6.71	1.74	
9-oxoODE	132.71	112.51	30.71	11.93	33.42	19.57	
9-HODE:9- oxoODE	0.29	0.10	0.61	0.31	0.03	0.16	
5-HETE:5- oxoETE	132.71	112.51	30.71	11.93	33.42	19.57	
15-HETE:15- oxoETE	0.29	0.10	0.61	0.31	0.03	0.16	

¹ PG = prostaglandin; TX = thromboxane; LT = leukotriene; RvD = resolvin D; PD = protectin; HETE = hydroxyeicosatetraenoic acid; oxoETE = oxoeicosatetraenoic acid; HODE = hydroxyoctadecadienoic acid; oxoODE = oxooctadecadienoic acid.

 $^{^{2}}$ 0 = prior to intramammary infusion on d of challenge, 3 = 3 d post-challenge, 7 = 7 d post-challenge, n=5 for all time points.

Table 6. Fatty acid composition of linoleic acid (LA) and α-Linolenic acid (ALA) infusions

Fatty Acid	LA	ALA
ratty Acid	g/d	g/d
Myristic acid (C14:0)	0.06	0.05
Palmitic acid (C16:0)	4.06	3.98
Palmitoleic acid (C16:1 9c)	0.11	0.03
Stearic acid (C18:0)	1.55	1.58
Oleic acid (C18:1 9c)	10.2	9.52
LA (C18:2n-6)	38.6	8.39
ALA (C18:3n-3)	6.77	37.8
Σ SFA	6.10	5.90
Σ MUFA	10.8	10.0
Σ PUFA	45.4	46.3
Σ n-3 PUFA	6.79	37.9
Σ n-6 PUFA	38.7	8.41

Table 7. Ingredient and nutrient composition of the treatment diet¹

Ingredient	% DM
Corn silage	28.4
Alfalfa silage	16.7
Wheat straw	3.2
Dry ground corn	17.5
High moisture corn	8.5
Soybean meal	14.8
Cottonseed with lint	7.4
Vitamin-mineral mix ¹	2.1
Limestone	0.76
Sodium bicarbonate	0.75
Nutrient Composition	% DM
DM	58.7
NDF	30.6
CP	17.5
Starch	26.3
FA	3.3

¹ Vitamin and mineral mix contained 34.1% dry ground shell corn, 25.6% white salt, 21.8% calcium carbonate, 9.1% Biofos, 3.9% magnesium oxide, 2% soybean oil, and < 1% of each of the following: manganese sulfate, zinc sulfate, ferrous sulfate, copper sulfate, iodine, cobalt carbonate, vitamin E, vitamin A, vitamin D, and selenium.

Table 8. Concentration (mM) of plasma FA following ex vivo microbial exposure¹

Fatty acid ²	Unstin	ulated	S. ub	peris	LPS	
ratty actu	Mean ³	SEM	Mean ⁴	SEM	Mean	SEM
LA	225.56	44.13	188.15	41.84	273.01	82.56
ArA	28.68	7.41	13.26*	2.25	30.48	12.22
ALA	54.09	10.34	45.76	9.46	57.04	16.00
EPA	5.69	1.81	2.52	0.52	5.72	2.33
DHA	1.61	0.33	1.26	0.26	1.84	0.47
Palmitic acid	933.34	326.46	744.19	201.83	1,861.58	1,010.93
Oleic acid	105.49	18.89	95.94	32.72	144.16	56.42
Stearic acid	39.23	14.67	59.27	38.8	90.90	46.85

¹Blood samples from the non-supplemented group (CON) were collected and exposed to heat-killed *S. uberis* or LPS for 4 h. Plasma then was collected and plasma FA were quantified by LC-MS.

 $^{^2}$ LA=Linoleic acid, ArA=Arachidonic acid, ALA= α -Linolenic acid, EPA=Eicosapentaenoic acid, DHA=Docosahexaenoic acid.

³Arithmetic means are shown for unstimulated, heat-killed *S. uberis*-challenged, and LPS-challenged plasma FA concentrations.

⁴Fatty acid concentrations within microbial agonist columns with an asterisk (*) are significantly different from control as determined by Student's t-tests ($P \le 0.05$).

Table 9. Concentration (μM) of significantly changed plasma oxylipids following *ex vivo* microbial exposure^{1,2}

Oxylipid ³	PUFA	Oxidation	Unstimulated		S. uberis		LPS	
Oxympia	substrate ⁴	pathway ⁵	Mean ⁶	SEM	Mean ⁷	SEM	Mean ⁷	SEM
13-oxoODE	LA	LOX	13.62	4.97	19.78*	5.63	15.08	1.76
15-oxoETE	ArA	LOX	0.25	0.06	0.92*	0.19	0.37	0.08
12-HETE	ArA	LOX	48.12	10.56	87.28*	15.91	81.48	27.07
5,6-LXA ₄	ArA	LOX	1.60	0.35	1.18	0.31	0.68*	0.18
11,12-EET	ArA	CYP	0.10	0.00	0.09	0.04	0.04*	0.02
12-HHTrE	ArA	COX	2.58	0.79	2.67	0.86	3.83*	0.76
14,15-DiHETE	EPA	CYP	25.32	3.55	38.65*	6.29	37.60	7.71
17,18-DiHETE	EPA	CYP	244.40	33.69	328.55*	44.80	291.70	28.07
11,12-								
EET/11,12-	EPA							
DHET			0.042	0.011	0.018	0.006	0.009*	0.003

¹Blood samples from the non-supplemented group (CON) were collected and exposed to heat-killed *S. uberis* or LPS for 4 h. Plasma then was collected and oxylipids were quantified by LC-MS/MS.

²Only oxylipids significantly changed following *S. uberis* or LPS exposure relative to control are displayed.

³oxoODE=oxooctadecadienoic acid, oxoETE – oxoeicosatetraenoic acid,

HETE=hydroxyeicosatetraenoic acids, LX=Lipoxin, EET=epoxyeicosatrienoic acid, DHET=dihydroxyeicosatrienoic acid, HHTrE= hydroxyheptadecatrienoic acid, TX=Thromboxane, DiHETE= dihydroxyeicosatetraenoic acid.

⁴LA=Linoleic acid, ArA=Arachidonic acid, EPA=Eicosapentaenoic acid,

DHA=Docosahexaenoic acid, ALA=α-Linolenic acid, DGLA=Dihomo-γ-Linoleic acid.

⁵LOX=Lipoxygenase, CYP=Cytochrome P450, COX=Cyclooxygenase

⁶Arithmetic means are shown for unstimulated, heat-killed *S. uberis*-challenged, and LPS-challenged plasma oxylipid concentrations.

⁷Oxylipid concentrations within microbial agonist columns with an asterisk (*) are different from control as determined by Student's t-tests ($P \le 0.05$).

Table 10. Changes in plasma FA from PUFA-supplemented cows following ex vivo S. uberis

challenge

Fatty acid ¹ —	CON^2		LA		ALA	
	$\Delta Mean^{3,4}$	SEM	Δ Mean	SEM	ΔMean	SEM
LA	↓ 37.41	54.73	↓ 93.37	68.90	↑ 86.07	113.24
ArA	↓ 15.42 ^a	6.27	♦ 8.19 a,b	5.18	↑ 9.30 ^b	6.62
ALA	♦ 8.34	11.82	↓ 51.76	13.86	↓ 3.95	93.56
EPA	↓ 3.18	1.43	↓ 1.25	0.98	↑ 0.74	0.90
DHA	↓ 0.36	0.35	↓ 0.18	0.40	↑ 0.58	0.55
Palmitic acid	↓ 189.16	175.84	↑ 59.86	543.60	↑ 399.64	238.69
Oleic acid	♦ 9.55	24.11	↓ 34.59	27.34	↑ 72.61	76.61
Stearic acid	↑ 20.04	26.05	↑ 1.22	9.63	↑ 58.04	24.75

¹LA=Linoleic acid, ArA=Arachidonic acid, ALA= α-Linolenic acid, EPA=Eicosapentaenoic acid, DHA=Docosahexaenoic acid.

²CON=Ethanol carrier, LA=Linoleic acid supplementation, ALA=α-Linolenic acid supplementation.

 $^{^3\}Delta$ Mean for each replicate was quantified by subtracting *S. uberis*-induced plasma FA concentration (mM) from unstimulated plasma FA concentration (mM). Means in table represent arithmetic means. A \spadesuit indicates greater plasma FA following *S. uberis* exposure compared to unstimulated samples, whereas \blacktriangledown indicates less plasma FA following *S. uberis* exposure compared to unstimulated samples.

⁴Different letters within each FA row represent statistically significant differences among treatments ($P \le 0.05$).

Table 11. Changes in plasma oxylipids from PUFA-supplemented cows following ex vivo S. uberis challenge¹

Ovvdini d ²	PUFA Oxidation		CON ⁵		LA	LA		ALA	
Oxylipid ²	substrate ³	pathway ⁴	ΔMean ^{6,7}	SEM	ΔMean	SEM	ΔMean	SEM	
12,13-EpOME	LA	CYP	↑ 2.00 ^a	4.49	↓ 12.26 ^b	4.53	♦ 8.33 ^b	4.49	
9-oxoODE	LA	LOX	↑ 25.3 ^a	11.50	↓ 47.6 ^b	13.96	↑ 11.12 ^{a,b}	11.50	
9-HETE	ArA	Non	↓ 0.36 ^a	0.26		0.28	↑ 0.68 ^b	0.26	
15-oxoETE	ArA	LOX	↑ 0.67 ^a	0.17	↓ 0.17 ^b	0.18	↑ 0.23 ^{a,b}	0.17	
20-HETE	ArA	CYP	↑ 0.07 ^{a,b}	0.22	↑ 0.37 ^a	0.24	↓ 0.30 ^b	0.22	

¹Only significant changes in oxylipids are displayed.

²EpOME=epoxyoctadecenoic acid, oxoODE=oxooctadecadienoic acid, HETE=hydroxyeicosatetraenoic acid, oxoETE=oxoeicosatetraenoic acid.

³LA=Linoleic acid, ArA=Arachidonic acid.

⁴CYP=Cytochrome P450, LOX=Lipoxygenase, Non=Non-enzymatic.

⁵CON=Ethanol carrier, LA=Linoleic acid supplementation, ALA=α-Linolenic acid supplementation.

 $^{^6\}Delta$ Mean for each replicate was quantified by subtracting *S. uberis*-induced plasma oxylipid concentrations (μM) from unstimulated plasma oxylipid concentrations (μM). Means in table represent arithmetic means. A ↑ indicates greater plasma oxylipids following *S. uberis* exposure compared to unstimulated samples, whereas \checkmark indicates less plasma oxylipids following *S. uberis* exposure compared to unstimulated samples.

⁷Different letters within each oxylipid row represent statistically significant differences among treatments ($P \le 0.05$). exposure, whereas a negative value indicates less abundant oxylipid biosynthesis as a result of *S. uberis* exposure.

Table 12. Changes in plasma FA from PUFA-supplemented cows following ex vivo LPS

challenge

Fatty acid ¹ -	CON^2		LA	1	ALA	
	Δ Mean ^{3,4}	SEM	Δ Mean	SEM	ΔMean	SEM
LA	↑ 47.45	68.94	₩ 29.59	45.98	↑ 120.79	27.12
ArA	1 .80	14.25	↑ 8.51	10.88	↑ 4.27	2.66
ALA	↑ 2.94 ^{a,b}	12.31	↓ 21.05 ^a	9.25	↑ 60.83 ^b	26.00
EPA	↑ 0.02	2.88	1 .80	1.60	↑ 0.67	0.60
DHA	↑ 0.23	0.52	↓ 0.05	0.21	↑ 1.07	0.29
Palmitic acid	↑ 928.23	745.06	↑ 37.33	413.70	↑ 678.18	292.73
Oleic acid	↑ 38.67	48.62	↓ 22.28	30.73	↑ 74.13	25.23
Stearic acid	↑ 51.67	51.58	1 2.38	17.26	↑ 72.20	55.02

¹LA=Linoleic acid, ArA=Arachidonic acid, ALA= α-Linolenic acid, EPA=Eicosapentaenoic acid, DHA=Docosahexaenoic acid.

²CON=Ethanol carrier, LA=Linoleic acid supplementation, ALA=α-Linolenic acid supplementation.

³ΔMean for each replicate was quantified by subtracting LPS-induced plasma FA concentration (mM) from unstimulated plasma FA concentration (mM). Means in table represent arithmetic means. A ↑ indicates greater plasma FA following LPS exposure compared to unstimulated samples, whereas ▶ indicates less plasma FA following LPS exposure compared to unstimulated samples.

⁴ Different letters within each FA row represent statistically significant differences among treatments ($P \le 0.05$).

Table 13. Changes in plasma oxylipids from PUFA-supplemented cows following *ex vivo* LPS challenge¹

Oxylipid ²	PUFA Oxidation		CON ⁵		LA		ALA	
	substrate ³	pathway ⁴	ΔMean ^{6,7}	SEM	ΔMean	SEM	ΔMean	SEM
9- oxoODE	LA	LOX/Non	↓ 12.5 ^a	8.30	↓ 30.3ª	9.59	↑ 30.4 ^b	8.3
13- oxoODE	LA	LOX	↓ 1.77 ^a	3.93	↓ 0.75 ^{a,b}	4.54	↑ 15.4 ^b	3.93
5,6 LXA ₄	ArA	LOX	↑ 0.92 ^a	0.35	↓ 0.23 ^{a,b}	0.39	↑ 0.37 ^b	0.35

¹Only significant changes in oxylipids are displayed.

²oxoODE=oxooctadecadienoic acid, LX=Lipoxin.

³LA=Linoleic acid, ArA=Arachidonic acid.

⁴LOX=Lipoxygenase, Non=Non-enzymatic.

⁵CON=Ethanol carrier, LA=Linoleic acid supplementation, ALA=α-Linolenic acid supplementation.

 $^{^6\}Delta$ Mean for each replicate was quantified by subtracting LPS-induced plasma oxylipid concentrations (μM) from unstimulated plasma oxylipid concentrations (μM). Means in table represent arithmetic means. A ↑ indicates greater plasma oxylipids following LPS exposure compared to unstimulated samples, whereas \checkmark indicates less plasma oxylipids following LPS exposure compared to unstimulated samples.

⁷Different letters within each oxylipid row represent statistically significant differences among treatments ($P \le 0.05$).

Table 14. Concentration (μM) of plasma oxylipids not significantly changed following ex vivo microbial exposure^{1,2}

Oxylipid ³	PUFA	Oxidation	Con	trol	S. ul	peris	LPS	
Oxynpid	substrate ⁴	pathway ⁵	Mean	SEM	Mean	SEM	Mean	SEM
9-HODE	LA	LOX/Non	69.00	6.07	82.50	13.94	60.00	6.76
9-oxoODE	LA	LOX/Non	38.88	9.56	64.20	17.28	26.40	3.61
13-HODE	LA	LOX	221.25	21.28	243.25	33.99	203.08	15.00
9,10-EpOME	LA	CYP	24.67	2.29	23.33	2.46	21.00	1.44
9,10-DiHOME	LA	CYP	142.00	29.68	163.50	48.84	156.83	22.70
12,13-EpOME	LA	CYP	73.00	6.38	75.00	10.34	69.67	11.61
12,13-DiHOME	LA	CYP	2305.5	374.1	2812.8	767.3	3020.5	586.8
PGE_2	ArA	COX	2.17	1.19	0.67	0.28	1.22	0.36
PGD_2	ArA	COX	0.42	0.09	0.29	0.06	0.83	0.29
6-keto $PGF_{1\alpha}$	ArA	COX	0.88	0.33	1.35	0.42	1.13	0.20
TXB_2	ArA	COX	2.22	1.23	3.13	1.24	3.37	0.85
8-iso-PGA ₁	ArA	Non	1.27	0.57	1.50	0.24	1.83	0.89
8-iso-PGA ₂	ArA	Non	0.23	0.08	0.18	0.09	0.37	0.09
8-iso-PGE ₂	ArA	Non	1.58	0.71	1.13	0.53	1.97	0.77
8-iso-PGF _{2α}	ArA	Non	0.85	0.16	0.60	0.23	0.88	0.22
5-HETE	ArA	LOX	4.85	0.62	5.15	0.84	4.67	0.69
5-oxoETE	ArA	LOX	1.43	0.44	1.08	0.46	0.74	0.27
15-HETE	ArA	LOX	5.55	0.56	2.35	0.49	5.78	0.87
11-HETE	ArA	Non	2.48	0.27	2.68	0.29	2.78	0.40
20-HETE	ArA	CYP	0.93	0.23	1.00	0.12	0.38	0.18
9-НЕТЕ	ArA	Non	1.75	0.85	0.26	0.15	0.50	0.30
LTB_4	ArA	LOX	0.63	0.20	0.53	0.16	0.33	0.14
14,15-EET	ArA	CYP	0.53	0.16	0.58	0.15	0.28	0.09
14,15-DHET	ArA	CYP	25.32	3.55	38.65	6.29	37.60	7.71
8,9-DHET	ArA	CYP	0.60	0.12	0.54	0.14	0.48	0.14
11,12-DHET	ArA	CYP	3.50	0.94	4.53	1.43	3.90	0.90
5,6-DiHETE	EPA	CYP	3.45	1.03	10.77	4.79	6.60	1.12

Table 14. (cont.)								
19,20-EpDPE	DHA	CYP	2.08	0.51	3.21	1.22	2.32	0.31
19,20-DiHDPA	DHA	CYP	1.45	0.20	1.25	0.37	1.20	0.32
RD1	DHA	LOX	0.25	0.06	0.38	0.11	0.18	0.05
RD2	DHA	LOX	0.63	0.15	0.93	0.27	1.22	0.38
15-HETrE	DGLA	LOX	2.55	0.23	2.35	0.49	2.02	0.49
5-HETE/5-oxoETE	ArA		13.29	6.81	14.74	8.57	26.25	13.01
15-HETE/15-oxoETE	ArA		28.38	7.10	9.59	1.79	18.36	3.91
14,15-EET/14,15-DHET	ArA		0.020	0.004	0.055	0.016	0.010	0.005
9-HODE/9-oxoODE	LA		2.44	0.68	1.46	0.16	2.45	0.41
13-HODE/13-oxoODE	LA		20.50	8.00	12.09	5.00	14.16	1.38
9,10-EpOME/9,10-DiHOME	LA		0.218	0.056	0.174	0.022	0.154	0.029
12,13-EpOME/12,13-DiHOME	LA		0.036	0.006	0.031	0.005	0.026	0.004

¹Blood samples from the non-supplemented group (CON) were collected and exposed to heat-killed *S. uberis* or LPS for 4 h. Plasma then was collected and oxylipids were quantified by LC-MS/MS.

²Oxylipids not significantly changed following *S. uberis* or LPS exposure relative to control are displayed.

³HODE= hydroxyoctadecadienoic acid, oxoODE=oxooctadecadienoic acid, oxoETE – oxoeicosatetraenoic acid, EpOME= epoxyoctadecenoic acid, DiHOME=dihydroxyoctadecenoic acid, PG=Prostaglandin, HETE=hydroxyeicosatetraenoic acid, oxoETE=oxoeicosatetraenoic acid, LT=Leukotriene, EET= epoxyeicosatrienoic acid, DHET= dihydroxyeicosatrienoic acid, DiHETE= dihydroxyeicosatetraenoic acid, EpDPE=epoxydocosapentaenoic acid, DiHDPA= dihydroxydocosapentaenoic acid, RD=Resolvin, HOTrE= hydroxyoctadecatrienoic acid, HETrE=hydroxyeicosatrienoic acid.

⁴LA=Linoleic acid, ArA=Arachidonic acid, EPA=Eicosapentaenoic acid, DHA=Docosahexaenoic acid, ALA=α-Linolenic acid, DGLA=Dihomo-γ-Linoleic acid.

⁵LOX=Lipoxygenase, Non=Non-enzymatic, CYP=Cytochrome P450, COX=Cyclooxygenase.

⁶Arithmetic means are shown for unstimulated, heat-killed S. uberis-challenged, and LPS-challenged plasma oxylipid concentrations.

Table 15. Changes in plasma oxylipids from PUFA-supplemented cows following ex vivo S. uberis challenge¹

Overlini d2	PUFA	PUFA Oxidation		N^5	LA		ALA	
Oxylipid ²	substrate ³ pathway ⁴	pathway ⁴	Δ Mean ⁶	SEM	ΔMean	SEM	ΔMean	SEM
9-HODE	LA	LOX/Non	1 3.50	9.31	↓ 7.62	10.34	4 4.58	9.31
13-HODE	LA	LOX	↑ 22.00	31.46	↓ 28.13	35.85	↓ 36.42	31.46
13-oxoODE	LA	LOX	↑ 6.17	9.58	↓ 3.47	10.63	1 9.08	9.58
9,10-EpOME	LA	CYP	↓ 1.33	3.09	↓ 1.20	3.20	↓ 6.33	3.09
9,10-DiHOME	LA	CYP	1 21.50	25.67	↓ 18.26	28.93	↓ 1.67	25.67
12,13-DiHOME	LA	CYP	↑ 507.33	431.69	↓ 477.22	478.19	↑ 258.83	431.69
PGE_2	ArA	COX	↓ 1.50	0.65	1 0.52	0.72	↑ 0.18	0.65
PGD_2	ArA	COX	↓ 0.13	0.14	↑ 0.41	0.15	↓ 0.04	0.14
6-keto $PGF_{1\alpha}$	ArA	COX	↑ 0.47	0.24	↓ 0.30	0.27	↑ 0.47	0.24
TXB_2	ArA	COX	↑ 0.92	0.77	↓ 0.66	0.87	↑ 0.12	0.77
12-HHTrE	ArA	COX	1 0.08	0.55	1 0.08	0.62	1 0.25	0.55
8-iso-PGA ₁	ArA	COX	↑ 0.23	0.41	↑ 0.14	0.46	↓ 0.58	0.41
8-iso-PGA ₂	ArA	COX	↓ 0.05	0.12	↑ 0.14	0.12	↓ 0.12	0.12
8 -iso-PGE $_2$	ArA	COX	↓ 0.45	0.73	1 1.28	0.83	↓ 0.53	0.73
8-iso-PGF _{2α}	ArA	COX	↓ 0.25	0.43	↑ 0.63	0.48	↑ 0.34	0.42
5-HETE	ArA	LOX	1 0.30	1.24	1 0.76	1.37	1 2.18	1.24
5-oxoETE	ArA	LOX	↓ 0.35	0.70	↓ 1.32	0.80	↓ 0.18	0.70
15-HETE	ArA	LOX	↑ 1.87	0.79	1 0.06	0.88	↑ 0.12	0.79
11-HETE	ArA	Non	1 0.20	0.30	↓ 0.02	0.33	↑ 0.53	0.30
12-HETE	ArA	LOX	↑ 39.17	17.88	₩8.08	19.83	↑ 13.52	17.88
$\mathrm{LTB_4}$	ArA	LOX	↓ 0.10	0.26	1 0.54	0.29	↓ 0.30	0.26
5,6 LXA ₄	ArA	LOX	↓ 0.42	0.43	↑ 0.13	0.48	↑ 0.23	0.43
14,15-EET	ArA	CYP	1 0.05	0.16	↓ 0.13	-0.03	↑ 0.16	
14,15-DHET	ArA	CYP	↑ 3.02	1.40	↓ 0.93	1.56	↑ 1.72	1.40
11,12-EET	ArA	CYP	↓ 0.02	0.06	↓ 0.05	0.07	↑ 0.02	0.06
11,12-DHET	ArA	CYP	↑ 1.03	0.84	↓ 0.75	0.97	↑ 0.83	0.84
8,9-DHET	ArA	CYP	$\mathbf{\Psi}_{0.06}$	0.18	↓ 0.20	0.20	↓ 0.35	0.18

Table 15. (cont.)								
5,6-DiHETE	EPA	CYP	↑ 7.32	3.37	↑ 3.05	3.58	↑ 1.65	3.37
14,15-DiHETE	EPA	CYP	↑ 13.33	5.57	↓ 1.34	6.68	↑ 6.03	5.57
17,18-DiHETE	EPA	CYP	↑ 84.15	46.82	↓ 26.20	51.94	↑ 61.7	46.82
19,20-EpDPE	DHA	CYP	↑ 1.13	0.57	↑ 0.28	0.64	↑ 0.42	0.57
19,20-DiHDPA	DHA	CYP	↓ 0.20	0.54	↓ 0.32	0.62	↓ 0.35	0.54
RD1	DHA	LOX	↑ 0.13	0.29	↑ 0.51	0.32	↑ 0.13	0.29
RD2	DHA	LOX	↑ 0.30	0.32	↑ 0.64	0.35	↑ 0.33	0.32
15-HETrE	DGLA	LOX	↓ 0.20	0.79	↓ 1.45	0.91	↑ 0.45	0.79
5-HETE/5-oxoETE	Ara		↓ 1.45	30.72	↓ 10.88	35.08	↓ 52.14	30.72
15-HETE/15-oxoETE	Ara		↓ 18.79	5.89	↓ 4.62	6.53	↓ 9.96	5.89
11,12-EET/11,12-DHET	Ara		↓ 0.02	0.02	↓ 0.007	0.02	↑ 0.003	0.02
14,15-EET/14,15-DHET	Ara		↓ 0.005	0.02	ullet0.00	0.02	↓ 0.009	0.02
9-HODE/9-oxoODE	LA		↑ 0.98	1.02	↓ 0.40	1.19	1 2.58	1.02
13-HODE/13-oxoODE	LA		↑ 14.71	9.11	↑ 8.82	10.11	↓ 0.24	9.11
9,10-EpOME/9,10-DiHOME	LA		↓ 0.04	0.03	↑ 0.004	0.03	$\mathbf{\Psi}_{0.05}$	0.03
12,13-EpOME/12,13-DiHOME	LA		1 0.003	0.004	↓ 0.006	0.005	↓ 0.004	0.004

¹Changes in table represent oxylipids not significantly changed due to PUFA supplementation.

²HODE= hydroxyoctadecadienoic acid, oxoODE=oxooctadecadienoic acid, oxoETE – oxoeicosatetraenoic acid, EpOME= epoxyoctadecenoic acid, DiHOME=dihydroxyoctadecenoic acid, PG=Prostaglandin, HETE=hydroxyeicosatetraenoic acid, oxoETE=oxoeicosatetraenoic acid, LT=Leukotriene, EET= epoxyeicosatrienoic acid, DHET= dihydroxyeicosatrienoic acid, DiHETE= dihydroxyeicosatetraenoic acid, EpDPE=epoxydocosapentaenoic acid, DiHDPA= dihydroxydocosapentaenoic acid, RD=Resolvin, HOTrE= hydroxyoctadecatrienoic acid, HETrE=hydroxyeicosatrienoic acid.

³LA=Linoleic acid, ArA=Arachidonic acid, EPA=Eicosapentaenoic acid, DHA=Docosahexaenoic acid, ALA=α-Linolenic acid, DGLA=Dihomo-γ-Linoleic acid.

⁴LOX=Lipoxygenase, Non=Non-enzymatic, CYP=Cytochrome P450, COX=Cyclooxygenase.

⁵CON=Ethanol carrier, LA=Linoleic acid supplementation, ALA=α-Linolenic acid supplementation.

 $^{^6}$ ΔMean for each replicate was quantified by subtracting *S. uberis*-induced plasma oxylipid concentrations (μM) from unstimulated plasma oxylipid concentrations (μM). Means in table represent arithmetic means. A ↑ indicates greater plasma oxylipids following *S. uberis* exposure compared to unstimulated samples, whereas \checkmark indicates less plasma oxylipids following *S. uberis* exposure compared to unstimulated samples.

Table 16. Changes in plasma oxylipids from PUFA-supplemented cows following ex vivo LPS challenge¹

Oxylipid ²	PUFA	Oxidation	СО	N ⁵	LA		ALA	
Oxympid	substrate ³	pathway ⁴	$\Delta Mean^6$	SEM	ΔMean	SEM	ΔMean	SEM
9-HODE	LA	LOX/Non	♦ 9.00	6.46	1 .94	7.17	\Pi 0.50	6.46
13-HODE	LA	LOX	↓ 18.17	20.73	↑ 26.51	23.00	↓ 30.67	20.73
9,10-EpOME	LA	CYP	↓ 3.67	2.72	↑ 3.15	3.02	↓ 5.33	2.72
9,10-DiHOME	LA	CYP	↑ 14.83	25.00	↑ 53.67	27.73	1 2.5	25.00
12,13-EpOME	LA	CYP	↓ 3.33	7.10	↓ 0.38	7.87	↓ 9.67	7.10
12,13-DiHOME	LA	CYP	↑ 715.00	412.24	↑ 1571.3	476.01	↑ 220.17	412.24
PGE_2	ArA	COX	↓ 0.95	0.55	1 0.46	0.63	↑ 0.33	0.55
PGD_2	ArA	COX	↑ 0.42	0.20	1 0.12	0.22	↑ 0.15	0.20
6-keto $PGF_{1\alpha}$	ArA	COX	↑ 0.25	0.22	↑ 0.31	0.25	↓ 0.15	0.22
TXB_2	ArA	COX	↑ 1.15	1.72	1 2.01	1.96	↑ 3.45	1.72
12-HHTrE	ArA	COX	↑ 1.25	1.47	1 2.08	1.63	↑ 3.42	1.47
8-iso-PGA ₁	ArA	COX	↑ 0.57	0.80	↓ 0.68	0.89	↓ 0.05	0.80
8-iso-PGA ₂	ArA	COX	↑ 0.13	0.15	↓ 0.09	0.17	↓ 0.18	0.15
8 -iso-PGE $_2$	ArA	COX	↑ 0.38	0.26	↑ 0.19	0.30	↑ 0.32	0.26
8 -iso-PGF _{2α}	ArA	COX	↑ 0.03	0.65	1 0.65	0.72	↑ 1.02	0.65
5-HETE	ArA	LOX	↓ 0.18	1.39	↓ 0.06	1.54	↑ 0.77	1.39
5-oxoETE	ArA	LOX	♦ 0.69	0.54	↓ 1.02	0.60	↑ 0.63	0.54
15-HETE	ArA	LOX	↑ 0.23	0.91	1 2.09	1.00	↑ 0.72	0.91
15-oxoETE	ArA	LOX	↑ 0.12	0.15	↓ 0.10	0.17	↑ 0.18	0.15
11-HETE	ArA	Non	↑ 0.30	0.53	1 .04	0.59	↑ 1.20	0.53
12-HETE	ArA	LOX	↑ 33.37	14.78	↓ 5.80	16.40	↑ 11.25	14.78
20- HETE	ArA	CYP	↓ 0.55	0.31	↑ 0.19	0.36	↓ 0.03	0.32
9-НЕТЕ	ArA	Non	↓ 1.25	0.62	↓ 0.13	0.71	↓ 0.33	0.62
LTB_4	ArA	LOX	↓ 0.30	0.17	1 0.06	0.19	↓ 0.33	0.17
14,15-EET	ArA	CYP	↓ 0.25	0.12	↓ 0.11	0.14	↓ 0.07	0.12
14,15-DHET	ArA	CYP	↑ 1.35	1.63	↑ 1.79	1.86	↑ 4.25	1.63
11,12-EET	ArA	CYP	↓ 0.06	0.05	↓ 0.01	0.05	↓ 0.02	0.05

Table 16. (cont.)								
11,12-DHET	ArA	CYP	↑ 0.40	0.73	↑ 1.13	0.83	1 2.47	0.73
8,9-DHET	ArA	CYP	↓ 0.12	0.22	1 0.03	0.26	↓ 0.43	0.22
5,6-DiHETE	EPA	CYP	↑ 3.15	2.52	↑ 5.63	2.86	↑ 0.63	2.52
14,15-DiHETE	EPA	CYP	↑ 12.28	5.42	↑ 8.87	6.12	↑ 15.93	5.42
17,18-DiHETE	EPA	CYP	↑ 47.30	42.59	↑ 58.68	47.25	↑ 134.50	42.59
19,20-EpDPE	DHA	CYP	↑ 0.23	0.40	1 0.02	0.46	↑ 0.93	0.40
19,20-DiHDPA	DHA	CYP	↓ 0.25	0.26	↓ 0.02	0.30	1 0.60	0.26
RD1	DHA	LOX	↓ 0.07	0.14	1 0.06	0.16	↓ 0.26	0.14
RD2	DHA	LOX	↑ 0.58	0.42	↑ 0.49	0.44	↑ 0.32	0.42
5-HETE/5-oxoETE	ArA		↑ 12.96	5.12	1 9.35	5.76	1 2.35	5.12
15-HETE/15-oxoETE	ArA		↓ 10.02	6.82	↑ 1.48	7.78	↑ 0.31	6.82
11,12-EET/14,15-DHET	ArA		↓ 0.03	0.02	$\mathbf{\Psi}_{0.00}$	0.02	ullet0.01	0.02
11,12-EET/14,15-DHET	ArA		↓ 0.01	0.00	$\mathbf{\Psi}_{0.01}$	-0.01	ullet0.01	0.00
9-HODE/9-oxoODE	LA		↑ 0.01	0.93	1 0.29	1.03	↓ 3.01	0.93
13-HODE/13-oxoODE	LA		↓ 6.39	5.31	♦ 6.31	5.90	↓ 22.16	5.31
9,10-EpOME/9,10-DiHOME	LA		↓ 0.06	0.03	↓ 0.00	0.03	↓ 0.02	0.03
12,13-EpOME/12,13-DiHOME	LA		↓ 0.01	0.00	$\mathbf{\Psi}_{0.00}$	-0.01	ullet0.00	0.00

¹Changes in table represent oxylipids not significantly changed due to PUFA supplementation.

²HODE= hydroxyoctadecadienoic acid, oxoODE=oxooctadecadienoic acid, oxoETE – oxoeicosatetraenoic acid, EpOME= epoxyoctadecenoic acid, DiHOME=dihydroxyoctadecenoic acid, PG=Prostaglandin, HETE=hydroxyeicosatetraenoic acid, oxoETE=oxoeicosatetraenoic acid, LT=Leukotriene, EET= epoxyeicosatrienoic acid, DHET= dihydroxyeicosatrienoic acid, DiHETE= dihydroxyeicosatetraenoic acid, EpDPE=epoxydocosapentaenoic acid, DiHDPA= dihydroxydocosapentaenoic acid, RD=Resolvin.

³LA=Linoleic acid, ArA=Arachidonic acid, EPA=Eicosapentaenoic acid, DHA=Docosahexaenoic acid, ALA=α-Linolenic acid, DGLA=Dihomo-γ-Linoleic acid.

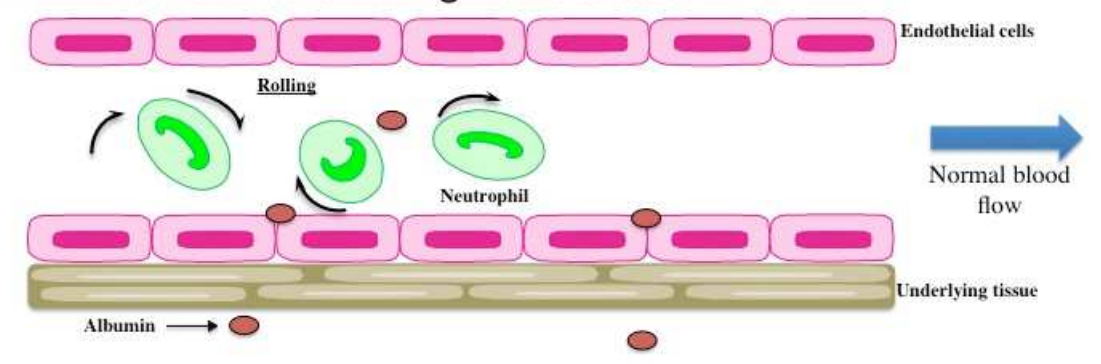
⁴LOX=Lipoxygenase, Non=Non-enzymatic, CYP=Cytochrome P450, COX=Cyclooxygenase.

⁵CON=Ethanol carrier, LA=Linoleic acid supplementation, ALA=α-Linolenic acid supplementation.

 $^{^6}$ ΔMean for each replicate was quantified by subtracting LPS-induced plasma oxylipid concentrations (μM) from unstimulated plasma oxylipid concentrations (μM). Means in table represent arithmetic means. A ↑ indicates greater plasma oxylipids following LPS exposure compared to unstimulated samples, whereas \checkmark indicates less plasma oxylipids following LPS exposure compared to unstimulated samples.

Appendix D. Figures

A. Endothelial cells during homeostasis



B. Endothelial cells during inflammation

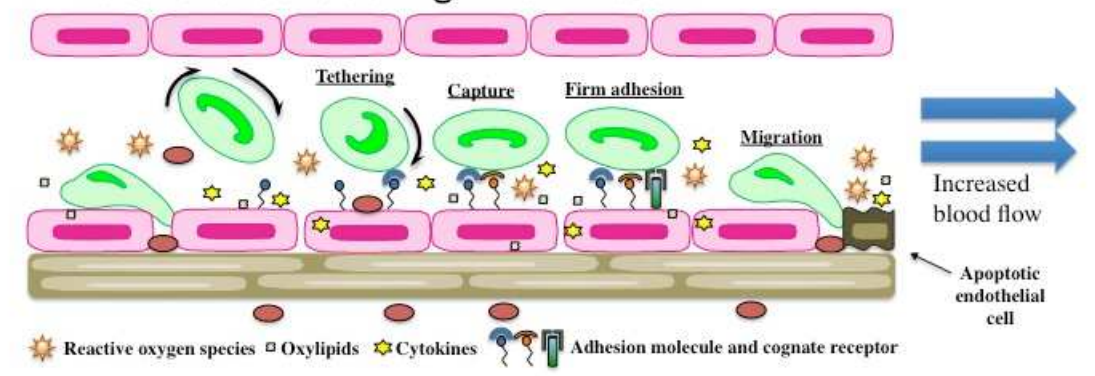
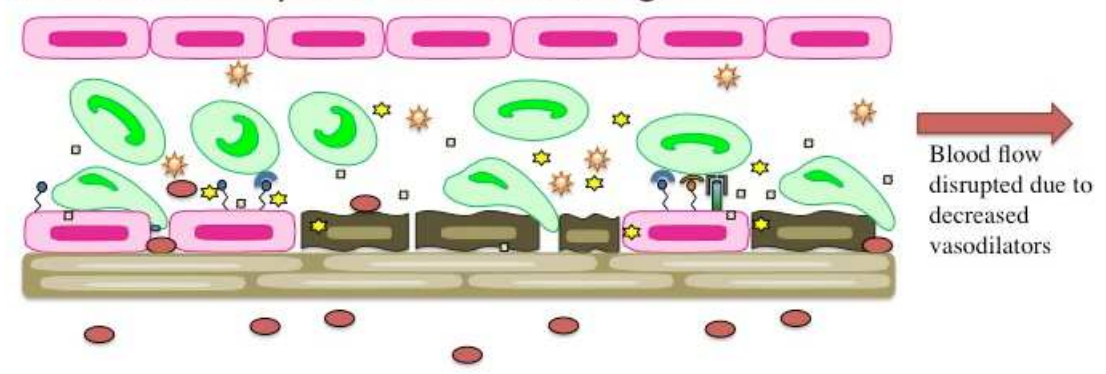


Figure 1A. During homeostasis, endothelial cells maintain adequate vascular tone, permeability, and leukocyte migration. B. At the onset of infection-induced inflammation, endothelial cells acquire new properties to facilitate clearance of the bacteria. Activated endothelial cell expression adhesion molecules and produce increased concentrations of reactive oxygen species, vasoactive lipid mediators, and cytokines. Increased vasodilation and chemokines elicit neutrophils to adhere to and cross the endothelium. Some endothelial cells may exhibit morphological changes during inflammation, those of which are eliminated during the resolution and wound healing phase of inflammation. C. An unregulated immune response results in prolonged activation of endothelial cells and accumulation of activated neutrophils at the endothelial surface causing irreversible cell damage. Oxidative stress as a result of accumulated ROS, free radicals, and lipid hydroperoxides further contributes to cellular damage and apoptosis of endothelial cells.

Figure 1. (cont.)

C. Endothelial dysfunction and damage



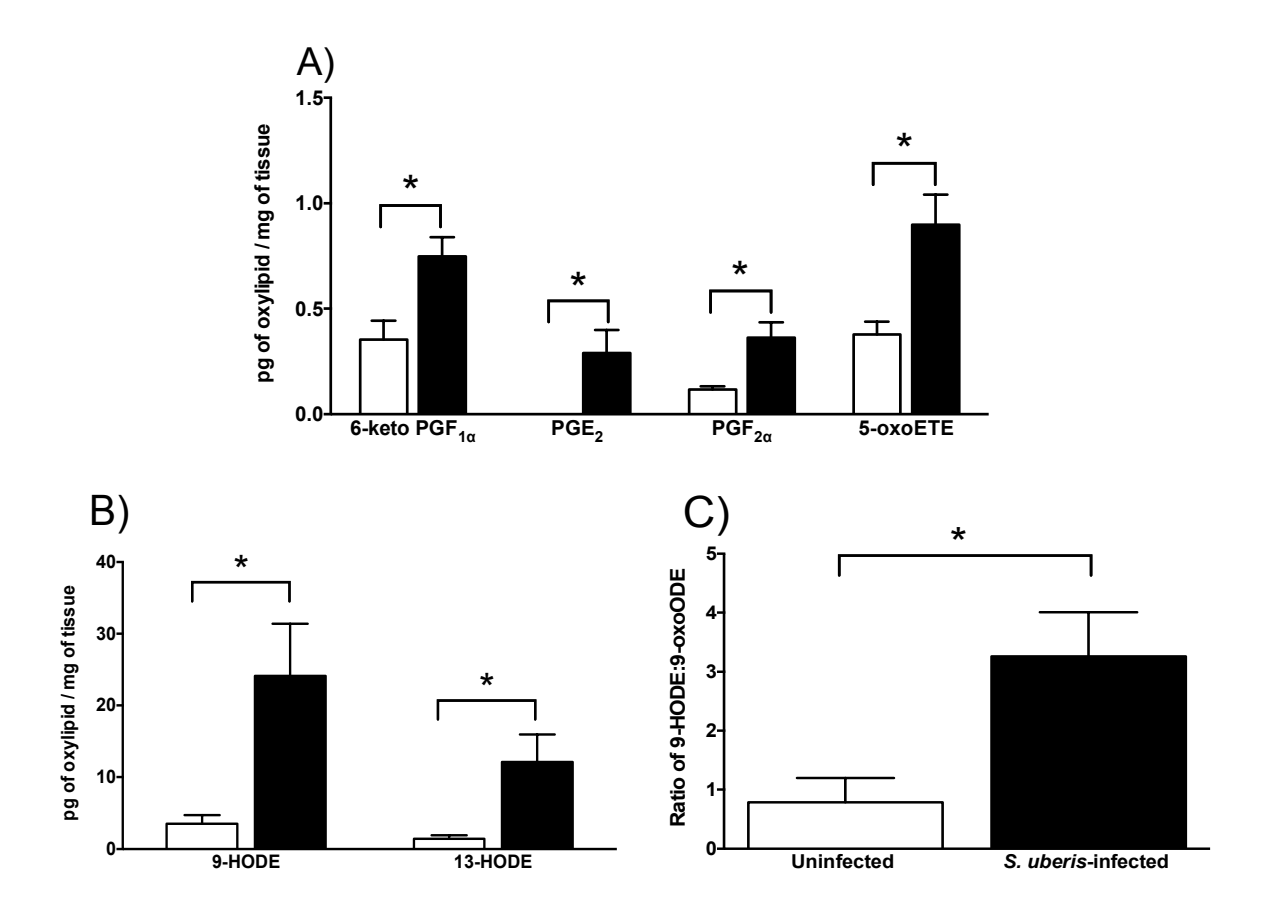


Figure 2. Means of oxylipid concentrations in tissue from uninfected cows (n=3) are displayed in open bars and means of oxylipid concentrations in tissue from *S. uberis*-infected cows (n=5) are displayed in closed bars. The concentration of tissue 6-keto-PGF_{1 α}, PGE₂, PGF_{2 α}, and 5-oxoETE (A) was significantly greater in *S. uberis*-infected mammary tissue. Similarly, the concentration of 9-HODE and 13-HODE (B), and the 9-HODE:9-oxoODE ratio (C) was significantly greater in *S. uberis*-infected mammary tissue. Values are means \pm SEM expressed in pg of oxylipid per mg of tissue or as a ratio of oxylipids. *Significance declared at $P \le 0.05$.

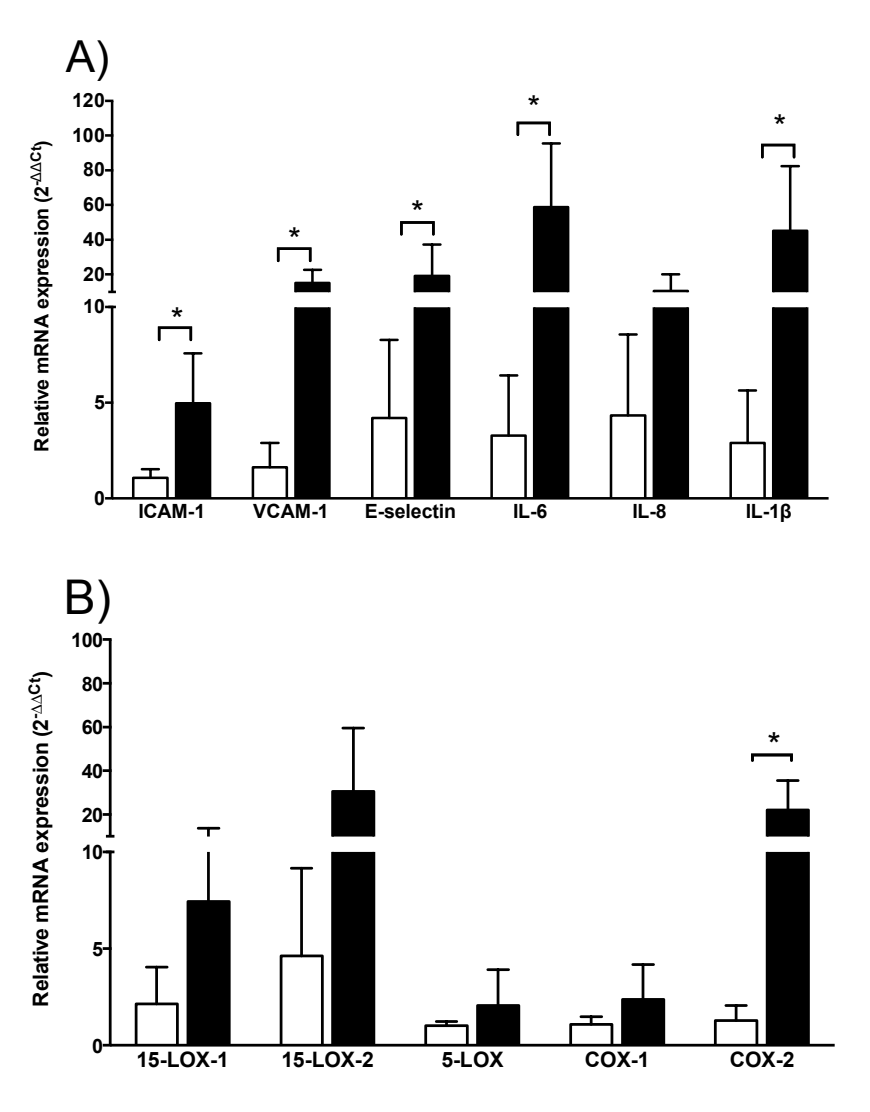


Figure 3. Means of relative mRNA expression in tissue from uninfected cows (n=3) are displayed in open bars and means of relative mRNA expression in tissue from *S. uberis*-infected cows (n=5) are displayed in closed bars. Pro-inflammatory marker (A) and oxylipid biosynthetic enzyme (B) mRNA expression of tissue from uninfected (n=3) and *S. uberis* (014J)-infected cows (n=5). The mRNA expression is expressed as $2^{-\Delta\Delta Ct} \pm SE$. Significance declared for differences in ΔCt at $P \le 0.05$.

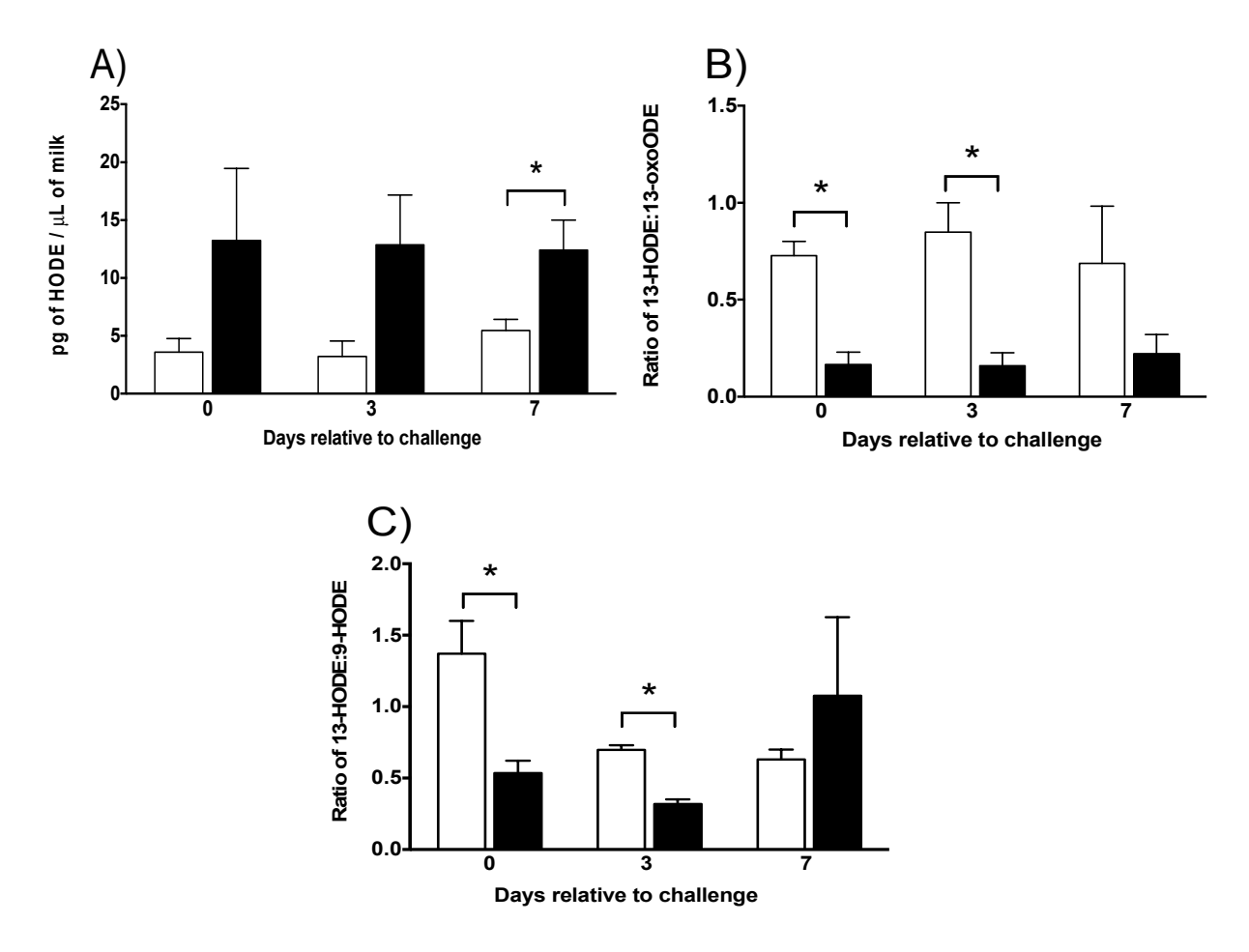


Figure 4. Means of oxylipid concentrations in milk from cows that failed to establish *S. uberis* mastitis (n=3) are displayed in open bars and means of oxylipid concentrations in milk from cows that established *S. uberis* mastitis (n=5) are in closed bars. Increased HODE was significant 7 d post-challenge in cows that established a *S. uberis* intramammary infection (A). In contrast, the milk 13-HODE:13-oxoODE ratio (B) and the milk 13-HODE:9-HODE ratio (C) was greater on the d of challenge and 3 d post-challenge in milk from cows that did not establish *S. uberis* mastitis compared to milk from cows that established mastitis. Values are means \pm SEM expressed in pg of oxylipid per μ L of milk or as a ratio of oxylipids. *Significance declared at $P \le 0.05$.

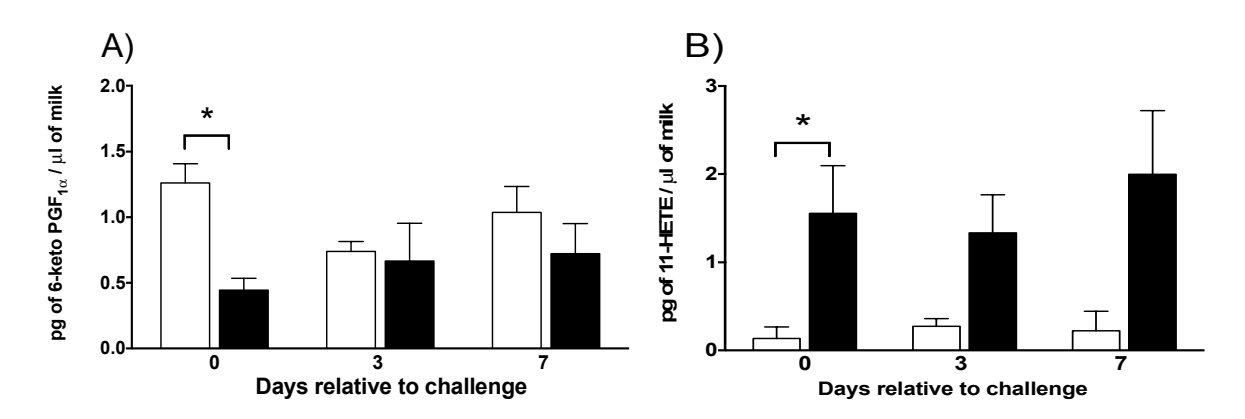


Figure 5. Means of oxylipid concentrations in milk from cows that failed to establish *S. uberis* mastitis (n=3) are displayed in open bars and means of oxylipid concentrations in milk from cows that established *S. uberis* mastitis (n=3) are in closed bars. The concentration of milk 6-keto-PGF_{1 α} (A) and 11-HETE (B) was different on the d of challenge between dairy cows that did not establish *S. uberis* mastitis compared to cows that established mastitis. Values are means \pm SEM expressed in pg of oxylipid per μ L of milk. *Significance declared at $P \le 0.05$.

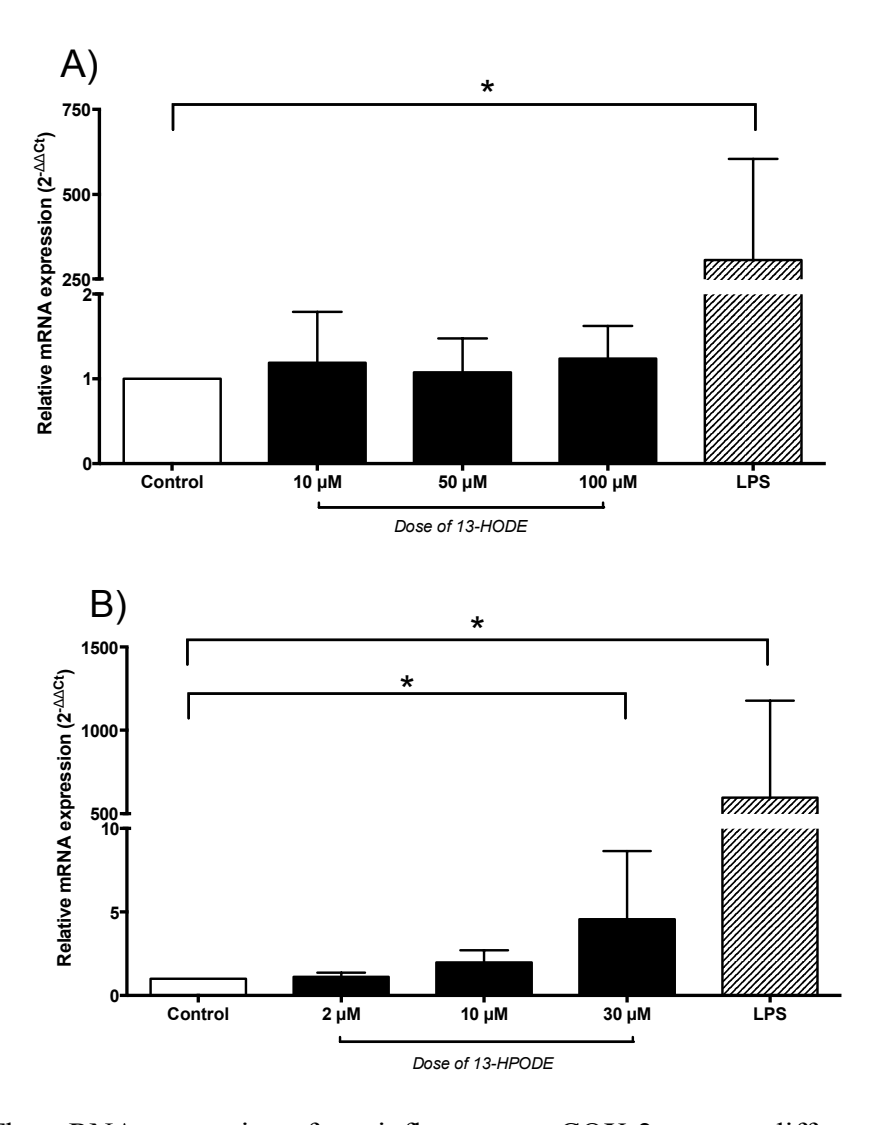


Figure 6. A) The mRNA expression of pro-inflammatory COX-2 was not different after 4 h 13-HODE exposure. (10 and 50 μ M n=7 and 100 μ M n=4). B) The mRNA expression of pro-inflammatory COX-2 was significantly greater after 4 h exposure to 30 μ M 13-HPODE (n=5). The positive control was LPS and was significantly greater during both experiments (A, B). The mRNA expression is expressed as $2^{-\Delta\Delta Ct} \pm SE$. Significance declared for differences in ΔCt at $P \le 0.05$.

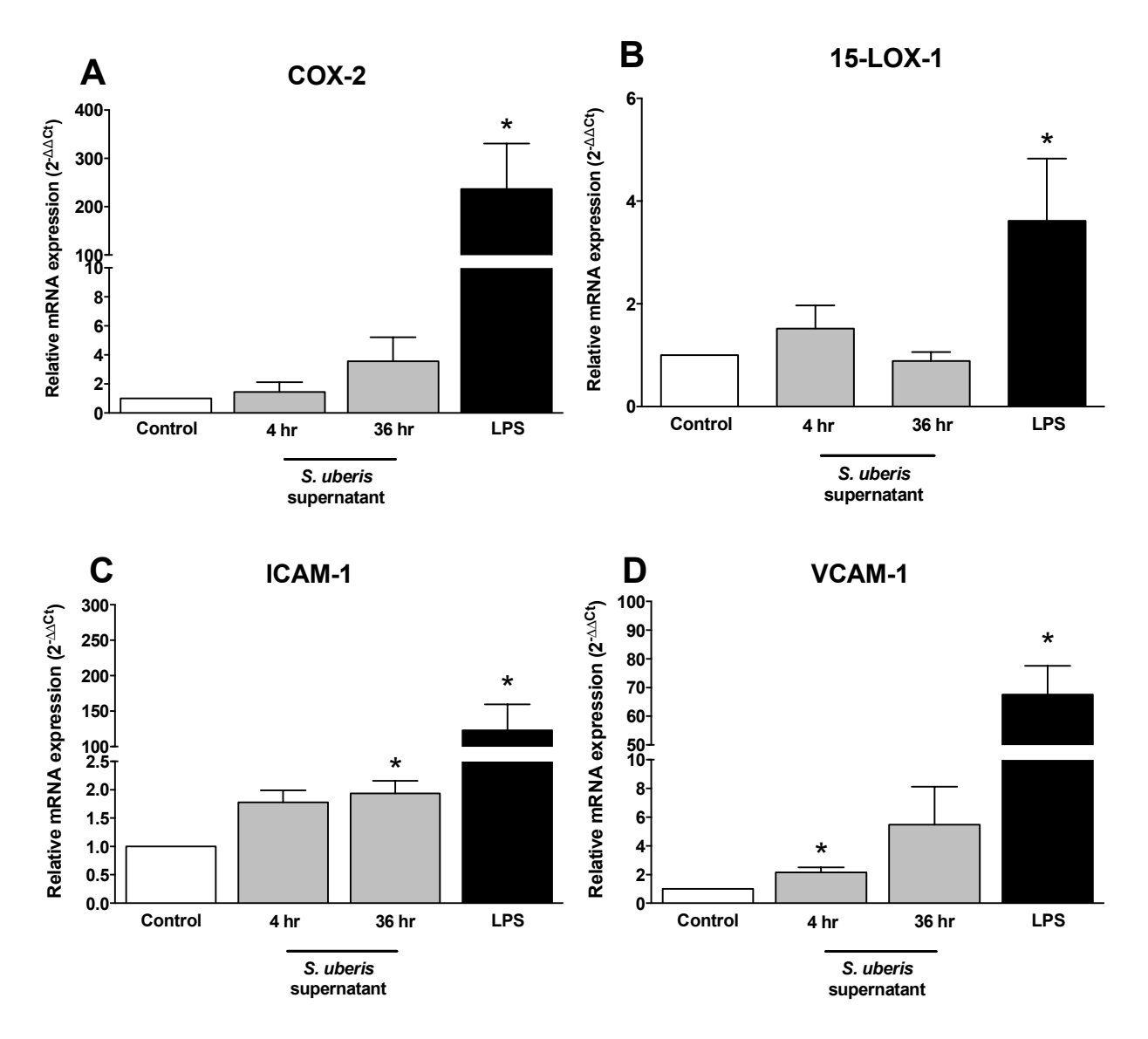
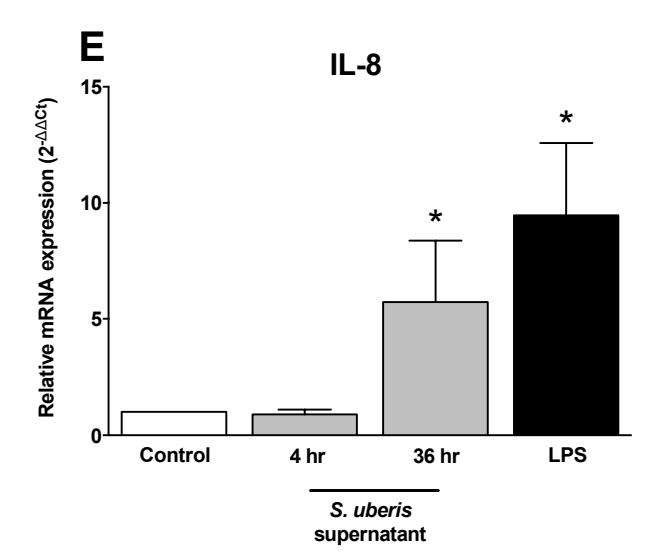


Figure 7. Mean changes in BMEC mRNA expression of oxylipid biosynthetic enzymes (A, B), adhesion molecules (C, D) and a chemotactic cytokine (E). Media controls are displayed as open bars. Positive control is 4 hr lipopolysaccharide (LPS) and displayed in closed bars are displayed. Light grey bars represent *S. uberis* supernatant exposure for 4 hr and 36 hr. The mRNA expression is expressed as $2^{-\Delta\Delta Ct} \pm SE$. Asterisks (*) denote differences between media control and treatments including *S. uberis* and positive control, LPS, as tested by Student's t-tests. Significance declared for differences in ΔCt at $P \le 0.05$ (n=3 for all genes).

Figure 7. (cont.)



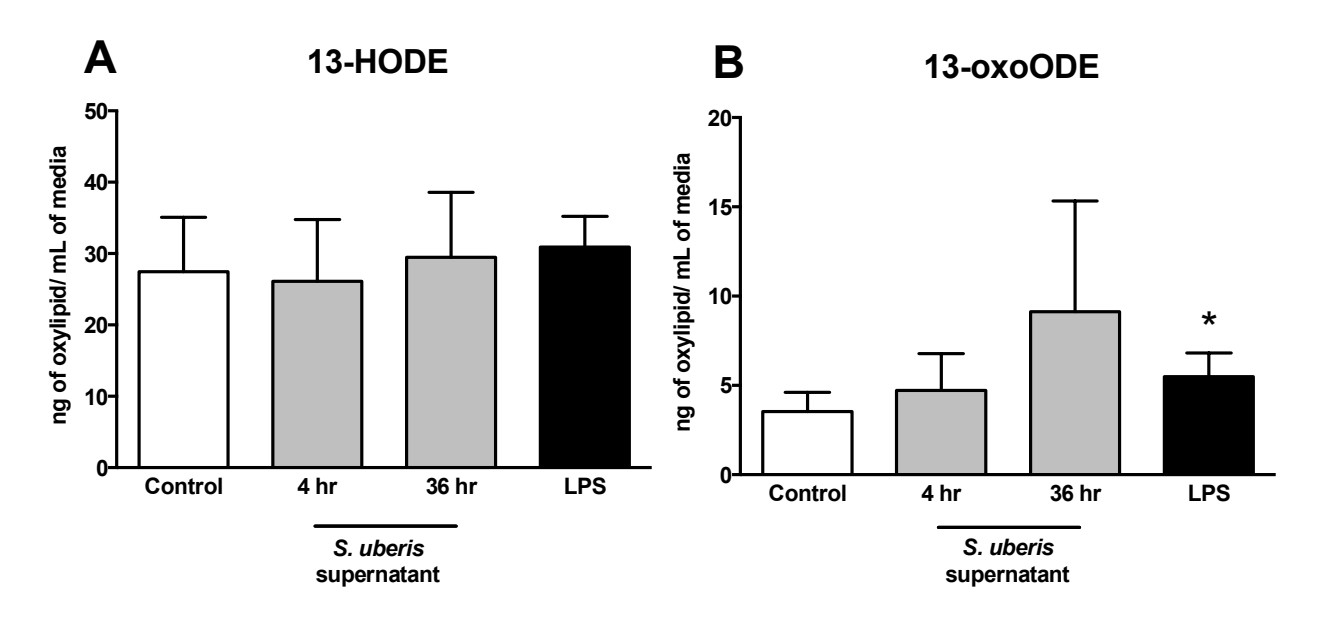


Figure 8. Oxylipid biosynthesis following 4 hr LPS (black bars) or *S. uberis* supernatant exposure for 4 hr and 36 hr (light grey bars) is displayed. Media controls are displayed as open bars. Mean oxylipid biosynthesis is expressed as ng of oxylipid/mL of media. Asterisks (*) denote differences between media control and positive control (LPS) as tested by Student's t-tests. Significance for differences declared at $P \le 0.05$ (n=3).

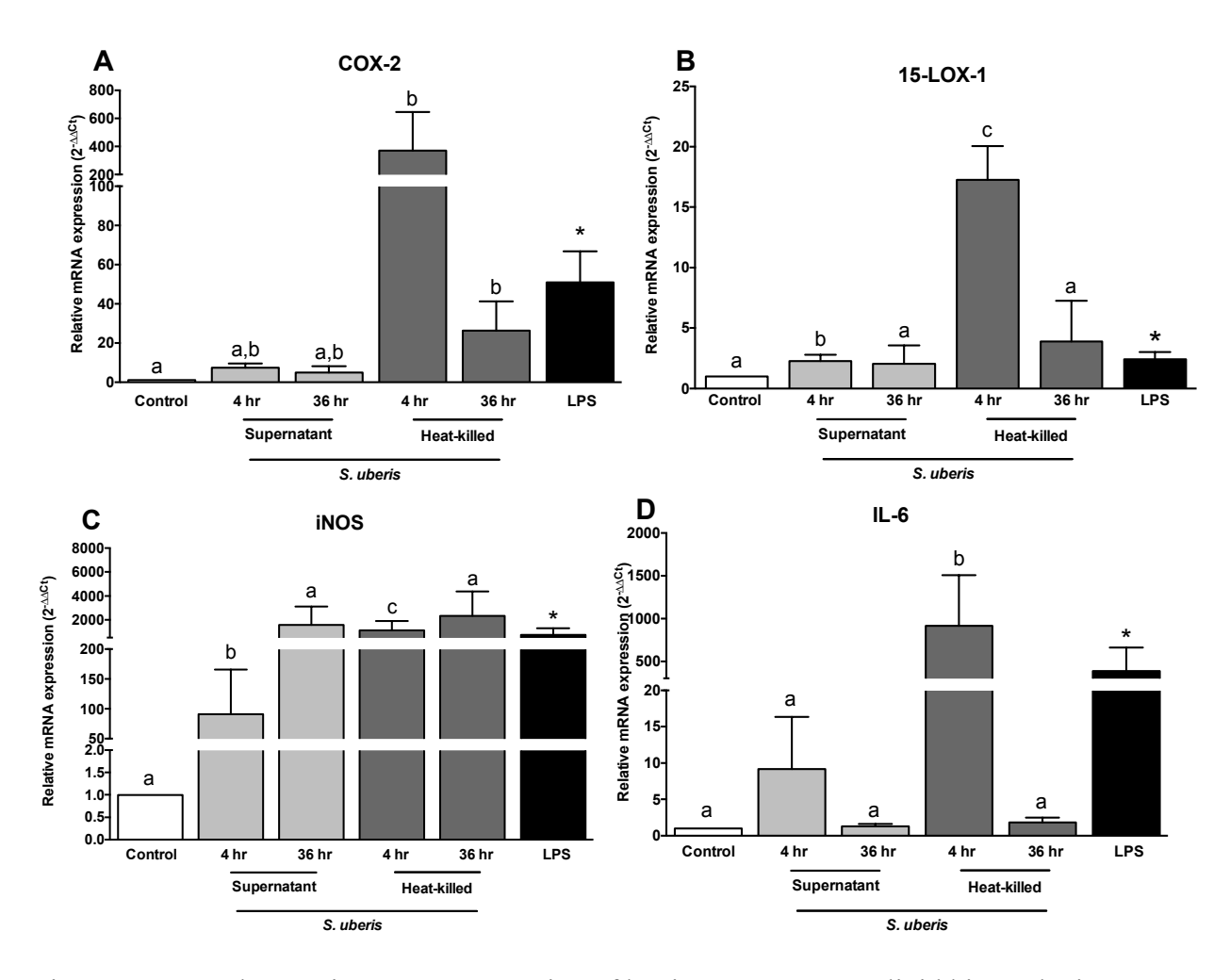
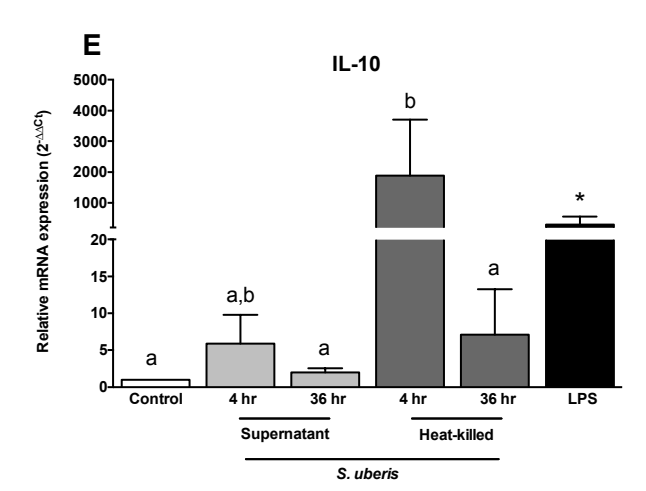


Figure 9. Mean changes in mRNA expression of bovine monocyte oxylipid biosynthetic enzymes (A, B), a marker of monocyte activation (C) and inflammatory cytokines (D, E). Media controls are displayed as open bars. Positive control is 4 hr LPS and displayed in closed bars. Light grey bars represent *S. uberis* supernatant exposure for 4 hr and 36 hr. Dark grey bars represent heat-killed *S. uberis* exposure for 4 hr and 36 hr. The mRNA expression is expressed as $2^{-\Delta\Delta Ct} \pm SE$. Asterisks (*) denote differences between media control and positive control (LPS) as tested by Student's t-tests. Letters that differ between control time points, 4 hr and 36 hr separately, denote significant differences between control and among treatments as measured by an ordinary one-way ANOVA with Tukey's post hoc correction. For example, 4 hr exposure to heat-killed *S. uberis* upregulated COX-2 mRNA expression compared to control but 4 hr exposure to *S. uberis* supernatant did not (Figure 3A). Additionally, COX-2 mRNA expression after *S. uberis* supernatant exposure (Figure 3A). A similar relationship can be described for 36 hr exposure of bovine monocytes to heat-killed and *S. uberis* supernatant. Significance declared for all tests using Δ Ct at $P \le 0.05$ (n=4 for 15-LOX-1, IL-6, and IL-10; n=3 for COX-2 and iNOS).

Figure 9. (cont.)



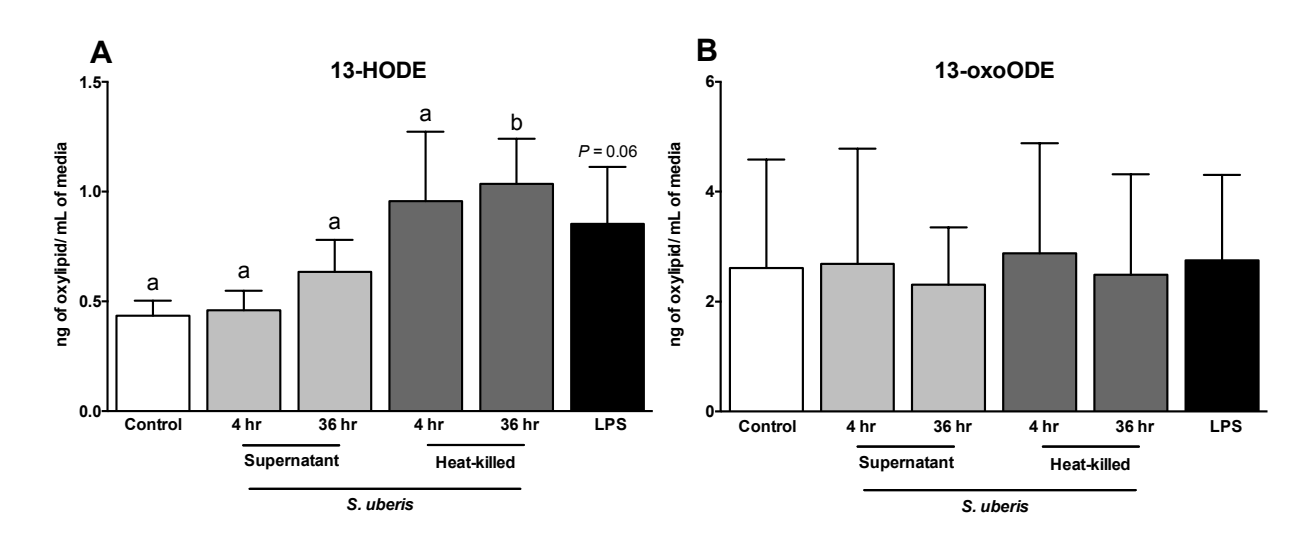


Figure 10. Oxylipid biosynthesis following 4 hr LPS (black bars) or *S. uberis* exposure. Media controls are displayed as open bars. Light grey bars represent *S. uberis* supernatant exposure for 4 hr and 36 hr. Dark grey bars represent heat-killed *S. uberis* exposure for 4 hr and 36 hr. Mean oxylipid biosynthesis is expressed as ng of oxylipid/mL of media. Asterisks (*) denote differences between media control and positive control (LPS) as tested by Student's t-tests. Letters that differ between control time points, 4 hr and 36 hr separately, denote significant differences between control and among treatments as measured by an ordinary one-way ANOVA with Tukey's post hoc correction. For example, 4 hr exposure to *S. uberis* supernatant or heat-killed *S. uberis* did not modify 13-HODE biosynthesis, whereas 36 hr exposure to heat-killed *S. uberis* did increase 13-HODE biosynthesis. No letters are displayed in Figure 4B as no differences were detected in any time points. Significance for differences declared at $P \le 0.05$ (n=4).

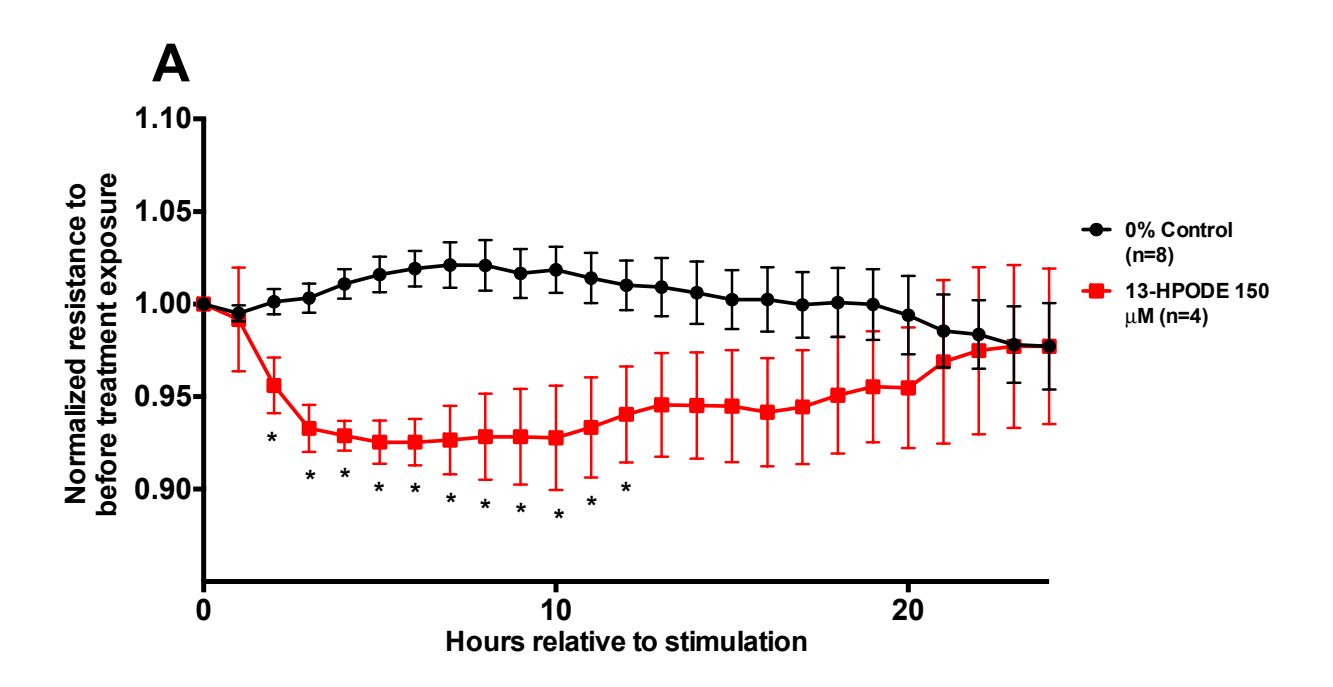


Figure 11. Mean normalized resistance across time during media control ($\stackrel{\bullet}{\bullet}$) and 150 μ M 13-HPODE ($\stackrel{\bullet}{\bullet}$) is displayed in Figure 5A. Mean normalized resistance for 100 μ M 13-HODE ($\stackrel{\bullet}{\bullet}$) exposure up to 6 hr is displayed in Figure 5B. Mean normalized resistance across time during media control ($\stackrel{\bullet}{\bullet}$) and 25 ng/mL LPS ($\stackrel{\bullet}{\bullet}$) is displayed in Figure 5C. Resistance for each group is normalized to prior to treatment addition. Significance declared for differences between media control and 13-HPODE at specific time points by Mann-Whitney tests ($P \le 0.05$).

Figure 11. (cont.)

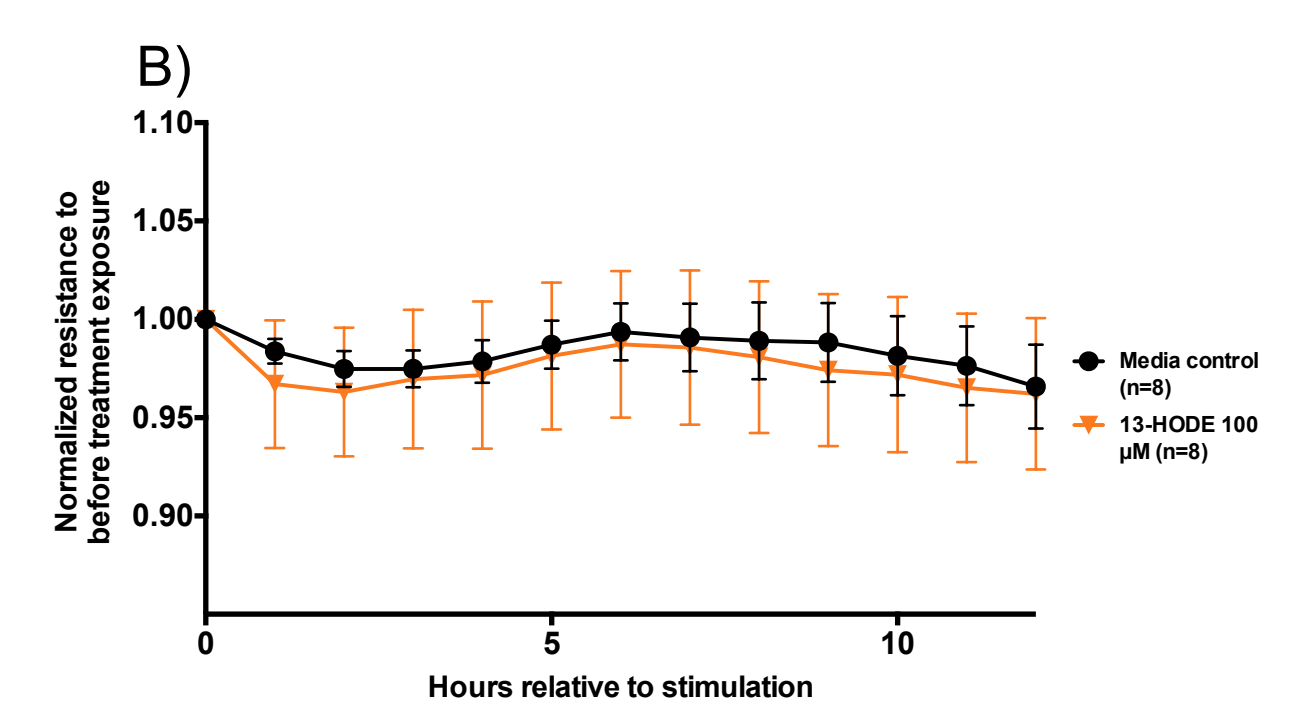
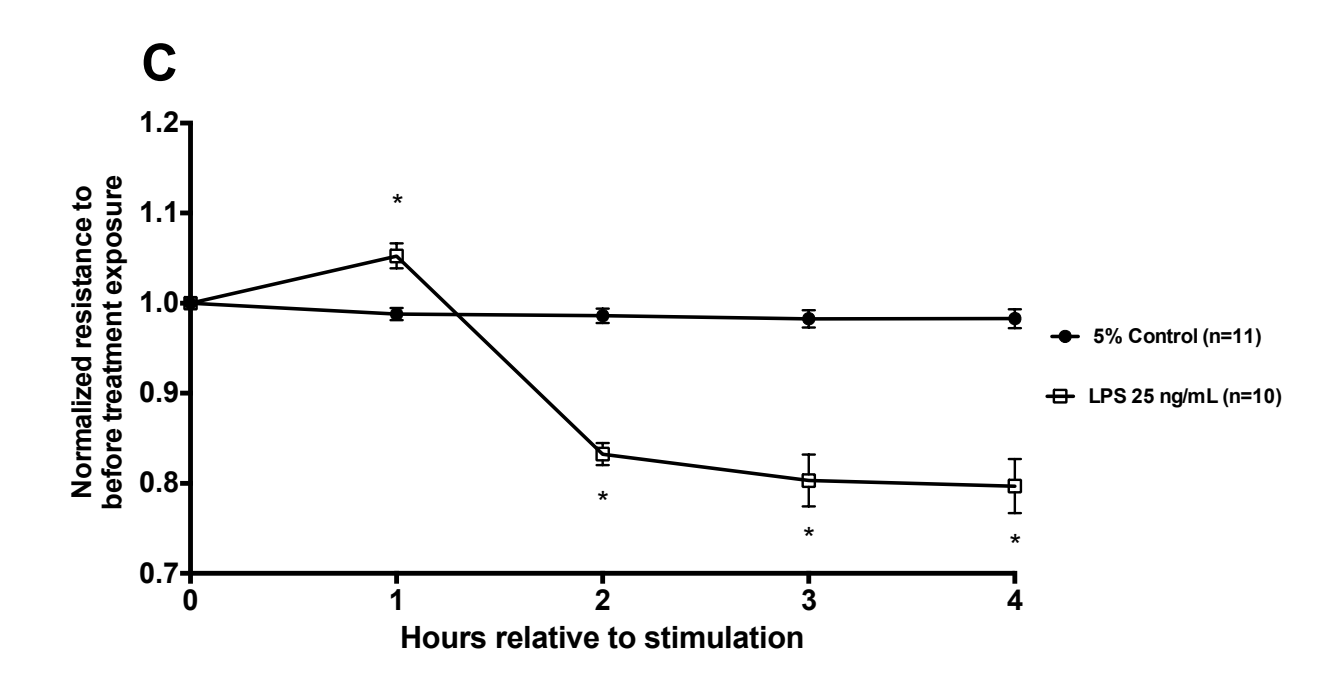
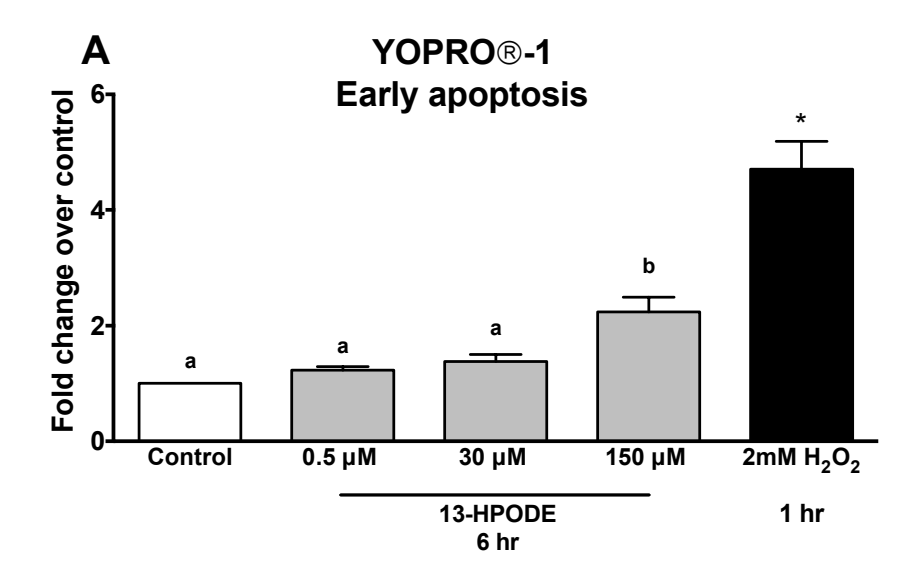


Figure 11. (cont.)





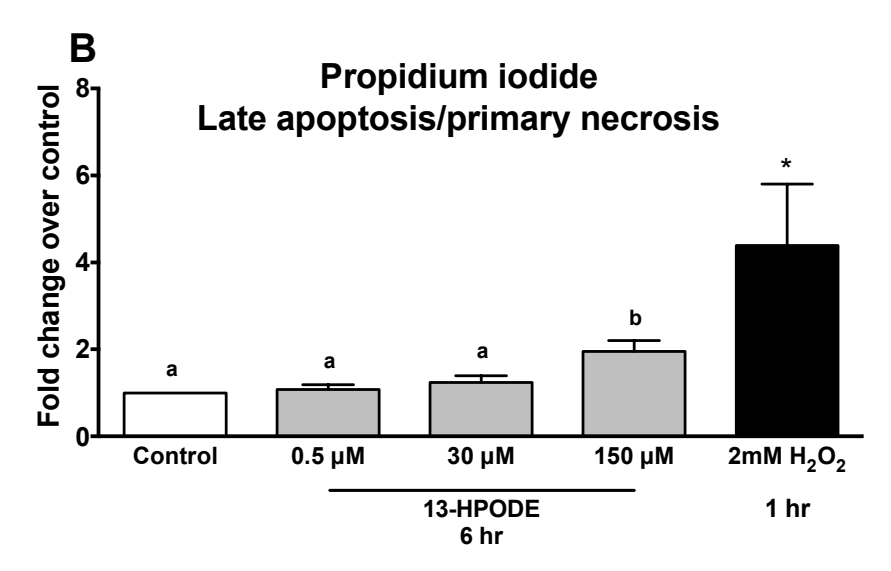
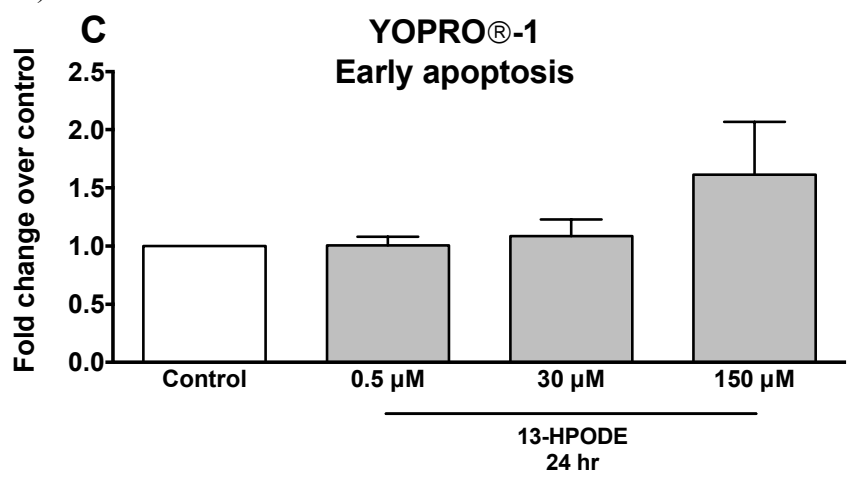
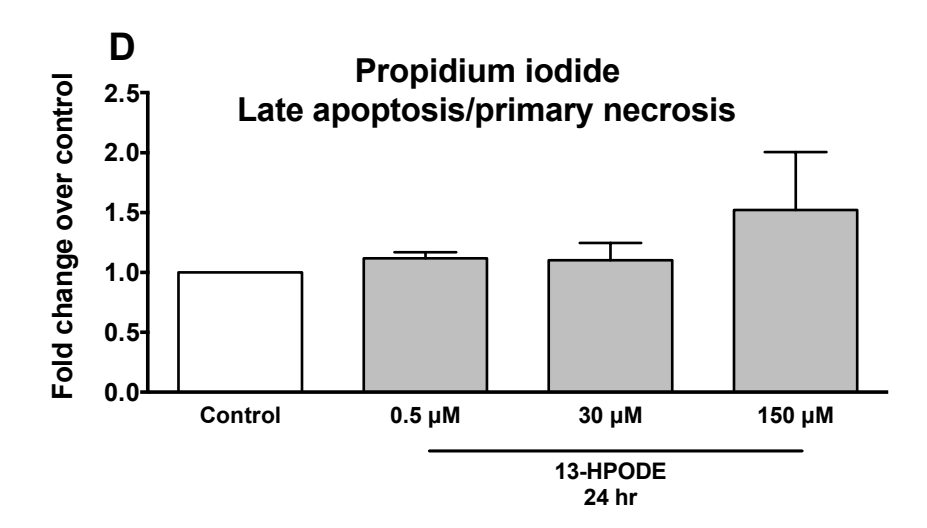


Figure 12. YOPRO®-1 and propidium iodide staining displayed as fold change over media control after 6 hr (Figure 6A & B) and 24 hr (Figure 6C & D) 13-HPODE exposure. Media controls are displayed in open bars and 13-HPODE treatments are in light grey bars. Positive control (1 hr 2mM H_2O_2 exposure) YOPRO®-1 and propidium iodide staining is displayed in Figure 6A & B and are the black bars. Different letters demonstrate a significant difference among media control and 13-HPODE treatments determined by one-way ANOVA with Tukey's post hoc correction. An asterisk (*) represents a significant difference between medial control and H_2O_2 as determined by Student's t-tests. Significance declared at $P \le 0.05$.

Figure 12. (cont.)





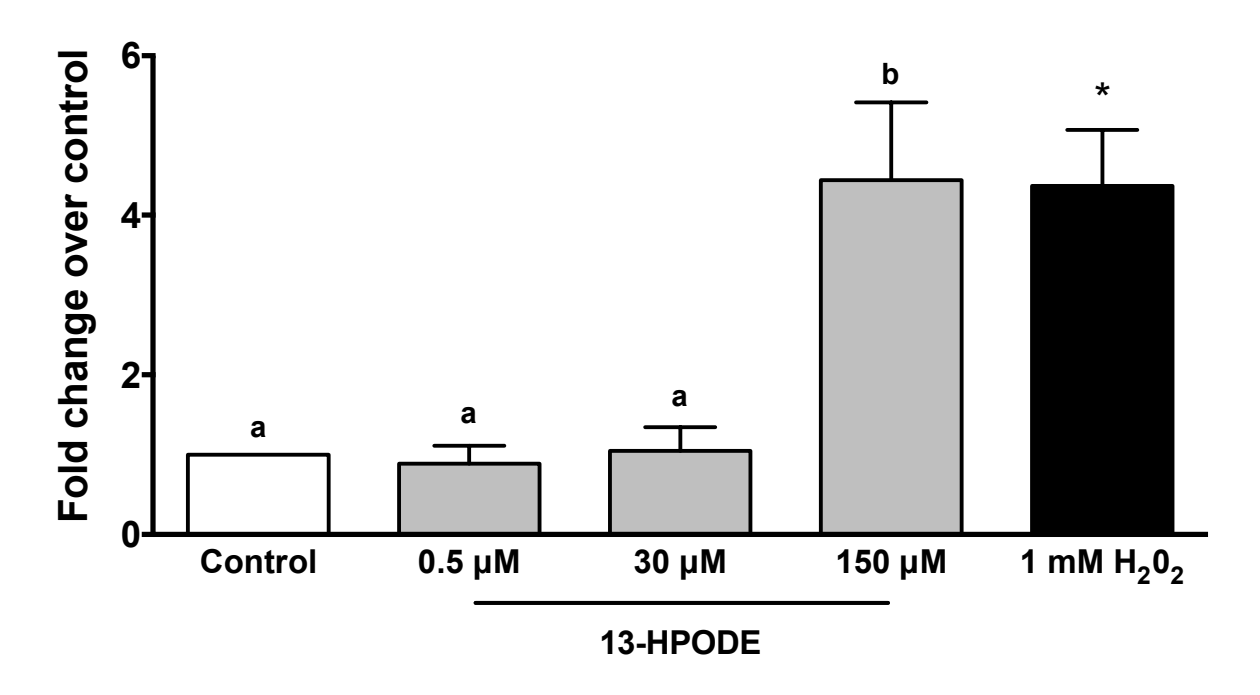


Figure 13. Mean change in caspase 3/7 activity displayed as fold change over media control (open bar) after 6 hr 13-HPODE (light grey bars) or 1 mM H_2O_2 exposure for 6 hr (black bar, positive control). Different letters demonstrate a significant difference among media control and 13-HPODE treatments determined by one-way ANOVA with Tukey's post hoc correction. An asterisk (*) represents a significant difference between medial control and H_2O_2 as determined by Student's t-tests. Significance declared at $P \le 0.05$.

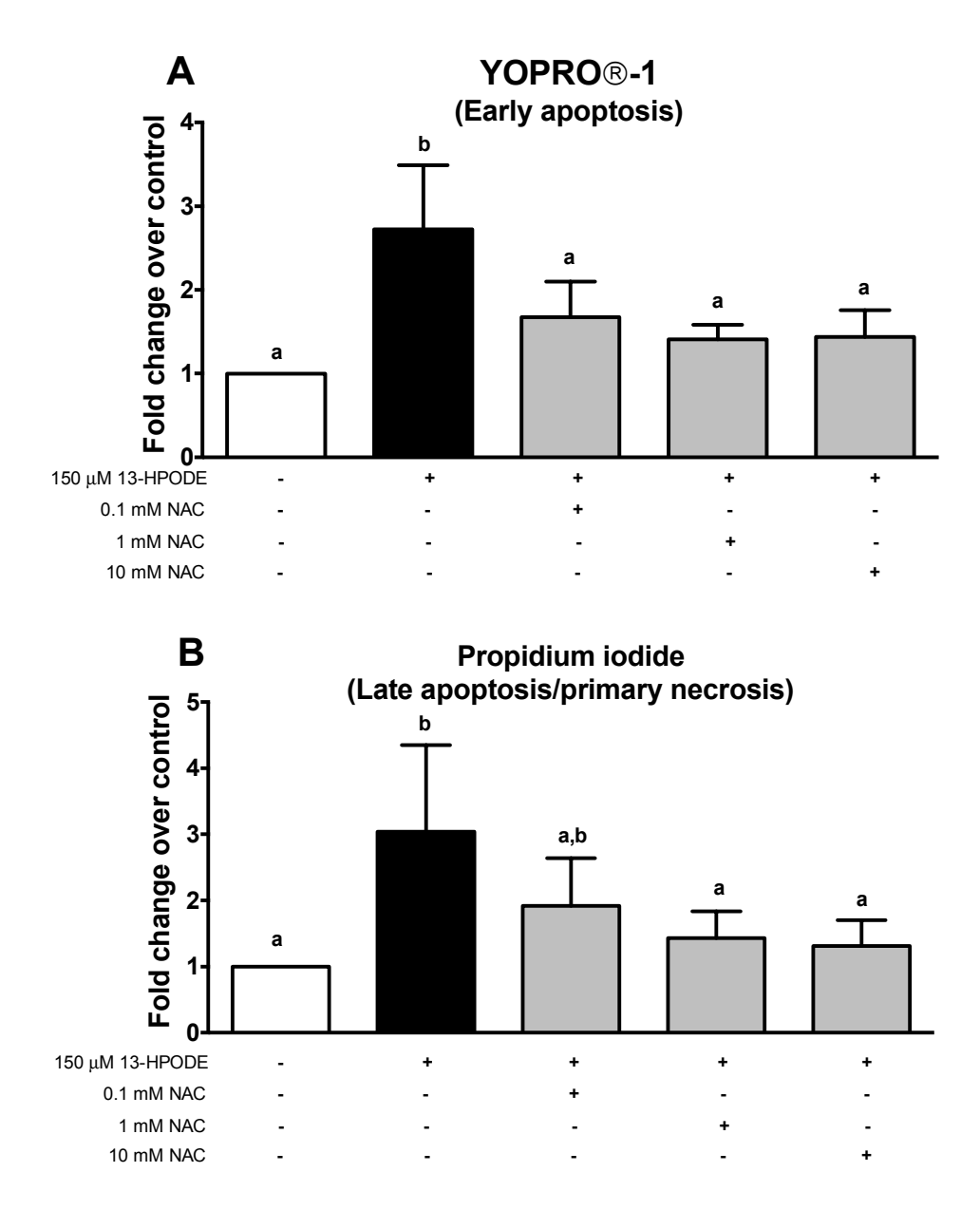


Figure 14. YOPRO-1 and propidium iodide staining displayed as fold change over media control (open bar) after 6 hr 150 μ M 13-HPODE (light grey bars) or 6 hr co-exposure with 150 μ M 13-HPODE or N-acetylcysteine (NAC, light grey bars). Different letters demonstrate a significant difference among media control and treatments as determined by a one-way ANOVA with Tukey's post hoc correction. Significance declared at $P \le 0.05$.

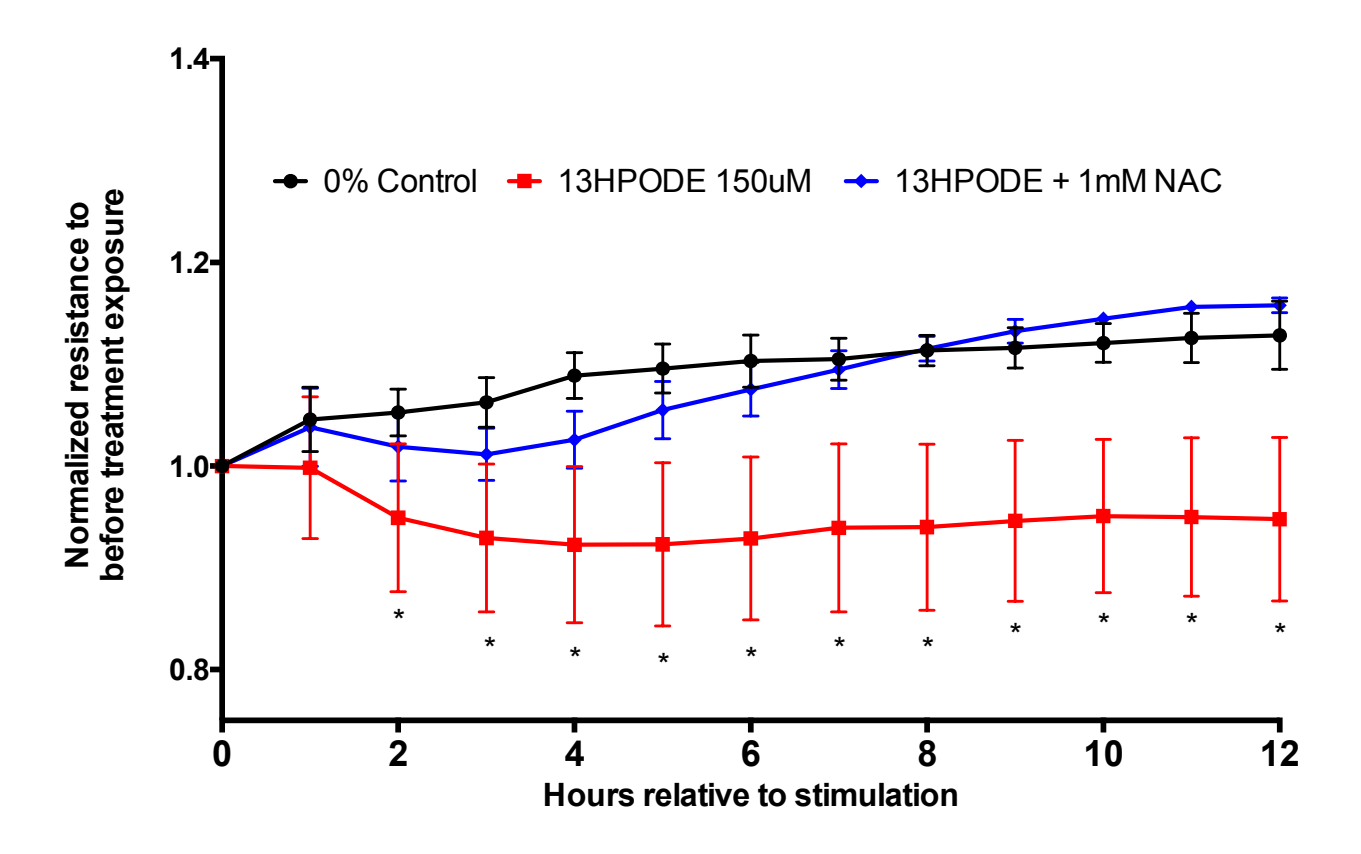


Figure 15. Mean normalized resistance across time during media control ($\stackrel{\bullet}{\bullet}$), 150 μ M 13-HPODE ($\stackrel{\bullet}{\bullet}$), and 150 μ M 13-HPODE + 1 mM N-acetylcysteine (NAC) ($\stackrel{\bullet}{\bullet}$) exposure is displayed in Figure 9. Resistance for each test group is normalized to prior to treatment addition. Significance declared for differences between media control and 13-HPODE at specific time points by Mann-Whitney tests ($P \le 0.05$). There were no significant differences detected between media control and 13-HPODE + 1mM NAC.

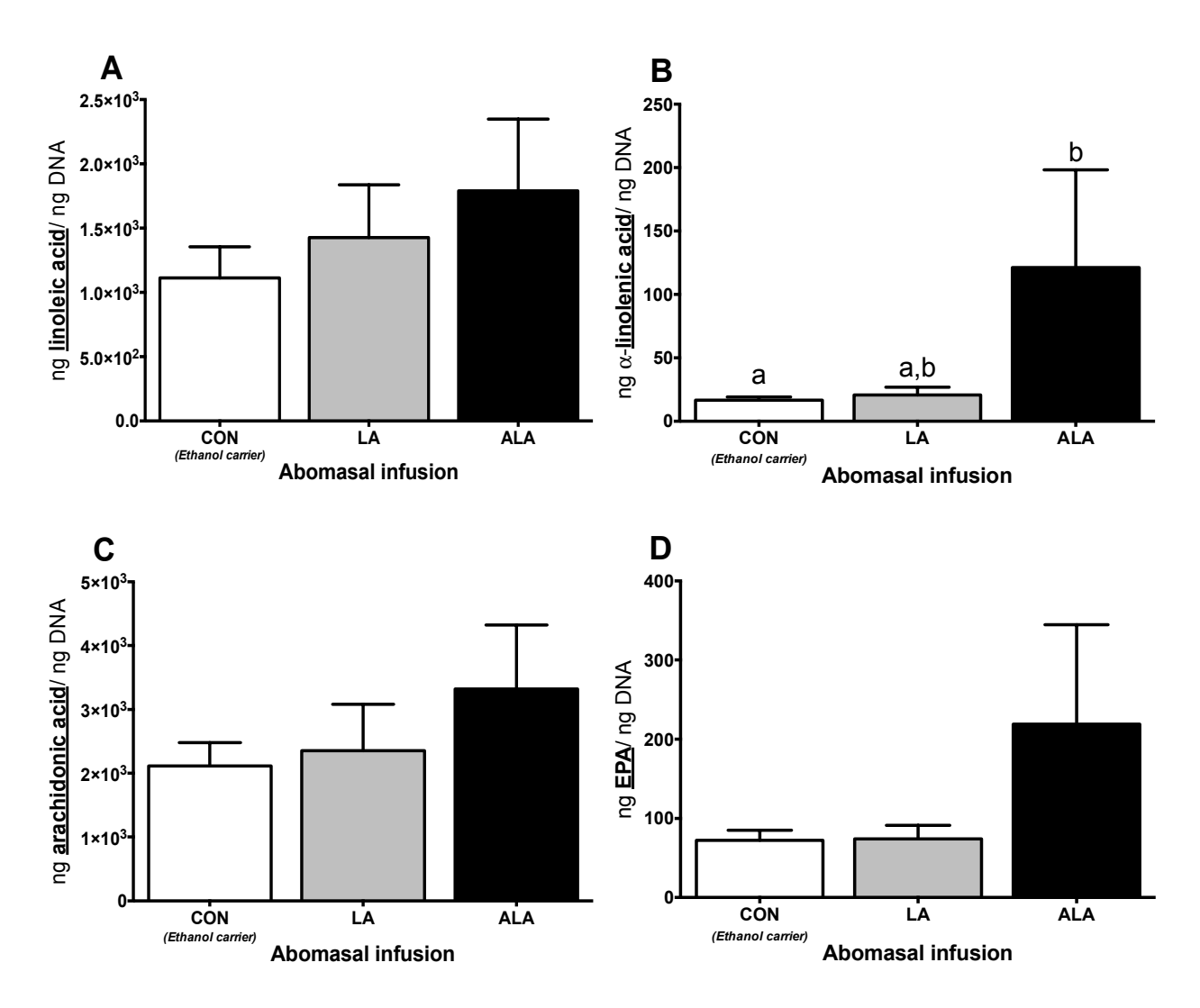
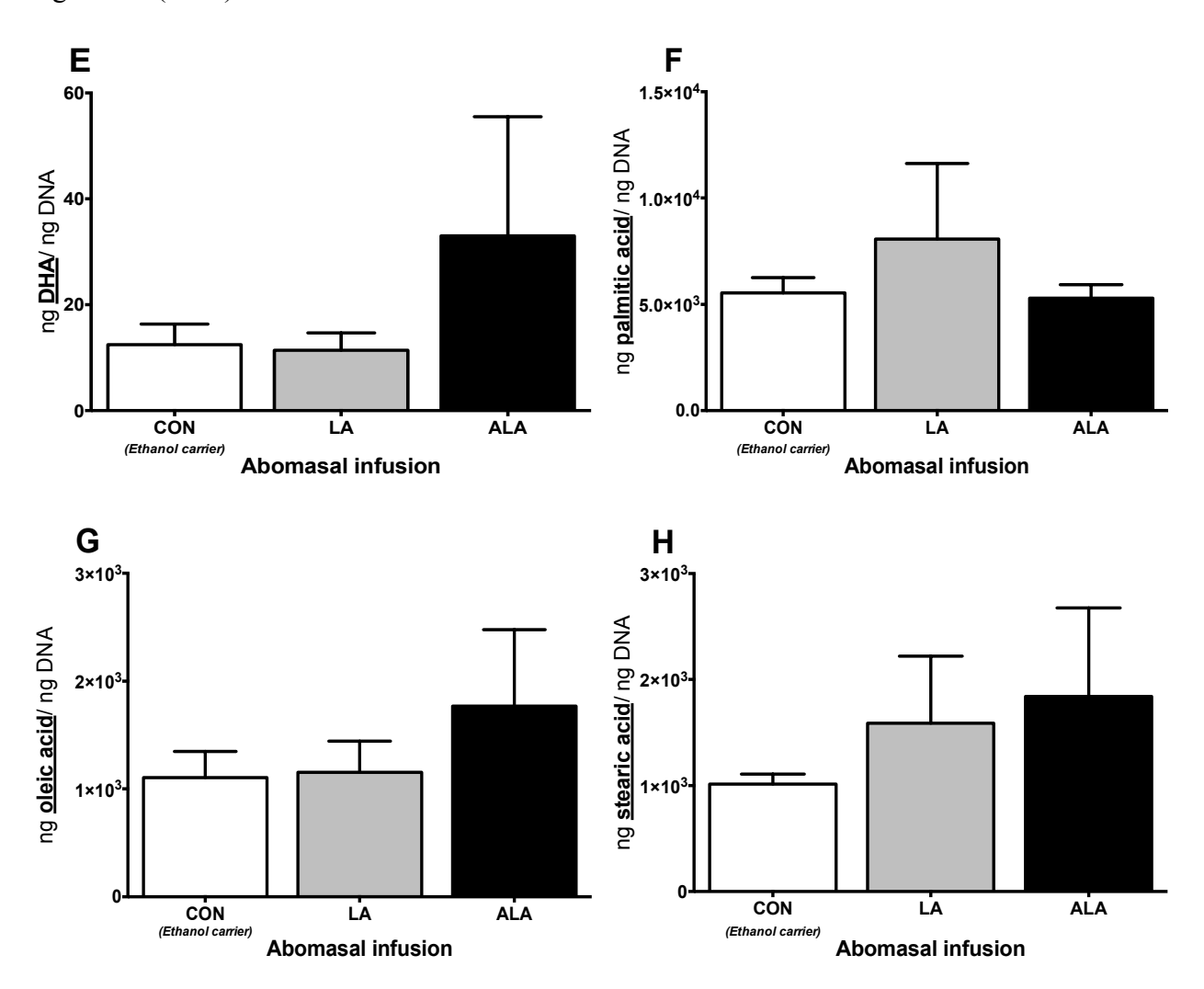


Figure 16. Normalized amount (ng FA/ ng DNA) of PUFA, SFA, and MUFA in bovine leukocytes following supplementation of the ethanol carrier (CON), LA at 45 g/d, or ALA at 45 g/d. Figures 1A-E depicts quantified PUFA (LA, ALA, ArA, EPA, and DHA). Figures 1F-G depicts quantified MUFA and SFA (palmitic acid, oleic acid, and stearic acid). Letters in Figure 1B represent significant differences across treatments groups as determined by a non-parametric one-way ANOVA with Dunn's correction ($P \le 0.05$).

Figure 16. (cont.)



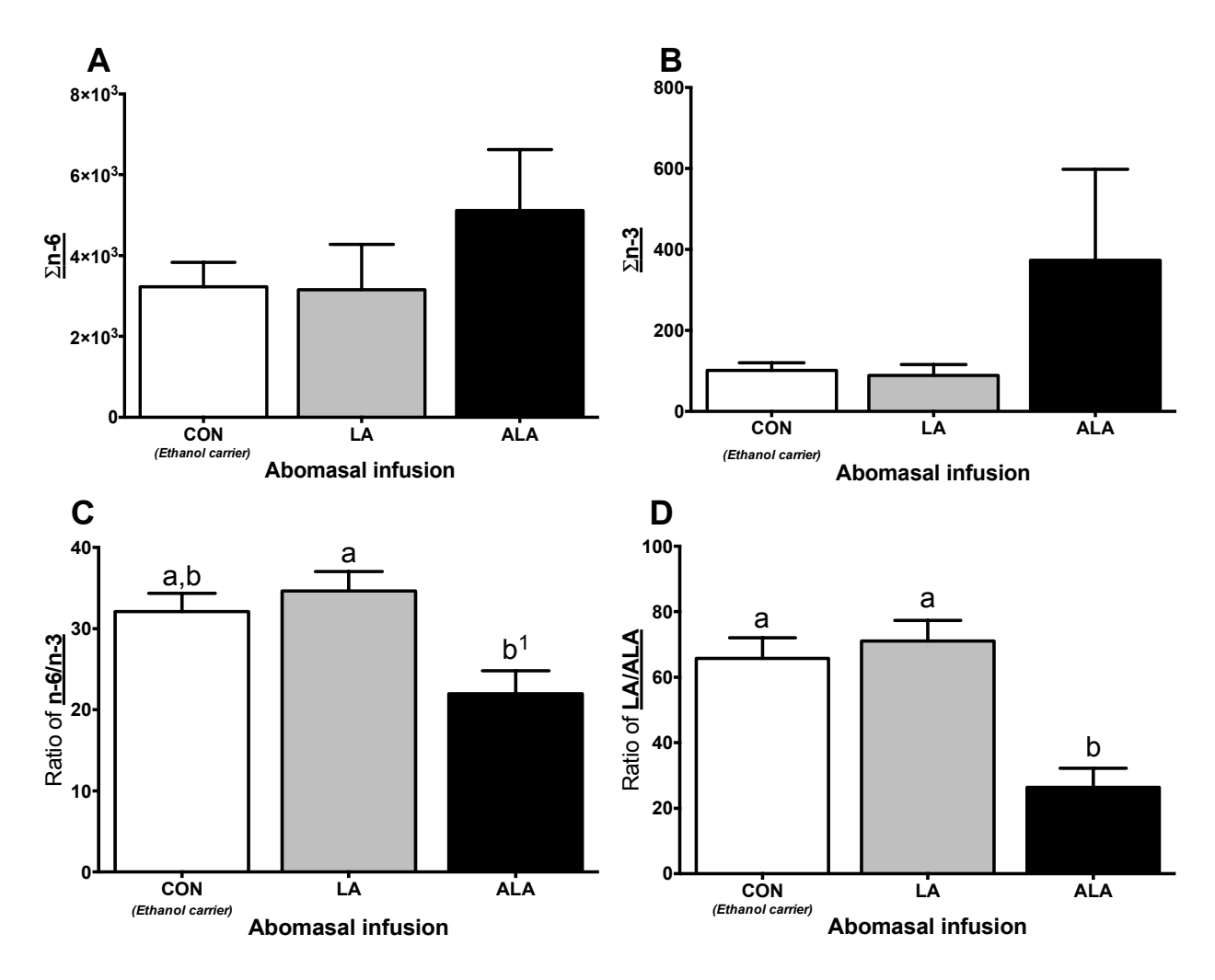


Figure 17. Normalized average sum of n-6 FA (ng FA/ ng DNA), n-6 FA (ng FA/ ng DNA), ratio of n-6/n-3, and ratio of LA/ALA in bovine leukocytes following supplementation of the ethanol carrier (CON), LA at 45 g/d, or ALA at 45 g/d. Figure 2A represents the normalized sum of n-6 PUFA (LA and ArA). Figure 2B represents the normalized sum of n-3 PUFA (ALA, EPA, and DHA). Figure 2C represents the ratio of total n-6 to n-3 (n-6/n-3). Figure 2D represents the ratio of LA to ALA (LA/ALA). Letters in Figure 2C & D represent significant differences across treatments groups as determined by an non-parametric one-way ANOVA with Dunn's correction ($P \le 0.05$).

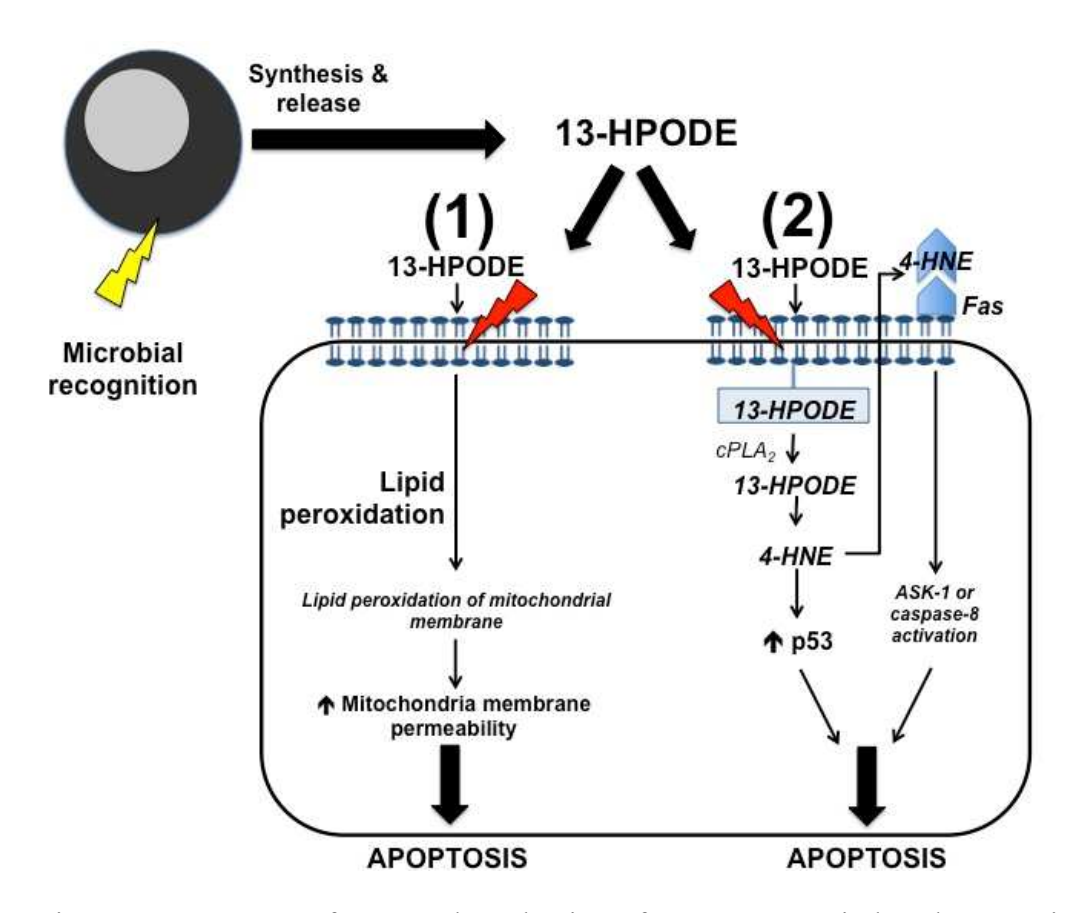


Figure 18. Summary of proposed mechanisms for 13-HPODE-induced apoptosis. (1) 13-hydroperxyoctadecadienoic acid (13-HPODE) may promote lipid peroxidation of endothelial membranes and contribute to increased lipid peroxyl radicals capable of propagating lipid peroxidation in the mitochondrial membrane. An inability to reduce pro-oxidant contributes to sustained increase in the permeability of the mitochondrial membrane and likely results in activation of intrinsic pathway of apoptosis. (2) 4-hydroxynonenal (4-HNE) may be formed as an end product of lipid peroxidation or from 13-HPODE cleaved from the membrane. Increased 4-HNE may activate cytoplasmic p53, which can promote transcription and translation of proteins that promote apoptosis. Conversely, 4-HNE is diffusible and can interact with the Fas death ligand to contribute to activate of the extrinsic apoptosis pathway through either caspase 8 activation or apoptosis signal-regulating kinase 1 (ASK-1).

Appendix E. Preparation of 13-HPODE

Preparation of 13-HPODE

Chemicals and solvents needed

Sodium borate (Fisher Science Education – blk bottle)
Linoleic acid (Sigma)
Lipoxidase type V from glycine max – soybean (Sigma) #L66632-IMU
Diethyl ether (JT Baker)
Millipure ddH₂0
Magnesium sulfate (JT Baker)
n-Hexane 99% (Fisher Scientific)
2-propanol (JT Baker) lot #151392
Ethyl Alcohol (Sigma)

Method

- 1) Rinse all glassware 3x with sterile EtOH.
 - a. Glassware needed: 2 250 mL bottles, 100 mL bottle (or 250 if not available), 2 100 mL graduated cylinders, 250 mL graduated cylinder, separation flask, rotary ball, solvent collector, several amber 5 mL bottles and clear 1.5 mL chromatography vial.
- 2) Fill water bath with DI water to 1 in. from top using beaker from precision water bath. Turn on Ecoline Rotary Evaporator to cool to -10°C and BUCH water bath to heat to 37°C.
- 3) Mix 14.29 g sodium borate in 250 mL millipure ddH₂0 in a rinsed 250 mL bottle with stir bar.
 - a. Stir on heat (100°C at 300rpm) for approximately 45 minutes.
- 4) Chill:
 - a. millipure ddH₂0 (at least 30 mL place in fridge across from sink)
 - b. diethyl ether (at least 60 mL pour in hood into an amber colored bottle in -20°C freezer)
 - c. 788mL:32mL hexane:propanol mixture until cold (in -20°C freezer)
- 5) Hexane and Propanol 1L bottles above Shimadzu machine Dump old and replace with **fresh** each time protocol run (hexane in TC hood beaker and Propanol in white jug in Mol. Bio. Lab). Gentle handling of line and filter when laying down. Be careful to do one at a time to keep line A for hexane ONLY and line B for propanol ONLY. Add enough for a full bottle each.
 - a. Hexane below hood fill in hood
 - b. Propanol –fill in hood
- 6) Turn on Shimadzu computer + 4 Shimadzu parts (buttons on machines to left of computer): 2 pumps, main controller, and PDA. → see Shimadzu Start-up Protocol
 - a. Make sure stopper in jug on floor sealed.
- 7) Once sodium borate buffer completely dissolved, pH to ≈ 9 (8.9 9.1 acceptable) and filter vacuum into new rinsed 250 mL bottle.
 - a. Chill at -20°C freezer until cold.

- 8) Transfer 30 mL sodium borate buffer in graduated cylinder to rinsed 100 mL *round bottom* bottle with stir bar.
 - a. Place bottle in gallon freezer bag on stirrer and get stirring well at gentle speed (75-100 rpm) BEFORE packing ice around bottle.
- 9) Linoleic acid suspension prep:
 - a. Shake liquid in vial down before popping top off (serrated).
 - b. Add 1 mL of borate buffer to new vial of linoleic acid with glass pipette (1 vial = 100mg; need 50mg)
 - c. Mix thoroughly with Pasteur pipette (gets very clumpy; will never go completely into solution).
 - d. Transfer 0.5 mL linoleic acid suspension to 30 mL borate buffer on ice, continue stirring, and LIGHTLY cap.
- 10) Add 118.89 uL (300,000 U) of lipoxidase type V to linoleic acid suspension- adding straight into buffer.
 - a. Stir bottle on ice for 1 h with **cap off.** Ensure bottle is in bag surrounded by ice to keep cold. (SEE **SHIMADZU START-UP** DURING THIS INCUBATION)
- 11) Stop reaction by adjusting pH to 3 (at least 3, below 3 ok too; slow down addition at 6 quick drop after) with 1 N HCl using pipette filler (in drawer below pH meter).
- 12) Screw round bottom flask on ratavapor machine with clamp.
- 13) Chill 2 blue topped waters vials + place sodium borate solution on ice.
- 14) Add 60 mL cold diethyl ether (in freezer) to linoleic acid suspension **in hood** and transfer to rinsed separation flask that has been purged with argon (make sure valve in closed position); cap. Complete these steps in the fume hood:
 - a. Invert separation flask and shake vigorously.
 - b. Burp/release valve to release gas.
 - c. Continue shaking and burping at least 5-10x.
 - d. Let separation of phases occur: upper = diethyl ether and lower = water.
 - e. Decant lower phase (water) to separation line.
 - f. Flip back over, release cap, and let separate into two phases again.
- 15) Add 30 mL cold millipure ddH20 and repeat step 14, waiting 30s at separation step.
 - a. Final release of water and shake/burp.
- 16) Add magnesium sulfate until it no longer "sticks" and crystals begin to move/roll with movement. (movement = all water has bound to magnesium sulfate)
- 17) Ensure rinsed rotary ball flask is flushed with argon and transfer diethyl ether extract slowly straight down into bottom of rotary ball flask. Attach flask to rotavapor, clamp down, and twist until locked into position.
- 18) Lower flask into water bath using lever. Slowly turn on rotary evaporator to a speed of 15 rpm, turn on vacuum, increase rotation speed to 115 rpm and vacuum to 22psi. (Watch for bubbles whole time!)

- a. If bubbles appear, release gas by turning valve on rotary evaporator arm.
- 19) Add ice around new rotary ball flask at bottom of condenser, packing around sides up to neck.
- 20) Once all liquid is gone (may be a slight oily residue) ie nothing actively dripping off coils, use lever to lift up flask in water bath slowly (not enough to disturb ice around condenser flask) and wipe water off side of flask and rotate (make sure not liquid left in water bath flask). If no liquid, shut off vacuum and release water bath flask and transfer to ice (this is now your extract collected).
- 21) **Raw Fraction Extract** = Resuspend extract collected first in 1 mL cold hexane:propanol (788 mL hexane:32 mL propanol or mobile phase) using a glass pipette.
 - a. Tilt flask to a flat orientation and roll ball around to ensure extract is collected. Remove extract and transfer to rinsed amber colored vial. Record volume of collection.
 - b. Top with argon. Place on ice.
- 22) **Raw Fraction Extract** = Add an additional 1 mL hexane:propanol (mobile phase) using a glass pipete and swirl/rotate ball to ensure extract is collected from the entire surface.
 - a. Remove extract and transfer to rinsed vial from step 15. Record volume of collection.
 - b. Top with argon. Place on ice.
- 23) Prepare 13-HPODE standard mixture (3 uL in 400 uL mobile phase should work). This standard doesn't have to exact as quantification will be done on LC/MS.
- 24) When ready to inject, press "load data" to load appropriate flow parameters for the method.
- 25) Ensure that pressure remains stable before injecting (355-370 psi).
- 26) Inject 2 syringe fulls (1000 μL) of mobile phase solution to injection site on column.
 - a. Hit "Start Stable Run"
 - b. Change name to standard prep or fraction# (13 HPODE standard prep 2 4 16)
 - c. Copy & paste to sample ID
 - d. Open semi prep methods (yellow folder icon) \rightarrow new date folder \rightarrow save
 - e. BEFORE clicking ok, make sure injector lever in up position.
 - f. Click ok.
- 27) Inject 200 uL 13-HPODE standard to determine approximate time of collection.
 - a. Take note of retention time.
 - b. If standard does not look clean, re-inject and if need be, make a new standard mixture.
- 28) Inject 200 uL raw fraction and collect at respective time. May not be able to collect first injection if peaks are a bit "messy".
 - a. Collect into blue topped waters bottles.
 - b. Top with argon.
- 29) Continue injecting and collecting all fractions until done with prepared extract. Top with argon each time.
 - a. At end of run (14min long) take out syringe and turn lever to up position.

30) Clean up:

- a. Clean separation column/flask with DI water to clean out magnesium. Rinse 1x with ethyl alcohol.
- b. Sodium borate can go down sink.
- c. Turn off bath, column, and machine.

Pour out condenser column flask liquid. Rinse 1x with ethyl alcohol.

Appendix F. Electric Cell-Substrate Impedance Sensing Experimental Protocol

BMEC ECIS EXPERIMENTS

ECIS: Day 1

- 1. Warm L-cysteine (10mM solution in sterile water, Morgan and Katie know how to make if you give them a couple days warning) to room temperature. Warm 0.15M NaCl solution, sterile ddH2O, sterile HBSS, several tubes of trypsin, 10% FBS F12k +Se BMEC media, and 5% FBS F12k +Se BMEC media.
- 2. Make sure you close out any open runs on the ECIS system and reopen software.
- 3. Add 200 uL 10mM L-cysteine to each well and allow to sit at room temperature for 10 minutes.
- 4. Make up bovine collagen at 4 uL/mL (usually make 5 mL for 2 arrays) with warmed NaCl solution.
- 5. Aspirate L-cysteine from each well and wash 2x with ddH2O. Ensure all water has been aspirated before moving to step 6. Avoid bubbles.
- 6. Add 200 uL bovine collagen solution to each well and incubate for approximately 45 minutes to 1 hr at 37C. While this is incubating, go trypsinize, collect, count cells, and resuspend cells with the following steps.
- 7. Aspirate media from desired flasks and wash with 10 mL HBSS. Aspirate all HBSS from flasks and add 4.5 mL trypsin. Incubate for 2 min, then tap cells loose, and quench with at least 9 mL 10% FBS F12k +Se BMEC media per flask. Collect all cell suspensions from flasks and deposit into 50 mL tube. Collect an aliquot for cell counting. Take note of media volume.
- 8. Spin cell suspensions at 1000 rpm for 10 min. Count cells while spinning and resuspend at $2x10^6$ cells/mL or $4x10^6$ cells/mL.
- 9. Resuspend cells in 5% FBS F12k +Se BMEC media and make a cell suspension at 2x10⁵ cells/mL. In addition to the cell suspension, aliquot about 10 mL 5% FBS F12k +Se BMEC media into another tube. This will be used to wash arrays and to fill cell-free well of array.
- 10. Seed 100 mm plates in 5% FBS F12k +Se BMEC media if necessary at 2x10⁶ and seed back flasks in 10% FBS F12k +Se BMEC media at desired concentration (usually either 2x10⁶ for about 4 days time to confluent or 1x10⁶ for about 6 days time to confluent).
- 12. Remove ECIS arrays and wash 2x with 5% FBS F12k +Se BMEC media. Gently mix cell suspension by pipetting and seed 500 uL into all but one array. I leave top left array "empty", but this well still needs 500 uL 5% FBS F12k +Se BMEC media.

- 13. Allow cells to sit in the hood at room temperature for 10-15 minutes.
- 14. Carefully place/slide array in holder and screw the holder to "finger tight" while limiting the time the door is open.
- 15. Press setup and ensure that all arrays in holder are green in the bottom left corner. Also select 8W10E+ below the boxes that light up.
- 16. On the right side of the screen, select MFT (multiple frequency) and change time interval to 180 seconds.
- 17. Press check connection and wait to ensure all wells are transmitting.
- 18. Once resistances are displayed and look "normal", press start. Add comments as necessary.
- 19. Ensure that the initial data displays on the graph.
- 20. Let incubate until resistances stabilize (observe at the default of 4000Hz).

ECIS: Day 2 (Part 1)

1. Warm media at least 30 min before needed. You need 0% FBS F12k +Se BMEC media and 5% FBS F12k +Se. I usually warm the media in tissue culture and pull out about 10 mL from each bottle into prelabeled tubes. These tubes I will take to BacT. Do NOT take media bottles out of tissue culture.

Be sure media is thoroughly warmed to 37C as temperature can affect the measurements

- 2. Press pause on the ECIS software and wait for box to pop up indicating the measurements are paused.
- 3. Carefully unscrew the holder and carefully remove the array from the holder without shaking.
- 3. <u>Slowly</u> aspirate all media from each well (500 uL) and <u>slowly</u> add <u>400 uL</u> fresh media to each well. I usually aspirate and add in a corner, not straight onto the monolayer.
- *Be careful not to introduce any bubbles. Also, be diligent, but move quickly because a drastic reduction in temperature will affect the measurements*
- 4. Carefully replace array in holder and screw the holder to "finger tight" while limiting the time the door is open.
- 5. Press check connection and wait to ensure all wells are transmitting.
- 6. Once resistances are displayed and look "normal", press continue.

7. Allow BMEC and measurements to equilibrate for approximately 4. The length of time depends on the severity of the change due to the temperature, flow from media change, and difference in media. I have had to wait up to 8 hours before, but hopefully this does not become an issue.

ECIS: Day 2 (Part 2)

1. Warm media at least 30 min before needed. You need 0% FBS F12k +Se BMEC media and 5% FBS F12k +Se. I usually warm the media in tissue culture and pull out about 10 mL from each bottle into prelabeled tubes. These tubes I will take to BacT. Do NOT take media bottles out of tissue culture.

Be sure media is thoroughly warmed to 37C as temperature can affect the measurements

- 3. Prepare experimental reagents at 5x the required concentration in warm media.
- 4. Press pause on the ECIS software and wait for box to pop up indicating the measurements are paused.
- 5. Carefully unscrew the holder and carefully remove the array from the holder without shaking.
- 6. Slowly add 100 uL of either % FBS F12k +Se BMEC media and 5% FBS F12k +Se to control wells or treatments to respective wells. Make sure they are labeled or diligently recorded in your notebook.
- 12. Carefully replace array in holder and screw the holder to "finger tight" while limiting the time the door is open.
- 13. Press check connection and wait to ensure all wells are transmitting.
- 14. Once resistances are displayed and look "normal", press continue.
- 15. Allow instrument to collect measurements for however long you prefer. At the conclusion press finish and add comments as needed. Save the data file
- 16. Export data as a CSV.

REFERENCES

REFERENCES

Abarikwu SO, Pant AB and Farombi EO. 2012. 4-Hydroxynonenal induces mitochondrial-mediated apoptosis and oxidative stress in SH-SY5Y human neuronal cells. *Basic Clin Pharmacol Toxicol* 110:441-448.

Abdul Awal M, Matsumoto M, Toyoshima Y and Nishinakagawa H. 1996. Ultrastructural and morphometrical studies on the endothelial cells of arteries supplying the abdomino-inguinal mammary gland of rats during the reproductive cycle. *J Vet Med Sci* 58: 29-34.

Aherne K, Davis M and Sordillo L. 1995. Isolation and characterization of bovine mammary endothelial cells. *Methods Cell Sci* 17: 41-46.

Aitken SL, Corl CM and Sordillo LM. 2011a. Immunopathology of mastitis: insights into disease recognition and resolution. *J Mammary Gland Biol Neoplasia* 16: 291-304.

Aitken SL, Corl CM and Sordillo LM. 2011b. Pro-inflammatory and pro-apoptotic responses of TNF-alpha stimulated bovine mammary endothelial cells. *Vet Immunol Immunopathol* 140: 282-290.

Aleman G, Lopez A, Ordaz G, Torres N and Tovar AR. 2009. Changes in messenger RNA abundance of amino acid transporters in rat mammary gland during pregnancy, lactation, and weaning. *Metabolism* 58: 594-601.

Altmann R, Hausmann M, Spöttl T, Gruber M, Bull AW, Menzel K, Vogl D, Herfarth H, Schömerich J, Falk W and Roger G. 2007. 13-Oxo-ODE is an endogenous ligand for PPARgamma in human colonic epithelial cells. *Biochem Pharmacol* 74: 612-622.

Anderson KL, Kindahl H, Smith AR, Davis LE and Gustafsson BK. 1986. Endotoxin-induced bovine mastitis: arachidonic acid metabolites in milk and plasma and effect of flunixin meglumine. *Am J Vet Res* 47: 1373-1377.

Andreotti CS, Pereyra EA, Baravalle C, Renna MS, Ortega HH, Calvinho LF and Dallard BE. 2014. Staphylococcus aureus chronic intramammary infection modifies protein expression of transforming growth factor beta (TGF-beta) subfamily components during active involution. *Res Vet Sci* 96: 5-14.

Andres AC and Djono V. 2010. The mammary gland vasculature revisited. *J Mammary Gland Biol Neoplasia* 15: 319-328.

Aon MA, Stanley BA, Sivakumaran V, Kembro JM, O'rourke B, Paolocci N and Cortassa S. 2012. Glutathione/thioredoxin systems modulate mitochondrial H2O2 emission: an experimental-computational study. *J Gen Physiol* 139: 479-491.

Atroshi F, Parantainen J, Kangasniemi R and Osterman T. 1987. Milk prostaglandins and electrical conductivity in bovine mastitis. *Vet Res Commun* 11: 15-22. Atroshi F, Sankari S, Rizzo A, Westermarck T and Parantainen J. 1990. Prostaglandins, glutathione metabolism, and lipid peroxidation in relation to inflammation in bovine mastitis. *Adv Exp Med Biol* 264: 203-207.

Baker N, O'meara SJ, Scannell M, Maderna P and Godson C. 2009. Lipoxin A4: anti-inflammatory and anti-angiogenic impact on endothelial cells. *J Immunol* 182: 3819-3826.

Balvers MG, Verhoeckx KC, Meijerink J, Bijlsma S, Rubingh CM, Wortelboer HM and Witkamp RF. 2012. Time-dependent effect of in vivo inflammation on eicosanoid and endocannabinoid levels in plasma, liver, ileum and adipose tissue in C57BL/6 mice fed a fish-oil diet. *Int Immunopharmacol* 13: 204-214.

Bannerman DD, Paape MJ, Goff JP, Kimura K, Lippolis JD and Hope JC. 2004a. Innate immune response to intramammary infection with Serratia marcescens and *Streptococcus uberis*. *Vet Res* 35: 681-700.

Bannerman DD, Paape MJ, Lee JW, Zhao X, Hope JC and Rainard P. 2004b. *Escherichia coli* and *Staphylococcus aureus* elicit differential innate immune responses following intramammary infection. *Clin Diagn Lab Immunol* 11: 463-472.

Bannerman DD, Sathyamoorthy M and Goldblum SE. 1998. Bacterial lipopolysaccharide disrupts endothelial monolayer integrity and survival signaling events through caspase cleavage of adherens junction proteins. *J Biol Chem* 273: 35371-35380.

Bazzoni G and Dejana E. 2004. Endothelial cell-to-cell junctions: molecular organization and role in vascular homeostasis. *Physiol Rev* 84: 869-901.

Bergholte JM, Soberman RJ, Hayes R, Murphy RC and Okita RT. 1987. Oxidation of 15-hydroxyeicosatetraenoic acid and other hydroxy fatty acids by lung prostaglandin dehydrogenase. *Arc Biochem Biophys* 257: 444-450.

Bjornstedt M, Xue J, Huang W, Akesson B and Holmgren A. 1994. The thioredoxin and glutaredoxin systems are efficient electron donors to human plasma glutathione peroxidase. *J Biol Chem* 269: 29382-29384.

Blaho VA, Buczynski MW, Brown CR and Dennis EA. 2009. Lipidomic analysis of dynamic eicosanoid responses during the induction and resolution of Lyme arthritis. *J Biol Chem* 284: 21599-21612.

Blum J and Fridovich I. 1985. Inactivation of glutathione peroxidase by superoxide radical. *Arch Biochem Biophys* 240: 500-508.

Blum MS, Toninelli E, Anderson JM, Balda MS, Zhou J, O'donnell L, Pardi R and Bender JR. 1997. Cytoskeletal rearrangement mediates human microvascular endothelial tight junction modulation by cytokines. *Am J Physiol* 273: H286-294.

Bolick DT, Orr AW, Whetzel A, Srinivasan S, Hatley ME, Schwartz MA and Hedric. 2005. 12/15-lipoxygenase regulates intercellular adhesion molecule-1 expression and monocyte adhesion to endothelium through activation of RhoA and nuclear factor-kappaB. *Arterioscler Thromb Vasc Biol* 25:2301-2307.

Bombeli T, Karsan A, Tait JF and Harlan JM. 1997. Apoptotic vascular endothelial cells become procoagulant. *Blood* 89: 2429-2442.

Bombeli T, Schwartz BR and Harlan JM. 1999. Endothelial cells undergoing apoptosis become proadhesive for nonactivated platelets. *Blood* 93: 3831-3838.

Boutet P, Bureau F, Degand G and Lekeux P. 2003. Imbalance between lipoxin A4 and leukotriene B4 in chronic mastitis-affected cows. *J Dairy Sci* 86: 3430-3439.

Bowler RP, Nicks M, Tran K, Tanner G, Chang LY, Young SK and Worthen GS. 2004. Extracellular superoxide dismutase attenuates lipopolysaccharide-induced neutrophilic inflammation. *Am J Respir Cell Mol Biol* 31: 432-439.

Breau WC and Oliver SP. 1985. Accelerated bovine mammary involution induced by infusion of concanavalin A or phytohemagglutinin. *Am J Vet Res* 46: 816-820.

Brenna JT, Salem N Jr, Sinclair AJ and Cunnane SC. . 2009. alpha-Linolenic acid supplementation and conversion to n-3 long-chain polyunsaturated fatty acids in humans. *Prostaglandins Leukot Essent Fatty Acids* 80:85-91.

Bryan DL, Hart P, Forsyth K and Gibson R. Incorporation of alpha-linolenic acid and linoleic acid into human respiratory epithelial cell lines. *Lipids* 36:713-717.

Bucci M, Roviezzo F, Posadas I, Yu J, Parente L, Sessa WC, Ignarro LJ and Cirino G. 2005. Endothelial nitric oxide synthase activation is critical for vascular leakage during acute inflammation in vivo. *Proc Natl Acad Sci USA* 102: 904-908.

Buchanan MR, Hass TA, Lagarde M and Guichardant M. 1985. 13-Hydroxyoctadecadienoic acid is the vessel wall chemorepellant factor, LOX. *J Biol Chem* 260:16056-16059.

Buckley CD, Gilroy DW, and Serhan CN. 2014. Proresolving lipid mediators and mechanisms in the resolution of acute inflammation. *Immunity* 40: 315-327.

Buczynski MW, Dumlao DS and Dennis EA. 2009. Thematic Review Series: Proteomics. An integrated omics analysis of eicosanoid biology. *J Lipid Res* 50:1015-1038.

Buettner GR. 1993. The pecking order of free radicals and antioxidants: lipid peroxidation, alpha-tocopherol, and ascorbate. *Arch Biochem Biophys* 300:535-543.

Bull AW, Bronstein JC, Earles SM and Blackburn ML. 1996. Formation of adducts between 13-oxooctadecadienoic acid (13-OXO) and protein-derived thiols, in vivo and in vitro. *Life sciences* 58: 2355-2365.

Burvenich C, Monfardini E, Mehrzad J, Capuco AV and Paape MJ. 2004. Role of neutrophil polymorphonuclear leukocytes during bovine coliform mastitis: physiology or pathology? *Verh K Acad Geneeskd Belg* 66: 97-150; discussion 150-153.

Busse R and Mulsch A. 1990. Calcium-dependent nitric oxide synthesis in endothelial cytosol is mediated by calmodulin. *FEBS Lett* 265: 133-136.

Calder PC. 2008. The relationship between the fatty acid composition of immune cells and their function. *Prostaglandins Leukot Essent Fatty Acids* 79:101-108.

Cao YZ, Reddy CC and Sordillo LM. 2000. Altered eicosanoid biosynthesis in selenium-deficient endothelial cells. *Free Radic Biol Med* 28: 381-389.

Cassuto J, Dou H, Czikora I, Szabo A, Patel VS, Kamath V, Belin De Chantemele E, Feher A, Romero MJ and Bagi Z. 2014. Peroxynitrite disrupts endothelial caveolae leading to eNOS uncoupling and diminished flow-mediated dilation in coronary arterioles of diabetic patients. *Diabetes* 63: 1381-1393.

Catala A. 2009. Lipid peroxidation of membrane phospholipids generates hydroxy-alkenals and oxidized phospholipids active in physiological and/or pathological conditions. *Chem Phys Lipids*, 157, 1-11.

Chaudhary P, Sharma R, Sharma A, Vatsyayan R, Yadav S, Singhal SS, Rauniyar N, Prokai L, Awasthi S and Awasthi YC: 2010. Mechanisms of 4-hydroxy-2-nonenal induced pro- and antiapoptotic signaling. *Biochemistry* 49:6263-6275.

Chiang CY, Veckman V, Limmer K and David M. 2012. Phospholipase Cgamma-2 and intracellular calcium are required for lipopolysaccharide-induced Toll-like receptor 4 (TLR4) endocytosis and interferon regulatory factor 3 (IRF3) activation. *J Biol Chem* 287:3704-3709.

Chiang N, Fredman G, Backhed F, Oh SF, Vickery T, Schmidt BA and Serhan CN. 2012. Infection regulates pro-resolving mediators that lower antibiotic requirements. *Nature* 484: 524-528.

Clesham G, Parsaee H, Joseph S, Mcewan JR and Macdermot J. 1992. Activation of bovine endothelial thromboxane receptors triggers release of prostacyclin but not EDRF. *Cardiovasc Res* 26: 513-517.

Clough G. 1991. Relationship between microvascular permeability and ultrastructure. *Prog Biophys Mol Biol* 55: 47-69.

Contreras GA, Mattmiller SA, Raphael W, Gandy JC and Sordillo LM. 2012a. Enhanced n-3 phospholipid content reduces inflammatory responses in bovine endothelial cells. *J Dairy Sci* 95: 7137-7150.

Contreras GA, O'Boyle NJ, Herdt TH and Sordillo LM. 2010. Lipomobilization in periparturient dairy cows influences the composition of plasma nonesterified fatty acids and leukocyte phospholipid fatty acids. *J Dairy Sci*, 93, 2508-16.

Contreras GA, Raphael W, Mattmiller SA, Gandy JC and Sordillo LM. 2012b. Nonesterified fatty acids modify inflammatory response and eicosanoid biosynthesis in bovine endothelial cells. *J Dairy Sci* 95: 5011-5023.

Conway EM and Rosenberg RD. 1988. Tumor necrosis factor suppresses transcription of the thrombomodulin gene in endothelial cells. *Mol Cell Biol* 8: 5588-5592.

Corl CM, Contreras GA and Sordillo LM. 2010. Lipoxygenase metabolites modulate vascular-derived platelet activating factor production following endotoxin challenge. *Vet Immunol Immunopathol* 136: 98-107.

Corl CM, Gandy JC and Sordillo LM. 2008. Platelet activating factor production and proinflammatory gene expression in endotoxin-challenged bovine mammary endothelial cells. *J Dairy Sci* 91: 3067-3078.

Cromack DT, Porras-Reyes B, Purdy JA, Pierce GF and Mustoe TA. 1993. Acceleration of tissue repair by transforming growth factor beta 1: identification of in vivo mechanism of action with radiotherapy-induced specific healing deficits. *Surgery* 113: 36-42.

Crossman DC, Carr DP, Tuddenham EG, Pearson JD and Mcvey JH. 1990. The regulation of tissue factor mRNA in human endothelial cells in response to endotoxin or phorbol ester. *J Biol Chem* 265: 9782-9787.

Dalleau S, Baradat M, Gueraud F, Huc L: 2013. Cell death and diseases related to oxidative stress: 4-hydroxynonenal (HNE) in the balance. *Cell Death Differ* 2013 20:1615-1630.

De Caterina R, Cybulsky MI, Clinton SK, Gimbrone MA, Jr. and Libby P. 1994. The omega-3 fatty acid docosahexaenoate reduces cytokine-induced expression of proatherogenic and proinflammatory proteins in human endothelial cells. *Arterioscler Thromb* 14: 1829-1836.

De Greeff A, Zadoks R, Ruuls L, Toussaint M, Nguyen TK, Downing A, Rebel J, Stockhoff-Zurwieden N and Smith H. 2013. Early host response in the mammary gland after experimental *Streptococcus uberis* challenge in heifers. *J Dairy Sci*, 96, 3723-36.

De Martin R, Vanhove B, Cheng Q, Hofer E, Csizmadia V, Winkler H and Bach F H. 1993. Cytokine-inducible expression in endothelial cells of an I kappa B alpha-like gene is regulated by NF kappa B. *Embo j* 12: 2773-2779.

Dhanasekaran A, Kotamraju S, Kalivendi SV, Matsunaga T, Shang T, Keszler A, Joseph J and Kalyanaraman B. 2004. Supplementation of endothelial cells with mitochondria-targeted antioxidants inhibit peroxide-induced mitochondrial iron uptake, oxidative damage, and apoptosis. *J Biol Chem* 279:37575-87.

Dhanasekaran A, Kotamraju S, Karunakaran C, Kalivendi SV, Thomas S, Joseph J and Kalyanaraman B. 2005. Mitochondria superoxide dismutase mimetic inhibits peroxide-induced oxidative damage and apoptosis: role of mitochondrial superoxide. *Free Radic Biol Med* 39:567-83.

Dickinson Zimmer JS, Voelker DR, Bernlohr DA, and Murphy RC. 2004. Stabilization of leukotriene A4 by epithelial fatty acid-binding protein in the rat basophilic leukemia cell. *J Biol Chem* 279: 7420-7426.

Djonov V, Andres AC and Ziemiecki A. 2001. Vascular remodelling during the normal and malignant life cycle of the mammary gland. *Microsc Res Tech* 52: 182-189. Dougherty RM, Galli C, Ferro-Luzzi A and Iacono JM. 1987. Lipid and phospholipid fatty acid composition of plasma, red blood cells, and platelets and how they are affected by dietary lipids: a study of normal subjects from Italy, Finland, and the USA. *Am J Clin Nutr* 45:443-55.

Drake WT, Lopes NN, Fenton JW, 2nd and Issekutz AC. 1992. Thrombin enhancement of interleukin-1 and tumor necrosis factor-alpha induced polymorphonuclear leukocyte migration. *Lab Invest* 67: 617-627.

Duda MK, O'Shea KM, Tintinu A, Xu W, Khairallah RJ, Barrows BR, Chess DJ, Azimzadeh AM, Harris WS, Sharov VG, Sabbah HN and Stanley WC. 2009. Fish oil, but not flaxseed oil, decreases inflammation and prevents pressure overload-induced cardiac dysfunction. *Cardiovasc Res* 81:319-27.

Dwarakanath RS, Sahar S, Reddy MA, Castanotto D, Rossi JJ and Natarajan R. 2004. Regulation of monocyte chemoattractant protein-1 by the oxidized lipid, 13-hydroperoxyoctadecadienoic acid, in vascular smooth muscle cells via nuclear factor-kappa B (NF-kappa B). *J Mol Cell Cardiol* 36:585-95.

Emken EA, Adlof RO and Gulley RM. 1994. Dietary linoleic acid influences desaturation and acylation of deuterium-labeled linoleic and linolenic acids in young adult males. *Biochim Biophys Acta* 1213:277-88.

Ereso AQ, Cureton EL, Cripps MW, Sadjadi J, Dua MM, Curran B and Victorino GP. 2009. Lipoxin a(4) attenuates microvascular fluid leak during inflammation. *J Surg Res* 156: 183-188.

Erlemann KR, Cossette C, Grant GE, Lee GJ, Patel P, Rokach J and Powell WS. 2007. Regulation of 5-hydroxyeicosanoid dehydrogenase activity in monocytic cells. *Bioch J* 403:157-165.

Fei H, Berliner JA, Parhami F and Drake TA. 1993. Regulation of endothelial cell tissue factor expression by minimally oxidized LDL and lipopolysaccharide. *Arterioscler Thromb* 13: 1711-1717.

Ferrari G, Cook BD, Terushkin V, Pintucci G and Mignatti P. 2009. Transforming growth factor-beta 1 (TGF-beta1) induces angiogenesis through vascular endothelial growth factor (VEGF)-mediated apoptosis. *J Cell Physiol* 219: 449-458.

Fitzpatrick FA and Soberman R. 2001. Regulated formation of eicosanoids. *J Clin Invest* 107:1347-1351.

Fortes GB, Alves LS, De Oliveira R, Dutra FF, Rodrigues D, Fernandez PL, Souto-Padron T, De Rosa MJ, Kelliher M, Golenbock D, Chan FK and Bozza MT. 2012. Heme induces programmed necrosis on macrophages through autocrine TNF and ROS production. *Blood* 119: 2368-2375.

Friedrichs B, Toborek M, Hennig B, Heinevetter L, Muller C and Brigelius-Flohe R. 1999. 13-HPODE and 13-HODE modulate cytokine-induced expression of endothelial cell adhesion molecules differently. *Biofactors* 9: 61-72.

Fukata M, Chen A, Klepper A, Krishnareddy S, Vamadevan AS, Thomas LS. Xu R, Inoue H, Arditi M, Dannenberg AJ and Abreu MT. 2006. Cox-2 is regulated by Toll-like receptor-4 (TLR4) signaling: Role in proliferation and apoptosis in the intestine. *Gastroenterology* 131:862-77.

Funk MO, Isacc R and Porter NA. 1976. Preparation and purification of lipid hydroperoxides from arachidonic and gamma-linolenic acids. *Lipids* 11: 113-117.

Gamble JR, Khew-Goodall Y and Vadas MA. 1993. Transforming growth factor-beta inhibits Eselectin expression on human endothelial cells. *J Immunol* 150: 4494-4503.

Giri SN, Chen Z, Carroll EJ, Mueller R, Schiedt MJ and Panico L. 1984. Role of prostaglandins in pathogenesis of bovine mastitis induced by *Escherichia coli* endotoxin. *Am J Vet Res* 45: 586-591.

Glasser F, Schmidley P, Sauvant D and Doreau M. 2008. Digestion of fatty acids in ruminants: a meta-analysis of flows and variation factors: 2. C18 fatty acids. *Animal* 2:691-704.

Goeckeler ZM and Wysolmerski RB. 1995.. Myosin light chain kinase-regulated endothelial cell contraction: the relationship between isometric tension, actin polymerization, and myosin phosphorylation. *J Cell Biol* 130: 613-627.

Guido DM, Mckenna R and Matthews WR. 1993. Quantitation of hydroperoxy-eicosatetraenoic acids and hydroxy-eicosatetraenoic acids as indicators of lipid peroxidation using gas chromatography-mass spectrometry. *Anal Biochem* 209:123-9.

Guillo H, Zadravec D, Martin PG and Jacobsson A. 2010. The key roles of elongases and desaturases in mammalian fatty acid metabolism: Insights from transgenic mice. *Prog Lipid Res* 49:186-99.

Gunther J, Czabanska A, Bauer I, Leigh JA, Holst O and Seyfert HM. 2016. Streptococcus uberis strains isolated from the bovine mammary gland evade immune recognition by mammary epithelial cells, but not of macrophages. *Vet Res* 47:13.

Haendeler J, Tischler V, Hoffmann J, Zeiher AM and Dimmeler S. 2004. Low doses of reactive oxygen species protect endothelial cells from apoptosis by increasing thioredoxin-1 expression. *FEBS Lett* 577: 427-433.

Hafezi-Moghadam A, Noda K, Almulki L, Iliaki EF, Poulaki V, Thomas KL, Nakazawa T, Hisatomi T, Miller JW and Gragoudas ES. 2007. VLA-4 blockade suppresses endotoxin-induced uveitis: in vivo evidence for functional integrin up-regulation. *FASEB J* 21: 464-474.

Haghiac M, Yang XH, Presley L, Smith S, Dettelback S, Minium J, Belury MA, Catalano PM and Hauguel-De Mouzon S. 2015. Dietary Omega-3 Fatty Acid Supplementation Reduces Inflammation in Obese Pregnant Women: A Randomized Double-Blind Controlled Clinical Trial. *PLoS One* 10:e0137309.

Haimovitz-Friedman A, Cordon-Cardo C, Bayoumy S, Garzotto M, Mcloughlin M, Gallily R, Edwards CK 3rd, Schuchman EH, Fuks Z and Kolesnick R. 1997. Lipopolysaccharide induces disseminated endothelial apoptosis requiring ceramide generation. *J Exp Med* 186:1831-41.

Hamberg, M., and B. Samuelsson. 1967. On the mechanism of the biosynthesis of prostaglandins E-1 and F-1-alpha. *J Biol Chem* 242: 5336-5343.

Hasdai D, Sangiorgi G, Spagnoli LG, Simari RD, Holmes DR Jr, Kwon HM, Carlson PJ, Schwartz RS and Lerman A. 1999. Coronary artery apoptosis in experimental hypercholesterolemia. *Atherosclerosis* 142:317-25.

Haug A, Hostmark AT and Harstad OM. 2007. Bovine milk in human nutrition--a review. *Lipids Health Dis* 6: 25.

Henricks PA, Engels F, Van Der Vliet H and Nijkamp FP. 1991. 9- and 13-hydroxy-linoleic acid possess chemotactic activity for bovine and human polymorphonuclear leukocytes. *Prostaglandins* 41:21-7.

Hill AW, Finch JM, Field TR and Leigh JA. 1994. Immune modification of the pathogenesis of *Streptococcus uberis* mastitis in the dairy cow. *FEMS Immunol Med Microbiol* 8: 109-117. Hill-Kapturczak N, Voakes C, Garcia J, Visner G, Nick HS and Agarwal A. 2003. A cis-acting region regulates oxidized lipid-mediated induction of the human heme oxygenase-1 gene in endothelial cells. *Arterioscler Thromb Vasc Biol* 23:1416-22.

Holst BD, Hurley WL and Nelson DR (1987). Involution of the bovine mammary gland: histological and ultrastructural changes. *J Dairy Sci* 70: 935-944.

Hordijk PL, Anthony E, Mul FP, Rientsma R, Oomen LC and Roos D (1999). Vascular-endothelial-cadherin modulates endothelial monolayer permeability. *J Cell Sci* 112: 1915-1923.

Hosoi T, Sugikawa E, Chikada A, Koguchi Y and Ohnuki T. 2005. TG1019/OXE, a Galpha(i/o)-protein-coupled receptor, mediates 5-oxo-eicosatetraenoic acid-induced chemotaxis. *Biochem Biophys Res Commun* 334:987-95.

Huo Y, Zhao L, Hyman MC, Shashkin P, Harry BL, Burcin T, Forlow SB, Stark MA, Smith DF, Clarke S, Srinivasan S, Hedrick CC, Pratico D, Witztum JL, Nadler JL, Funk CD and Ley K. 2004. Critical role of macrophage 12/15-lipoxygenase for atherosclerosis in apolipoprotein Edeficient mice. *Circulation* 110:2024-31.

Ignotz RA and Massague J. 1986. Transforming growth factor-beta stimulates the expression of fibronectin and collagen and their incorporation into the extracellular matrix. *J Biol Chem* 261: 4337-4345.

Il'yasova D, Morrow JD, Ivanova A and Wagenknecht LE. 2004. Epidemiological marker for oxidant status: comparison of the ELISA and the gas chromatography/mass spectrometry assay for urine 2,3-dinor-5,6-dihydro-15-F2t-isoprostane. *Ann Epidemiol* 14: 793-797.

Ismail ZA and Dickinson C. 2010. Alterations in coagulation parameters in dairy cows affected with acute mastitis caused by E. coli and S. aureus pathogens. *Vet Res Commun* 34: 533-539.

Itoh T, Fairall L, Amin K, Inaba Y, Szanto A, Balint BL, Nagy L, Yamamoto K and Schwabe JW. 2008. Structural basis for the activation of PPARgamma by oxidized fatty acids. *Nat Struct Mol Biol* 15:924-31.

Jasper J and Weary DM. 2002. Effects of ad libitum milk intake on dairy calves. *J Dairy Sci* 85: 3054-3058.

Jenkins TC, Wallace RJ, Moate PJ and Mosley. 2008. Board-invited review: Recent advances in biohydrogenation of unsaturated fatty acids within the rumen microbial ecosystem. *J Anim Sci* 86:397-412.

Jiang WG, Bryce RP, Horrobin DF and Mansel RE. 1998. Regulation of tight junction permeability and occludin expression by polyunsaturated fatty acids. *Biochem Biophys Res Commun* 244: 414-420.

Jurek D, Udilova N, Jozkowicz, Nohl H, Marian B and Schulte-Hermann R. 2005. Dietary lipid hydroperoxides induce expression of vascular endothelial growth factor (VEGF) in human colorectal tumor cells. *FASEB J* 19: 97-99.

Kadl A and Leitinger N. 2005. The role of endothelial cells in the resolution of acute inflammation. *Antioxid Redox Signal* 7: 1744-1754.

Kaduce TL, Fang X, Harmon SD, Oltman CL, Dellsperger KC, Teesch LM, Gopal VR, Falck JR, Campbell WB, Weintraub NL and Spector AA. 2004. 20-hydroxyeicosatetraenoic acid (20-HETE) metabolism in coronary endothelial cells. *J Biol Chem* 279: 2648-2656.

Kaplanski G, Farnarier C, Tissot O, Pierres A, Benoliel AM, Alessi MC, Kaplanski S and Bongrand P. 1993. Granulocyte-endothelium initial adhesion. Analysis of transient binding events mediated by E-selectin in a laminar shear flow. *Biophys J* 64: 1922-1933.

Karlsson A, Markfjall M, Stromberg N and Dahlgren C. 1995. Escherichia coli-induced activation of neutrophil NADPH-oxidase: lipopolysaccharide and formylated peptides act synergistically to induce release of reactive oxygen metabolites. *Infect Immun* 63: 4606-4612.

Kelly JJ, Moore TM, Babal P, Diwan AH, Stevens T and Thompson WJ. 1998. Pulmonary microvascular and macrovascular endothelial cells: differential regulation of Ca2+ and permeability. *Am J Physiol* 274: L810-L819.

Knepler JL, Jr, Taher LN, Gupta MP, Patterson C, Pavalko F, Ober MD and Hart CM. 2001. Peroxynitrite causes endothelial cell monolayer barrier dysfunction. *Am J Physiol Cell Physiol* 281: C1064-1075.

Kobayashi K, Oyama S, Numata A, Rahman MM and Kumura H. 2013. Lipopolysaccharide disrupts the milk-blood barrier by modulating claudins in mammary alveolar tight junctions. *PLoS One* 8: e62187.

Kobayashi M, Shimada K and Ozawa T. 1990. Human recombinant interleukin-1 beta- and tumor necrosis factor alpha-mediated suppression of heparin-like compounds on cultured porcine aortic endothelial cells. *J Cell Physiol* 144: 383-390.

Koltsida O, Karamnov S, Pyrillou K, Vickery T, Chairakaki AD, Tamvakopoulos C, Sideras P, Serhan CN and Andreakos E. 2013. Toll-like receptor 7 stimulates production of specialized proresolving lipid mediators and promotes resolution of airway inflammation. *EMBO molecular medicine* 5:762-775.

Komatsu T, Itoh F, Kushibiki S and Hodate K. 2005. Changes in gene expression of glucose transporters in lactating and nonlactating cows. *J Anim Sci* 83: 557-564.

Kozak KR, Crews BC, Morrow JD, Wang LH, Ma YH, Weinander R, Jakobssen PJ and Marnett LJ. 2002. Metabolism of the endocannabinoids, 2-arachidonylglycerol and anandamide, into prostaglandin, thromboxane, and prostacyclin glycerol esters and ethanolamides. *J Biol Chem* 277: 44877-44885.

Kronke G, Katzenbeisser J, Uderhardt S, Zaiss MM, Scholtysek C, Schabbauer G, Zarbock A, Koenders MI, Axmann R, Zwerina J, Baenckler HW, Van den Berg W, Voll RE, Kuhn H, Joosten LA and Schett G. 2009. 12/15-lipoxygenase counteracts inflammation and tissue damage in arthritis. *J Immunol* 183:3383-9.

Kuhn H, Banthiya S and Van Leyen K. 2015. Mammalian lipoxygenases and their biological relevance. *Biochim Biophys Acta* 1851:308-30.

Lacasse P, Farr VC, Davis SR and Prosser CG. 1996. Local secretion of nitric oxide and the control of mammary blood flow. *J Dairy Sci* 79: 1369-1374.

Lands WE, Inoue M, Sugiura Y and Okuyama H. 1982. Selective incorporation of polyunsaturated fatty acids into phosphatidylcholine by rat liver microsomes. *J Biol Chem* 257:14968-72.

Levi M, Van Der Poll T, Ten Cate H and Van Deventer SJ. 1997. The cytokine-mediated imbalance between coagulant and anticoagulant mechanisms in sepsis and endotoxaemia. *Eur J Clin Invest* 27: 3-9.

Levick JR and Smaje LH. 1987. An analysis of the permeability of a fenestra. *Microvasc Res* 33: 233-256.

Levin G, Duffin KL, Obukowicz MG, Hummert SL, Fujiwara H, Needleman P and Raz A. 2002. Differential metabolism of dihomo-gamma-linolenic acid and arachidonic acid by cyclo-oxygenase-1 and cyclo-oxygenase-2: implications for cellular synthesis of prostaglandin E1 and prostaglandin E2. *Biochem J* 365(Pt 2):489-496.

Levkau B, Kenagy RD, Karsan A, Weitkamp B, Clowes AW, Ross R and Raines EW. 2002. Activation of metalloproteinases and their association with integrins: an auxiliary apoptotic pathway in human endothelial cells. *Cell Death Differ* 9: 1360-1367.

Ley K, Bullard DC, Arbones ML, Bosse R, Vestweber D, Tedder TF and Beaudet AL. 1995. Sequential contribution of L- and P-selectin to leukocyte rolling in vivo. *J Exp Med* 181: 669-675.

Linzell JL and Peaker M. 1972. Day-to-day variations in milk composition in the goat and cow as a guide to the detection of subclinical mastitis. *Br Vet J* 128: 284-295.

Lock AL, Tyburczy C, Dwyer DA, Harvatine KJ, Destaillats F, Mouloungui Z, Candy L and Bauman DE. 2007. Trans-10 octadecenoic acid does not reduce milk fat synthesis in dairy cows. *J Nutr* 137:71-76.

Lombardo D, Fanni T, Pluckthun A and Dennis EA. 1986. Rate-determining step in phospholipase A2 mechanism. 18O isotope exchange determined by 13C NMR. *J Biol Chem* 261: 11663-11666.

Lubos E, Kelly NJ, Oldebeken SR, Leopold JA, Zhang YY, Loscalzo J and Handy DE. 2011. Glutathione peroxidase-1 deficiency augments proinflammatory cytokine-induced redox signaling and human endothelial cell activation. *J Biol Chem* 286: 35407-35417.

Maddox JF, Aherne KM, Reddy CC and Sordillo LM. 1999. Increased neutrophil adherence and adhesion molecule mRNA expression in endothelial cells during selenium deficiency. *J Leukoc Biol* 65: 658-664

Marcel YL, Christiansen K and Holmon RT. 1968. The preferred metabolic pathway from linoleic acid to arachidonic acid in vitro. *Biochim Biophys Acta* 164:25-34.

Maskrey BH, and O'Donnell VB. 2008. Analysis of eicosanoids and related lipid mediators using mass spectrometry. *Biochem Soc Trans* 36: 1055-1059.

Matsumoto M, Kurohmaru M, Hayashi Y, Nishinakagawa H and Otsuka J. 1994. Permeability of mammary gland capillaries to ferritin in mice. *J Vet Med Sci* 56: 65-70. Matsumoto M, Nishinakagawa H, Kurohmaru M, Hayashi Y and Otsuka J. 1992. Pregnancy and lactation affect the microvasculature of the mammary gland in mice. *J Vet Med Sci* 54: 937-943.

Mattmiller SA, Carlson BA, Gandy JC and Sordillo LM. 2014. Reduced macrophage selenoprotein expression alters oxidized lipid metabolite biosynthesis from arachidonic and linoleic acid. *J Nutr Biochem* 25 647-654.

Mattmiller SA, Corl CM, Gandy JC, Loor JJ and Sordillo LM. 2011. Glucose transporter and hypoxia-associated gene expression in the mammary gland of transition dairy cattle. *J Dairy Sci* 94: 2912-2922.

Mavangira V, Gandy JC, Zhang C, Ryman VE, Jones DA and Sordillo LM. 2015. Polyunsaturated fatty acids influence differential biosynthesis of oxylipids and other lipid mediators during bovine coliform mastitis. *J Dairy Sci* 98: 6202-6215.

Mayadas TN, Johnson RC, Rayburn H, Hynes RO and Wagner DD. 1993. Leukocyte rolling and extravasation are severely compromised in P selectin-deficient mice. *Cell* 74: 541-554.

Mcever RP, Beckstead JH, Moore KL, Marshall-Carlson L and Bainton DF. 1989. GMP-140, a platelet alpha-granule membrane protein, is also synthesized by vascular endothelial cells and is localized in Weibel-Palade bodies. *J Clin Invest* 84: 92-99.

Meade EA, McIntyre TM, Zimmerman GA and Prescott SM. 1999. Peroxisome proliferators enhance cyclooxygenase-2 expression in epithelial cells. *J Biol Chem* 274: 8328-8334.

Micciche F, van Haveren J, Oostveen E, Laven J, Ming W, Okan Oyman Z and van der Linde R.. 2005. Oxidation of methyl linoleate in micellar solutions induced by the combination of iron(II)/ascorbic acid and iron(II)/H2O2. *Arch Biochem Biophys* 443: 45-52.

Michel CC and Curry FE. 1999. Microvascular permeability. *Physiol Rev* 79: 703-761.

Min Y, Djahanbakhch O, Hutchinson J, Bhullar AS, Raveendran M, Hallot A, Eram S, Namugere I, Nateghian S and Ghebremeskel K. 2014. Effect of docosahexaenoic acid-enriched fish oil supplementation in pregnant women with Type 2 diabetes on membrane fatty acids and

fetal body composition--double-blinded randomized placebo-controlled trial. *Diabet Med* 3:1331-40.

Morgan AH, Dioszeghy V, Maskrey BH, Thomas CP, Clark SR, Mathie SA, Lloyd CM, Kuhn H, Topley N, Coles BC, Taylor PR, Jones SA and O'Donnell VB. 2009. Phosphatidylethanolamine-esterified eicosanoids in the mouse: tissue localization and inflammation-dependent formation in Th-2 disease. *J Biol Chem* 284: 21185-21191.

Morrow JD, Kill KE, Burk RF, Nammour TM, Badr KF and Roberts LJ 2nd. 1990. A series of prostaglandin F2-like compounds are produced in vivo in humans by a non-cyclooxygenase, free radical-catalyzed mechanism. *Proc Natl Acad Sci U S A 87*: 9383-9387.

Moyes KM, Larsen T, Sorensen P and Ingvartsen KL. 2014. Changes in various metabolic parameters in blood and milk during experimental Escherichia coli mastitis for primiparous Holstein dairy cows during early lactation. *J Anim Sci Biotechnol* 5,:47.

Muller WA, Weigl SA, Deng X and Phillips DM. 1993. PECAM-1 is required for transendothelial migration of leukocytes. *J Exp Med* 178: 449-460.

Murata T, Ushikubi F, Matsuoka T, Hirata M, Yamasaki A, Sugimoto Y, Ichikawa A, Aze Y, Tanaka T, Yoshida N, Ueno A, Oh-Ishi S and Narumiya S. 1997. Altered pain perception and inflammatory response in mice lacking prostacyclin receptor. *Nature* 388: 678-682.

Nadjar A, Tridon V, May MJ, Ghosh S, Dantzer R, Amedee T and Parnet P. 2005. NFkappaB activates in vivo the synthesis of inducible Cox-2 in the brain. *J Cereb Blood Flow Metab* 25: 1047-1059.

Nagy L, Tontonoz P, Alvarez JG, Chen H and Evans RM. 1998. Oxidized LDL regulates macrophage gene expression through ligand activation of PPARgamma. *Cell* 93: 229-240.

Nakamura MT and Nara TY. 2003. Essential fatty acid synthesis and its regulation in mammals. *Prostaglandins Leukot Essent Fatty Acids* 68:145-50.

National Mastitis Council. 2004. National Mastitis Council. Madison, WI.

Nawroth PP and Stern DM. 1986. Modulation of endothelial cell hemostatic properties by tumor necrosis factor. *J Exp Med* 163: 740-745.

NMC. 1999. Laboratory handbook on bovine mastitis. National Mastitis Council.

Nielsen MO, Fleet IR, Jakobsen K and Heap RB. 1995. The local differential effect of prostacyclin, prostaglandin E2 and prostaglandin F2 alpha on mammary blood flow of lactating goats. *J Endocrinol* 145: 585-591.

Nishida K, Harrison DG, Navas JP, Fisher AA, Dockery SP, Uematsu M, Nerem RM, Alexander RW and Murphy TJ. 1992. Molecular cloning and characterization of the constitutive bovine aortic endothelial cell nitric oxide synthase. *J Clin Invest* 90: 2092-2096.

Nitta T, Hata M, Gotoh S, Seo Y, Sasaki H, Hashimoto N, Furuse M and Tsukita S. 2003. Size-selective loosening of the blood-brain barrier in claudin-5-deficient mice. *J Cell Biol* 161: 653-660.

Niu XF, Smith CW and Kubes P. 1994. Intracellular oxidative stress induced by nitric oxide synthesis inhibition increases endothelial cell adhesion to neutrophils. *Circ Res* 74: 1133-1140. Noguchi N, Yamashita H, Hamahara J, Nakamura A, Kuhn H and Niki E. 2002. The specificity of lipoxygenase-catalyzed lipid peroxidation and the effects of radical-scavenging antioxidants. *Biol Chem* 383: 619-626.

O'Boyle NJ, Contreras GA, Mattmiller SA and Sordillo LM. 2012. Changes in glucose transporter expression in monocytes of periparturient dairy cows. *J Dairy Sci* 95:5709-5719.

O'Flaherty JT, Cordes JF, Lee SL, Samuel M and Thomas MJ. 1994. Chemical and biological characterization of oxo-eicosatetraenoic acids. *Biochim Biophys Acta* 1201:505-15.

Ohashi Y, Kawashima S, Hirata K, Yamashita T, Ishida T, Inoue N, Sakoda T, Kurihara H, Yazaki Y and Yokoyama M. 1998. Hypotension and reduced nitric oxide-elicited vasorelaxation in transgenic mice overexpressing endothelial nitric oxide synthase. *J Clin Invest* 102: 2061-2071.

Oliw EH, Bylund J and Herman C. 1996. Bisallylic hydroxylation and epoxidation of polyunsaturated fatty acids by cytochrome P450. *Lipids* 31: 1003-1021.

Olson ST, Richard B, Izaguirre G, Schedin-Weiss S and Gettins PG. 2010. Molecular mechanisms of antithrombin-heparin regulation of blood clotting proteinases. A paradigm for understanding proteinase regulation by serpin family protein proteinase inhibitors. *Biochimie* 92: 1587-1596.

Othman A, Ahmad S, Megyerdi S, Mussell R, Choksi K, Maddipati KR, Elmarakby A, Rizk N and Al-Shabrawey M. 2013. 12/15-Lipoxygenase-derived lipid metabolites induce retinal endothelial cell barrier dysfunction: contribution of NADPH oxidase. *PLoS One* 8:e57254.

Parnham MJ, Bittner C and Leyck S. 1987. Changes in glutathione peroxidase activities and the oxidative burst of leukocytes during inflammation in the mouse and rat. *Free Radic Res Commun* 4: 183-188.

Patterson E, Wall R, Fitzgerald GF, Ross RP and Stanton C. 2012. Health implications of high dietary omega-6 polyunsaturated Fatty acids. *J Nutr Metab* 2012:539426.

Pedersen LH, Aalbaek B, Rontved CM, Ingvartsen KL, Sorensen NS, Heegaard PM and Jensen HE. 2003. Early pathogenesis and inflammatory response in experimental bovine mastitis due to *Streptococcus uberis*. *J Comp Pathol* 128:156-164.

Pepper MS, Baetens D, Mandriota SJ, Di Sanza C, Oikemus S, Lane TF, Soriano JV, Montesano R and Iruela-Arispe ML. 2000. Regulation of VEGF and VEGF receptor expression in the rodent mammary gland during pregnancy, lactation, and involution. *Dev Dyn* 218: 507-524.

Petit HV, Dewhurst RJ, Scollan ND, Proulx JG, Khalid M, Haresign W, Twagiramungu H and Mann GE. 2002. Milk production and composition, ovarian function, and prostaglandin secretion of dairy cows fed omega-3 fats. *J Dairy Sci* 85:889-99.

Pezeshki A, Stordeur P, Wallemacq H, Schynts F, Stevens M, Boutet P, Peelman LJ, De Spiegeleer B, Duchateau L, Bureau F and Burvenich C. 2011. Variation of inflammatory dynamics and mediators in primiparous cows after intramammary challenge with *Escherichia coli. Vet Res* 42: 15.

Piotrowska-Tomala KK, Siemieniuch MJ, Szostek AZ, Korzekwa AJ, Wocławek-Potocka I, Galvao AM, Okuda K and Skarzynski DJ. 2012. Lipopolysaccharides, cytokines, and nitric oxide affect secretion of prostaglandins and leukotrienes by bovine mammary gland epithelial cells. *Domest Anim Endocrinol* 43: 278-288.

Phuektes P, Mansell PD, Dyson RS, Hooper ND, Dick JS and Browning GF. 2001. Molecular epidemiology of *Streptococcus uberis* isolates from dairy cows with mastitis. *J Clin Microbiol* 39: 1460-1466.

Porro B, Songia P, Squellerio I, Tremoli E and Cavalca V. 2014. Analysis, physiological and clinical significance of 12-HETE: a neglected platelet-derived 12-lipoxygenase product. J Chromatogr B 964:26-40

Poulsen RC, Gotlinger KH, Serhan CN and Kruger MC. 2008. Identification of inflammatory and proresolving lipid mediators in bone marrow and their lipidomic profiles with ovariectomy and omega-3 intake. *Am J Hematol* 83:437-45.

Poutrel B, Caffin JP and Rainard P. 1983. Physiological and pathological factors influencing bovine serum albumin content of milk. *J Dairy Sci* 66: 535-541.

Predescu S, Knezevic I, Bardita C, Neamu RF, Brovcovych V and Predescu D. 2013. Platelet activating factor-induced ceramide micro-domains drive endothelial NOS activation and contribute to barrier dysfunction. *PLoS One* 8: e75846.

Prosser CG, Davis SR, Farr VC and Lacasse P. 1996. Regulation of blood flow in the mammary microvasculature. *J Dairy Sci* 79: 1184-1197.

Quarrie LH, Addey CV and Wilde CJ. 1994. Local regulation of mammary apoptosis in the lactating goat. *Biochem Soc Trans* 22: 178s.

Quehenberger O, Armando AM, Brown AH, Milne SB, Myers DS, Merrill AH, Bandyopadhyay S, Jones KN, Kelly S, Shaner RL, Sullards CM, Wang E, Murphy RC, Barkley RM, Leiker TJ, Raetz CR, Guan Z, Laird GM, Six DA, Russell DW, McDonald JG, Subramaniam S, Fahy E and Dennis EA. 2010. Lipidomics reveals a remarkable diversity of lipids in human plasma. *J Lipid Res* 51: 3299-3305.

Rabot A, Sinowatz F, Berisha B, Meyer HH and Schams D. 2007. Expression and localization of extracellular matrix-degrading proteinases and their inhibitors in the bovine mammary gland during development, function, and involution. *J Dairy Sci* 90: 740-748. Rambeaud M, Almeida RA, Pighetti GM and Oliver SP. 2003. Dynamics of leukocytes and cytokines during experimentally induced *Streptococcus uberis* mastitis. *Vet Immunol Immunopathol* 96: 193-205.

Ramirez RA, Lee A, Schedin P, Russell JS and Masso-Welch PA. 2012. Alterations in mast cell frequency and relationship to angiogenesis in the rat mammary gland during windows of physiologic tissue remodeling. *Dev Dyn* 241: 890-900.

Ramsden CE, Ringel A, Feldstein AE, Taha AY, Macintos BA, Hibbeln JR, Majchrzak-Hong SF, Faurot KR, Rapoport SI, Cheon Y, Chung YM, Berk M & Mann JD. 2012. Lowering dietary linoleic acid reduces bioactive oxidized linoleic acid metabolites in humans. *Prostaglandins Leukot Essent Fatty Acids* 87:135-41.

Rao LV and Rapaport SI. 1987. Studies of a mechanism inhibiting the initiation of the extrinsic pathway of coagulation. *Blood* 69: 645-651.

Raphael W and Sordillo LM. 2013. Dietary polyunsaturated fatty acids and inflammation: the role of phospholipid biosynthesis. *Int J Mol Sci* 14:21167-88.

Raphael, W., L. Halbert, G. A. Contreras, and L. M. Sordillo. 2014. Association between polyunsaturated fatty acid-derived oxylipid biosynthesis and leukocyte inflammatory marker expression in periparturient dairy cows. *J Dairy Sci* 97:3615-3625.

Rippe B, Kamiya A and Folkow B. 1979. Transcapillary passage of albumin, effects of tissue cooling and of increases in filtration and plasma colloid osmotic pressure. *Acta Physiol Scand* 105: 171-187.

Romer LH, Mclean NV, Yan HC, Daise M, Sun J and Delisser HM. 1995. IFN-gamma and TNF-alpha induce redistribution of PECAM-1 (CD31) on human endothelial cells. *J Immunol* 154: 6582-6592.

Rossiter H, Barresi C, Ghannadan M, Gruber F, Mildner M, Fodinger D and Tschachler E. 2007. Inactivation of VEGF in mammary gland epithelium severely compromises mammary gland development and function. *FASEB J* 21: 3994-4004.

Ryman, V. E., Pighetti, G. M., Lippolis, J. D., Gandy, J. C., Applegate, C. M. & Sordillo, L. M. 2015. Quantification of bovine oxylipids during intramammary *Streptococcus uberis* infection. *Prostaglandins Other Lipid Mediat* 121:207-17.

Sans M, Panes J, Ardite E, Elizalde JI, Arce Y, Elena M, Palacin A, Fernandez-Checa JC, Anderson DC, Lobb R and Pique JM. 1999. VCAM-1 and ICAM-1 mediate leukocyte-endothelial cell adhesion in rat experimental colitis. *Gastroenterology* 116: 874-883.

Sandstrom PA, Pardi D, Tebbey PW, Dudek RW, Terrain DM, Folks and Buttke TM. 1995. Lipid hydroperoxide-induced apoptosis: lack of inhibition by Bcl-2 over-expression. *FEBS letters* 365: 66-70.

Scalia R and Lefer AM. 1998. In vivo regulation of PECAM-1 activity during acute endothelial dysfunction in the rat mesenteric microvasculature. *J Leukoc Biol* 64: 163-169.

Schenkel AR, Mamdouh Z, Chen X, Liebman RM and Muller WA. 2002. CD99 plays a major role in the migration of monocytes through endothelial junctions. *Nat Immunol* 3: 143-150.

Schmedtje JF Jr, Ji YS, Liu WL, DuBois RN and Runge MS. 1997. Hypoxia induces cyclooxygenase-2 via the NF-kappaB p65 transcription factor in human vascular endothelial cells. *J Biol Chem* 272: 601-608.

Schmelzer KR, Kubala L, Newman JW, Kim IH, Eiserich JP and Hammock BD. 2005. Soluble epoxide hydrolase is a therapeutic target for acute inflammation. *Proc Natl Acad Sci U S A* 102: 9772-7.

Schmidt KN, Amstad P, Cerutti P and Baeuerle PA. 1995. The roles of hydrogen peroxide and superoxide as messengers in the activation of transcription factor NF-kappa B. *Chem Biol* 2: 13-22.

Schmitz S, Pfaffl MW, Meyer HH and Bruckmaier RM. 2004. Short-term changes of mRNA expression of various inflammatory factors and milk proteins in mammary tissue during LPS-induced mastitis. *Domest Anim Endocrinol* 26: 111-126.

Scholz D, Devaux B, Hirche A, Potzsch B, Kropp B, Schaper W and Schaper J. 1996. Expression of adhesion molecules is specific and time-dependent in cytokine-stimulated endothelial cells in culture. *Cell Tissue Res* 284: 415-423.

Scuchardt JP, Schneider I, Willenberg I, Yang J, Hammock BD, Hahn A and Schebb NH. 2014. Increase of EPA-derived hydroxy, epoxy and dihydroxy fatty acid levels in human plasma after a single dose of long-chain omega-3 PUFA. *Prostaglandins Other Lipid Mediat* 109-111:23-31.

Serhan CN. 1994. Lipoxin biosynthesis and its impact in inflammatory and vascular events. *Biochim Biophys Acta* 1212:1-25.

Serhan CN and Petasis NA 2011. Resolvins and protectins in inflammation resolution. *Chem Rev* 111:5922-43.

Serhan CN, Chiang N and Van Dyke TE. 2008a. Resolving inflammation: dual anti-inflammatory and pro-resolution lipid mediators. *Nat Rev Immunol* 8: 349-361.

Serhan CN, Gotlinger K, Hong S, Lu Y, Siegelman J, Baer T, Yang R, Colgan SP and Petasis NA. 2006. Anti-inflammatory actions of neuroprotectin D1/protectin D1 and its natural stereoisomers: assignments of dihydroxy-containing docosatrienes. *J Immunol* 176: 1848-1859.

Serhan CN, Yacoubian S and Yang R. 2008b. Anti-inflammatory and pro-resolving lipid mediators. *Annual review of pathology* 3: 279.

Setty BN, Berger M and Stuart MJ. 1987. 13-Hydroxyoctadecadienoic acid (13-HODE) stimulates prostacyclin production by endothelial cells. *Biochem Biophys Res Comm* 146: 502-509.

Shao Y, Wellman TL, Lounsbury KM and Zhao FQ. 2014. Differential regulation of GLUT1 and GLUT8 expression by hypoxia in mammary epithelial cells. *Am J Physiol Regul Integr Comp Physiol*. 307: R237-247.

Shiraki T, Kamiya N, Shiki S, Kodama TS, Kakizuka A and Jingami H. 2005. Alpha,beta-unsaturated ketone is a core moiety of natural ligands for covalent binding to peroxisome proliferator-activated receptor gamma. *J Biol Chem* 280:14145-53.

Shuster DE, Kehrli ME, Jr., Rainard P and Paape M. 1997. Complement fragment C5a and inflammatory cytokines in neutrophil recruitment during intramammary infection with *Escherichia coli. Infect Immun* 65: 3286-3292.

Silva LP, Lorenzi PL, Purwaha P, Yong V, Hawke DH and Weinstein JN. 2013. Measurement of DNA concentration as a normalization strategy for metabolomic data from adherent cell lines. *Anal Chem* 85:9536-9542.

Sinclair AJ, Attar-Bashi NM and Li D. 2002. What is the role of alpha-linolenic acid for mammals? *Lipids* 37:1113-23.

Smith WL, Urade Y and Jakobsson PJ. 2011. Enzymes of the cyclooxygenase pathways of prostanoid biosynthesis. *Chem Rev* 111:5821-65.

Snyder NW, Golin-Bisello F, Gao Y, Blair IA, Freeman BA and Wendell SG. 2015. 15-Oxoeicosatetraenoic acid is a 15-hydroxyprostaglandin dehydrogenase-derived electrophilic mediator of inflammatory signaling pathways. *Chem Biol Interact* 234:144-53.

Sordillo L, Weaver JA, Cao YZ, Corl C, Sylte MJ and Mullarky IK. 2005. Enhanced 15-HPETE production during oxidant stress induces apoptosis of endothelial cells. *Prostaglandins Other Lipid Mediat* 76:19-34.

Sordillo LM, Contreras GA and Aitken SL. 2009. Metabolic factors affecting the inflammatory response of periparturient dairy cows. *Anim Health Res Rev* 10: 53-63.

Sordillo LM, Streicher KL, Mullarky IK, Gandy JC, Trigona W and Corl CM. 2008. Selenium inhibits 15-hydroperoxyoctadecadienoic acid-induced intracellular adhesion molecule expression in aortic endothelial cells. *Free Radic Biol Med* 44: 34-43.

Sordillo LM, Weaver JA, Cao YZ, Corl C, Sylte MJ and Mullarky IK. 2005. Enhanced 15-HPETE production during oxidant stress induces apoptosis of endothelial cells. *Prostaglandins Other Lipid Mediat* 76: 19-34.

Spector AA. 1975. Fatty acid binding to plasma albumin. *J Lipid Res* 16: 165-179. Stirling JW and Chandler JA. 1976. The fine structure of the normal, resting terminal ductal-lobular unit of the female breast. *Virchows Arch A Pathol Anat Histol* 372: 205-226. Strandberg Y, Gray C, Vuocolo T, Donaldson L, Broadway M and Tellam R. 2005. Lipopolysaccharide and lipoteichoic acid induce different innate immune responses in bovine mammary epithelial cells. *Cytokine* 31:72-86.

Suardiaz R, Masgrau L, Lluch JM and Gonzalez-Lafont A. 2013. An insight into the regiospecificity of linoleic acid peroxidation catalyzed by mammalian 15-lipoxygenases. *J Phys Chem* B 117: 3747-3754.

Swanson EW. 1965. Comparing continuous milking with sixty-day dry periods in successive lactations. *J Dairy Sci* 48: 1205-1209.

Swanson KM, Stelwagen K, Dobson J, Henderson HV, Davis SR, Farr VC and Singh K. 2009. Transcriptome profiling of *Streptococcus uberis*-induced mastitis reveals fundamental differences between immune gene expression in the mammary gland and in a primary cell culture model. *J Dairy Sci* 92: 117-129.

Szklenar M, Kalkowski J, Stangl V, Lorenz M and Ruhl R. 2013. Eicosanoids and docosanoids in plasma and aorta of healthy and atherosclerotic rabbits. *J Vasc Res*, 50, 372-82.

Tam VC. 2013. Lipidomic profiling of bioactive lipids by mass spectrometry during microbial infections. *Semin Immunol*, 25, 240-8.

Tam VC, Quehenberger O, Oshansky CM, Suen R, Armando AM, Treuting PM, Thomas PG, Dennis EA and Aderem A. 2013. Lipidomic profiling of influenza infection identifies mediators that induce and resolve inflammation. *Cell* 154: 213-227.

Tampo Y, Kotamraji S, Chitambar CR, Kalivendi SV, Keszler, Joseph J and Kalyanaraman B. 2003. Oxidative stress-induced iron signaling is responsible for peroxide-dependent oxidation of dichlorodihydrofluorescein in endothelial cells: role of transferrin receptor-dependent iron uptake in apoptosis. *Circ Res* 92: 56-63.

Tatarczuch L, Philip C and Lee CS. 1997. Involution of the sheep mammary gland. *J Anat* 190: 405-416.

Thomas LH, Haider W, Hill AW and Cook RS. 1994. Pathologic findings of experimentally induced *Streptococcus uberis* infection in the mammary gland of cows. *Am J Vet Res* 55: 1723-1728.

Thompson RD, Noble KE, Larbi KY, Dewar A, Duncan GS, Mak TW and Nourshargh S. 2001. Platelet-endothelial cell adhesion molecule-1 (PECAM-1)-deficient mice demonstrate a transient and cytokine-specific role for PECAM-1 in leukocyte migration through the perivascular basement membrane. *Blood* 97: 1854-1860.

Trigona WL, Mullarky IK, Cao Y and Sordillo LM. 2006. Thioredoxin reductase regulates the induction of haem oxygenase-1 expression in aortic endothelial cells. *Biochem J* 394: 207-216. Vangaveti V, Baune BT and Kennedy RL. 2010. Hydroxyoctadecadienoic acids: novel regulators of macrophage differentiation and atherogenesis. *Ther Adv Endocrinol Metab* 1: 51-60.

Van Nieuw Amerongen GP and Van Hinsbergh VW. 2002. Targets for pharmacological intervention of endothelial hyperpermeability and barrier function. *Vascul Pharmacol* 39: 257-272.

Vasquez-Vivar J, Kalyanaraman B, Martasek P, Hogg, N, Masters BS, Karoui H, Tordo P and Pritchard, KA, Jr. 1998. Superoxide generation by endothelial nitric oxide synthase: the influence of cofactors. *Proc Natl Acad Sci USA* 95: 9220-9225.

Vercesi AE, Kowaltowski AJ, Grijalba MT, Meinicke AR and Castilho RF. 1997. The role of reactive oxygen species in mitochondrial permeability transition. *Biosci Rep*, 17, 43-52.

Walker NI, Bennett RE and Kerr JF. 1989. Cell death by apoptosis during involution of the lactating breast in mice and rats. *Am J Anat* 185: 19-32.

Wang Y, Armando AM, Quehenberger O, Yan C and Dennis EA. 2014. Comprehensive ultraperformance liquid chromatographic separation and mass spectrometric analysis of eicosanoid metabolites in human samples. *J Chromatogr A* 1359: 60-69.

Weaver JA, Maddox JF, Cao YZ, Mullarky IK and Sordillo LM. 2001. Increased 15-HPETE production decreases prostacyclin synthase activity during oxidant stress in aortic endothelial cells. *Free Radic Biol Med* 30: 299-308.

Weisner R, Suzuki H, Walther M, Yamamoto S and Kuhn H. 2003. Suicidal inactivation of the rabbit 15-lipoxygenase by 15S-HpETE is paralleled by covalent modification of active site peptides. *Free Radic Biol Med* 34:304-15.

Weiss N, Zhang YY, Heydrick S, Bierl C and Loscalzo J. 2001. Overexpression of cellular glutathione peroxidase rescues homocyst(e)ine-induced endothelial dysfunction. *Proc Natl Acad Sci USA* 98: 12503-12508.

Wilde CJ, Addey CV, Li P and Fernig DG. 1997. Programmed cell death in bovine mammary tissue during lactation and involution. *Exp Physiol* 82: 943-953.

Winn RK and Harlan JM. 2005. The role of endothelial cell apoptosis in inflammatory and immune diseases. *J Thromb Haemost* 3: 1815-1824.

Wong BC, Wang WP, Cho CH, Fan XM, Lin MC, Kung HF and Lam SK. 2001. 12-Lipoxygenase inhibition induced apoptosis in human gastric cancer cells. *Carcinogenesis* 22:1349-1354.

Wrighton CJ, Hofer-Warbinek R, Moll T, Eytner R, Bach FH and De Martin R. 1996. Inhibition of endothelial cell activation by adenovirus-mediated expression of I kappa B alpha, an inhibitor of the transcription factor NF-kappa B. *J Exp Med* 183: 1013-1022.

Xia Y, Tsai AL, Berka V and Zweier JL. 1998. Superoxide generation from endothelial nitric-oxide synthase. A Ca2+/calmodulin-dependent and tetrahydrobiopterin regulatory process. *J Biol Chem* 273: 25804-25808.

Yao HT, Chang YM, Lan SJ, Chem CT, Hsu JT and Yeh TK. 2006. The inhibitory effect of polyunsaturated fatty acids on human CYP enzymes. *Life Sci* 79:2432-40.

Yasugi T, Kaido T and Uehara Y. 1989. Changes in density and architecture of microvessels of the rat mammary gland during pregnancy and lactation. *Arch Histol Cytol* 52: 115-122.

Zhang W, Zheng S, Storz P and Min W. 2005. Protein kinase D specifically mediates apoptosis signal-regulating kinase 1-JNK signaling induced by H2O2 but not tumor necrosis factor. *J Biol Chem* 280: 19036-19044.

Zhang X, Wang T, Gui P, Yao C, Sun W, Wang L, Wang H, Xie W, Yao S, Lin Y and Wu Q. 2013. Resolvin D1 reverts lipopolysaccharide-induced TJ proteins disruption and the increase of cellular permeability by regulating IkappaBalpha signaling in human vascular endothelial cells. *Oxid Med Cell Longev* 2013: 185715.

Zhao FQ and Keating AF. 2007. Expression and regulation of glucose transporters in the bovine mammary gland. *J Dairy Sci* 90 Suppl 1: E76-86.

Zhao X, Yamamoto T, Newman JW, Kim IH, Watanabe T, Hammock BD, Stewart J, Pollock JS, Pollock DM & Imig JD. 2004. Soluble epoxide hydrolase inhibition protects the kidney from hypertension-induced damage. *J Am Soc Nephrol*, 15, 1244-53.

Zia S, Giri SN, Cullor J, Emau P, Osburn BI and Bushnell RB. 1987. Role of eicosanoids, histamine, and serotonin in the pathogenesis of *Klebsiella pneumoniae*-induced bovine mastitis. *Am J Vet Res* 48: 1617-1625.

Zu L, He J, Jiang H, Xu C, Pu S and Xu G. 2009. Bacterial endotoxin stimulates adipose lipolysis via toll-like receptor 4 and extracellular signal-regulated kinase pathway. *J Biol Chem* 284:5915-26.

Zweier JL, Broderick R, Kuppusamy P, Thompson-Gorman S and Lutty GA. 1994. Determination of the mechanism of free radical generation in human aortic endothelial cells exposed to anoxia and reoxygenation. *J Biol Chem* 269: 24156-2416.